THE EFFECT OF HEAT TREATMENT ON MECHANICAL PROPERTIES AND MICROSTRUCTURE OF LOW CARBON STEEL WELDED JOINT WITH ER70S FILLER METAL

NUR ALIYA ALINA BT AB RADZAK

BACHELOR OF MANUFACTURING ENGINEERING TECHNOLOGY (PROCESS AND TECHNOLOGY) WITH HONOURS

2022

Faculty of Mechanical and Manufacturing Engineering Technology

THE EFFECT OF HEAT TREATMENT ON MECHANICAL PROPERTIES AND MICROSTRUCTURE OF LOW CARBON STEEL WELDED JOINT WITH ER70S FILLER METAL

Nur Aliya Alina Binti Ab Radzak

Bachelor of Manufacturing Engineering Technology (Process and Technology) with Honours

2022

THE EFFECT OF HEAT TREATMENT ON MECHANICAL PROPERTIES AND MICROSTRUCTURE OF LOW CARBON STEEL WELDED JOINT WITH ER70S FILLER METAL

NUR ALIYA ALINA BINTI AB RADZAK

A thesis submitted
in fulfillment of the requirements for the degree of
Bachelor of Manufacturing Engineering Technology (Process and Technology) with Honours

Faculty of Mechanical and Manufacturing Engineering Technology

UNIVERSITI TEKNIKAL MALAYSIA MELAKA

2022

DECLARATION

I declare that this Choose an item. entitled “The Effect of Heat Treatment on Mechanical Properties and Microstructure of Low Carbon Steel Welded Joint with ER70s Filler Metal” is the result of my own research except as cited in the references. The Choose an item. has not been accepted for any degree and is not concurrently submitted in candidature of any other degree.

Signature : 

Name : Nur Aliya Alina Binti Ab Radzak

Date : 16 January 2022

APPROVAL

I hereby declare that I have checked this thesis and in my opinion, this thesis is adequate in terms of scope and quality for the award of the Bachelor of Manufacturing Engineering Technology (Process and Technology) with Honours.

Signature : 

NUR AIMAN HANIS BINTI HASIM
Pensyarah
Jabatan Teknologi Kejuruteraan Pembuatan
Fakulti Teknologi Kejuruteraan Mekanikal dan Pembuatan
Universiti Teknikal Malaysia Melaka

Supervisor Name : Puan Nur Aiman Hanis Binti Hasim

Date : 18 January 2022

Signature : 

Co Supervisor Name : Dr Mohd Fauzi Bin Mamat

DR. MOHD FAUZI BIN MAMAT
Pensyarah kanan
Jabatan Teknologi Industri
Fakulti Teknologi Kejuruteraan Mekanikal Dan Pembuatan (FTKMP)
Universiti Teknikal Malaysia Melaka

Date : 18 January 2022

DEDICATION

This report is dedicated to my beloved family in perticular, for their endless love, support and encouragement. To my main supervisor Puan Nur Aiman Hanis Binti Hasim and my co supervisor, Dr Mohd Fauzi Bin Mamat who has guided me along the way to finish this project. Thank you for all your support, and give me strength untill this project is finished.

ABSTRACT

Welding process such as GMAW appears to be growing the fastest, with recent years showing the greatest growth. However, the process during welding, rapid heating and cooling takes place which produce severe thermal cycle near weld line region of any metal that gets submerged in the heating zone. Gas Metal Arc Welding (GMAW), sometimes known as metal inert gas (MIG) welding, is a type of welding method in which an electric arc is produced between a consumable wire electrode and the workpiece metal(s), heating, melting, and joining them. The main objective of this study were to study the welded joint of low carbon steel joint with filler metal ER70s. Next, to carry out the non-destructive test by using radiography testing and liquid penetrant inspection. Last but not least,to study the effect of heat treatment on the mechanical and microstructure properties by performing hardness and impact test. Radiography and liquid penetrant test were conducted to investigate the surface defects on the sample. After that, the sample were cut into 9 samples with the dimension of 55mm x 10mm x 12mm using abrasive water jet. The samples were prepared through two types of heat treatment process which is annealing with the temperature of 900˚C and tempering 450˚C. Next, the material characterization were confirmed through optical microscope and Scanning Electron Microscope (SEM/EDX). The macro hardness test were done by using Rockwell machine to evaluate the microhardness behaviour of treated and untreated samples. Meanwhile, for the impact test, the Charpy test were used to determine the relative toughness or impact toughness of the sample. The impact test results showed similar value of three samples with value 49.885J for untreated sample, 49.860J for tempered sample and 49.884J for annealed were tough and strong enough to break at the welded connection, however at the HAZ area, the annealed sample with value 49.884J is stronger than the tempered which have 48.860J and untreated samples with 47.885J. At annealed sample, the result of the graph showed that the line pattern of each area were in average compared to graph of untreated and tempered sample. Even though the line pattern of annealed sample were in average, but the annealed sample have the lowest value of hardness at HAZ and weld joint compared to tempered and untreated sample. Next, by performing SEM, it shown the presence of Iron (Fe) in the welded joint with 94.95% at untreated sample meanwhile after performing a heat treatment test, it showed that the structure has changed by showing the presence of manganese in the welded join area with 97.56% at tempered sample and 92.72% at annealed sample.

ABSTRAK

Proses kimpalan seperti GMAW nampaknya berkembang dengan pantas, dengan beberapa tahun kebelakangan ini menunjukkan pertumbuhan yang paling besar. Walau bagaimanapun, proses semasa mengimpal, pemanasan pantas dan penyejukan berlaku yang menghasilkan kitaran haba yang teruk berhampiran kawasan garisan kimpalan mana-mana logam yang terendam dalam zon pemanasan. Kimpalan Arka Logam Gas (GMAW), kadang-kadang dikenali sebagai kimpalan gas lengai logam (MIG), ialah sejenis kaedah kimpalan di mana arka elektrik dihasilkan antara elektrod wayar boleh guna dan logam bahan kerja, pemanasan, lebur, dan menyertai mereka. Objektif utama kajian ini adalah untuk mengkaji sambungan kimpalan sambungan keluli karbon rendah dengan pengisi ER70s. Seterusnya, untuk menjalankan ujian tanpa musnah dengan menggunakan ujian radiografi dan pemeriksaan penembus cecair. Akhir sekali, untuk mengkaji kesan rawatan haba ke atas sifat mekanikal dan struktur mikro dengan melakukan ujian kekerasan dan hentaman. Radiografi dan ujian penembusan cecair telah dijalankan untuk menyiasat kecacatan permukaan pada sampel. Selepas itu, sampel dipotong kepada 9 sampel berdimensi 55mm x 10mm x 12mm menggunakan pancutan air yang kasar. Sampel disediakan melalui dua jenis proses rawatan haba iaitu *annealing* dengan suhu 900˚C dan *tempering* 450˚C. Seterusnya, pencirian bahan disahkan melalui mikroskop optik dan Mikroskop Elektron Pengimbasan (SEM/EDX). Ujian kekerasan makro dilakukan dengan menggunakan mesin *Rockwell* untuk menilai tingkah laku kekerasan mikro bagi sampel yang dirawat dan tidak dirawat. Manakala bagi ujian impak, ujian *Charpy* digunakan untuk menentukan keliatan relatif atau keliatan impak sampel. Keputusan ujian impak menunjukkan nilai yang hampir sama bagi tiga sampel dengan nilai 49.885J untuk sampel yang tidak dirawat, 49.860J untuk sampel *tempered* dan 49.884J untuk *annealed* adalah lasak dan cukup kuat untuk pecah pada sambungan yang dikimpal, namun pada kawasan HAZ, sampel *annealed* dengan nilai 49.884J adalah lebih kuat daripada sampel *tempered* yang mempunyai nilai 48.860J dan sampel yang tidak dirawat dengan nilai 47.885J. Pada sampel *annealed*, keputusan graf menunjukkan bahawa corak garisan setiap kawasan adalah secara purata berbanding dengan graf sampel yang tidak dirawat dan *tempered*. Walaupun corak garisan sampel *annelaed* adalah secara purata, tetapi sampel *annealed* mempunyai nilai kekerasan yang paling rendah pada HAZ dan sambungan kimpalan berbanding sampel *tempered* dan tidak dirawat. Seterusnya, dengan melakukan SEM menunjukkan kehadiran *Iron* (Fe) dalam sambungan kimpalan dengan 94.95% pada sampel yang tidak dirawat manakala selepas melakukan ujian rawatan haba, ia menunjukkan bahawa struktur telah berubah dengan menunjukkan kehadiran *manganese* dalam cantuman yang dikimpal. kawasan dengan 97.56% pada sampel *tempered* dan 92.72% pada sampel *annealed.*

ACKNOWLEDGEMENTS

In the Name of Allah, the Most Gracious, the Most Merciful

First and foremost, I would like to thank and praise Allah the Almighty, my Creator, my Sustainer, for everything I received since the beginning of my life. I would like to extend my appreciation to the Universiti Teknikal Malaysia Melaka (UTeM) for providing the research platform.

My utmost appreciation goes to my main supervisor, Puan Nur Aiman Hanis Binti Hasim and my co supervisor, Dr. Mohd Fauzi Bin Mamat for all their support, advice, and inspiration. Their constant patience for guiding and providing priceless insights will forever be remembered.

I would like to give a special thanks to my beloved mother, Hasmah Binti Yong for her endless support, love, and prayers. I dedicated this thesis for you. I would also like to thank my friends especially to my housemates, 807-K for the great supports and friendship. I also would like to thank seven beautiful individuals, BTS for always being there along ups and down in my life. Finally, thank you to all the individual(s) who had provided me the assistance, support, and inspiration to embark on my study.

TABLE OF CONTENTS

		PAGE
DECLARATION		
APPROVAL		
DEDICATION		
ABSTRACT		**i**
ABSTRAK		**ii**
ACKNOWLEDGEMENTS		**iii**
TABLE OF CONTENTS		**iv**
LIST OF TABLES		**vi**
LIST OF FIGURES		**vii**
LIST OF SYMBOLS AND ABBREVIATIONS		**x**
APPENDICES		**xi**
CHAPTER 1	**INTRODUCTION**	**1**
1.1	Background of Study	1
1.2	Problem Statement	2
1.3	Objective of Study	3
1.4	Scope of Study	3
1.5	Significant of Study	4
CHAPTER 2	**LITERATURE REVIEW**	**5**
2.1	Introduction	5
2.2	Welding Process	5
2.2.1	Welding Gas Metal Arc Welding (GMAW)	7
2.2.2	Filler metal	9
2.3	Welding Metallurgy	10
2.3.1	Area at fusion weld – Heat Affected Zone (HAZ)	11
2.4	Welding Parameter	12
2.5	Defects in Welding	12
2.6	Carbon Steel as Base Material	19
2.6.1	Low Carbon Steel	21
2.6.2	Medium Carbon Steel	22
2.6.3	High Carbon Steel	22
2.6.4	Application of Carbon Steel in Oil and Gas Industry	23
2.7	Heat Treatment Process	23
2.7.1	Stages of Heat Treatment	26

2.7.2 Types of Heat Treatment 28
2.7.3 Heat Treatment on Welded Joint 35
2.8 Summary of Literature Review 36

CHAPTER 3 METHODOLOGY 38
3.1 Introduction 38
3.2 Preparation of Sample 40
3.2.1 Welding Procedures 40
3.3 Non-Destructive Test (NDT) 41
3.3.1 Liquid Penetrant Inspection 42
3.3.2 Radiographic Testing 44
3.4 Sample Preparation for Testing 45
3.4.1 Procedures of waterjet cutting 46
3.5 Heat Treatment Process 47
3.6 Mechanical Test 48
3.6.1 Hardness Test (Rockwell Hardness) 49
3.6.2 Impact Test 50
3.7 Microstructure Characterization 53
3.7.1 Optical Microscope 53
3.7.2 Scanning Electron Microscopy (SEM) Energy Dispersive X-Ray Spectroscopy (EDX) 55

CHAPTER 4 RESULTS AND DISCUSSION 56
4.1 Introduction 56
4.2 Composition of analysis 56
4.3 Complete welded joint 57
4.4 Non destructive test 58
4.4.1 Radiographic testing 58
4.4.2 Liquid penetrant testing 59
4.5 Heat Treatment Process 60
4.6 Mechanical Test 61
4.6.1 Impact Testing 61
4.6.2 Macro hardness Analysis 64
4.7 Microstructure Analysis 71
4.7.1 Optical microscope 71
4.7.2 Line Scanning 75
4.7.3 Elemental Mapping 78

CHAPTER 5 CONCLUSION AND RECOMMENDATIONS 80
5.1 Conclusion 82
5.2 Recommendations for future 85

REFERENCES 86

APPENDICES 91

LIST OF TABLES

TABLE	TITLE	PAGE
Table 2.1	Typical welding parameters of mild and low alloy for GMAW	8
Table 2.2	The comparison of the carbon content, microstructure, and properties	20
Table 2.3	The comparison result of heat treatment on welded joint of previous study	24
Table 2.4	Table comparison of heat treatment process	29
Table 4.1	Chemical composition of low carbon steel	57
Table 4.2	Result of Charpy test	62
Table 4.3	Result from the macro hardness test of untreated sample	65
Table 4.4	Result from the macro hardness test of tempered sample	67
Table 4.5	Result from the macro hardness test of annealed sample	69

LIST OF FIGURES

FIGURE	TITLE	PAGE
Figure 2.1	Types of welding process	6
Figure 2.2	Gas Metal Arc Welding (GMAW)	7
Figure 2.3	The letter-number designations of filler metal	9
Figure 2.4	Zones and boundaries in the heat affected zone	11
Figure 2.5	Classification of welding defects	13
Figure 2.6	Welding crack	15
Figure 2.7	Spatter	16
Figure 2.8	Uniformly distributed porosity	17
Figure 2.9	Diagram of incomplete fusion	19
Figure 2.10	The example of pipeline structure in oil and gas	23
Figure 2.11	a) Temperature b) Its reaction to the TTT diagram	27
Figure 2.12	Iron-carbon phase diagram	29
Figure 2.13	Grain metals in annealing stages	32
Figure 2.14	Hardening process	33
Figure 2.15	Tempering steel colour chart used	34
Figure 2.16	Difference on pearlitic structure due to annealing and normalizing	35
Figure 3.1	Process flow chart of study	39
Figure 3.2	Dimension of sample preparation	40
Figure 3.3	The procedure of liquid penterant inspection	43
Figure 3.4	The applicant used in liquid penentrant testing	44
Figure 3.5	Indication using liquid penetrant inspection	44

Figure 3.6	Radiography using x-ray	45
Figure 3.7	Flow Mach 2 1313B Abrasive Water Jet Machine	46
Figure 3.8	The procedures of waterjet cutting	46
Figure 3.9	Workpiece that were cut by waterjet machine	47
Figure 3.10	The procedure of the sample for tempering process	48
Figure 3.11	The procedure of the sample for annealing process	48
Figure 3.12	Mitutoyo HR-400 Rockwell Hardness Tester	49
Figure 3.13	The sample were put to get the value of hardness of each layers	50
Figure 3.14	Instron CEAST 9050 Pendulum Impact Tester	51
Figure 3.15	The Charpy test	52
Figure 3.16	Charpy (Simple-Beam) impact test specimens (ASTM, 2015)	52
Figure 3.17	Zeiss AxioLab A1 Upright Light Microscope with AxioCam Erc 5s	54
Figure 3.18	ZEISS EC EPIPLAN objectives lens	54
Figure 3.19	JEOL JSM 6010 PLUS/LV Scanning Electron Microscope	55
Figure 4.1	Complete welded low carbon steel plate	58
Figure 4.2	The film of workpiece under film viewer	59
Figure 4.3	Sample after developer were applied	60
Figure 4.4	Visual appearances after treated	61
Figure 4.5	The bar graph of impact test for welded joint (centre)	62
Figure 4.6	The bar graph of impact test for Heat Affected Zone (HAZ)	63
Figure 4.7	Indentation done on multiple layer on the same surface	64
Figure 4.8	Graph result of macro hardness of untreated sample	66
Figure 4.9	Graph result of macrohardness of tempered sample	68
Figure 4.10	Graph result of macrohardness of annealed sample	70

Figure 4.11 Microstructure of each area on untreated sample 72

Figure 4.12 Microstructure of each area of tempered sample 73

Figure 4.13 Microstructure of each area of annealed sample 74

Figure 4.14 Interface of untreated sample 76

Figure 4.15 Interface of tempered sample 77

Figure 4.16 Interface of annealed sample 78

Figure 4.17 Elemental mapping analysis for untreated sample 79

Figure 4.18 Elemental mapping analysis for tempered sample 80

Figure 4.19 Elemental mapping analysis for annealed sample 81

LIST OF SYMBOLS AND ABBREVIATIONS

GMAW	-	Gas Metal Arc Welding
MIG	-	Metal Inert Gas
GTAW		Gas Tungsten Arc Welding
HAZ	-	Heat Affected Zone
NDT	-	Non-Destructive Test
SEM	-	Scanning Electron Microscope
LPT	-	Liquid Penetrant Testing
EDX	-	Energy Dispersive X-Ray
FCC	-	Face Centered Cubic
BCC	-	Body Centered Cubic
CO_2	-	Carbon Dioxide
ASRC	-	Alloy Steels Research Committee
HSLA	-	High- Strength, Low-Alloy Steel
PWHT	-	Post-Weld Heat Treatment
EBSD	-	Electron Backscatter Diffraction

APPENDICES

APPENDIX	TITLE	PAGE
APPENDIX A	ASTM E23	90
APPENDIX B	Gantt Chart (BDP 1)	116
APPENDIX C	Gantt Chart (BDP 2)	117
APPENDIX D	Turnitin Report	118

CHAPTER 1

INTRODUCTION

1.1 Background of Study

The arc welding segment of the industry appears to be growing the fastest, with recent years showing the greatest growth. Welding is the most common joining method, and most common steels are weldable. These days, it become the most important activity in any manufacturing process, and the quality of welding has a direct effect on the performance of the endproduct. Welding can be defined as the process of joining materials into a single piece (Vural, 2014). As widely known, GMAW is a popular welding technique, particularly in industrial sectors. Gas Metal Arc Welding (GMAW), sometimes known as metal inert gas (MIG) welding, is a type of welding method in which an electric arc is produced between a consumable wire electrode and the workpiece metal(s), heating, melting, and joining them (Hajili, 2017). GMAW produces welds with enhanced mechanical characteristics and is often used because it results in welds that are more attractive as well as of higher quality. This technology is increasingly being applied in the construction industry, as well as pipe joining in the oil and gas industry.

Although the oil and gas industries has an incredible safety record over many decades, failures occasionally occur. Corrosion failures, fatigue failures, and ductile and brittle metal failures are the most common reasons of these failures. Due to the heat treatment process, infrastructure and equipments used in the oil and gas industry tend to last for many years because of the properties in the structures and it became stronger, and can survive severe pressures, temperatures, weights, and conditions (Pourazizi et al.,

2020). Heat treatment is the process of heating a metal to a specified temperature, keeping it there, and then cooling it down (Chandra Kandpal et al., 2020). Mechanical characteristics of the metal part will alter during the process. This is due to the fact that high temperatures affect the microstructure of the metal. To sum up, heat treatment is critical for obtaining the appropriate mechanical characteristics and microstructure for a variety of applications. The present study will investigate the mechanical properties and microstructure of low carbon steel joint with ER70s filler metal with different type of heat treatments.

1.2 Problem Statement

During the welding process, rapid heating and cooling occur, causing a severe thermal cycle along the weld line region of any metal submerged in the heating zone. Due to the thermal cycle, the material is not uniformly heated and cooled, resulting in a harder heat affected zone (HAZ), sustaining stress, and a preponderance of cold cracking in the weld metal and base metal. Hazardous stressors that persist regularly cause and impact a wide variety of heating and cooling temperatures. When steel is heated to a certain temperature, it welds well; moreover, the heat generated on it has an unique microstructure from that of the base metal, referred to as the heat affected zone (HAZ) (Pisarski & Pargeter, 1984). Why do weld usually fails in HAZ? It is because when the HAZ is exposed to enough heat for a long enough time, the layer develops microstructure and properties that are different from the parent metal. These property adjustments are normally undesirable, and they end up becoming the component's weakest point. Microstructural changes, for example, can result in residual stresses, decreased material strength, increased brittleness, and decreased corrosion and/or crack resistance (Nayak et al., 2015). As a result, there are several faults in the HAZ. A pre- and/or post-weld heat

treatment can help to reduce HAZ issues. Heat treatment, as is well known, modifies the mechanical and microstructural qualities of the material, making it suitable for the purpose for which it is intended. Nam et al., (1999) proposed that during annealing, the microstructure softens and sometimes recrystallizes and recovers. They also proposed that the morphology of carbides is bound to vary throughout time. Steel's machinability, ductility, hardness, tensile strength, and impact strength are all improved by heat treatment. In this project, two types of heat treatment process which is annealing and tempering will be used.

1.3 Objective of Study

i. To study the welded joint of low carbon steel joint with filler ER70s.

ii. To carry out the non-destructive test by using radiography testing and liquid penetrant inspection.

iii. To study the effect of heat treatment on the mechanical and microstructure properties by performing hardness and impact test.

1.4 Scope of Study

The scope of this study:

i. Gas metal arc welding (GMAW) are used as welding method on the low carbon steel joint.

ii. Performing non –destructive test (NDT) by using radiography testing and liquid penetrant inspection to detect internal and external defects in the welded joint.

iii. Using abrasive water jet to cut the welded metal to the dimension 55mm x 10mm x 12mm.

iv. Mechanical testing of microhardness is carried out on the sample to investigate the resistant of the sample to indentation or penetration.

v. Investigate the material characterization using optical microscope, scanning electron microscope (SEM) and energy dispersive x-ray analysis (EDX) to analyse microstructure and fracture mode on welded cross section.

vi. Visual observation and inspection of the experiments are used to evaluate and analyse them.

1.5 Significant of Study

The oil and gas industry plays a very important role in the global energy supply as well as the world economy. Many technologies are crucial to the existence and functioning of this multi-billion-dollar industry. The oil and gas industry utilizes various highly complex infrastructure such as rigs, pipelines, platforms, bridges, offshore and onshore structure and ships. The vast majority of these infrastructures are built using welding technologies. Welding is important in oil and gas operations, both for new project construction and for the maintenance of existing facilities. Regarding this project, heat treatment will help to increase the mechanical properties. The purpose of this research is to help the oil and gas industry so that they will improve the future production in term of using suitable heat treatment process and reduce the cost of processing, time and energy of the workers.

CHAPTER 2

LITERATURE REVIEW

2.1 Introduction

Welding is the most critical operation in any manufacturing process, and the quality of the welding directly affects the ultimate product's quality. According to Kumar et al., (2019), welding is a procedure that permanently binds two materials (typically metals) together through the use of a specific mixture formed by the proper combination of temperature, weight, and metallurgical conditions. Additionally, he claimed that a range of welding forms have been developed depending on the relationship between temperature and weight, ranging from high temperatures with no weight to large weights with a low temperature. Nowadays, numerous welding techniques are used. The most often used varieties in industrial sectors are Gas Metal Arc Welding (GMAW) or MIG, Gas Tungsten Arc Welding (GTAW) or TIG, Flux Core Arc Welding, and Stick Welding. Apart from that, welding can be done underwater; nevertheless, this demands highly skilled operators who are aware with the conditions and scenarios encountered while working in the water.Welding Process

Metal is melted to form a bridge between the components to be connected, and when the weld metal solidifies, the components become connected. Welding is frequently accomplished by the use of pressure, perhaps in combination with heat (Jenney & O'Brien, 1991). Welding processes are classified into two categories as shown in figure 2.1:

i) Fusion - The surfaces of two components to be connected are cleaned, pressed together, and heated, resulting in the formation of a pool of molten metal connecting the components.

ii) Solid state - The joining metals are not melted. Rather than that, they are heated by friction created by the components moving together under normal load. This process softens the metals and cleans the surface. After then, the sliding is halted, the normal load is raised, and the two surfaces are joined.

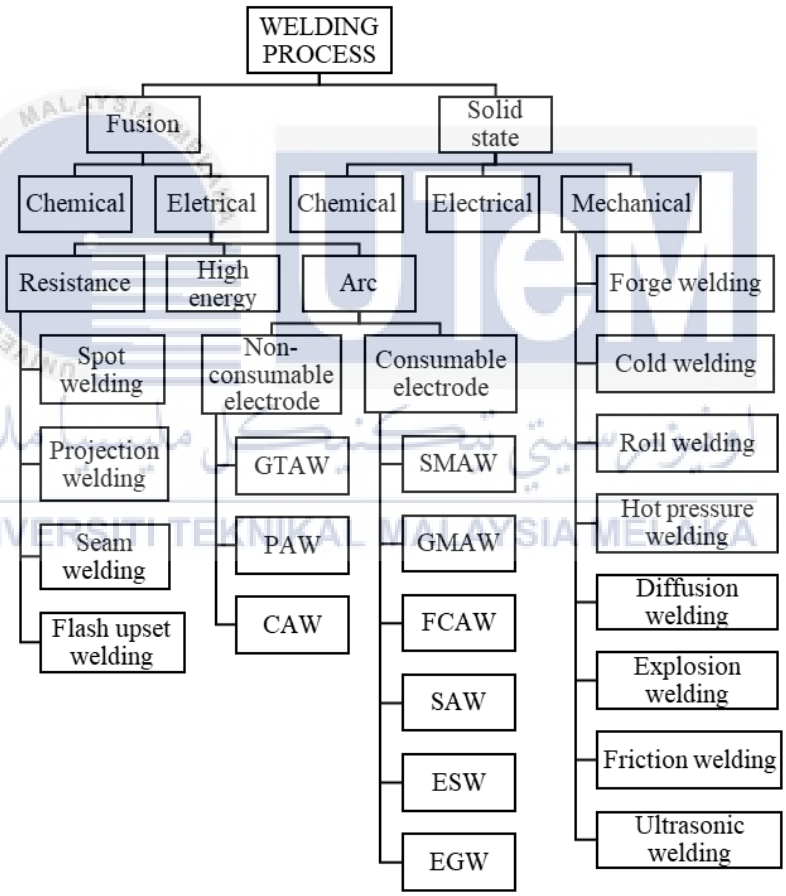

Figure 2.1: Types of welding process (https://www.weldingandndt.com/, 2017)

2.1.1 Welding Gas Metal Arc Welding (GMAW)

Gas Metal Arc Welding (GMAW), also known as metal inert gas (MIG) welding, is a process that involves the formation of an electric arc between a consumable wire electrode and the workpiece metal(s), heating and pressing them together to melt and join (Hajili, 2017). In addition to the wire electrode, a shielding gas is fed into the welding gun, effectively isolating the process from airborne pollutants. Techniques might be semi-automatic or totally automated. While GMAW is commonly driven by a constant voltage, direct current source, it can also be run on constant current or alternating current. External shielding gas protects molten metal from ambient oxides and nitrides during the welding process. There are four fundamental metal transfer processes in GMAW as in Figure 2.2 which were globular, short-circuiting, spray, and pulsed-spray, each having its own set of characteristics, advantages, and disadvantages.

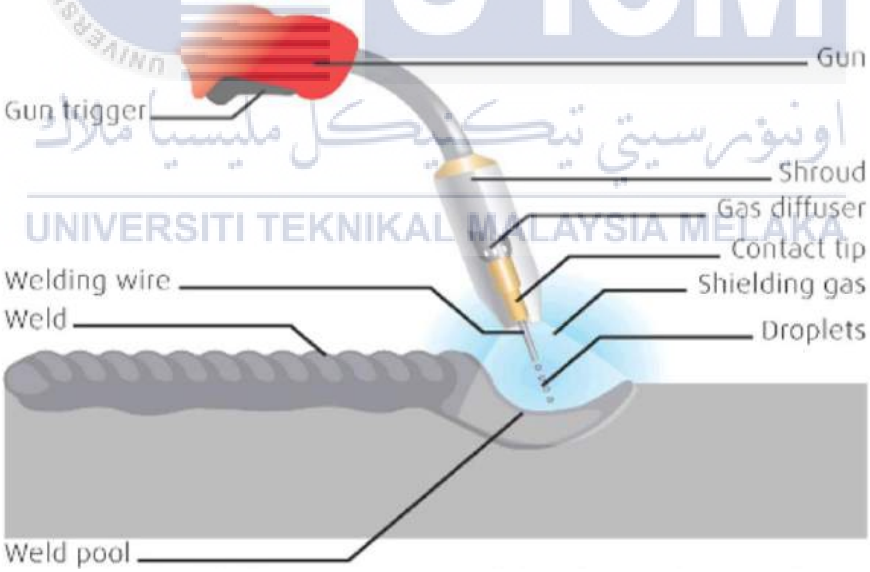

Figure 2.2: Gas Metal Arc Welding (GMAW) (https://www.sparkerweld.com/en, 2018)

Gas metal arc welding (GMAW) is a regularly utilised arc welding technology for joining large metal sections due to its unique properties. These advantages include an enhanced rate of wire electrode deposition, regulated high thermal energy dissipation, no

oxidation due to the use of shielding gas, and increased process efficiency (Wahab, 2014). Additionally, GMAW produces weldments with improved mechanical qualities and is frequently employed because it produces more visually appealing and high-quality welds than the shielded metal arc welding (SMAW) process (Abioye et al., 2019). This technique is increasingly being utilised in the construction industry, as well as the oil and gas business, to link pipes. In GMAW, argon is frequently utilised as the shielding gas. This is because the single-atom gas has a low thermal conductivity and ionisation potential, resulting in inefficient heat transmission to the arc's surface. As a result, argon offers deep but limited penetration into welds.

Table 2.1 showed the typical welding parameters of mild and low alloy for GMAW. These two methods of metal transfer usually used as parameter when welding the mild and low alloy steels.

Table 2.1: Typical welding parameters of mild and low alloy for GMAW (https://www.haynesintl.com/, 2017)

Process	Diameter Of Wire		Voltage (V)	Amperage (A)	Shielding Gas
	inch	mm			
Spray transfer	.035	0.9	28 – 32	165 – 200	98% Argon + 2% Oxygen or 75% Argon + 25% CO_2
	.045	1.14	30 – 34	180 – 220	
	1/16	1.6	30 – 34	230 – 260	
Short circuiting transfer	.035	0.9	22 – 25	100 – 140	100% CO_2
	.045	1.14	23 – 26	120 – 150	75% Argon + 25% CO_2

2.1.2 Filler metal

Filler metals liquefy and melt when heated, providing a brazed or soldered connection between two closely fitted components. Capillary attraction distribution occurs in correctly prepared joints when a filler metal has suitable melting and flow characteristics. Filler metals contribute to the formation of joints that meet service requirements for strength and corrosion resistance, among other characteristics. Seven factors must be considered when selecting a filler metal: the base material to be welded, the welding location, regulatory specifications and regulations, design requirements, shielding gas, post-weld heat treatment, and welding equipment. The welder can select an appropriate filler metal by referring to the letter-number designations for each type of filler metal as indicated in Figure 2.3.

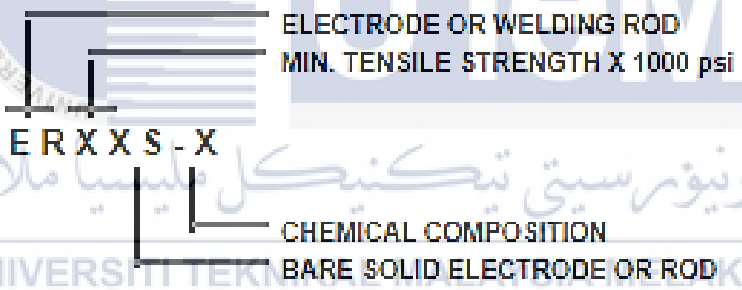

Figure 2.3: The letter-number designations of filler metal (Primo, 2014)

The silicon level in carbon steel electrodes is determined by the electrode classification, with ER70S-3 and ER70S-6 being the most popular. Because of its lower silicon levels, ER70S-2, ER70S-4, and ER70S-7 are sometimes used in pipe applications for open-root work. Lower silicon results in a firmer puddle and more control over the back bead design (Primo, 2014). Because the S-6 type has a larger degree of silicon and the puddle is more fluid, it can be used with less inductance in an open-root weld than an S-2 type electrode (Primo, 2014). It is critical to maintain a steady contact tip-to-work distance

in short-circuit transfer to ensure a smooth transfer. For carbon steel electrodes, the most common shielding gas and short-circuit transfer mode is 75% Ar and 25% CO_2.

2.2 Welding Metallurgy

Metallurgy is the science that investigates how metals behave. It explains how metals behave, their properties, and their internal structure are determined. Additionally, metallurgy refers to the treatments and techniques that enable us to customise a metal's qualities to a certain use. The metallurgy described in this case study is gas metal arc welding's ability to join two mechanically identical or different metals, specifically ferrous and non-ferrous metals. As Rahman et al., (2016) mentioned in their research, several studies in the field of metallurgical engineering are being conducted to investigate how heat treatment can be used to improve the physical and mechanical properties of low carbon steel. As is generally known, the atomic structure of a material has an effect on its properties; for instance, face-centered cubic FCC metals and alloys exhibit extraordinary ductility. Each crystal (grain) contains an ordered array of atoms, and when the grains come into contact, a mismatch in the ordered atoms causes a grain boundary. Imperfections in the crystal structure, such as point defects (such as solute atoms and vacancies) and dislocations, have a wide range of characteristics (Krauss, 2017).

The crystal structure of the metal determines the welding type that is required to meet the weldment criteria. Low carbon steels have body centred cubic (BCC) microstructures that can fluctuate during weld pool formation and joining, resulting in a heterogeneous microstructure on the welded surface. Due to the fact that welding employs heat to unite the metals, the required melting ranges, which span from solid to liquid, for the efficient application of the steel welding process are often referred to as phase diagrams. When a sufficient amount of heat is given to a surface, the ferrite BCC structure

converts to the face-centred cubic (FCC) structure known as austenite. While welding may be advantageous for the connecting method, the temperature variations induced by the welding process may damage the features in certain cases (Magudeeswaran et al., 2018).

2.2.1 Area at fusion weld – Heat Affected Zone (HAZ)

The heat affected zone (HAZ) of a metal or thermoplastic material is the area that is exposed to heat. While HAZ does not melt, heat-intensive processing can alter the material's characteristics and microstructure. Typically, mechanical qualities are altered during welding or high-heat cutting. HAZ refers to the region between the welded or cut surface and the base metal. These zones vary in size and severity depending on the material properties, the heat intensity and concentration, and the procedure used. When subjected to high temperatures for a sustained length of time, the HAZ undergoes structural and physical changes that identify it from the parent metal (Jeong et al., 2021). Typically, these property changes are undesirable and contribute to the material's weakness. For example, microstructural changes may result in residual stresses, decreased material strength, increased brittleness, and reduced resistance to corrosion or cracking. As a result of this, the HAZ has a high rate of failure. The zones and bounds of the heat-affected zone are illustrated in Figure 2.4 below.

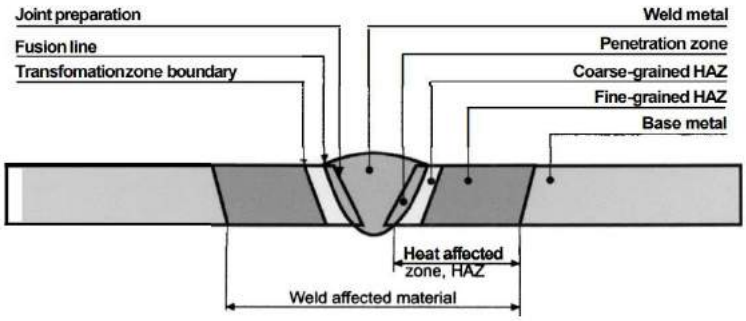

Figure 2.4: Zones and boundaries in the heat affected zone (https://whatispiping.com/, 2021)

2.3 Welding Parameter

The GMAW welding parameters have an impact on the quality, productivity, and cost of the welding joint. If all the welding parameters are in place, the perfect arc will be achieved. Major parameters contain:

i. welding current and voltage
ii. welding travel speed
iii. Flow rate of gas

According to Owolabi et al., (2016), the welding current is the most critical variable in the arc welding process since it affects the melting rate, deposition rate, penetration depth, and amount of base metal melted. His research proved that raising the welding current increases the hardness of the weld up to 115A and 116A for mild steel and low carbon steel, respectively, but declines with increasing the welding current. The ultimate tensile strength of mild steel decreases with increasing welding current but increases with 200A and 115A welding currents, respectively. The yield and impact strengths of the two samples decrease with increasing welding current.

2.4 Defects in Welding

As with any other industrial process, welding is prone to faults. The shape and size of the metal structure may alter slightly during the operation. It is likely that this condition is produced by the employment of an ineffective welding approach or technique. While it is difficult to achieve a defect-free welding joint, various procedures can help minimise defects to a considerable extent. Welding flaws are classified into two types: exterior defects and internal problems. External flaws are visible on the welded material's upper

surface, whereas internal imperfections are visible at a greater depth. Figure 2.5 below is the classification of some of welding defects in GMAW.

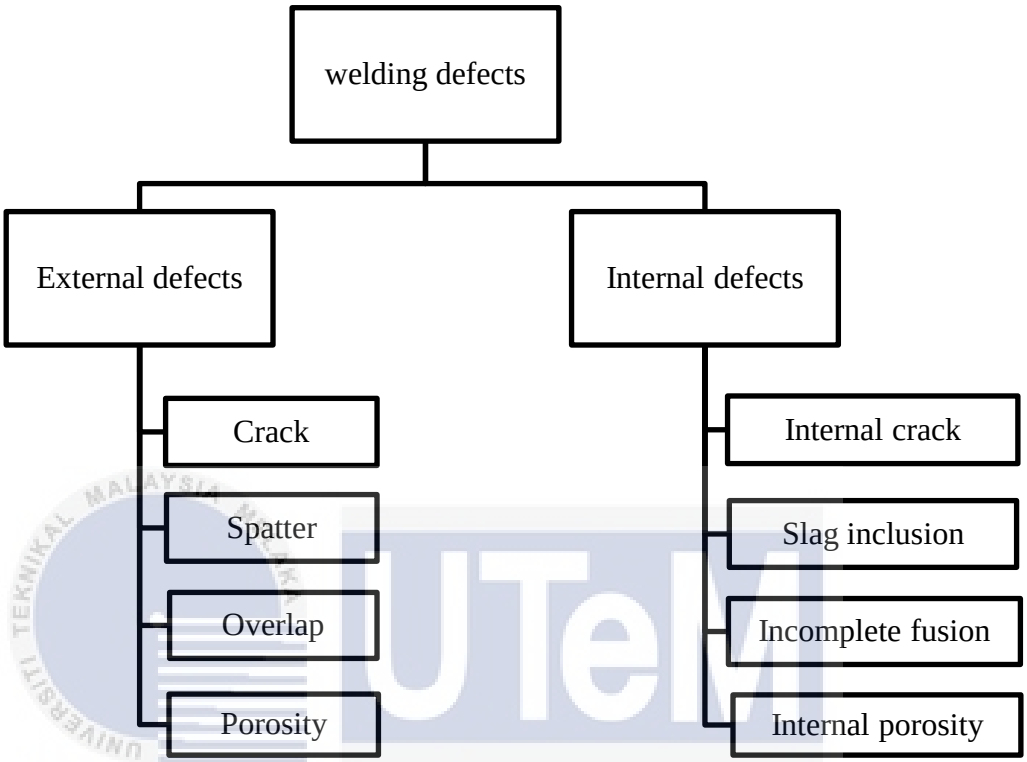

Figure 2.5: Classification of welding defects (https://whatispiping.com/, 2020)

2.4.1.1 Type of Defects

There are some of the most common welding flaws that can be found in welding field such as crack, spatter, porosity and incomplete fusion. These are the sort of flaws that commonly can be see found when a weld is complete either a single pass or a complete weld, depending on the defect itself. Most of it are easy to be detected.

1) Crack

Cracks are frequently planar discontinuities with a large distance between their length and diameter. Cracks can form at either elevated or low temperatures and in three locations: the weld, the base metal's heat affected zone, or at the weld-to-base metal fusion

line. Furthermore, cracking indicates a breakdown in metallurgical control. Cracks can be classified into several types based on the temperature at which they occur:

i. Hot cracks: Hot weld cracking occurs at high temperatures, typically exceeding 1000 degrees Fahrenheit (538 degrees Celsius), and the fault appears practically immediately (though not always visibly) after the weld hardens. Hot cracking nearly always occurs parallel to or immediately next to the longitudinal direction of the weld bead.

ii. Cold cracks: Occurs primarily when the weldment's temperature has returned to atmospheric levels. It can happen instantly or a week later, and it can happen with or without loading. Additionally, it may arise as a result of loading stress or as a result of stress concentrations generated by the notch effect of surface discontinuities.

iii. Crater cracks: These take place at the end of the welding process, shortly before the operator makes a pass over the weld joint. They are often seen after the finish of a weld. When the weld pool cools and solidifies, it must retain enough volume to compensate for any shrinkage in the weld metal. If this is not done, a crater fracture will form.

As a result, cracks, particularly surface cracks, are regarded as the most harmful of all flaws, and practically all specifications restrict the admission of any crack observable by conventional methods of analysis. Cracks can reveal themselves in a variety of forms and locations. Factors that contribute to crack formation include the following:

i. Temperature gradients that result in thermal stresses in the weld zone as a result of the weld bead's solidification and contraction relative to the surrounding structure.

ii. Differences in the weld zone's composition.

iii. Grains' borders become fragile.

iv. Lack of contraction of the welded metal during cooling.

Figure 2.6 below shows the example of cracks that usually happen in weldment.

Figure 2.6: Welding crack (https://allgas.us/, 2019)

Select base and filler materials with care to avoid cracks. Additionally, it may be quite advantageous to store the filler material appropriately. Cracks created by spreading the bead too thinly can be rectified by applying sufficient filler and ensuring that the parts fit together properly. Apart from the base and filler materials, adjusting the travel speed and voltage settings frequently results in sufficient filler material to withstand internal pressures caused by metal shrinkage. Contaminants can also have an effect on the strength of the weld, therefore thoroughly clean the workpiece. In some instances, preheating may be required.

2) Spatter

Spatter is a term that refers to droplets of molten material that occur at or near the welding arc. It is frequently regarded as a nuisance and should be taken into account while developing an application. Spatter happens when the weld pool is disrupted to the point where molten metal spits or sprays out of the weld, as illustrated in figure 2.7. Spatter is a frequent occurrence during GMAW welding. The primary reason for this is that wire transmission into the weld causes a disruption in the molten weld pool. This is frequently

the result of an amperage-voltage mismatch. This occurs when the welding voltage is either too high or too low for the particular wire and gas combination. The arc is too cool in this scenario to keep the wire and pool molten, resulting in a stubbing action on the wire. This can occur when the current is either too high or too low. Additionally, as a result of the gas created, scattering may occur. While using CO_2 in GMAW increases arc energy and is extremely cost effective, but it results in increased weld spatter. Argon is commonly used to prevent CO_2 splatter.

Figure 2.7: Spatter (https://weldguru.com/, 2021)

There are some ways to reduce the spatter. Firstly, the arc voltage should be adjusted. If the voltage setting is not adjusted properly, it can result in a large number of spatters. Low voltage settings produce spatter because the wire is repeatedly shorted in the weld pool, resulting in small explosions at the wire tip. This is typical for short-arc MIG welding, but if the arc voltage is set properly, the expelled spatter will be extremely little and will not adhere to your workpiece or surrounding fixtures. On the other hand, due to the massive arc force, an excessive voltage might result in severe splatter. Another option is to eliminate the protrusion. The stick-out length, or the length of wire that extends beyond the contact tip that forms the weld, has an effect on the arc's amperage. If the stick-out is excessively long, it can reduce amperage, resulting in spatter escaping the weld due

to the weld not reaching deep enough. If it is too short, the amperage is increased, which results in material falling out of the weld owing to the arc's force.

Apart from that, welding equipment should be improved. Due to the high expense of spatter, certain modern welding power sources place a premium on spatter reduction. They also provide other benefits that enhance overall weld quality and readily justify the cost.

3) Porosity

Cavities or pores formed by trapped gases in molten metal during the solidification process are referred to as porosity. In other words, porosity can be thought of as a trapped gas bubble within the welded metal. Porosity can take on a variety of shapes and sizes, including dispersed pores, wormhole pores, surface-breaking pores, and crater pipes.

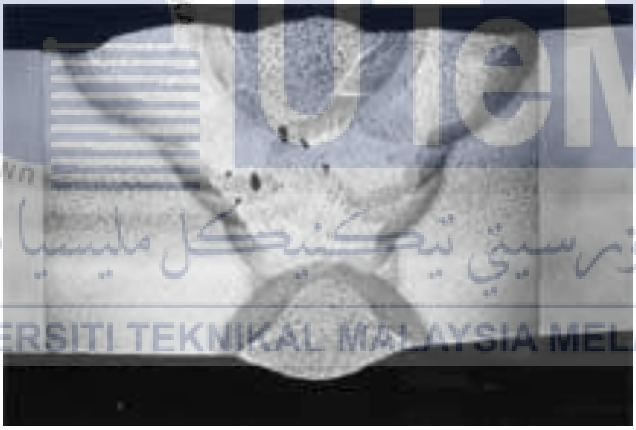

Figure 2.8: Uniformly distributed porosity (https://www.twi-global.com/)

The porosity is created when nitrogen, oxygen, and hydrogen are absorbed in the molten weld pool and subsequently released and trapped in the solidified weld metal. Inadequate gas shielding is the most common source of nitrogen and oxygen absorption in the weld pool. Distributed porosity may be created with as little as 1% air entrainment in the shielding gas, but more than 1.5% results in gross surface breaking pores. Apart from that, porosity is typically caused by gas line leaks, high gas flow rates, draughts, and an

excessive amount of weld pool turbulence. Hydrogen can be generated when moisture from wet electrodes, fluxes, or the workpiece surface condenses.

There are a few methods for overcoming it. To begin, pretreatment of material surfaces before to welding can be just as critical to creating a clean weld as welding itself. Without proper cleaning, the aftereffects of manufacturing might result in surface contamination and porosity. Next, take note on the flow of gas from the gas shield. The more powerful the gas flow, the more air is disrupted. This can result in impurities combining with the weld puddle, resulting in an impure weld. Although flow rates might vary, it is critical to choose the appropriate flow rate for each application. Last but not least, always do checking on the equipment. Hoses might leak and wire might become exposed or damaged over time. Before striking an arc, double-check all connections to ensure an exact flow from the gas shield. Check the weld gun tip for cleanliness; sometimes the tip becomes clogged, resulting in contaminants in the weld.

4) Incomplete fusion

Incomplete fusion occurs when there is insufficient fusion between the weld metal and the fusion faces or nearby weld beads, as seen in Figure 2.9. This absence of fusion can occur in any location inside the weld joint, but is most visible in fillet and groove welds. Incomplete fusion can occur as a result of the base material's or previously deposited weld metal's melting temperature not being increased sufficiently during the welding process. It is frequently encountered on one leg of a fillet weld and is produced by an insufficient welding angle, which results in an uneven distribution of heat between the two sides of the joint. Additionally, it could be caused by a failure to clean the surface of the base material with which the deposited weld metal must fuse.

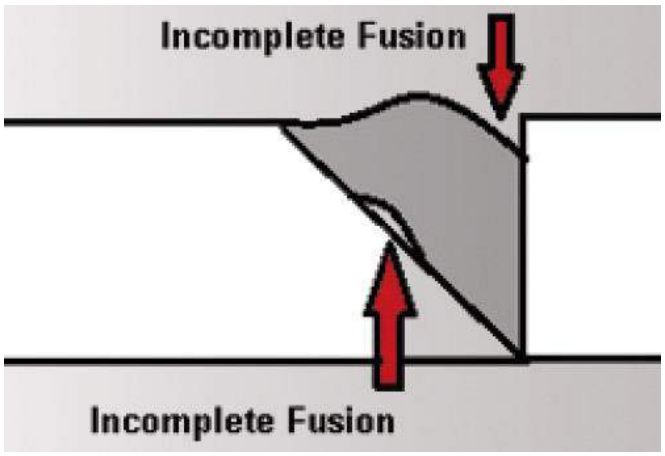

Figure 2.9: Diagram of incomplete fusion (https://weldingengineers.co.nz/)

Numerous precautions must be taken to ensure the full fusion of two or more pieces of metal. After completing a weld, always clear away any slag. Leaving slag in place can result in structural discontinuities, such as insufficient fusion. Incomplete fusion, like a large number of other welding problems, is typically the result of insufficient technique. Inadequate travel speed and welding angle will make thoroughly fusing separate pieces of metal problematic. Additionally, it is vital to select the appropriate welding procedure for the application. Attempting to fuse together thick metal pieces with GMAW welding is an example of selecting the inappropriate welding procedure. The strength of the MIG welding method is its ability to join a wide variety of thinner metals.

2.5 Carbon Steel as Base Material

Steel is an alloy metal that is generally made of iron and carbon, as well as trace metals. Due to its high tensile strength and low manufacturing cost, it is a preferred metal among manufacturers. However, steel comes in a variety of varieties, each with its unique set of properties. Carbon steel, for instance, is frequently preferred over other types of steel. Carbon steels are defined by the Alloy Steels Research Committee (ASRC) as "steels that include less than 0.5% manganese and 0.5% silicon, with all other steels classed as

alloy steels" (Metals. & International., 1997). The fundamental alloying elements used in steel are manganese, lead, nickel, chromium, molybdenum, vanadium, niobium, silicon, and cobalt (Metals. & International., 1997),(Frihat, 2015). Carbon steels are categorised into three groups based on their carbon content: low carbon steel, medium carbon steel, and high carbon steel. The carbon content, microstructure, and characteristics of these materials are compared in Table 2.2 below.

Table 2.2: The comparison of the carbon content, microstructure, and properties (https://matmatch.com/)

Type of Carbon	**Carbon Content (Wt.%)**	**Microstructure**	**Properties**	**Examples**
Low carbon steel	< 0.25	Ferrite, pearlite	• Low hardness and cost. • High ductility, toughness, machinability and weldability.	AISI 304, ASTM A815, AISI 316L
Medium carbon steel	0.25 – 0.60	Martensite	• Low hardenability, medium strength, ductility and toughness.	AISI 409, ASTM A29, SCM 435
High carbon steel	0.60 – 1.25	Pearlite	• High hardness, strength, low ductility.	AISI 440C, EN 10088-3

2.5.1 Low Carbon Steel

Low-carbon steel is the most often used kind of carbon steel. Typically, these steels have a carbon content of less than 0.25 percent. Due of these materials' inability to be hardened through heat treatment (to form martensite), they are frequently hardened using cold work. Frequently, carbon steels are delicate and brittle. They do, however, possess a high degree of ductility, which makes them ideal for machining and welding, as well as being reasonably priced. While high-strength, low-alloy steels (HSLA) are occasionally referred to as low-carbon steels, they also include other elements such as copper, nickel, vanadium, and molybdenum. These can make up up to 10% of the steel's composition. As the name implies, high-strength, low-alloy steels have been heat treated to improve their strength. Additionally, they retain their ductility, allowing them to be moulded and machined easily. Corrosion resistance is increased in HSLA steels over ordinary low-carbon steels.

It is primarily composed of ferrite, a solid solution phase of carbon dissolved in alpha-iron that crystallises as a body-centered cubic (BCC) crystal (Evans, 2012). Ferrite is steel's softest phase, and it substantially contributes to low carbon steel's superior machinability as compared to other carbon and alloyed steels. As the carbon content of steel increases, the amount of pearlite produced in the microstructure of the metal increases proportionally. The microstructure of pearlite is made of alternating layers of ferrite and iron carbide (cementite). Low carbon steels are frequently employed in the fabrication of pipes, structural forms (I-beams, channel, and angle iron), building and bridge components, food cans, and vehicle body components.

2.5.2 Medium Carbon Steel

Carbon concentrations vary between 0.25 and 0.60 percent, whereas manganese concentrations range between 0.60 and 1.65 percent. The autenitising, quenching, and tempering processes improve the mechanical characteristics of this steel, resulting in a martensitic microstructure. Although heat treatment is only possible on extremely thin sections, extra alloying elements such as chromium, molybdenum, and nickel can be added to improve the steel's heat treatment capacity and therefore hardening capability. While hardened medium-carbon steels provide more strength than low-carbon steels, they sacrifice ductility and toughness in the process. These steels are mostly used to produce shafts, axles, gears, crankshafts, couplings, and forgings. Rails, railway wheels, and rail axles are composed of steels containing between 0.40 and 0.60 percent carbon (Singh, 2020).

2.5.3 High Carbon Steel

The carbon level is between 0.60 and 1.25 percent by weight, whereas the manganese concentration is between 0.30 and 0.90 percent by weight. It is the strongest and most durable carbon steel available, but it is also the least ductile. High-carbon steels are extremely resistant to wear due to their virtually universal hardening and tempering. Tool and die steels are chromium-vanadium-molybdenum-tungsten-alloyed high-carbon steels. Combining these metals results in a highly hard, wear-resistant steel due to the creation of carbide compounds such as tungsten carbide (WC) (Qiao et al., 2021). High-carbon steels are applied in cutting tools, springs, great-strength wire, and dies due to their high wear resistance and toughness.

2.5.4 Application of Carbon Steel in Oil and Gas Industry

Carbon steel, as we all know, is a strong metal with a great resistance to wear. It is the most often used steel type in the oil and gas industries. It is used to construct pipelines, structural components, platforms, and other objects. Carbon steel is critical in the oil and gas sectors because it is an iron alloy that contains up to 2% carbon, which enhances the material's strength and offers corrosion resistance (Wahab, 2014). Furthermore, the steel contains trace quantities of other metals such as nickel and chromium. Additionally, carbon steel has enough structural and thermal strength, is economical, and its surfaces may be protected against corrosion using well-known corrosion inhibitors. The figure 2.10 below illustrates a typical oil and gas pipeline structure.

Figure 2.10: The example of pipeline structures in oil and gas

(https://www.codesteel.com/2017)

2.6 Heat Treatment Process

Heat treatment is widely utilised in the steelmaking and welding and joining sectors today, with post-weld heat treatment focusing on the weld bead and joining metal. Heat treatment is a procedure that includes controlling the rate of heating and cooling and involves the application of a range of steel treatments for a variety of metalworking purposes (Rahman et al., 2016). The physical and mechanical characteristics of the metal

will change during annealing, tempering, annealing, and quenching, and other variables will also impact the heat-treated metal. The hardness, toughness, and strength of the metal, as well as its brittleness, may be increased by heat treatment, resulting in more dependable and superior characteristics (Chandra Kandpal et al., 2020). Apart from that, it is a method of enhancing the shapeability, machining, and manufacturability of the metal (Hnizdil & Chabicovsky, 2018). Heat treatment is employed in this study to determine the efficacy of changes made to the characteristics of low carbon steel in order to make it more stable and steady.

Table 2.3: The comparison result of heat treatment on welded joint of previous study

Author	Title	Material	Process	Finding
Kučerová et al., (2019)	Microstructure analysis and mechanical properties of low alloyed steel with retained austenite obtained by heat treatment	Low carbon low alloyed steel.	Annealing	With decreasing retained austenite volume fraction, the retained austenite carbon content dropped. For all treatments, the volume fraction of retained austenite ranged between 11% and 18%. Slower cooling produced coarser microstructures, longer retained austenite laths, lower retained austenite carbon concentrations, and more prominent retained austenite lath bainite morphology.
Reyes et al., (2017)	Effect of heat treatment on the mechanical and microstructural properties of a low carbon steel	Low carbon steel	Annealing Tempering Hardening Normalizing	The investigation of the effect of heat treatment on the steel sample reveals that there is always a trade-off between two properties. Tempering reduces the steel's toughness and tensile strength while increasing its hardness slightly. The microstructure of the untreated control phases exposes ferrite and pearlite, while the hardened

				micrograph displays mainly coarse martensite. The microstructure of the tempered sample indicates a martensite phase with recrystallization of ferrite.
Chandra Kandpal et al., (2020)	Effect of heat treatment on properties and microstructure of steels	Alloy steel (EN 31, EN 24 and EN 8)	Annealing Normalizing Hardening	From the data obtained, it can be claimed that mechanical qualities depend greatly on the different heat treatment processes and cooling rate. It will deliver satisfactory results for high ductility and minimum toughness. This treatment is indicated as final following manufacture. Hardened sample showed the maximum tensile strength and hardness compared to other heat-treated samples, with the lowest ductility and impact strength.
Prabakaran & Kannan, (2021)	Effects of post-weld heat treatment on dissimilar laser welded joints of austenitic stainless steel to low carbon steel	Austenitic stainless steel (AISI316) and low carbon steel (AISI1018)	Annealing	The effects of PWHT on a variety of metal complexes were thoroughly investigated. Tensile strength and elongation of the joint were significantly increased with PWHT at 960°C. Following PWHT at 960°C, the chromium carbide was successfully dissolved and did not precipitate again in the weld zone's grain and grain boundaries.
Valdes-Tabernero et al., (2020)	The sensitivity of the microstructure and properties to the peak temperature in an ultrafast heat treated low carbon-steel	Hot-rolled 6 mm thick low carbon steel sheets	Annealing	The rise in peak temperature favours the production of austenite. These activities result in a decrease in the volume fraction of ferrite as the volume fraction of inter-critical austenite increases. Due to the increased dislocation density of non-recrystallized ferrite, it is tougher than recrystallized ferrite.

2.6.1 Stages of Heat Treatment

To achieve the desired outcome, the metal or alloy is heated to a specific temperature, sometimes as high as 1300°C, held there for a specified amount of time, and then cooled. When a metal is heated, its physical structure, sometimes referred to as microstructure, changes, resulting in changes in the metal's physical properties. The period of time required to heat the metal is referred to as the'soak time.' The duration of the soak time has an influence on the properties of a metal, as metal that has been soaked for an extended period of time will exhibit distinct microstructure changes in comparison to metal that has been soaked for a brief period of time (Mesquita et al., 2017). After the soak time, the cooling procedure has an influence on the metal's outcome. Metals can be swiftly cooled, a process known as quenching, or gradually cooled in the furnace to ensure the correct end is obtained. The soak temperature, soak time, cooling temperature, and cooling duration all contribute to the desirable characteristics of a metal or alloy. When a metal is heat treated numerous times throughout the production process, the characteristics of the metal are altered, and some metals may be treated several times.

Based on figure 2.11, heat treatment is comprised of three steps: progressively heating the metal to provide uniform temperature distribution, soaking the metal at a certain temperature for a specified period of time, and cooling the metal to room temperature to achieve the desired characteristics. The heating stage, the soaking stage, and the cooling stage are the three steps of heat treatment.

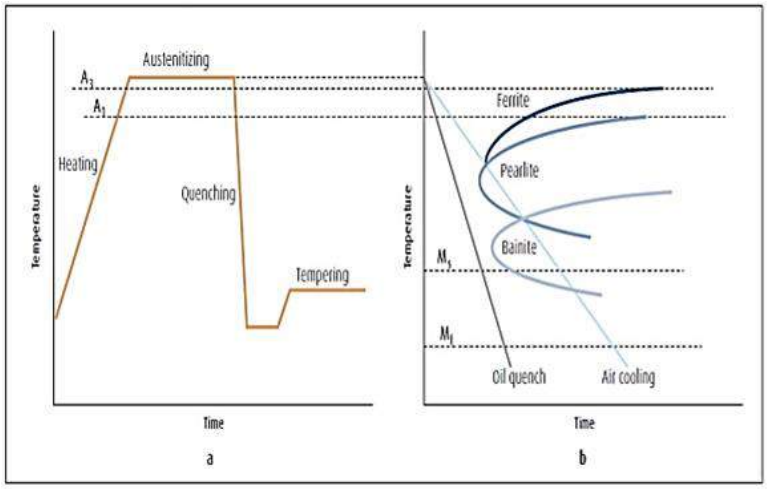

Figure 2.11: a) Temperature b) Its relation to the TTT diagram

(https://www.slideshare.net/,2015)

1) The heating stage

The first step in a heat-treating procedure is heating. When alloys are heated to a given temperature, it is done to change their structure. At room temperature, the alloy is said to be either a solid solution, a mechanical mixture, or a combination of both. In a solid solution, two or more metals are bonded together to generate a solution which does not show the elements when observed under the microscope. The elements and compounds are easily noticeable and compressed by a base metal matrix in a mechanical mixture.

2) The soaking stage

Soaking is the stage when the entire structure of the heated metal undergoes a thorough transformation. The objective of the soaking stage is to maintain a constant temperature for the metal until the necessary internal structure develops. The time required to soak the metal is dependent by its mass. In other terms, soaking happens when a section of a metal becomes evenly red as a result of prolonged exposure to heat.

3) The cooling stage

The third and last stage of the heat treatment procedure is cooling. Additionally, depending on the cooling method used, it alters the chemical properties of the soaked metal. The metal can be directly contacted with a cooling medium, which can be a gas, a liquid, or a solid, or a mixture of these. The speed at which the metal cools is determined by the metal itself and the desired end result.

There is no way to bypass any of the three phases of heat treatment. The heating stage assists in the change of the metal's structure from room temperature to the soaking stage, which occurs when the metal develops a consistent red colour. Cooling is the stage at which the metal completely transforms into its new characteristics as a result of the cooling process.

2.6.2 Types of Heat Treatment

Heat treatment is important for achieving the optimal characteristics of a metal and can be used to soften or condition it, as in normalising and annealing, or to harden it, as in hardening, quenching, and tempering. These treatments result in the formation of three distinct microstructures: pearlite, bainite, and martensite. There are four primary types of heat treatment processes that are often employed in the steelmaking industry: annealing, tempering, hardening, and normalizing. The exact heat treatment required in manufacturing will be determined by the metal chemistry, the part's size, and the desired characteristics. Heat treatment is frequently used in forging and post weld heat treatment, or preheat (Singh, 2020). The iron-carbon phase diagram (figure 2.12) is often used to understand the various phases of steel and cast iron. As we know, steel and cast iron are both made of iron and carbon. In table 2.3, there are table comparison of each of the heat treatment process.

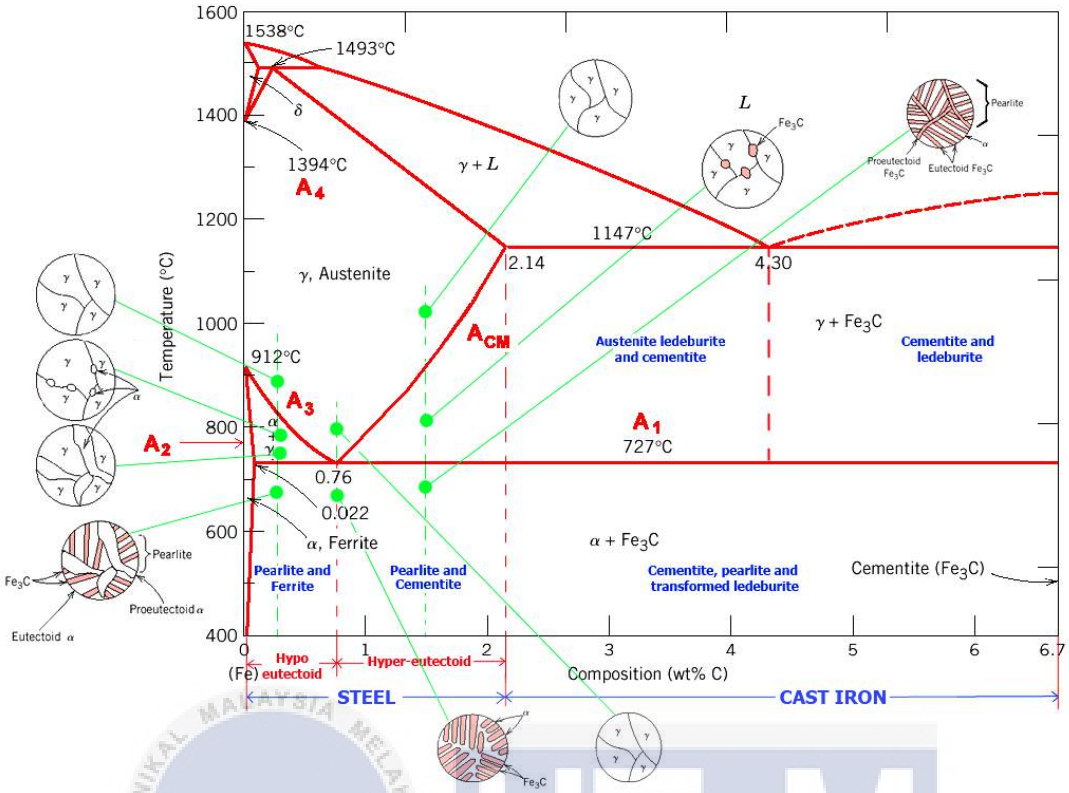

Figure 2.12: Iron-carbon Phase Diagram (https://www.tf.uni-kiel.de/en, 2021)

Table 2.4: Table comparison of heat treatment process

Type of Heat Treatment	Definition	Process	Temperature	Purpose	Application
Annealing	Is a process to soften metal in order to get desired chemical and physical properties.	Involves heating a metal to or near critical temperature and then slowly cooling it to room temperature.	260˚C- 950˚C	To soften the materials.	Used for metals and metal alloys.
Hardening	Is a process used to increase the hardness of a metal.	The metal is heated until it reaches the austenitic crystal phase, then rapidly cooled.	Between 800˚C- 900˚C	To increase the hardness of a metal.	Used for metal alloys with a high carbon and alloy content.
Tempering	Is the process of removing excess hardness,	By heating it to produce austenite and then quenching it to produce	As high as 950 °C for up to 20 hours	To make metals less brittle.	Used mainly for steel.

	and thus brittleness, caused by hardening.	martensite.			
Normalizing	Is a process used to relieve internal tensions produced by processes such as welding, casting, or quenching.	Involves heating the steel to about 40˚Celsius beyond its upper critical temperature limit, holding it at this temperature for a period of time, and then cooling it in air.	Between 750°C-980°C	To improves toughness, ductility while still maintaining high strength level.	Used mainly for material that require impact strength or have to withstand huge external stresses.

The following subject will go into full detail about the types of heat treatment that are usually advantageous in welding.

i. Annealing

Annealing is a chemical and physical process that softens metals to get the desired chemical and physical properties. During annealing, the metal is heated to its upper critical temperature and then slowly cooled to room temperature. It improves the ability of the metal to be cold worked and formed. Additionally, it improves the machinability, ductility, and toughness of the metal. Annealing is a process that is commonly used in ferrous alloys. It involves heating the metal over the upper critical temperature and then cooling slowly to create pearlite or ferrite. Annealing is used to soften pure metals and a range of alloys that cannot be heat treated (Reyes et al., 2017). The metal is sufficiently heated to produce recrystallization, which corrects defects caused by plastic deformation. (Phoumiphon et al., 2016). In general, the pace at which these metals cool has little influence on them. The bulk of heat treatable nonferrous alloys are also

annealed to reduce the hardness of cold working. These can be gradually chilled to cause full crystallisation and the formation of a fine microstructure.

Ferrous alloys are frequently referred to be 'completely annealed' or 'process annealed'. Full annealing requires extremely slow cooling rates to create coarse pearlite. In process annealing, the cooling rate may be increased up to and including normalizing. The fundamental objective of process annealing is to produce a microstructure that is consistent. Nonferrous alloys are often annealed in a number of ways, including 'recrystallization annealing,' 'partial annealing,' 'complete annealing,' and 'final annealing'. The figure 2.13 below shows the grain of metals in annealing stages. In figure 2.13, a small increase in the annealing temperature initiates the second step, which entails dislocation rearrangement and elimination. At rearrangement temperature, opposing dislocations caused by diffusion are reduced, resulting in a reduction in the material's total internal stresses. Following the annihilation of opposite sign dislocations, the remaining dislocations begin to expand in order to mitigate the effects of internal stresses. This process of rearranging remaining dislocations is referred to as polygonization, in which edge dislocations unite to form tilt boundaries and screw dislocations combine to form twist boundaries. As the steel annealing temperature is increased higher, the activation energy increases and the high-angle grain boundary begins to migrate. Only dislocations and point defects are moving entities that reduce internal stresses in the material below the recrystallization temperature. Following the recrystallization process, freshly created grains begin to expand. The growth of large grains occurs at the expense of crystallised fine grains. The greater the steel annealing temperature, the more aggressive the growing process will be. This force is linked to grain boundaries. Higher grain border area in conjunction with increased grain size results in a decrease in total energy per unit area.

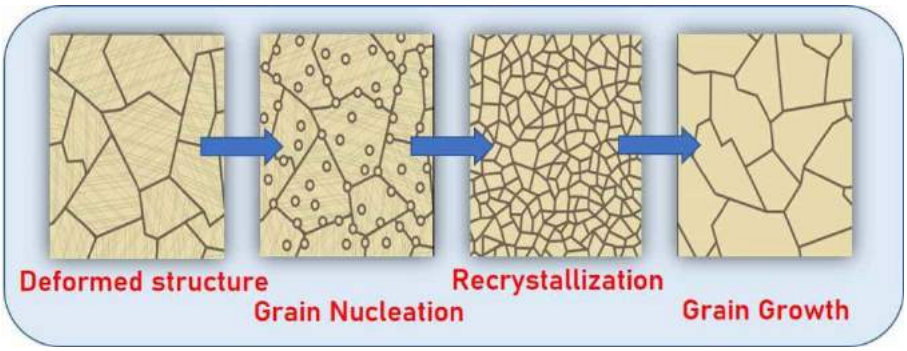

Figure 2.13: Grain of metals in annealing stages (https://materials-today.com/, 2020)

ii. Hardening

The most often used heat treatment procedure is hardening, which is used to improve a metal's hardness. To harden a metal (usually steel or cast iron) by quenching, it must be heated above its upper critical temperature and then rapidly cooled. Cooling can be accomplished using forced air or other gases, depending on the alloy and other factors (such as the exchange between maximum hardness and fracture and distortion) (such as nitrogen). Liquids such as oil, water, a polymer diluted in water, or brine may be used because of their increased heat resistance (Rahman et al., 2016). When austenite is rapidly cooled (depending on the alloy composition), a part of it changes into martensite, a hard, brittle crystalline structure. The chemical composition and quenching process of a metal determine its quenched hardness. The figure 2.14, it shows the steel rapidly cooled by using water after heated.

Figure 2.14: Hardening process (https://www.wasatchsteel.com/, 2018)

iii. Tempering

Tempering is a process that improves the toughness of hardened steel by heating it to produce austenite and then quenching it to produce martensite. Untempered martensite is a strong, tough, brittle material. The more brittle it is, the stronger and tougher it is. The strength and hardness of martensite are due to elastic strain within the martensite, which is caused by an excess of carbon atoms in the gaps between the iron atoms in the martensite. The martensite strength and hardness increase as the quantity of carbon in a steel increases (up to roughly 0.8w% carbon).

During the tempering process, the carbon atoms in martensite migrate out of the spaces between the iron atoms, forming iron carbide particles (Singh, 2020). The strain is released as the carbon atoms separate from the iron atoms in martensite. As a result, steel toughness is improved at the price of strength. The amount of tempering required is dependent on the steel's intended usage. Because toughness is not always needed, tempering at a low temperature for a brief period of time is sometimes suitable. When extremely strong and tough steel is required, a high carbon steel tempered at a high

temperature may be used. Figure 2.15 below shows the tempering steel colour chart that used in heat treatment process.

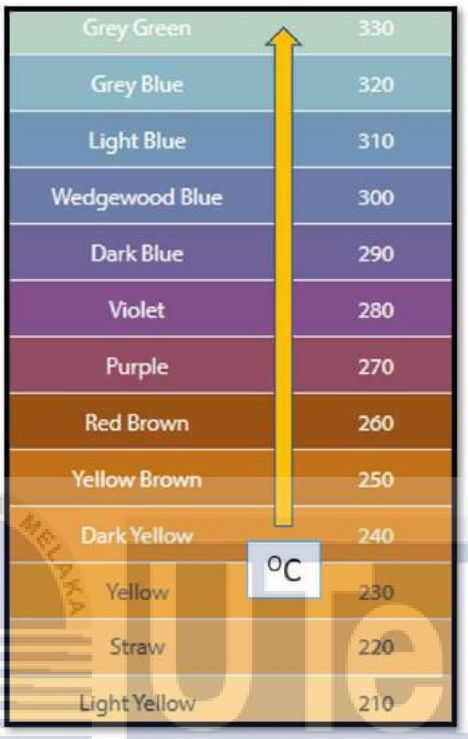

Figure 2.15: Tempering steel colour chart used (https://materials-today.com/, 2020)

iv. Normalizing

Normalizing is a type of heat treatment that is used to relieve internal stresses caused by welding, casting, or quenching. Normalizing produces not just pearlite but also martensite and, in certain circumstances, bainite, resulting in a harder, stronger steel with less ductility than complete annealing of the same composition. The normalization process involves heating the steel to about 40˚Celsius over its upper critical temperature limit, keeping it there for an extended length of time, and then cooling it in air. Normalized steels are more difficult to work with and stronger than annealed steel (Rahman et al., 2016). Indeed, steel is stronger than any other material in

its normalized state. This is why parts requiring impact resistance or the ability to tolerate extremely high external pressures are often normalized. The figure 2.16 below illustrates the variation in the spacing of the cementite plates in pearlite between annealing and normalising. Ferrite is a very soft structure, whereas cementite is extremely hard. By bringing the cementite plates closer together in normalised medium pearlite, they tend to stiffen the ferrite, preventing it from yielding as easily, hence enhancing hardness.

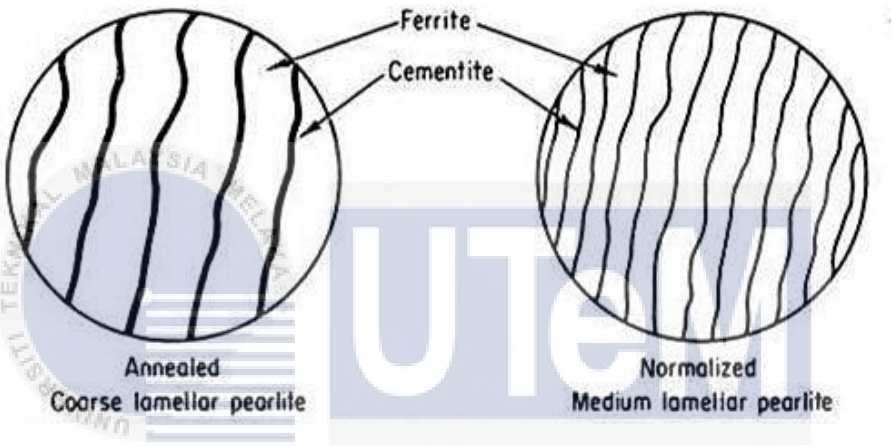

Figure 2.16: Difference on pearlitic structure due to annealing and normalizing (https://www.ques10.com/, 2018)

2.6.3 Heat Treatment on Welded Joint

Welding is a critical component in operating and maintaining assets in the oil and gas (upstream, midstream, and downstream) industries, as well as the chemical processing industries. While welding has a wide range of applications, it can unintentionally damage equipment by transferring residual stresses into the material, resulting in decreased material properties. Post Weld Heat Treatment (PWHT) is a process that is routinely used to guarantee that the material strength of a component is maintained following welding. PWHT can be used to reduce residual stresses, control hardness, and assist in material

strength enhancement (Moore & Booth, 2015). Heat treatment may be conducted following welding for one or more of the following reasons:

i. To achieve dimensional stability in order to preserve tolerances during machining operations or during service shake-down.

ii. To design and fabricate novel metallurgical structures in order to achieve the necessary mechanical properties.

iii. To reduce the possibility of in-service problems such as stress corrosion or brittle fracture by reducing the residual stress in the welded component.

If PWHT is conducted incorrectly or not at all, residual stresses can combine with load stresses to exceed the design limitations of a material. This can result in weld failures, enhanced cracking potential, and increased sensitivity to brittle fracture. In general, the higher the carbon content of a material, the more probable it will require PWHT following welding procedures. Similarly, the higher the alloy content and the greater the cross-sectional thickness of the material, the more likely it will require PWHT.

2.7 Summary of Literature Review

Gas Metal Arc Welding (GMAW), sometimes referred to as metal inert gas (MIG) welding, is a type of welding in which an electric arc is formed between a wire electrode and the workpiece metal. GMAW produces welds that are more attractive and of higher quality than those produced by shielded metal arc welding (SMAW). In the arc welding process, the welding current is the most important variable. Carbon steels are defined by the Alloy Steels Research Committee (ASRC) as "steels containing less than 0.5 percent manganese and 0.5 percent silicon, with all other steels classed as alloy steels." Carbon steel is classified into three types based on its carbon content which is low carbon, medium carbon, and high carbon steel. Carbon steel is critical in the oil and gas industries because

it is an iron alloy that contains up to 2% carbon, which indirectly enhances the material's strength. Heat treatment is frequently employed in steel manufacturing, as well as welding and joining, with post-weld heat treatment concentrating on the weld bead and joining metal. The duration of the soak time has an effect on the characteristics of a metal, since metal that has been soaked for a long period of time will exhibit differential microstructure changes compared to metal that has been soaked for a short amount of time. Heat treatment is essential for attaining the best characteristics and may be used to soften or condition a metal, as with normalizing and annealing, or to harden a metal, as with hardening, quenching, and tempering.

CHAPTER 3

METHODOLOGY

3.1 Introduction

This chapter were described in details the process of finding the effects of heat treatment on mechanical properties and microstructure of low carbon steel joint with 70s filler metal. Based on previous study, the students or professors had also researched, tested and performed the effect of heat treatment on low carbon steel. This information were provided more perspectives into how this work is to be carried out and the studies and processes for potential use of particular fields and areas that are included in this subject.

The flowchart of overall process in this study were depicted in Figure 3.1. This study began by initiating specimen preparation and were proceed with the welding process which were GMAW with butt joint design. And then, were followed by carried out non-destructive test to check any flaws of the specimen. After that, the sample were cut into small pieces with the dimensions of 55mm x 10mm x 12mm. These samples were carried out in two heat treatment process which are annealing and tempering. When the samples are done with heat treatment process, the samples were tested to observe the mechanical by hardness test and impact test. To identified the material characterization, analytical scanning such as optical microscope, Energy Dispersive X-Ray Spectroscopy (EDX) and Electron Backscatter Diffraction (EBSD) were used to study the microstructure element of the welded low carbon steel. Lastly, all the data were analyzed to conclude the study.

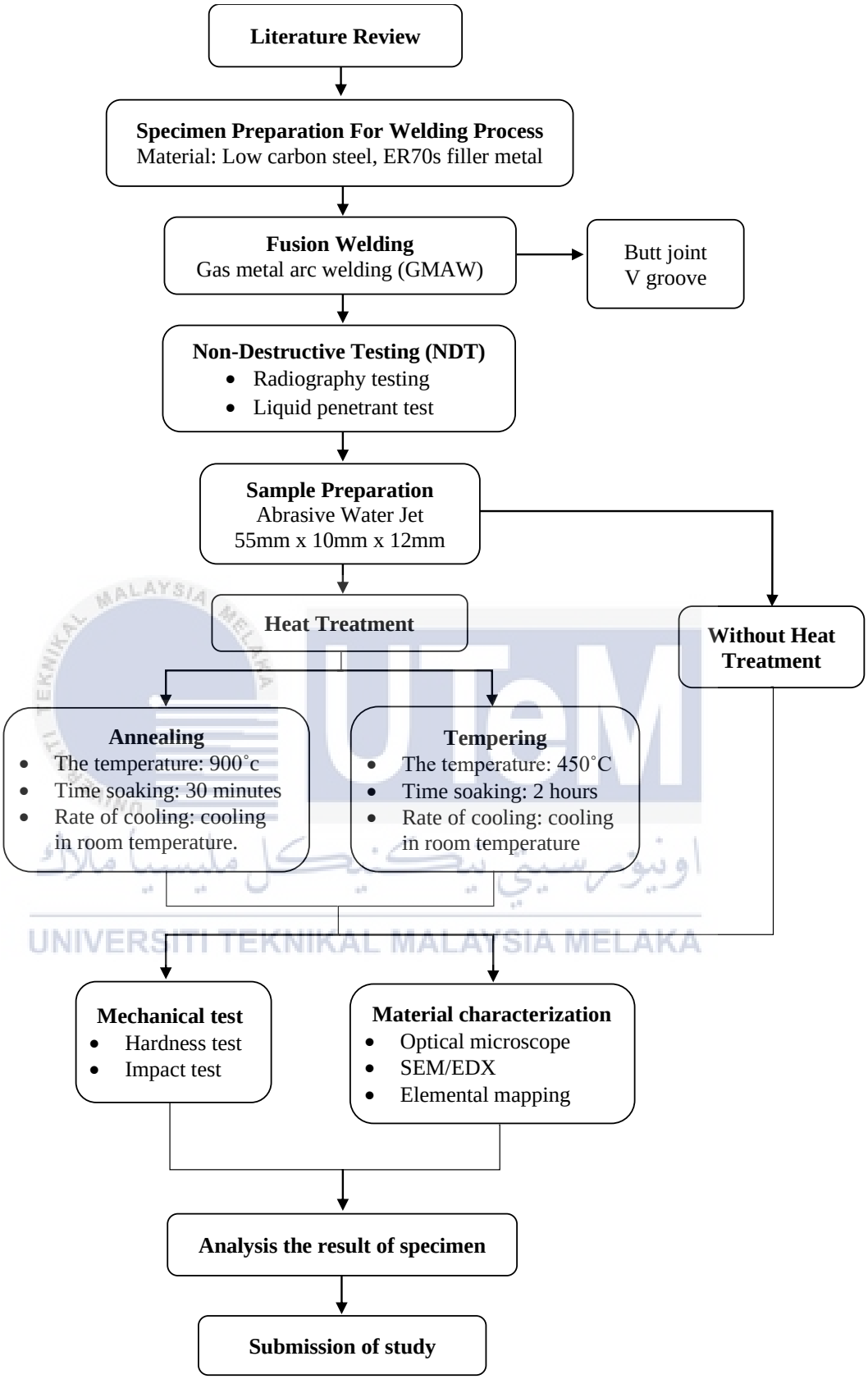

Figure 3.1: Process flow chart of study

3.2 Preparation of Sample

Prior to cut the sample to the desired size, the metal was inspected for flaws and defects and then were cleansed to remove foreign objects such as small holes or indentation that could result in the development of pitting corrosion and to ensured that the raw materials are free of microstructure changes.

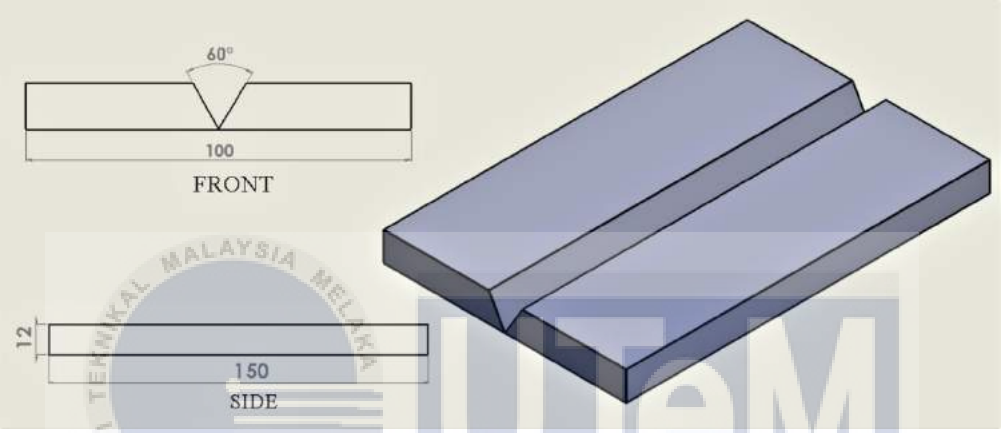

Figure 3.2: Dimension of sample preparation

The dimensions of the samples were cut to a smaller length and width by using an appropriate cutting tool for the desired dimension. The type of joint used in this study is the butt joint, which were the most commonly used and widely recognized as the simplest design welding to manufacture weldment.

3.2.1 Welding Procedures

The joint type that were used in this study is a butt joint, which were a well-known form of joint that was applied in accordance with the American Welding Society (AWS) standard. The idea of the butt joint is similar to that seen in the welding industry. The welding technique that must be applied in order to maintain the quality of welding activity were shielded metal arc welding, and the welding type used in this study were shielded

metal arc welding (GMAW). GMAW was chosen because of its support of a wide variety of industries and its simplicity of use, needing no additional safeguards. Precautions must be taken, however, to guarantee safety and good welding. The process for performing GMAW welding were as follows:

i. The butt joint design can take on a variety of forms however, the V groove was chosen for this study.
ii. The electrode used in the welding butt joint were ER70s filler metal.
iii. Current setup and amp were set as appropriated.
iv. The travel speed of the welding to ensure the good penetration on the welded joint.

This parameter must be monitored closely in ordered to avoid and eliminate internal flaws and cracks produced by inadequate welding techniques. When the current were abnormally weak, the suitable speed should also be reduced. The groove must be entirely filled to eliminated corrosion risk and ensured the welded joint's integrity.

3.3 Non-Destructive Test (NDT)

Non-destructive testing (NDT) were a method of analyzing the properties of a material, component, structure, or system for unique variations or welding defects and discontinuities without causing damage to the original part. This type of inspection were performed to check the sample's quality prior to the sample set's heat treatment test. To ensure the quality of the sample, the welded joint, and the continuity of the sample used in this study, liquid penetrant tests and radiography were used.

3.3.1 Liquid Penetrant Inspection

The sample were inspected using liquid penetrant testing, which would look for undetected defects on the weld sample. Firstly, the sample were first be cleaned using a cleaner to eliminate any foreign substance from its surface. Following that, the liquid penetrant were softly sprayed onto the clean surface of the test plate. The sample were allowed to dry for around 7-10 minutes, depending on the base metal's temperature. Then, the surface were wiped cleanly using the cleanser to eliminate any remaining penetrant. Then, wait another 2-5 minutes till it dried completely. The developer were applied by spraying a little layer on the surface and wait approximately 10 minutes for the indication to appear as shown the process in figure 3.3. The figure 3.4 showed the applicant used in liquid penentrant testing meanwhile figure 3.5 showed the indication using liquid penetrant inspection.

1. 	2. 
First of all, brush the surface of the plate using a wire brush to remove any rust.	Then, spray the cleaner on the lint-free cloth and rubbed it on top of the surface plate to remove any foreign substance. Allow for a while for it to evaporate.

3. 	4. 
Next, spray the liquid penetrant on top of the surface and allow to dry for around 7-10 minutes.	And then, wipe the surface off to remove all the penetrant. Allow it dry around 2-5 minutes.
5. 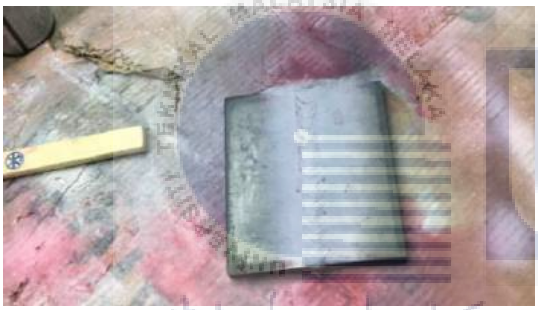	6. 
Lastly, spray light coating of the developer on the surface. Wait around 4-6 minutes for the indication to appear.	After done evaluating the weld, clean the surface by using a cleaner.

Figure 3.3: The procedure of liquid penetrant inspection

Figure 3.4: The applicant used in liquid penentrant testing; (a) Fluxo S190 Solvent Remover, (b) Fluxo P125 Red Dye Penetrant, (c) Fluxo R175 Developer

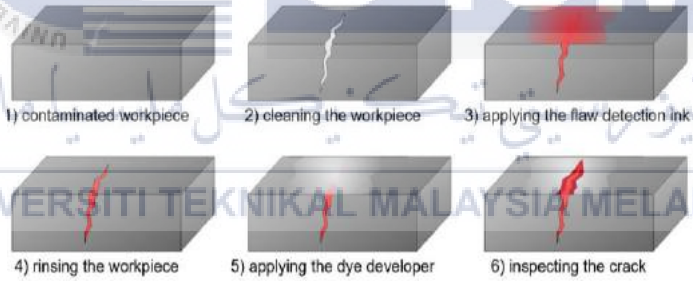

Figure 3.5:Indication using liquid penetrant inspection (https://www.tec-science.com/)

3.3.2 Radiographic Testing

Radiographic Testing (RT), as seen in Figure 3.6, is a non-destructive testing (NDT) technique that used x-rays or gamma rays to analyzed the internal structure of produced components in order to discover defects or flaws. The sample were sandwiched between the radiation source and a piece of sensitive film or detector during radiography testing. Once the x-ray or gamma-ray radiation were initiated, the test part's material density and

thickness would absorbed some of the radiation. A thicker, denser specimen were enabled less radiation to flow through it. The film (or electronic device) captured the quantity of radiation (referred to as radiograph) that passed through the test specimen and reached the film. Defects can simply be identified by examining the radiograph data. If the material were sound and free of defects, whole rays were flowed through it equally. However, for materials with imperfections, rays traveling through the faults were absorbed to a minor level due to the density changed. Due to the fact that defects in the parent metal diminished its density, they transmitted radiation far more efficiently than the sound metal. As a result, the radiograph film were looked darker in the defect-exposes area.

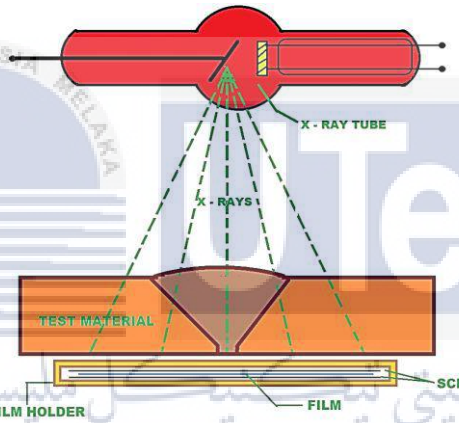

Figure 3.6: Radiography using x-ray (https://www.weldingandndt.com/, 2017)

3.4 Sample Preparation for Testing

To enhance the data collection, the sample were cut to the measurements required for sample analysis and experimentation. Before started the weld, the raw material were selected and were processed to remove any impurities. After butted the plates together, the welded plate were cut to the correct length and width using an watejet machine as shown in figure 3.7 below. Before undergone waterjet process, the drawing of the sample were done using Solidworks and the sample size is 55mm x 10mm x 12mm.

Figure 3.7: Flow Mach 2 1313B Abrasive Water Jet Machine

3.4.1 Procedures of waterjet cutting

The waterjet machine was used to cut into small samples by cutting a tiny line into a piece of material using a high-pressure spray of water as shown in figure 3.8. A granular abrasive is added to the waterjet to enhance the cutting power required to cut to the specified dimension. Figure 3.9 is the finished workpiece after were cut by using abrasive water jet.

The workpiece were placed on the slats and were clamped on the worktable by using speader.

The water nozzle were cut right to the place that want to be cut.

Figure 3.8: The procedures of waterjet cutting

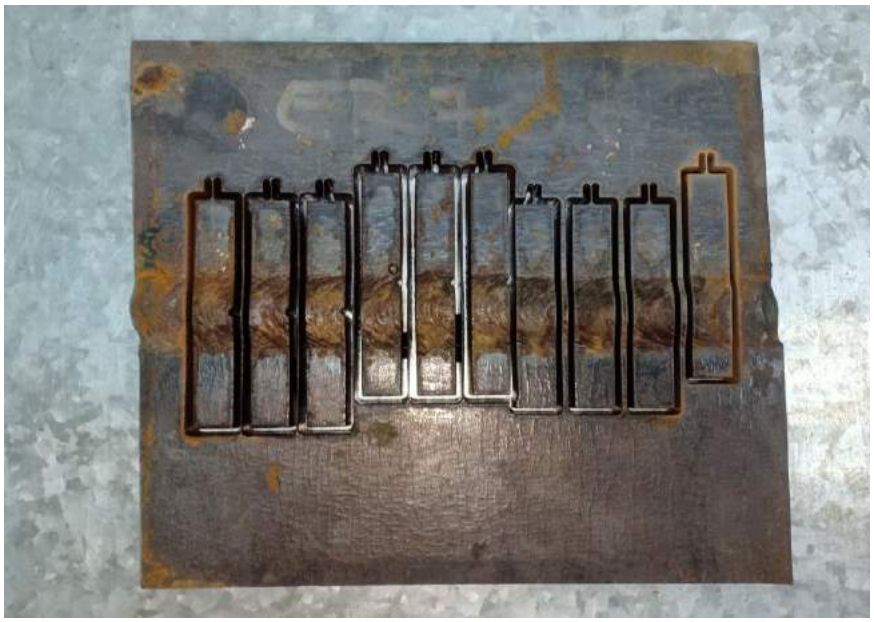

Figure 3.9: Workpiece that were cut by waterjet machine

3.5 Heat Treatment Process

Among the other tests, heat treatment were the most important for this research. This due to the fact that whether or not heat treatment affected the performance of the sample had a significant impact on the overall research. In this project, two types of heat treatment process which was tempering and annealing were used as parameter. The figure 3.10 below showed the procedure of the sample for tempering process meanwhile figure 3.11 shown the procedure of the sample for annealing process.

The samples were put in the furnace with the temperature 450˚C	The samples were soak for about 2 hours.	Lastly, the samples were cooled to the room temperature

Figure 3.10: The procedure of the sample for tempering process

The samples were put in the furnace with the temperature 900˚C	The samples were soak for about 30 minutes.	Lastly, the samples were cooled to the room temperature.

Figure 3.11: The procedure of the sample for annealing process

To sum up, three temperature were used during the testing process which are 900°C for annealing, 450°C for tempering, and 30°C for the untreated sample and lastly were cooled in room temperature.

3.6 Mechanical Test

Mechanical properties are those of materials that need a response to an applied load. The mechanical characteristics of metals influenced the material's range of utility and, consequently, the expected service life. The most often examined characteristics are strength, ductility, hardness, impact resistance, and fracture strength. Mechanical

characteristics of the material are not constant and regularly fluctuated in response to temperature, loading rate, and other variables. Macro hardness test and impact resistance of materials were evaluated using Rockwell hardness and their behaviour at high deformation rates were investigated using Charpy testing.

3.6.1 Macro Hardness Test (Rockwell Hardness)

A macro hardness tester as depicted in figure 3.12 were the most often used technique to evaluated the macrohardness behaviour of treated and untreated materials. The samples were indented with a ball indenter. The indentation were produced on the surface of three primary regions: base metal, weld material, and heat-affected zone (HAZ). Additionally, numerous layers of indentation testing were done to verified and confirmed the sample data.

Figure 3.12: Mitutoyo HR-400 Rockwell Hardness Tester

Figure 3.13: The sample were put to get the value of hardness of each layers

3.6.2 Impact Test

Impact testing were used to evaluate the relative toughness or impact toughness of materials. Impact tests are beneficial because they can determined the amount of energy absorbed by a material during fracture. This absorbed energy is an indicator for a material's toughness and would used to investigate the temperature-dependent brittle-ductile transition. The purpose were to determined if a material is brittle or ductile. For this experiment, the impact test were conducted using the Charpy technique and ASTM E23 standards. The aim is to analyze whether the materials are brittle or ductile. Also, the Charpy test and ASTM E23 standards were used as when do impact test.

3.6.2.1 The Charpy Test

The Charpy impact tester as shown in figure 3.15 also known as the Charpy V-notch test, is a strain rate test that included impacting a standard notched sample with a controlled weight pendulum swinging from a predetermined height. The specimens shown in figure 3.14 were those most widely used and most generally satisfactory. For this study, a specimen of type A as in figure 3.16 which are the typical Charpy V-notch specimen with dimension 55mm long, 10mm square, and has a 2mm deep notch machines on one

face with a tip radius of 0.25mm were used. The sample were supported at both ends by an anvil and struck by the pendulum on the opposite face to the notch. The amount of energy absorbed in breaking the sample were measured, and this would give an approximation of the test material's notch toughness. During the test, the pendulum swings over, with the height of the swing represented the amount of energy absorbed in breaking the sample.

Figure 3.14: Instron CEAST 9050 Pendulum Impact Tester

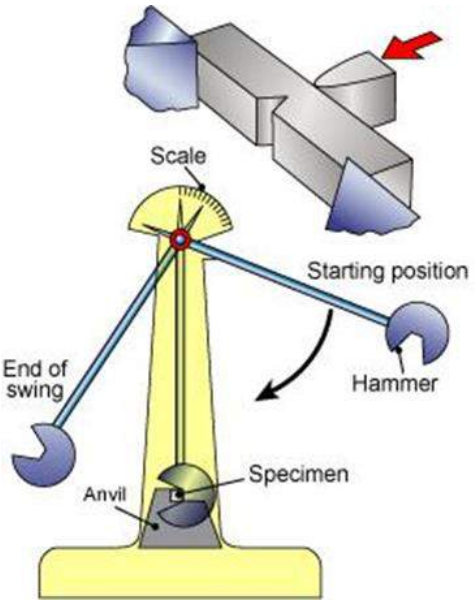

Figure 3.15:The Charpy test (https://builderssolutiongroup.blogspot.com/)

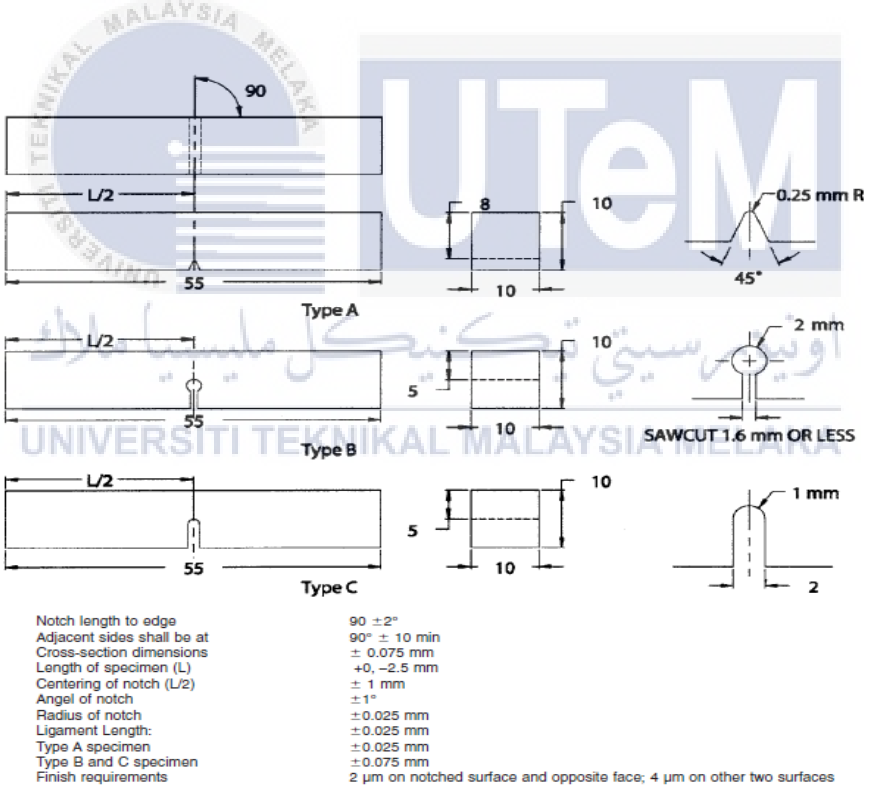

Notch length to edge	90 ±2°
Adjacent sides shall be at	90° ± 10 min
Cross-section dimensions	± 0.075 mm
Length of specimen (L)	+0, –2.5 mm
Centering of notch (L/2)	± 1 mm
Angel of notch	±1°
Radius of notch	±0.025 mm
Ligament Length:	±0.025 mm
Type A specimen	±0.025 mm
Type B and C specimen	±0.075 mm
Finish requirements	2 µm on notched surface and opposite face; 4 µm on other two surfaces

Figure 3.16: Charpy (Simple-Beam) impact test specimens (ASTM E23, 2015)

3.7 Microstructure Characterization

The microstructure is a material that were a very tiny scale structure, defined as the structure of a material's prepared surface as revealed by an optical microscope over 25 magnification. The microstructure of a material (such as metals, polymers, ceramics, or composites) could have a significant impact on physical properties including strength, toughness, ductility, hardness, corrosion resistance, high or low temperature behaviour, or wear resistance. The microstructural analysis were crucial. Generally, the microstructure is were examined using an optical microscope in conjunction with suitable metallurgical preparation and Scanning Electron Microscopy (SEM) Energy Dispersive X-Ray Spectroscopy (EDX). The sample is polished with sandpaper of various sizes, including 1000µ, 2000µ, and diamond polishing pieces, to achieve a mirror-like surface. The sample will then be etched for 10 seconds in Nital solution to allow the microstructure machine to see the sample structure.

3.7.1 Optical Microscope

An optical microscope as in figure 3.17 combined one or more lenses to magnified the image of a sample placed inside the lens's focal plane. The components of an optical microscope were sometimes rather complicated, and it is critical that the microscope is set up properly in order to obtain an accurate image. The fundamental principles related to the operation of an optical microscope are rather simple. An optical microscope's objective lens as in figure 3.18 were comparable to that of an extremely strong magnifying glass. As it is a small focal length lens, it should be held near to the sample that were study. This caused the light from the sample to concentrate around 160 mm within the microscope's tube, resulting in an enlarged and inverted picture of the subject. The objective lens created the genuine picture, which the ocular lens enlarged further so that it may be viewed by an

individual. The compound lens eyepiece used on the majority of optical microscopes has one lens in the front and another at the back of the eyepiece tube. This results in the formation of a couplet, which enabled the virtual image to focus between the lenses, allowing the eye to concentrate on it. The stage were lowered after utilized an optical microscope to facilitate the removal of the microscope slide.

Figure 3.17: Zeiss AxioLab A1 Upright Light Microscope with AxioCam Erc 5s

Figure 3.18 : ZEISS EC EPIPLAN objectives lens (http://zeiss-campus.magnet.fsu.edu/)

3.7.2 Scanning Electron Microscopy (SEM) Energy Dispersive X-Ray Spectroscopy (EDX)

Scanning electron microscopy (SEM) is a technique used to examine cells in a sample at a high magnification. Sample preparation is fairly simple, and when it comes to diverse samples, it does not require processing for ultra-thin sheets to perform the SEM procedure. This is due to the fact that SEM may be used to analyse and calculate evaluations on a millimetre or nanometer scale. SEM can receive a large sample size at one time at low magnification, while at greater magnification, high-resolution images of specific regions can be acquired. Each SEM has energy-dispersive X-ray (EDX, commonly known as EDS) spectroscopy functions. When subjected to an electron beam, an atom generates characteristic X-rays that are unique to its atomic number; this allows the elemental composition of a material to be analysed, whether at a single spot or over a vast region, using techniques such as line scanning and elemental mapping. Semi-quantitative analysis can also be used to determine the chemical composition of a material. When combined with standard SEM analysis, EDX can provide a more comprehensive view of a sample's local composition.

Figure 3.19: JEOL JSM 6010 PLUS/LV Scanning Electron Microscope

CHAPTER 4

RESULTS AND DISCUSSION

4.1 Introduction

The outcomes of this study are used to forecast the likely outcome or result of the upcoming test that was being researched. However, when the analyzed actual results are obtained, the findings may be debated. The preliminary outcomes from the sample tests are also discussed, although they are not the final data that will define the research's course. This subject is used to identify and investigate the original data expectations.

4.2 Composition of analysis

Chemical composition involves qualitative approach testing of numerous sample components, combined with structured analytical approaches, which may require the synthesis and production of delicate chemical composites and chemical reactions. In addition to quantitative analysis to analyze the correlation coefficients of substances in various chemical reagents, the molecular structure of the discovered substance was detected and validated throughout many platforms (Boumerzoug et al., 2010). Table 4.1 showed the chemical composition of the ER70s filler metal material and the low carbon steel material.

Table 4.1: Chemical composition (%wt) of low carbon steel and filler used

Alloy Elements	**Low carbon steel**	**Filler metal ER70s**
C	0.137	0.104
Mn	0.560	0.521
P	0.0320	0.0229
S	0.0337	0.0108
Si	0.140	0.238
Cr_2	0.127	0.0702
Ni_2	0.157	0.486
Cu_2	0.276	0.277
Fe	98.4	98.1

Carbon content on low carbon steel showing at table 4.1 proved that the carbon content is below than <0.30%.

4.3 Complete welded joint

Low carbon steel plate was welded together as in figure 4.1 using current and voltage that were appropriate for the speed and thickness of the steel plate. The slag on the weld bead was then carefully scraped away to avoid any damage to the weld bead itself or to the surface of the plate. Following the completion of the weld, the steel plate is allowed to cool to room temperature slowly by being exposed to the air rather than being immersed in water.

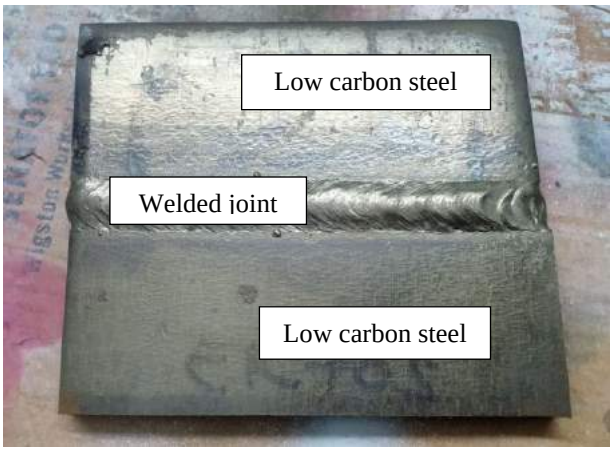

Figure 4.1: Complete welded low carbon steel plate

4.4 Non destructive test

Non-Destructive Testing refers to a group of inspection methods that allow inspectors to evaluate and collect data about a material, system, or component without permanently affecting it. Radiographic and liquid penetrant tests are used in this study to ensure the quality of the sample, the welded joint, and the continuity of the sample.

4.4.1 Radiographic testing

Radiographic Testing (RT) is a non-destructive testing (NDT) approach that examines the interior structure of produced components to discover flaws or defects using either x-rays or gamma rays. The test-part is positioned between the radiation source and the film in radiography testing (or detector). It is based on the idea that radiation is absorbed and scattered as it travels through an item. If the thickness or density of an object varies (for example, due to faults), more or less radiation goes through and affects the film exposure (Deepak et al., 2020). Flaws appear on the film as dark patches. The figure 4.2 below showed the film of workpiece. Based on figure 4.2 below, theres no signs of cracks at the workpiece.

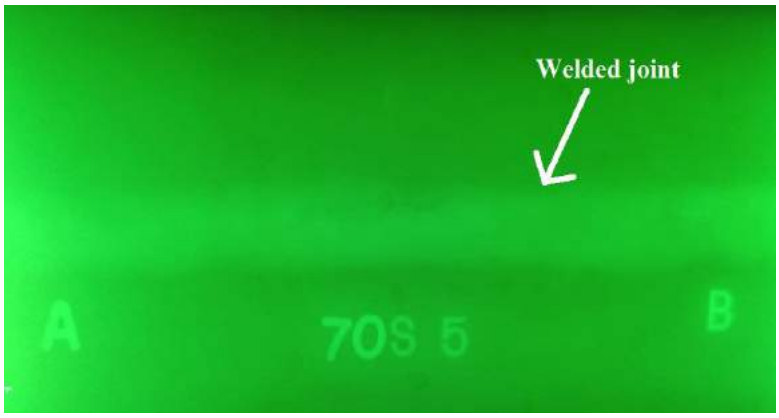

Figure 4.2: The film of workpiece under film viewer

4.4.2 Liquid penetrant testing

The liquid penetrant is pulled into the surface-breaking crack by capillary action, and surplus surface penetrant is then removed; a developer (usually a dry powder) is then applied to the surface, drawing out the penetrant in the fracture and producing a surface indication (Deepak et al., 2020). It is possible to detect cracks as small as 150 nanometres. The created indicators are significantly wider than the real fault and hence more obvious.

Liquid penetrant testing can be used on any non-porous clean material, metallic or non-metallic, although it is not appropriate for unclean or extremely rough surfaces (Deepak et al., 2020). Surface cleaning is an important step in the penetrant testing process. The process can be fully automated, semi-automatic, or manual. Penetrant inspection and continuous-operation production lines, in which specimens are cleaned, dipped, rinsed, dried, and so on, are prevalent. As can see in figure 4.3, after a few minutes were sprayed by developer there are no signs of cracks or any defects on the surface of workpiece and welding area.

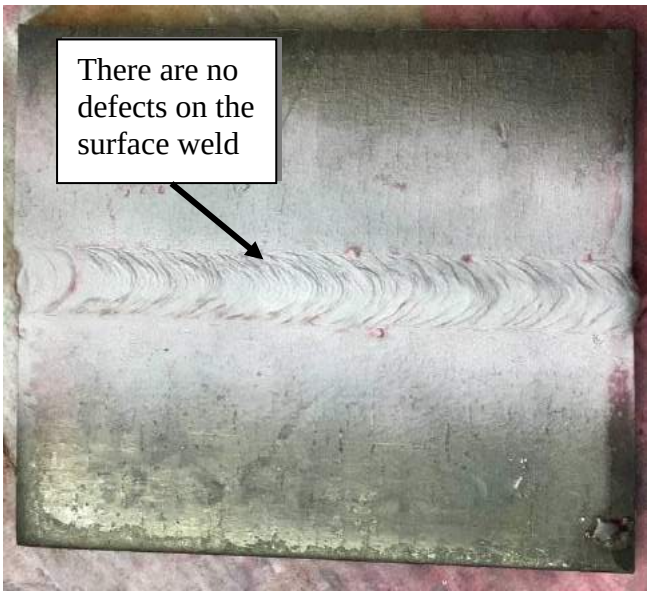

Figure 4.3: Sample after developer were applied

4.5 Heat Treatment Process

There were three parameters that were determined for each sample group to be evaluated and studied. The first treatment parameter is annealing, which has a high temperature but is below the melting point of low carbon steel. The sample was heated to 900˚C inside the furnace before being allowed to cool down with the furnace's lowering ambient temperature. The second treatment parameter is tempering, which has a temperature of 450˚C and was left in the furnace for 2 hours before the sample was taken out to cool to the surrounding temperature. Finally, the third sample group was made up of untreated samples. The look of each sample varied as shown in figure 4.4 below. The looks of each sample group can be identified by naked eyes, with the annealed sample having a crispy dark grey coating outside its surface, the tempered sample having a brownish colour, and the untreated sample retaining its original appearance.

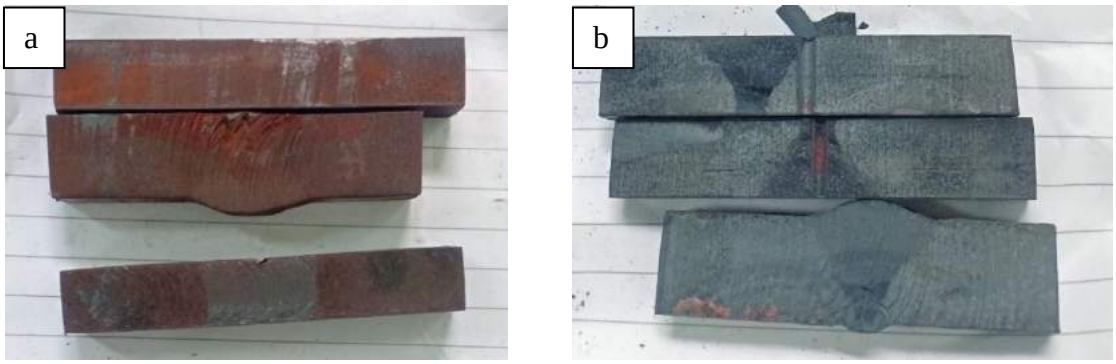

Figure 4.4: Visual appearances after treated; (a) Annealed, (b) Tempered

4.6 Mechanical Test

Mechanical properties are the characteristics of materials that must respond to a load applied to them. The mechanical properties of metals had an impact on the material's range of application and, as a result, on the estimated service life of the material. Strength, ductility, hardness, impact resistance, and fracture strength are the qualities that are most frequently investigated (Adedayo et al., 2010). The mechanical characteristics of the material are not constant and fluctuate on a regular basis in reaction to changes in temperature, loading rate, and other variables (Owolabi et al., 2016). Macro hardness testing was used to evaluate material hardness and impact resistance, while Charpy testing was used to explore their behaviour at high deformation rates.

4.6.1 Impact Testing

An impact test is performed to observe the mechanics that a material will exhibit when subjected to a shock loading that causes the specimen to immediately deform, fracture, or break completely. In addition, the Charpy test and ASTM E23 standard were applied for performing impact tests. Table 4.2 below showed the result of impact test meanwhile for figure 4.5 and 4.6 depicted the bar graph of impact test.

Table 4.2: Result of Charpy test

Type of sample	Part	Impact value(kJ/m^2)	Energy consumed (J)
Untreated	Centre	1293.56	49.885
	HAZ	1293.53	47.884
Tempering	Centre	1292.92	49.860
	HAZ	1292.92	48.860
Annealing	centre	1293.53	49.884
	HAZ	1293.53	49.884

The figure 4.5, the bar graph showed that the toughness of the heat-treated samples and untreated sample were not have significant result of values. This is because the welded joint area is strong, the structure remains the same so thats why the result does not show a significant difference.

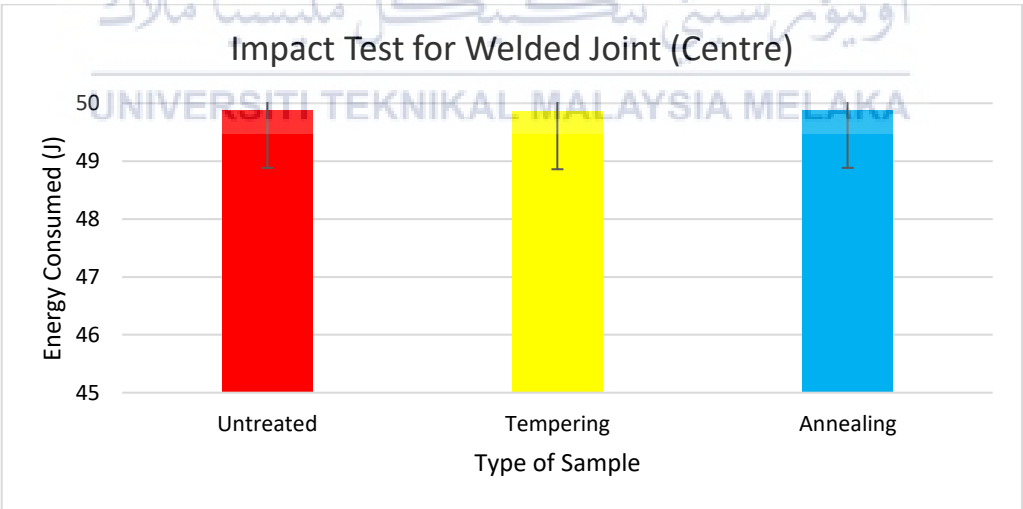

Figure 4.5: The bar graph of impact test for welded joint (centre)

However in figure 4.6, it showed there were significant value at the HAZ area for each sample. As can see, annealed sample still does not show a change in value compared to annealed value at welded joint. This is because each surface of the annealed sample is approximately have the same structure. The toughness of tempered sample were decrease at HAZ area because the structure of surface area were more subtle (Adedayo et al., 2010).

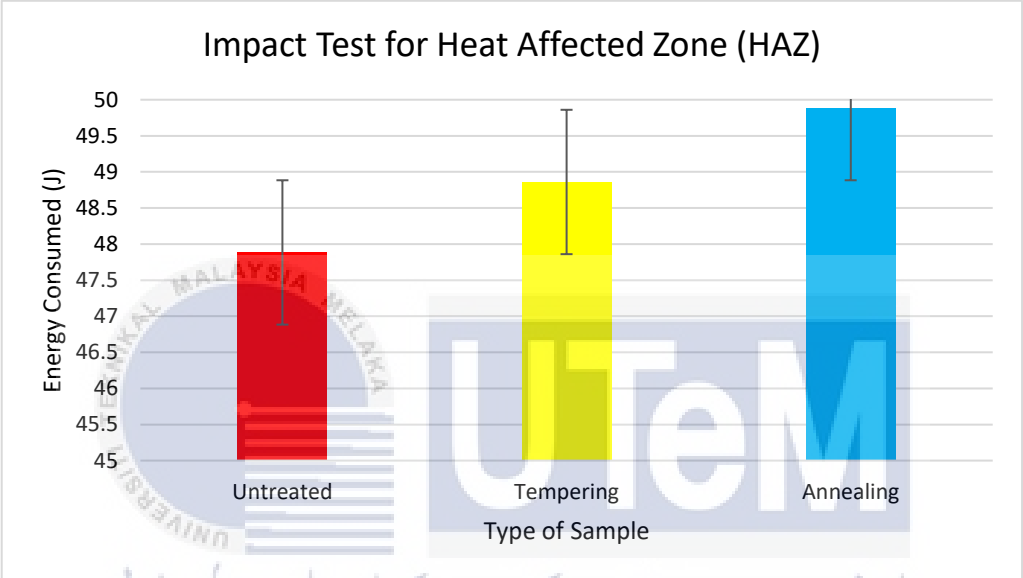

Figure 4.6: The bar graph of impact test for Heat Affected Zone (HAZ)

4.6.2 Macro hardness Analysis

Macro hardness is a phrase that is commonly used in the testing of hardness by applied load impacting materials. For this testing, Rockwell method were chosen and used ball indenter because of type of material were low carbon steel. Macro hardness variability were measured at three separate layers, with micro hardness tests done at the top, centre, and bottom of the sample as shown in figure 4.7.

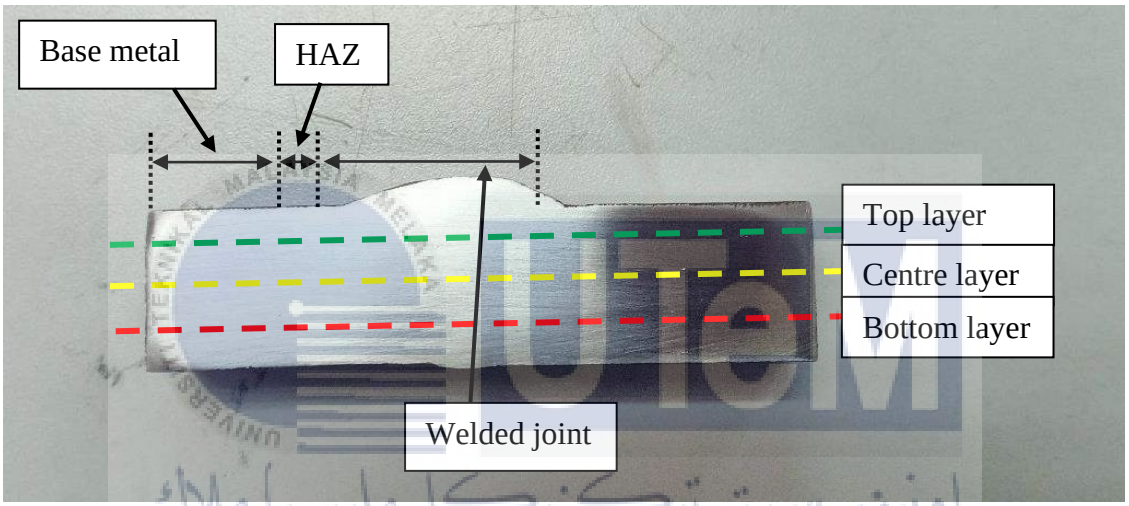

Figure 4.7: Indentation done on multiple layer on the same surface

The measurement was conducted in a distributed way, and the transverse area of cross sectional area that was given the most attention is the area of Heat Affected Zone (HAZ) and weld joint , in which the fusion reaction and microstructure variations growing actively occur (Boumerzoug et al., 2010), as shown in table 4.3.

Table 4.3: Result from the macro hardness test of untreated sample

No	Area	Top (HRB)	Centre (HRB)	Bottom (HRB)
1	Base metal	74.3	74.2	73.8
2		73.9	76.8	75.8
3		74.2	77.5	76.0
4		76.3	75.9	75.4
5		75.8	75.6	75.2
6	HAZ	79.7	78.7	76.9
7		81.3	77.6	79.2
8		81.5	79.2	79.2
9	Welded joint	83.9	82.9	80.5
10		84.4	84.6	85.6
11		85.9	84.3	82.5
12		85.7	82.6	83.5
13	HAZ	78.6	80.0	78.1
14		75.2	81.3	79.5
15		77.1	78.2	79.5
16	Base metal	77.1	75.3	75.0
17		74.8	76.7	76.0
18		74.6	75.0	76.3
19		75.6	74.9	74.0
20		75.8	75.5	74.5

Figure 4.8 showed a line graph for an untreated sample. The line patten is not in average. As can see at the weld joint area it were higher than the HAZ and base metal. This is because the structure at weld joint were subtle compared to other areas.

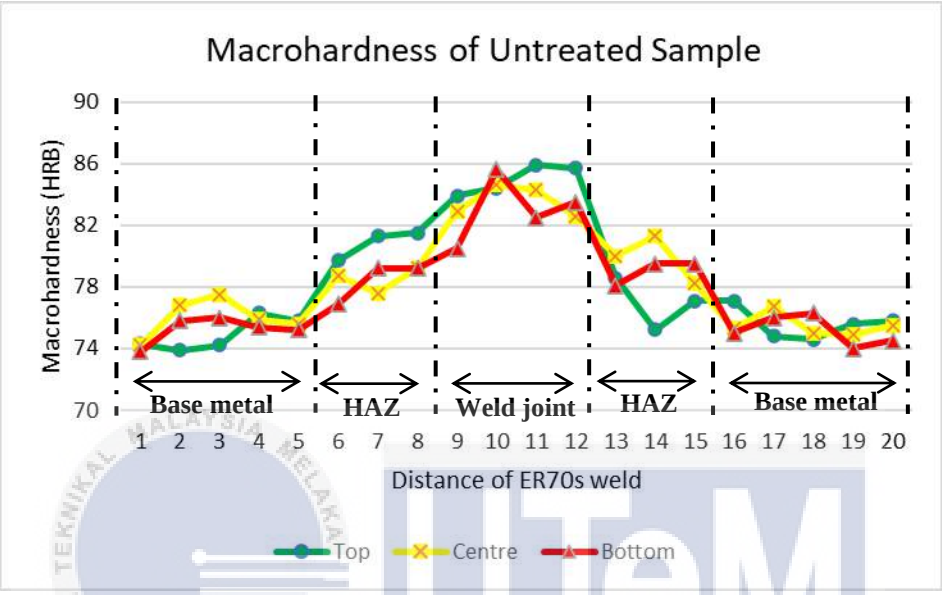

Figure 4.8: Graph result of macro hardness of untreated sample

Table 4.4: Result from the macro hardness test of tempered sample

No	Area	Top (HRB)	Centre (HRB)	Bottom (HRB)
1	Base metal	75.0	75.3	74.5
2		75.0	74.6	75.3
3		75.7	74.9	75.7
4		74.8	75.1	75.4
5		75.6	76.3	76.3
6	HAZ	80.0	79.9	79.5
7		81.3	81.8	80.9
8		81.5	80.3	81.3
9	Welded joint	84.8	82.2	82.2
10		85.6	82.1	84.2
11		84.2	82.5	84.2
12		82.4	81.8	83.6
13	HAZ	81.2	80.8	80.2
14		80.7	79.8	79.1
15		80.2	79.9	78.6
16	Base metal	74.9	75.8	75.9
17		74.9	75.5	75.1
18		74.8	75.2	75.3
19		75.7	74.7	75.4
20		75.1	74.9	74.9

According to the graph in figure 4.9 below as for tempered sample, it also showed that the line pattern were not in average. At the HAZ area, we can see that the line pattern were higher compared to the line pattern for untreated sample. This because tempered sample have more subtle structure surface compared from untreated sample. Other than that, at area weld joint, we can see that it has similar line pattern to the untreated sample. The smoother the surface structure, the higher the hardness value.

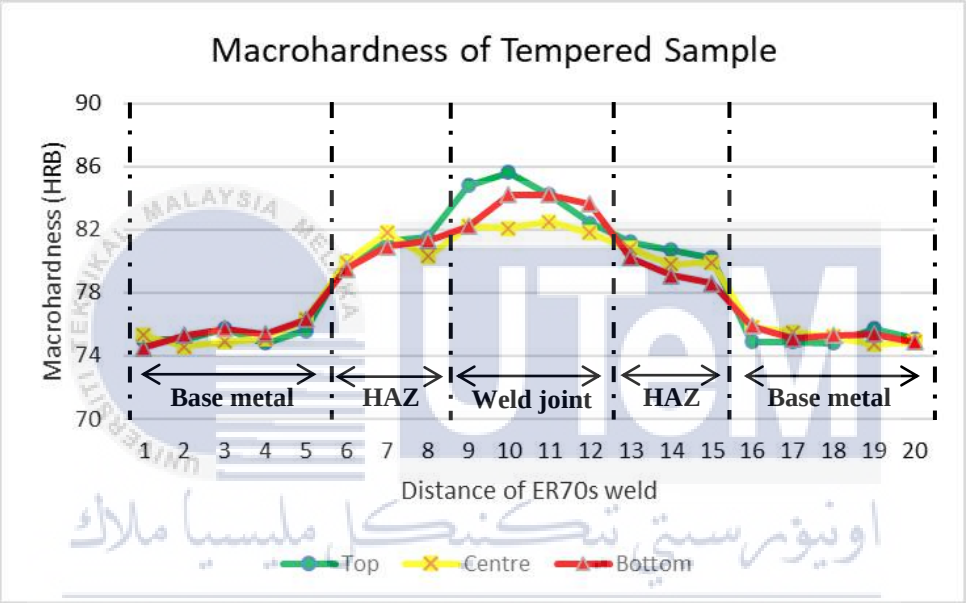

Figure 4.9: Graph result of macrohardness of tempered sample

Table 4.5: Result from the macro hardness test of annealed sample

No	Area	Top (HRB)	Centre (HRB)	Bottom (HRB)
1	Base metal	75.8	75.7	74.0
2		76.0	76.0	75.2
3		76.6	75.7	75.5
4		75.6	75.9	75.8
5		76.1	77.2	75.3
6	HAZ	77.7	79.5	76.8
7		79.3	79.8	77.2
8		76.3	78.0	78.4
9	Welded joint	77.1	79.6	80.6
10		76.4	79.9	78.8
11		77.0	78.7	80.9
12		76.9	78.7	80.1
13	HAZ	76.7	75.9	75.1
14		78.7	77.7	75.4
15		78.2	77.5	75.3
16	Base metal	76.2	75.8	73.2
17		76.2	75.9	72.4
18		76.0	76.3	74.5
19		76.4	76.6	74.2
20		76.1	75.7	73.4

Figure 4.10 showed the result of annealed sample for macro hardness. The line pattern of each area were in average compared to untreated sample of graph. The value at each area quite similar because annealing process were helped to stabilize the microstructure of the sample. Even though the line pattern in average but the annealed sample have the lowest value of hardness at HAZ and weld joint compared to tempered and untreated sample.

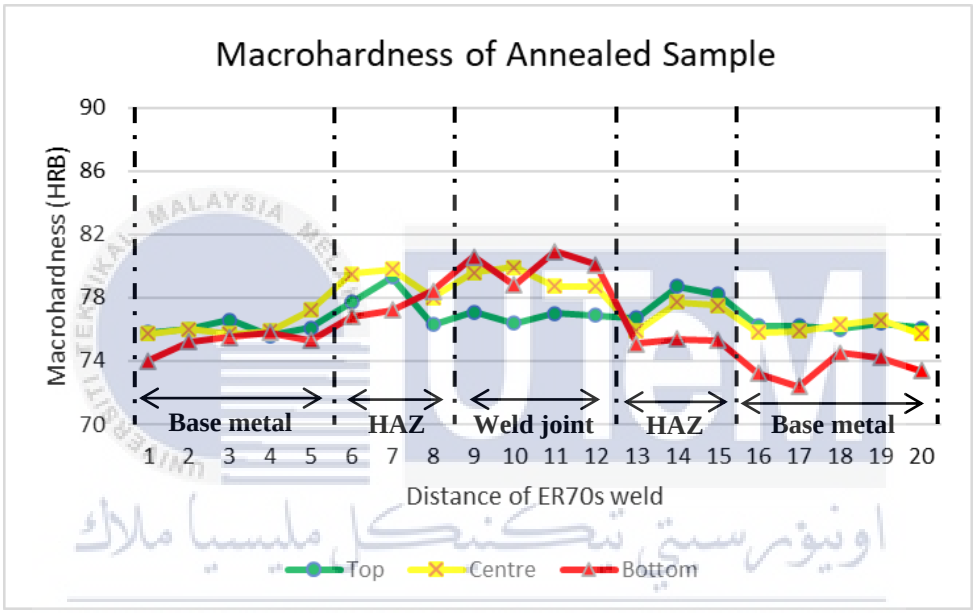

Figure 4.10: Graph result of macrohardness of annealed sample

4.7 Microstructure Analysis

The microstructure resting method was an alternative strategy to identifying and recognizing the characteristics of all three group samples. This testing is used to identify grit size by employing microscope-assisted equipment, as stated in the methodology.

4.7.1 Optical microscope

This test is used to determine the grain size utilising microscope-assisted equipment, as discussed in the methodology.

Figure 4.11 depicted the appearance of untreated sample's grain growth. According to the figure below, the results of the microstructural examination revealed that the initial grain size had a significant impact on the phases formed in the intercritical HAZ (b). Also, there is the presence of pearlite and martensite as can be seen in (c) and (e). The fusion line of HAZ and welded metal low carbon steel can be seen in (d).

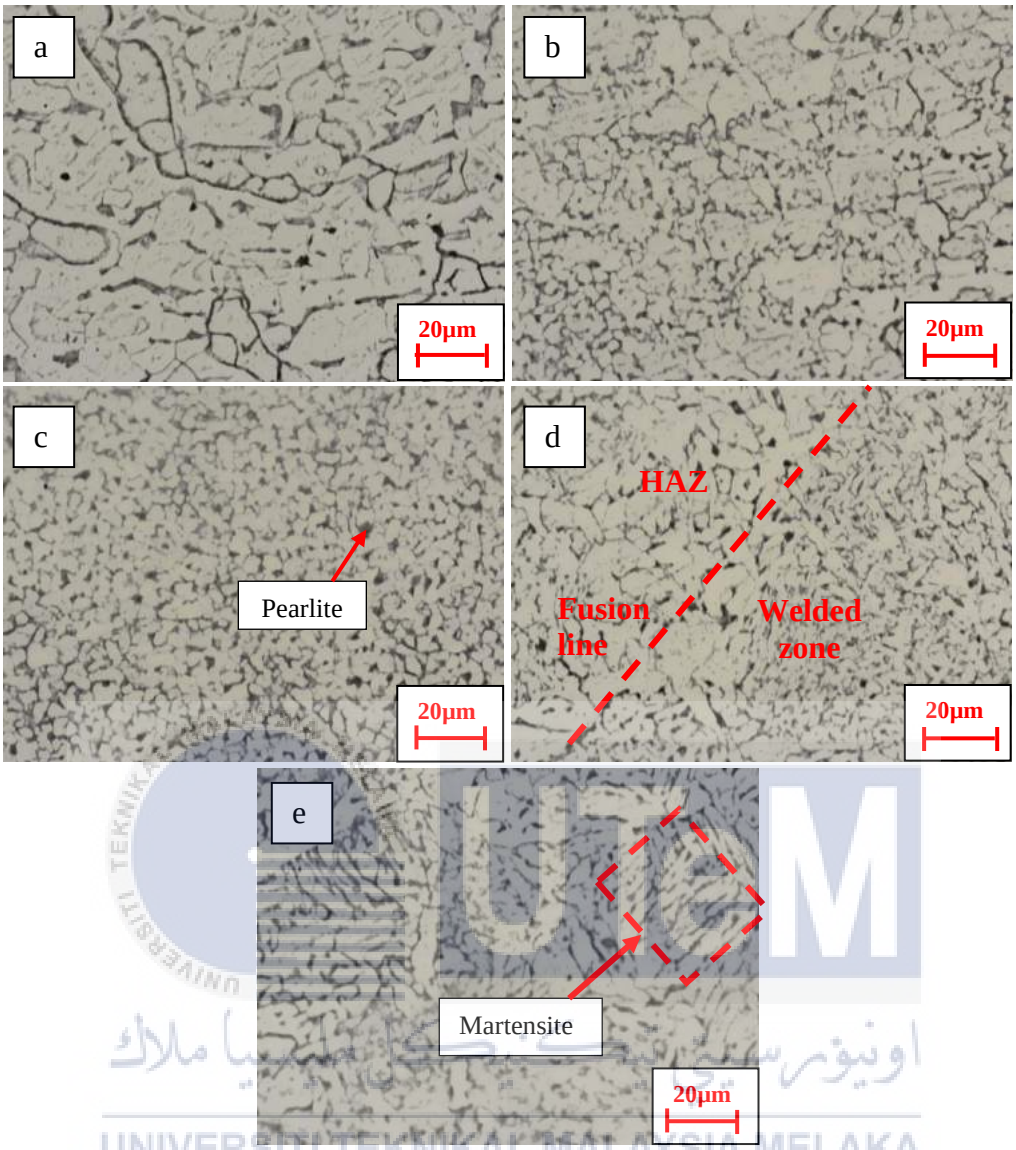

Figure 4.11: Microstructure of each area on untreated sample; (a) base material, (b) Intercritical zone (IGHAZ), (c) Fine grained zone (FGHAZ), (d) Fusion boundary between HAZ and welded zone, (e) Welded zone

After done tempered at 450˚C, the microstructure as in figure 4.12 below, the pearlite were seen at the (b). White areas indicated ferrite formation, while black patches indicated pearlite or cementite formation. At the welded zone (e), its being gradually transformed into fine needle-like (fragmented) tempered martensite.

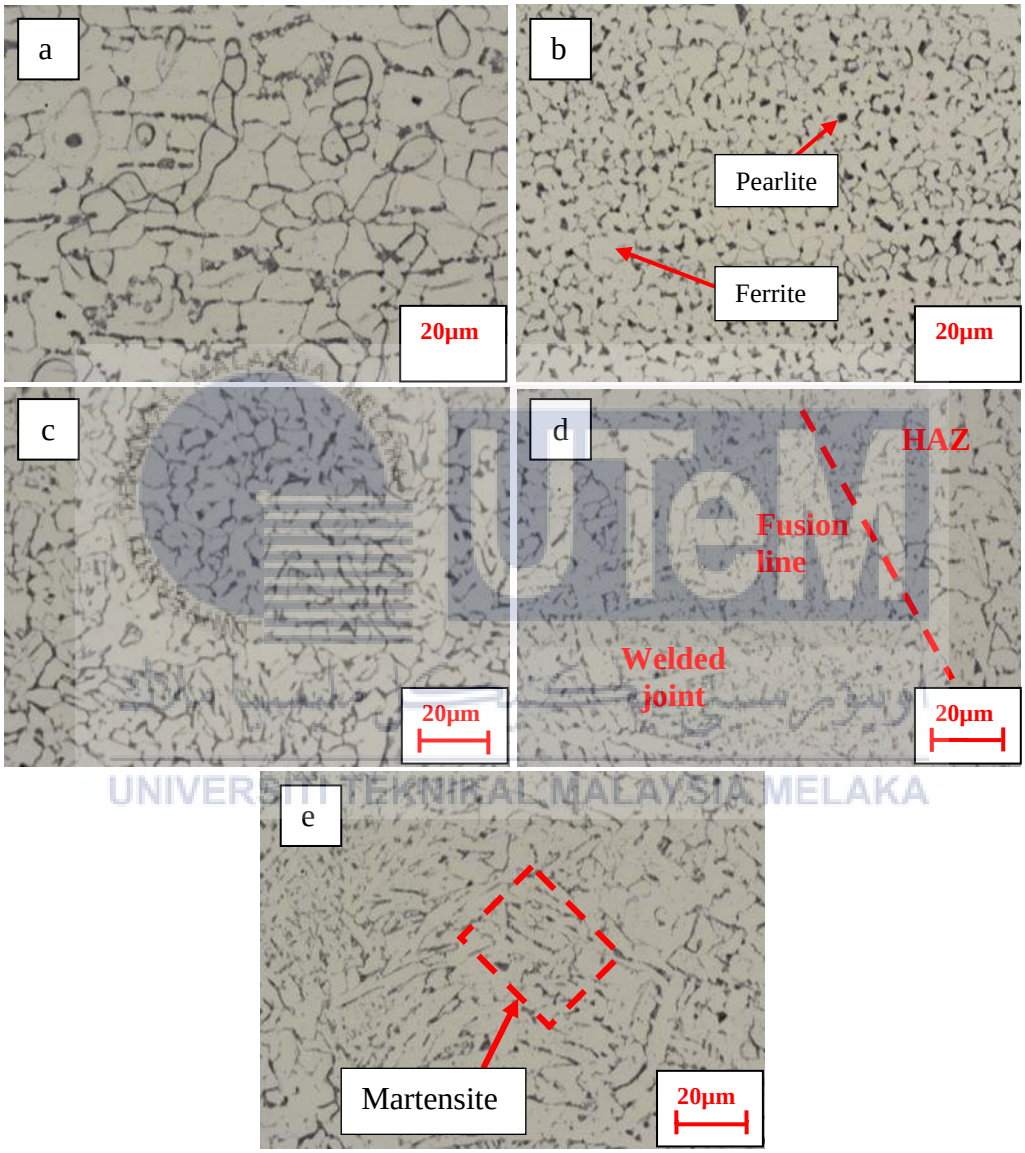

Figure 4.12: Microstructure of each area of tempered sample; (a) base material, (b) Fine grained zone (FGHAZ), (c) Coarse grained zone (CGHAZ), (d) Fusion boundary between HAZ and welded zone, (e) Welded zone

Figure 4.13 depicted the microstructure of each area of annealed sample. Slow cooling in annealing, which is room temperature cooling, led in the change of austenite to soft pearlite, which was then combined with ferrite or cementite (Chandra Kandpal et al., 2020). At the base metal (a), the grain size of the microstructure were more small compared to grain size of untreated sample. The more pearlite gives the steel higher strength, but lower ductility (Owolabi et al., 2016). Also, there were no significant microstructure changes between each area. This is because there were no structure fine needle-like at the welded area.

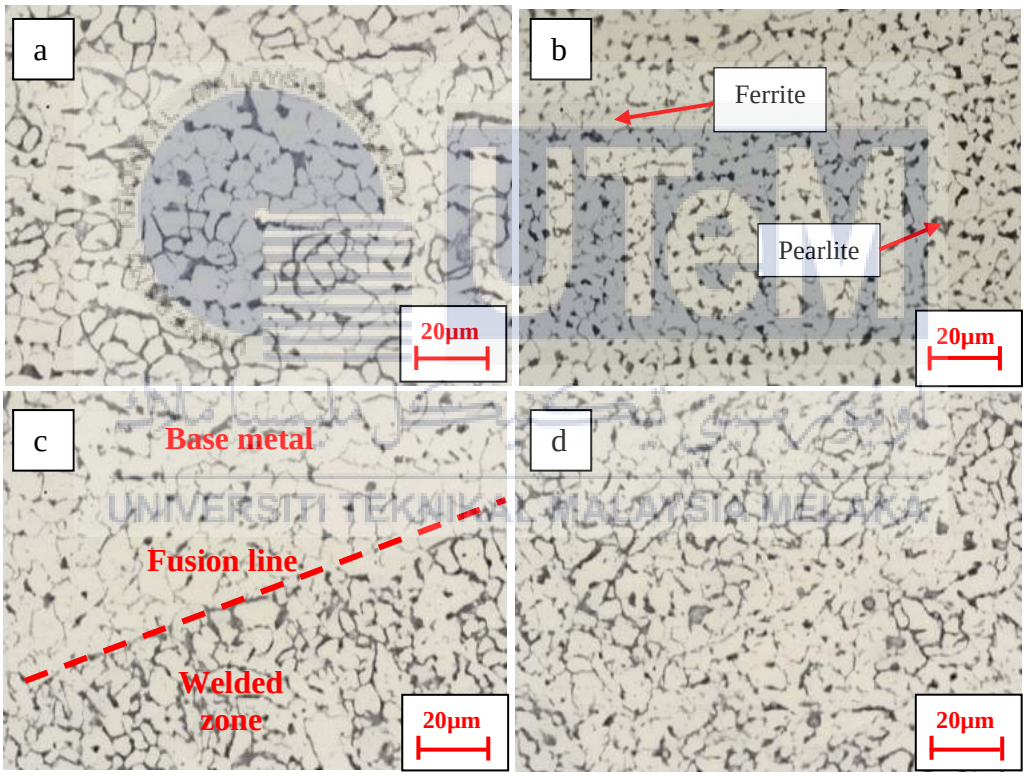

Figure 4.13: Microstructure of each area of annealed sample; (a) base material, (b) Fine grained zone (FGHAZ), (c) Fusion Boundary between base metal and welded zone, (d) Welded zone

4.7.2 Line Scanning

One of the features of an EDX machine is the ability to evaluate the elements and compounds detected in the sample utilizing a low vacuum mode (Saito et al., 2021). It has displayed the results of the analysis of the sample provided.

A line scanning test was performed on the surface of the low carbon steel sample, as shown in figure 4.14. The colour that represents the element content in the sample between the base and welded areas. Based on figure 4.14, it showed elements that have in untreated sample which is Carbon (C), Silicon (Si), Iron (Fe), and Manganese (Mn). Red colour graph represent for Carbon (C) element, green colour showed Silicon (Si) meanwhile blue light showed Iron (Fe) element detected on sample and purple colour for Manganese (Mn) element. It showed that Iron element have highest weight percentage with 94.95% compared to other elements, followed by Carbon with 4.06% and Silicon 0.99%.

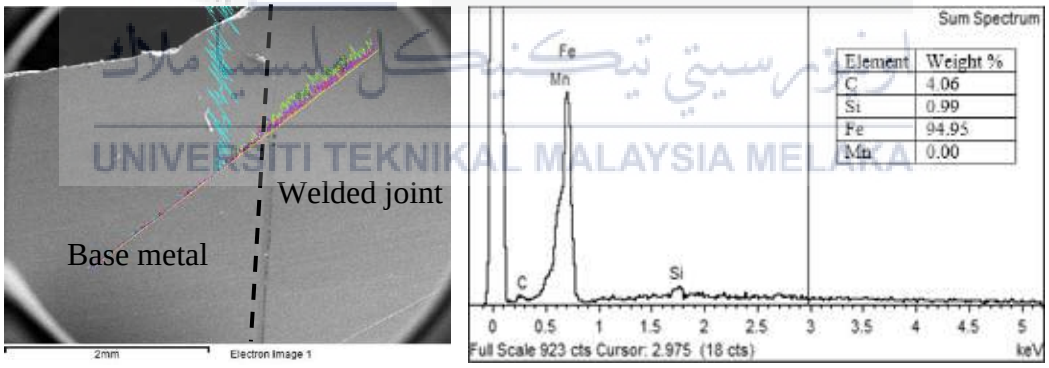

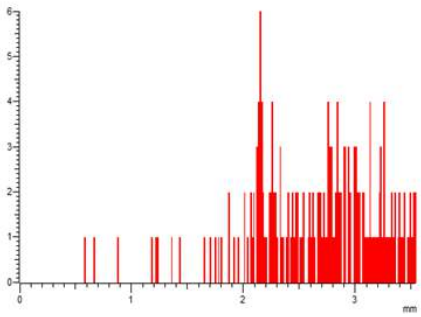

Carbon, C

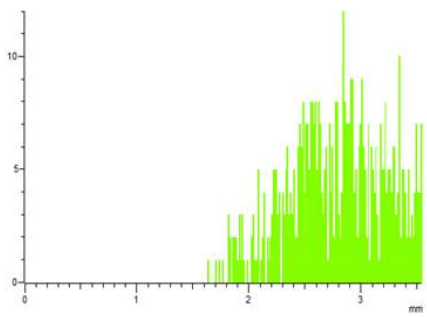

Silicon, Si

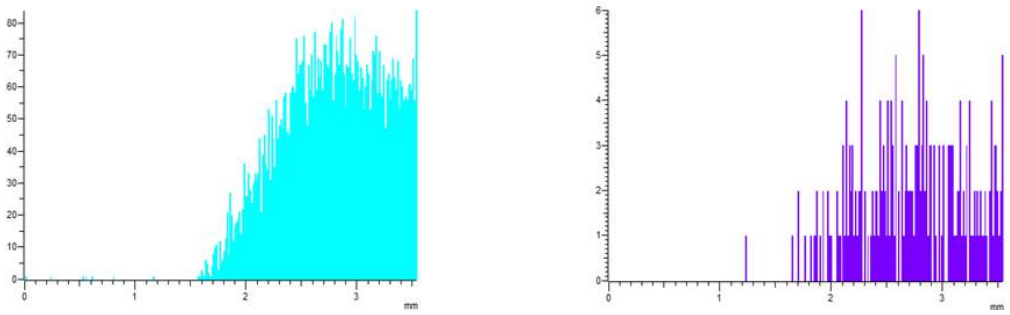

Iron, Fe Manganese, Mn

Figure 4.14: Interface of untreated sample

The surface of base metal and welded joint area sample was performed a line scanning test was conducted on, referring to Figure 4.15, the colour representing the content of the element between the base metal and welded joint. Based on figure 4.15, it showed the element content found between base metal and welded joint area. Different colours have shown the sample contains various type of elements. The red graph was showed an element containing Carbon (C) meanwhile the green graph has shown that the sample contains the element Silicon (Si). In addition, the blue light coloured graph containing Iron (Fe) element and the purple graph showed Manganese (Mn). Manganese elements were shown that the manganese element have a high chemical contain in the welded metal area compared to the base metal in tempered sample.

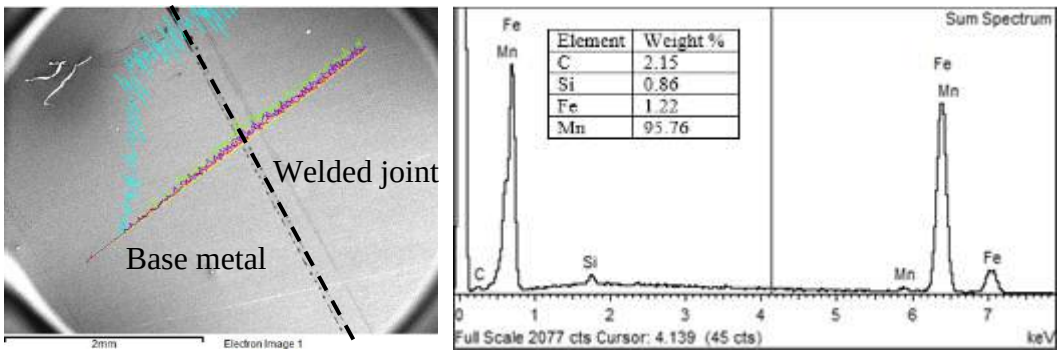

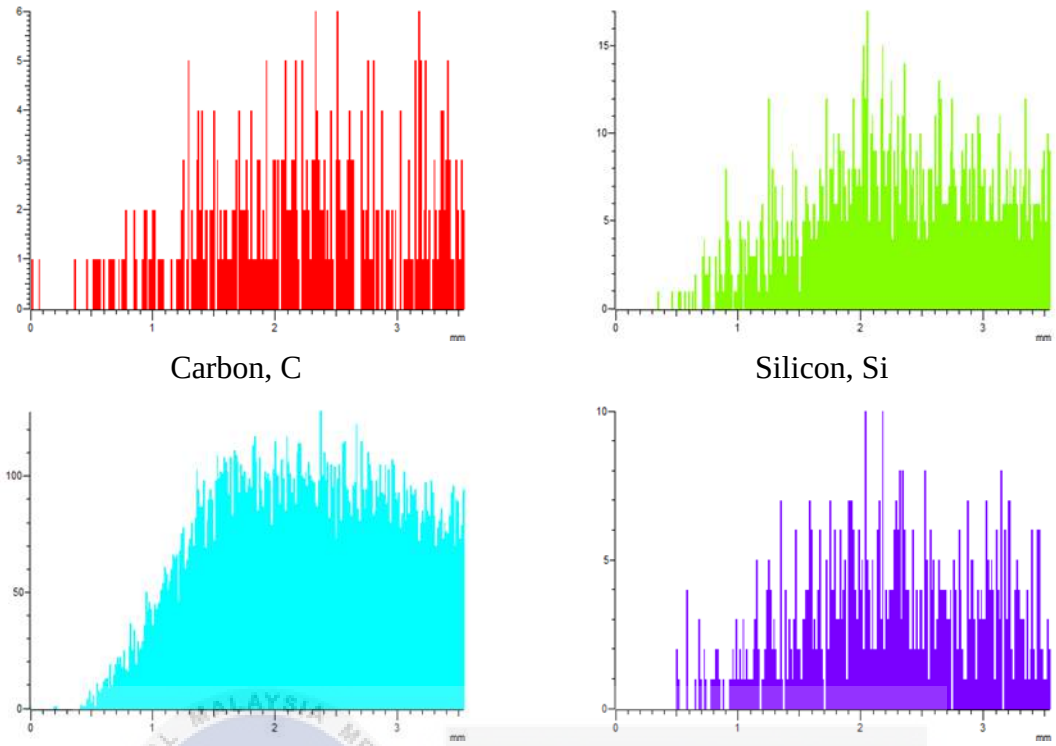

Figure 4.15: Interface of tempered sample

Based on figure 4.16, it showed the element content found between base metal and welded joint area. Different colours have shown the sample contains various type of elements. The red graph was showed an element containing Carbon (C) meanwhile the green graph has shown that the sample contains the element Silicon (Si). In addition, the blue light coloured graph containing Iron (Fe) element and the purple graph showed Manganese (Mn). Manganese elements were shown that the manganese element have a high chemical contain in the base metal compared to the welded metal area in annealed sample.

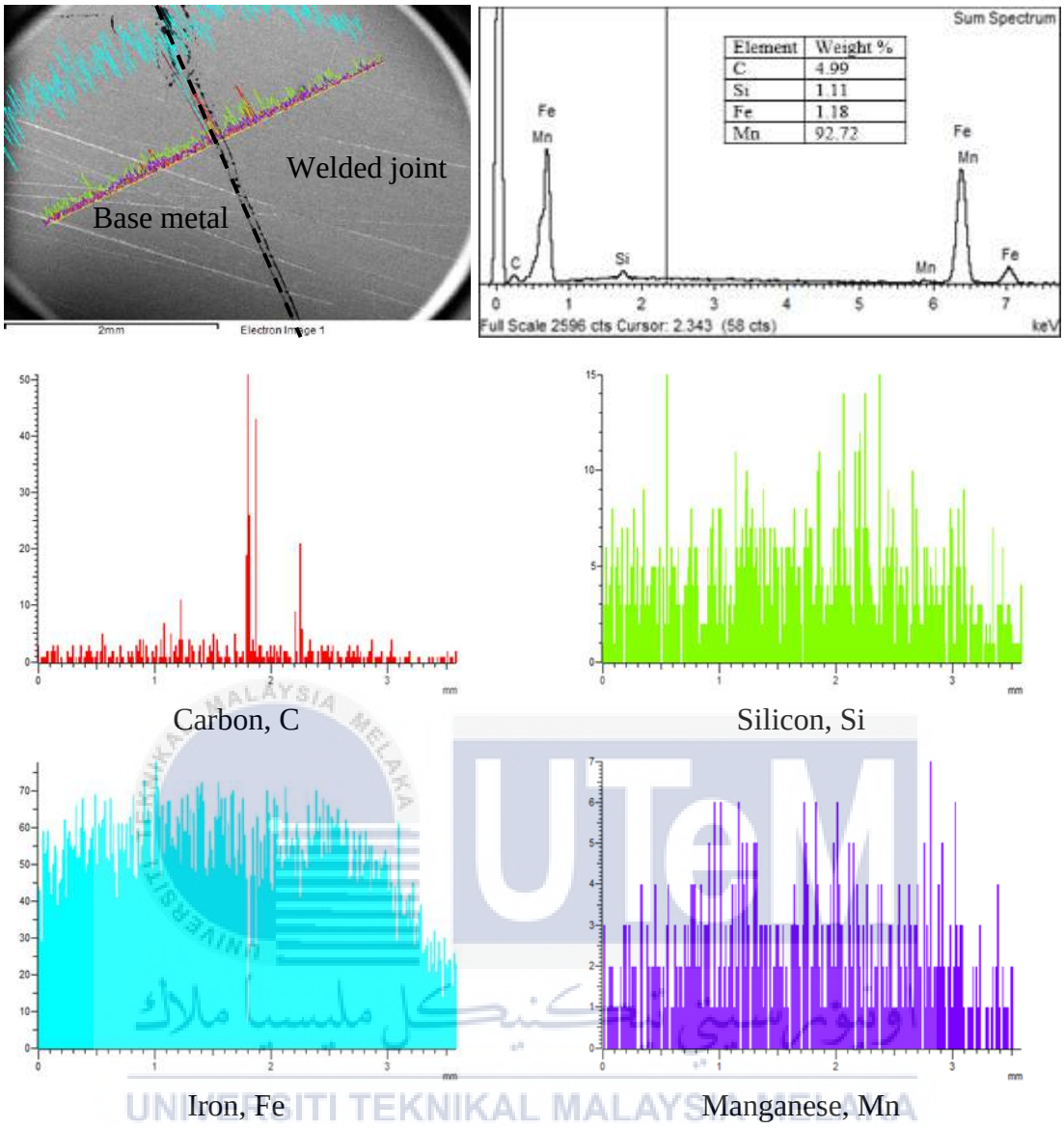

Figure 4.16: Interface of annealed sample

4.7.3 Elemental Mapping

One of the procedures used for element analysis or chemical characterization of samples is EDX analysis. This is to prove the presence of other chemical elements after the sample were done do heat treatment (Senthur Prabu et al., 2021).

Based on figure 4.17, the content of the element can be seen in the graph where the highest content on the graph is the Iron (Fe) element which in blue colour have 94.95% at

welded area. Carbon (C) elements that were in red colour have 4.06% in surface between base metal and welded zone for untreated sample.

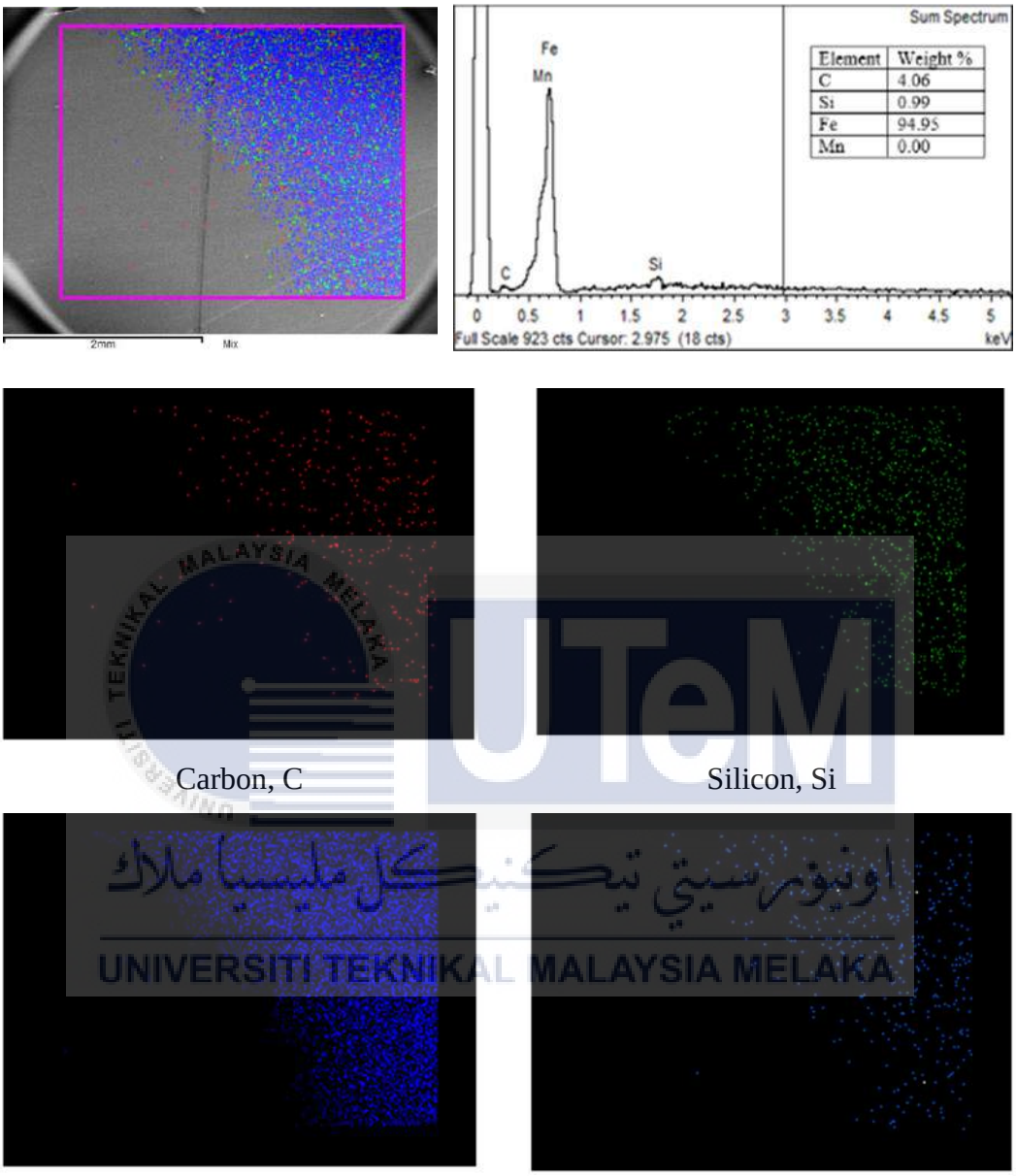

Figure 4.17: Elemental mapping analysis for untreated sample

For the figure 4.18, supposedly there are manganese (Mn) in blue color covering the surface because it has the highest content of element which is 95.76% compared to other elements. Besides, Carbon (C) elements which is in red colour have 2.15% in welded zone meanwhile Iron (Fe) elements were 1.22% and Silicon (Si) elements were 0.86% for tempered sample.

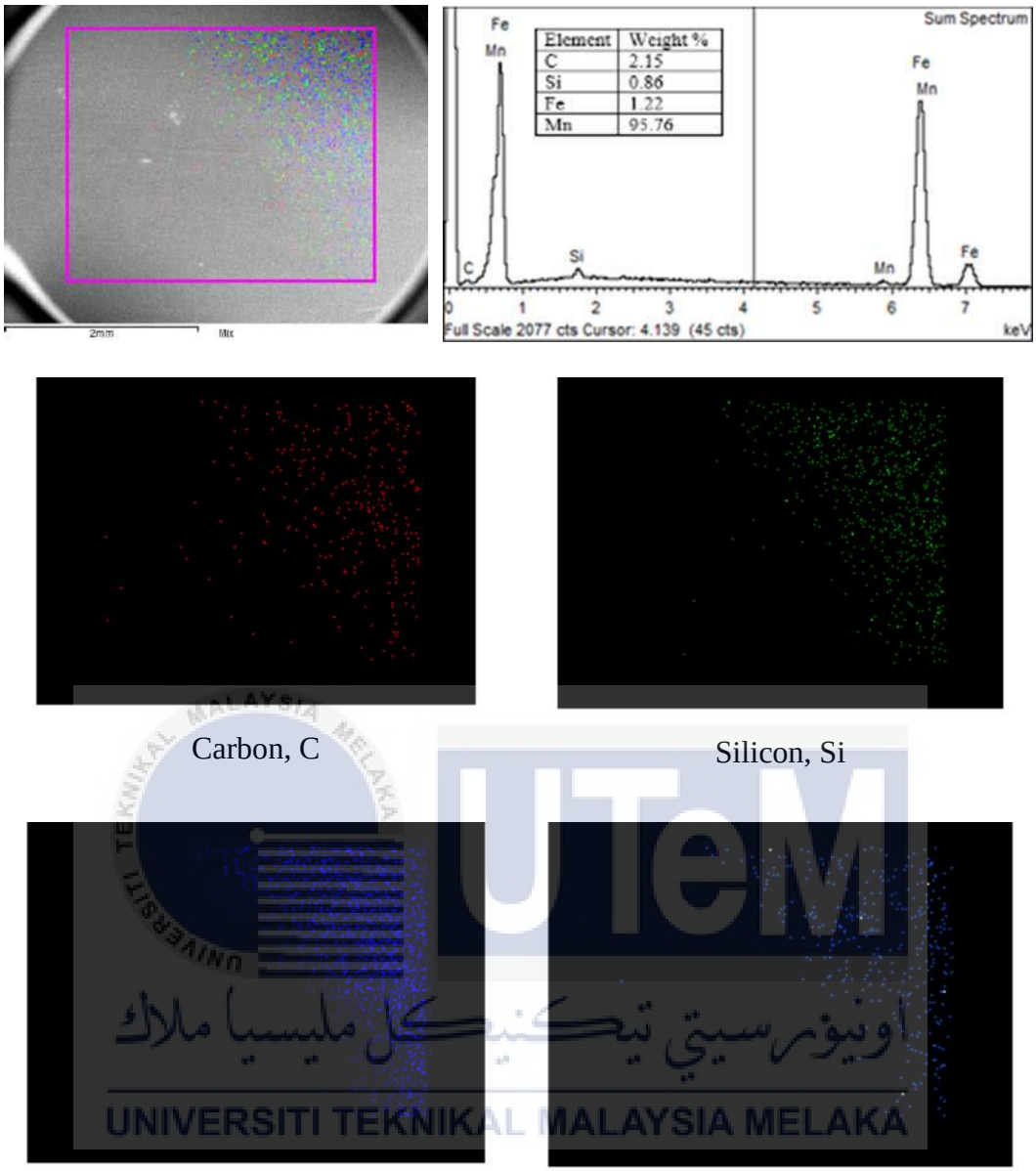

Figure 4.18: Elemental mapping analysis for tempered sample

Based on figure 4.19, the blue colour elements containing Manganese (Mn) which have the highest content percentage which are 92.71% when compared to other elements. The red graph depicted element containing Carbon (C) where it have 4.99% content element in the sample, whereas the Iron (Fe) have 1.18% slight higher than Silicon (Si) which is 1.11%.

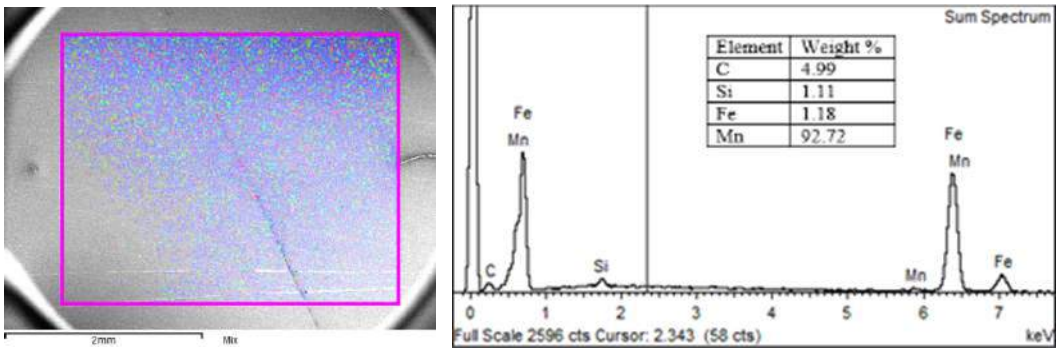

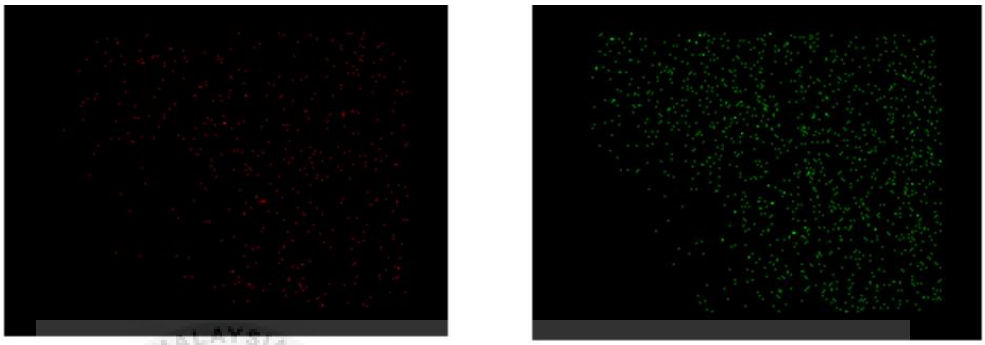

Carbon, C Silicon, Si

Iron, Fe Manganese, Mn

Figure 4.19: Elemental mapping analysis for annealed sample

CHAPTER 5

CONCLUSION AND RECOMMENDATIONS

5.1 Conclusion

i. During this process, were able to study the welded joint of low carbon steel joint with filler ER70s and the effect of heat treatment on the mechanical and microstructure properties by performing hardness and impact test. In addition, were able to carry out the non-destructive test by using radiography testing and liquid penetrant inspection. This study was conducted to find out how heat treatment can effect on the mechanical and microstructure at HAZ and welded joint area. This study is also used in the oil and gas industry.

ii. NDT is a non-destructive test that is always used on non-porous materials to detect surface defects using two separate procedures. These tests are particularly effective because the specimens are tested in methods that do not affect the reliability or functionality of the material being analyzed. After completing a dye penetrant test and radiography testing to examine if there was a surface defect against the welded joint, the specimen showed that no surface defect was found.

iii. After being cut with an abrasive water jet, the specimen must go through the tempering and annealing processes. This study includes three parameters: untreated, tempered, and annealed samples. The sample for tempering had to soak for 2 hours in the furnace at 450˚celsius, while the sample for annealing had to soak for 30 minutes in the furnace at 900˚celsius, and both had to be cooled in

room temperature. The outcome of the heat treatment method is that the looks of each sample group can be recognized by naked eyes, with the annealed sample having a crispy dark grey coating outside its surface, the tempered sample having a brownish colour, and the untreated sample preserving its original appearance.

iv. After the heat treatment is completed, a mechanical test must be performed. The impact and hardness tests were conducted for mechanical testing. The impact test results showed similar value of three samples with value 49.885J for untreated sample, 49.860J for tempered sample and 49.884J for annealed were tough and strong enough to break at the welded connection, however at the HAZ area, the annealed sample with value 49.884J is stronger than the tempered which have 48.860J and untreated samples with 47.885J.

v. For hardness test, Rockwell method were chosen and used ball indenter because of type of material were low carbon steel. Macro hardness variability were measured at three separate layers, with micro hardness tests done at the top, centre, and bottom of the sample. At annealed sample, the result of the graph showed that the line pattern of each area were in average compared to graph of untreated and tempered sample. Even though the line pattern of annealed sample were in average, but the annealed sample have the lowest value of hardness at HAZ and weld joint compared to tempered and untreated sample. Hardness test also revealed that heat treatment can strengthen the structure, resulting in a more ductile and stronger sample.

vi. material characterization, two methods were used, including an optical microscope and a Scanning Electron Microscopy (SEM) machine. First, the

sample must be polished with sandpaper and a diamond polisher sheet until it resembles a mirror. The sample must next be etched for 10 seconds with Nital. Nital is used to see the structure more clearly under an optical microscope with different lens diameters. The microstructure test results showed at the tempered sample have subtle structure especially at welded joint area and there's have fine grained structure at HAZ area meanwhile for annealed sample, the microstructure were similar at each area. There also no structure fine needle-like at the welded area were detected.

5.2 Recommendations for future

During the period, some difficulties and limitations in this study were encountered. During the polishing process to prepare the sample for microstructure and etching, the polished surface must not be touched or swept with a dry cloth since contact with a foreign surface may reduce the integrity of the polished surface and a scratch may occur. In addition to the process before the microstructure analyses, the duration spend immersing the sample in the Nital solution liquid during the etching should not exceed 10 seconds to avoid over etching on the surface sample. If over etching occurs, the polishing procedure must be repeated from the beginning.

Excessive heat from equipment and tools must not be introduced to the samples throughout the heat treatment study's sample preparation and data collecting phase prior to the heat treatment performed on the samples. This is done to avoid changes in microstructure and grain growth caused by the affected heat apart from heat treatment. Other test such as Electron Backscatter Diffraction (EBSD) to examine the microstructure, also can be done. In addition to all the recommendations, we can undertake additional heat treatment studies in the future to prevent failure in the region of HAZ, particularly at pipeline structures that were used in the oil and gas industry.

REFERENCES

Abioye, T. E., Ariwoola, O. E., Ogedengbe, T. I., Farayibi, P. K., & Gbadeyan, O. O. (2019). Effects of welding speed on the microstructure and corrosion behavior of dissimilar gas metal arc weld joints of AISI 304 stainless steel and low carbon steel. Materials Today: Proceedings, 17, 871–877. https://doi.org/10.1016/j.matpr.2019.06.383

Adedayo, A. V, Ibitoye, S. A., & Oyetoyan, O. A. (2010). Annealing Heat Treatment Effects on Steel Welds. 9(6), 547–557.

ASTM. (2015). E23-07a - Standard Test Methods for Notched Bar Impact Testing of Metallic Materials. ASTM International, 14(C), 28. https://doi.org/10.1520/E0023-07AE01.2

Boumerzoug, Z., Derfouf, C., & Baudin, T. (2010). Effect of Welding on Microstructure and Mechanical Properties of an Industrial Low Carbon Steel. Engineering, 02(07), 502–506. https://doi.org/10.4236/eng.2010.27066

Chandra Kandpal, B., Gupta, D. K., Kumar, A., Kumar Jaisal, A., Kumar Ranjan, A., Srivastava, A., & Chaudhary, P. (2020). Effect of heat treatment on properties and microstructure of steels. Materials Today: Proceedings, 44, 199–205. https://doi.org/10.1016/j.matpr.2020.08.556

Deepak, J. R., Bupesh Raja, V. K., Srikanth, D., Surendran, H., & Nickolas, M. M. (2020). Non-destructive testing (NDT) techniques for low carbon steel welded joints: A review and experimental study. Materials Today: Proceedings, 44, 3732–3737. https://doi.org/10.1016/j.matpr.2020.11.578

Evans, R. (2012). 2 - Selection and testing of metalworking fluids. In V. P. Astakhov & S. Joksch (Eds.), Metalworking Fluids (MWFs) for Cutting and Grinding (pp. 23–78). Woodhead Publishing. https://doi.org/https://doi.org/10.1533/9780857095305.23

Frihat, M. H. (2015). Effect of Heat Treatment Parameters on the Mechanical and Microstructure Properties of Low-Alloy Steel. Journal of Surface Engineered Materials and Advanced Technology, 05(04), 214–227. https://doi.org/10.4236/jsemat.2015.54023

Hajili, S. (2017). School Of Industrial And Information Welding processes for joining dissimilar metals and plastics.https://www.researchgate.net/ publication/323254307_ Advanced_Manufacturing_Welding_processes_for_joining_dissimilar_metals_and_plastic s/references

Hnizdil, M., & Chabicovsky, M. (2018). Experimental study of in-line heat treatment of 1.0577 structural steel. Procedia Manufacturing, 15, 1596–1603. https://doi.org/https://doi.org/10.1016/j.promfg.2018.07.305

Jenney, C. L., & O'Brien, A. (1991). Welding Handbook_Volume 1_Welding Science And Technology. American Welding Society, 1, 982.

Jeong, S., Lee, Y., Park, G., Kim, B., Moon, J., Park, S.-J., & Lee, C. (2021). Phase transformation and the mechanical characteristics of heat-affected zones in austenitic Fe–Mn–Al–Cr–C lightweight steel during post-weld heat treatment. Materials Characterization, 177, 111150. https://doi.org/https://doi.org/10.1016/j.matchar.2021.111150

Krauss, G. (2017). 4 - Physical metallurgy of steels: An overview.In R. Rana & S. B. Singh (Eds.), Automotive Steels (pp. 95–111). Woodhead Publishing. https://doi.org/https://doi.org/10.1016/B978-0-08-100638-2.00004-3

Kučerová, L., Jandová, A., & Rubešová, K. (2019). Microstructure analysis and mechanical properties of low alloyed steel with retained austenite obtained by heat treatment. Manufacturing Technology, 19(2), 243–247. https://doi.org/10.21062/ujep/277.2019/a/1213-2489/mt/19/2/243

Kumar, H., Kumar, N., & Engineering, R. N. C. (2019). A Survey on Gas Metal Arc Welding (GMAW) -Review. 7(01), 595–600.

Magudeeswaran, G., Balasubramanian, V., & Madhusudan Reddy, G. (2018). Metallurgical characteristics of armour steel welded joints used for combat vehicle construction. Defence Technology, 14(5), 590–606. https://doi.org/10.1016/j.dt.2018.07.021

Mesquita, R. A., Barbosa, C. A., & Machado, A. R. (2017). 2.9 Heat Treatment of Tool Steels. In M. S. J. Hashmi (Ed.), Comprehensive Materials Finishing (pp. 214–245). Elsevier. https://doi.org/https://doi.org/10.1016/B978-0-12-803581-8.09191-8

Metals., A. S. for, & International., A. S. M. (1997). Metals handbook. Volume 1, Volume 1,. ASM International.

Moore, P., & Booth, G. (2015). 13 - Improving the fracture performance and fatigue life of welded joints. In P. Moore & G. Booth (Eds.), The Welding Engineer's Guide to Fracture and Fatigue (pp. 185–195). Woodhead Publishing. https://doi.org/https://doi.org/10.1533/9781782423911.2.185

Nayak, S. S., Biro, E., & Zhou, Y. (2015). 5 - Laser welding of advanced high-strength steels (AHSS). In M. Shome & M. Tumuluru (Eds.), Welding and Joining of Advanced High Strength Steels (AHSS) (pp. 71–92). Woodhead Publishing. https://doi.org/https://doi.org/10.1016/B978-0-85709-436-0.00005-9

Owolabi, O. B., Aduloju, S. C., Metu, C. S., Chukwunyelu, C. E., & Okwuego, E. C. (2016). Evaluation of the Effects of Welding Current on Mechanical Properties of Welded Joints Between Mild Steel and Low Carbon Steel. American Journal of Materials Science and Application, 4(1), 1–4.

Phoumiphon, N., Othman, R., & Ismail, A. B. (2016). Improment in Mechanical Properties Plain Low Carbon Steel Via Cold Rolling and Intercritical Annealing. Procedia Chemistry, 19, 822–827. https://doi.org/https://doi.org/10.1016/j.proche.2016.03.108

Pisarski, H. G., & Pargeter, R. J. (1984). Fracture Toughness Of Weld Heat Affected Zones (Hazs) In Steels Used In Constructing Offshore Platforms. In Welding in Energy-Related Projects (pp. 415–428). Pergamon. https://doi.org/https://doi.org/10.1016/B978-0-08-025412-8.50044-9

Pourazizi, R., Mohtadi-Bonab, M. A., & Szpunar, J. A. (2020). Investigation of different failure modes in oil and natural gas pipeline steels. Engineering Failure Analysis, 109, 104400. https://doi.org/10.1016/j.engfailanal.2020.104400

Prabakaran, M. P., & Kannan, G. R. (2021). Effects of post-weld heat treatment on dissimilar laser welded joints of austenitic stainless steel to low carbon steel. International Journal of Pressure Vessels and Piping, 191(January), 104322. https://doi.org/10.1016/j.ijpvp.2021.104322

Primo, J. (2014). Gas Metal Arc Welding – GMAW Best Practices. ME Mechanical, 514.

Qiao, L., Zhu, J., & Wang, Y. (2021). Coupling physics in machine learning to predict interlamellar spacing and mechanical properties of high carbon pearlitic steel. Materials Letters, 293, 129645. https://doi.org/https://doi.org/10.1016/j.matlet.2021.129645

Rahman, S. M. M., Karim, K. E., & Simanto, M. H. S. (2016). Effect of Heat Treatment on Low Carbon Steel: An Experimental Investigation. Applied Mechanics and Materials, 860, 7–12. https://doi.org/10.4028/www.scientific.net/amm.860.7

Reyes, A., Bedolla, E., Perez, R., & Contreras, A. (2017). Effect of heat treatment on the mechanical and microstructural characterization of Mg-AZ91E/TiC composites. Composite Interfaces, 24(6), 593–609. https://doi.org/10.1080/09276440.2017.1248201

Saito, G., Zhang, T., Sakaguchi, N., Ohno, M., Matsuura, K., Takeuchi, M., Sano, T., Minoguchi, K., & Yamaoka, T. (2021). In-situ observation of abnormal grain growth in a low-alloyed carbon steel using SEM-EBSD. Materialia, 15, 100985. https://doi.org/10.1016/j.mtla.2020.100985

Senthur Prabu, S., Devendranath Ramkumar, K., & Arivazhagan, N. (2021). Microstructural evolution and elemental variation across the fusion interface of AISI 904L and Inconel 625 dissimilar weldments. Materials Today: Proceedings, 46(xxxx), 8260–8265. https://doi.org/10.1016/j.matpr.2021.03.246

Singh, R. (2020). 6 - Classification of steels. In R. Singh (Ed.), Applied Welding Engineering (Third Edition) (Third Edit, pp. 53–60). Butterworth-Heinemann. https://doi.org/https://doi.org/10.1016/B978-0-12-821348-3.00014-8

Valdes-Tabernero, M. A., Kumar, A., Petrov, R. H., Monclus, M. A., Molina-Aldareguia, J. M., & Sabirov, I. (2020). The sensitivity of the microstructure and properties to the peak temperature in an ultrafast heat treated low carbon-steel. Materials Science and Engineering A, 776(January), 138999. https://doi.org/10.1016/j.msea.2020.138999

Vural, M. (2014). 6.02 - Welding Processes and Technologies. In S. Hashmi, G. F. Batalha, C. J. Van Tyne, & B. Yilbas (Eds.), Comprehensive Materials Processing (pp. 3–48). Elsevier. https://doi.org/https://doi.org/10.1016/B978-0-08-096532-1.00603-8

Wahab, M. A. (2014). 6.03 - Manual Metal Arc Welding and Gas Metal Arc Welding. In S. Hashmi, G. F. Batalha, C. J. Van Tyne, & B. Yilbas (Eds.), Comprehensive Materials Processing (pp. 49–76). Elsevier. https://doi.org/https://doi.org/10.1016/B978-0-08-096532-1.00610-5

APPENDICES

APPENDIX A, ASTM E23

Designation: E23 – 07a$^{\varepsilon 1}$

An American National Standard

Standard Test Methods for Notched Bar Impact Testing of Metallic Materials[1]

This standard is issued under the fixed designation E23; the number immediately following the designation indicates the year of original adoption or, in the case of revision, the year of last revision. A number in parentheses indicates the year of last reapproval. A superscript epsilon (ε) indicates an editorial change since the last revision or reapproval.

This standard has been approved for use by agencies of the Department of Defense.

ε^1 NOTE—Editorial changes made throughout in September 2007.

1. Scope

1.1 These test methods describe notched-bar impact testing of metallic materials by the Charpy (simple-beam) test and the Izod (cantilever-beam) test. They give the requirements for: test specimens, test procedures, test reports, test machines (see Annex A1) verifying Charpy impact machines (see Annex A2), optional test specimen configurations (see Annex A3), precracking Charpy V-notch specimens (see Annex A4), designation of test specimen orientation (see Annex A5), and determining the percent of shear fracture on the surface of broken impact specimens (see Annex A6). In addition, information is provided on the significance of notched-bar impact testing (see Appendix X1), methods of measuring the center of strike (see Appendix X2).

1.2 These test methods do not address the problems associated with impact testing at temperatures below −196 °C (−320 °F, 77 K).

1.3 The values stated in SI units are to be regarded as the standard. Inch-pound units are provided for information only.

1.4 *This standard does not purport to address all of the safety concerns, if any, associated with its use. It is the responsibility of the user of this standard to establish appropriate safety and health practices and determine the applicability of regulatory limitations prior to use.* Specific precautionary statements are given in Section 5.

2. Referenced Documents

2.1 *ASTM Standards:*[2]

B925 Practices for Production and Preparation of Powder Metallurgy (PM) Test Specimens

E177 Practice for Use of the Terms Precision and Bias in ASTM Test Methods

E399 Test Method for Linear-Elastic Plane-Strain Fracture Toughness K_{Ic} of Metallic Materials

E604 Test Method for Dynamic Tear Testing of Metallic Materials

E691 Practice for Conducting an Interlaboratory Study to Determine the Precision of a Test Method

E1313 Guide for Recommended Formats for Data Records Used in Computerization of Mechanical Test Data for Metals (Discontinued 2000)[3]

3. Summary of Test Method

3.1 The essential features of an impact test are: a suitable specimen (specimens of several different types are recognized), a set of anvils, and specimen supports on which the test specimen is placed to receive the blow of the moving mass, a moving mass that has sufficient energy to break the specimen placed in its path, and a device for measuring the energy absorbed by the broken specimen.

4. Significance and Use

4.1 These test methods of impact testing relate specifically to the behavior of metal when subjected to a single application of a force resulting in multi-axial stresses associated with a notch, coupled with high rates of loading and in some cases with high or low temperatures. For some materials and temperatures the results of impact tests on notched specimens, when correlated with service experience, have been found to predict the likelihood of brittle fracture accurately. Further information on significance appears in Appendix X1.

5. Precautions in Operation of Machine

5.1 Safety precautions should be taken to protect personnel from the swinging pendulum, flying broken specimens, and hazards associated with specimen warming and cooling media.

6. Apparatus

6.1 *General Requirements:*

6.1.1 The testing machine shall be a pendulum type of rigid construction.

[1] These test methods are under the jurisdiction of ASTM Committee E28 on Mechanical Testing and are the direct responsibility of Subcommittee E28.07 on Impact Testing.

Current edition approved June 1, 2007. Published July 2007. Originally approved in 1933. Last previous edition approved 2007 as E23 – 07. DOI: 10.1520/E0023-07AE01.

[2] For referenced ASTM standards, visit the ASTM website, www.astm.org, or contact ASTM Customer Service at service@astm.org. For *Annual Book of ASTM Standards* volume information, refer to the standard's Document Summary page on the ASTM website.

[3] Withdrawn. The last approved version of this historical standard is referenced on www.astm.org.

4. Summary of Test Method

4.1 The essential features of an impact test are: a suitable specimen (specimens of several different types are recognized), a set of anvils, and specimen supports on which the test specimen is placed to receive the blow of the moving mass, a moving mass that has sufficient energy to break the specimen placed in its path, and an indicating device for measuring the absorbed energy of the broken specimen.

5. Significance and Use

5.1 These test methods of impact testing relate specifically to the behavior of metal when subjected to a single application of a force resulting in multi-axial stresses associated with a notch, coupled with high rates of loading and in some cases with high or low temperatures. For some materials and temperatures the results of impact tests on notched specimens, when correlated with service experience, have been found to predict the likelihood of brittle fracture accurately. Further information on significance appears in Appendix X1.

6. Precautions in Operation of Machine

6.1 Safety precautions should be taken to protect personnel from the swinging pendulum, flying broken specimens, and hazards associated with specimen warming and cooling media.

7. Apparatus

7.1 *General Requirements:*

7.1.1 The testing machine shall be a pendulum type of rigid construction.

7.1.2 The testing machine shall be designed and built to conform with the requirements given in Annex A1.

7.2 *Inspection and Verification:*

7.2.1 Procedures for direct verification of impact machines are provided in A2.2 and A2.3. The items listed in A2.2 require direct verification annually.

7.2.2 Procedures for indirect verification of Charpy machines, using verification specimens, are given in A2.4. Charpy impact machines require direct and indirect verification annually.

8. Test Specimens

8.1 *Configuration and Orientation:*

8.1.1 Specimens shall be taken from the material as specified by the applicable specification.

8.1.2 The type of specimen chosen depends largely upon the characteristics of the material to be tested. A given specimen may not be equally satisfactory for soft nonferrous metals and hardened steels; therefore, many types of specimens are recognized. In general, sharper and deeper notches are required to distinguish differences in very ductile materials or when using low testing velocities.

8.1.3 The specimens shown in Fig. 1 and Fig. 2 are those most widely used and most generally satisfactory. They are particularly suitable for ferrous metals, excepting cast iron.[3] The Charpy specimen designations are V-notch and U-notch.

[3] Report of Subcommittee XV on Impact Testing of Committee A03 on Cast Iron, Proceedings, ASTM, Vol 33 Part 1, 1933.

NOTE 1—Keyhole notch specimen is similar to U-notch, except the notch width is 1.6 mm or less.

8.1.4 The specimens commonly found suitable for powder metallurgy materials are shown in Fig. 3 and Fig. 4. Powder metallurgy impact test specimens shall be produced following the procedure in Practices B925. The impact test results of these materials are affected by specimen orientation. Therefore, unless otherwise specified, the position of the specimen in the machine shall be such that the pendulum will strike a surface that is parallel to the compacting direction. For powder metallurgy materials the impact test results are reported as unnotched absorbed energy.

8.1.5 Sub-size and supplementary specimen recommendations are given in Annex A3.

8.2 *Specimen Machining:*

8.2.1 When heat-treated materials are being evaluated, the specimen shall be finish machined, including notching, after the final heat treatment, unless it can be demonstrated that the impact properties of specimens machined before heat treatment are identical to those machined after heat treatment.

8.2.2 Notches shall be smoothly machined, but polishing has proven generally unnecessary.

NOTE 2—Variations in notch dimensions will affect the results of the tests. Appendix X1.2 illustrates the effects from varying notch dimensions on V-notch specimens.

NOTE 3—In keyhole notch specimens, carefully drill the round hole with a slow feed rate. Exercise care in cutting the slot to ensure that the surface of the drilled hole opposite the slot is not damaged.

8.2.3 Identification marks shall only be placed in the following locations on specimens: either of the 10-mm square ends; the side of the specimen that faces up when the specimen is positioned in the anvils (see Note 4); or the side of the specimen opposite the notch. No markings, on any side of the specimen, shall be within 10 mm of the center line of the notch. Permanent markers, laser engraving, scribes, electrostatic pencils, and other reasonable marking methods may be used for identification purposes. However, some marking methods can result in damage to the specimens if not used correctly. For example, excessive heat from electrostatic pencils or deformation to the specimen from stamping can change the mechanical properties of the specimen. Therefore, care shall always be taken to avoid damage to the specimen. Stamping and other marking processes that result in deformation of the specimen should only be used on the ends of the specimens, prior to notching.

NOTE 4—Careful consideration should be given before placing identification marks on the side of the specimen to be placed up when positioned in the anvils. If the test operator is not careful, the specimen can be placed in the machine with the identification marking resting on the specimen supports (that is, facing down). Under these circumstances, the absorbed energy value obtained may be unreliable.

8.2.4 Test specimens shall conform to the dimensions and tolerances shown in Fig. 1 or any other applicable figure in this test method.

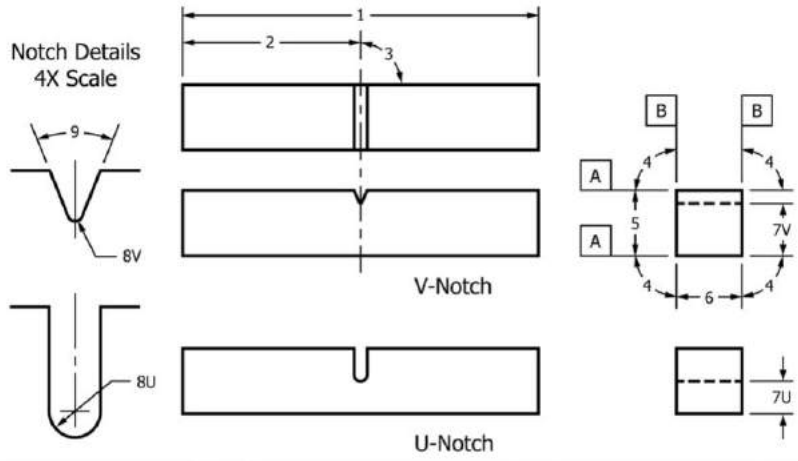

ID Number	Description	Dimension	Tolerance
1	Length of specimen	55 mm	+0/-2.5 mm
2	Centering of notch		±1 mm
3	Notch length to edge	90°	±2°
4	Adjacent sides angle	90°	±0.17°
5	Width	10 mm	±0.075 mm
6	Thickness	10 mm	±0.075 mm
7V	Ligament length, Type V	8 mm	±0.025 mm
7U	Ligament length, Type U	5 mm	±0.075 mm
8V	Radius of notch, Type V	0.25 mm	±0.025 mm
8U	Radius of notch, Type U	1 mm	±0.025 mm
9	Angle of notch	45°	±1°
A	Surface finish requirements	2 µm (Ra)	≤
B	Surface finish requirements	4 µm (Ra)	≤

FIG. 1 Charpy (Simple-Beam) Impact Test Specimens, V-Notch and U-Notch

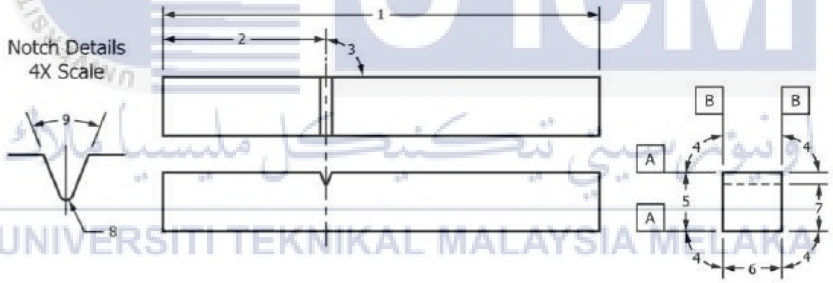

ID Number	Description	Dimension	Tolerance
1	Length of specimen	75 mm	+0/-2.5 mm
2	Notch to top	28 mm	
3	Notch length to edge	90°	±2°
4	Adjacent sides angle	90°	±0.17°
5	Width	10 mm	±0.025 mm
6	Thickness	10 mm	±0.025 mm
7	Ligament length	8 mm	±0.025 mm
8	Radius of notch	0.25 mm	±0.025 mm
9	Angle of notch	45°	±1°
A	Surface finish requirement	2 µm (Ra)	≤
B	Surface finish requirement	4 µm (Ra)	≤

FIG. 2 Izod (Cantilever-Beam) Impact Test Specimen

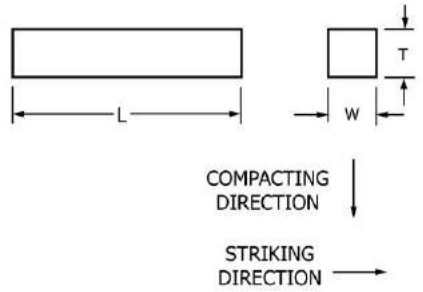

	Dimensions mm
L- Overall Length	55.0 ± 1.0
W-Width	10.00 ± 0.13
T-Thickness	10.00 ± 0.13

NOTE 1—Adjacent sides shall be at 90° ± 10 min.

FIG. 3 Unnotched Charpy (Simple Beam) Impact Test Specimen for Metal Powder Structural Materials

	Dimensions mm
L- Overall Length	75.0 ± 1.5
W-Width	10.00 ± 0.13
T-Thickness	10.00 ± 0.13

NOTE 1—Adjacent sides shall be at 90° ± 10 min.

FIG. 4 Izod (Cantilever-Beam) Impact Test Specimen for P/M Structural Materials

9. Procedure

9.1 *Preparation of the Apparatus:*

9.1.1 Perform a routine procedure for checking impact machines at the beginning of each day, each shift, or just prior to testing on a machine used intermittently. The results of these routine checks should be kept in a log book for the machine. After the testing machine has been ascertained to comply with Annex A1 and Annex A2, carry out the routine check as follows:

9.1.1.1 Visually examine the striker and anvils for obvious damage and wear.

9.1.1.2 Check the machine with a free swing. The indicating device shall indicate zero on machines reading directly in absorbed energy. On machines reading in degrees, the reading shall correspond to zero absorbed energy on the conversion chart furnished by the machine manufacturer. On machines that do not compensate for total frictional losses, the analog scale will not indicate zero. In this case, the indicated values, when converted to absorbed energy, shall be corrected for total frictional losses that are assumed to be proportional to the arc of the swing.

9.1.1.3 The percent friction and windage loss shall not exceed 0.4 % of the range capacity being tested and should not change by more than 10 % of the percent friction and windage loss measurements previously recorded on the machine. If the percent friction and windage loss does exceed 0.4 % or is significantly different from previous measurements, check the indicating device, the latch height, and the bearings for wear

and damage. However, if the machine has not been used recently, let the pendulum swing for 50 to 100 cycles, and repeat the percent friction and windage loss test before undertaking repairs to the machine. To ensure that percent friction and windage loss is within allowable tolerance, use one of the following evaluation procedures:

(1) For a machine equipped with an analog scale:

Raise the pendulum to the latched position;
Move the analog scale pointer to the range capacity being used;
Release the pendulum (without a specimen in the machine);
Allow the pendulum to cycle five times (a forward and a backward swing together count as one cycle);
Prior to the sixth forward swing set the analog scale pointer to between 5 and 10 % of the range capacity being used;
After the sixth forward swing record the value indicated by the analog scale pointer (convert to absorbed energy if necessary);
Divide the energy reading by 10;
Divide by the range capacity being used, and
Multiply by 100 to get the percent friction and windage loss.

(2) A machine equipped with a digital display:
Determine the percent friction and windage loss per manufacturer's procedure.

(3) For machine equipped with both an analog scale and digital display:
Determine the percent friction and windage loss using the same indicating device used to report absorbed energy (11.2.5 and A2.4).

NOTE 5—Prior to the 2012 version, the percent friction and windage loss was based on 11 (half) swings and the analog scale pointer was not engaged on the first swing. Now the pointer is engaged on the first swing. The difference is that the friction, windage, and analog scale pointer mechanism losses associated with the first swing are no longer assumed to be zero. On the first swing the pointer should go to 0.00, so any friction and windage losses that will be recorded will only show up on the following 10 (half) swings.

9.2 *Test Temperature Considerations:*

9.2.1 The temperature of testing affects the impact properties of most materials. For materials with a body centered cubic structure, a transition in fracture mode occurs over a temperature range that depends on the chemical composition and microstructure of the material. Test temperatures may be chosen to characterize material behavior at fixed values, or over a range of temperatures to characterize the transition region, lower shelf, or upper shelf behavior, or all of these. The choice of test temperature is the responsibility of the user of this test method and will depend on the specific application. For tests performed at room temperature, the temperature should be 20 °C ± 5 °C.

9.2.2 The temperature of a specimen can change significantly during the interval it is removed from the temperature conditioning environment, transferred to the impact machine, and the fracture event is completed (see Note 8). When using a heating or cooling medium near its boiling point, use data from the references in Note 8 or calibration data with thermocouples to confirm that the specimen is within the stated temperature tolerances when the striker contacts the specimen. If excessive adiabatic heating is expected, monitor the specimen temperature near the notch during fracture.

9.2.3 Verify temperature-measuring equipment at least every six months. If liquid-in-glass thermometers are used, an initial verification shall be sufficient, however, the device shall be inspected for problems, such as the separation of liquid, at least twice annually.

9.2.4 Hold the specimen at the desired temperature within ±1 °C (±2 °F) in the temperature conditioning environment. Any method of heating or cooling or transferring the specimen to the anvils may be used provided the temperature of the specimen immediately prior to fracture is essentially the same as the holding temperature (see Note 8). The maximum change in the temperature of the specimen allowed for the interval between the temperature conditioning treatment and impact is not specified here, because it is dependent on the material being tested and the application. The user of nontraditional or lesser used temperature conditioning and transfer methods (or specimen sizes) shall show that the temperature change for the specimen prior to impact is comparable to or less than the temperature change for a standard size specimen of the same material that has been thermally conditioned in a commonly used medium (oil, air, nitrogen, acetone, methanol), and transferred for impact within 5 s (see Note 8). Three temperature conditioning and transfer methods used in the past are: liquid bath thermal conditioning and transfer to the specimen supports with centering tongs; furnace thermal conditioning and robotic transfer to the specimen supports; placement of the specimen on the supports followed by in situ heating and cooling.

9.2.4.1 For liquid bath cooling or heating use a suitable container, which has a grid or another type of specimen positioning fixture. Cover the specimens, when immersed, with at least 25 mm (1 in.) of the liquid, and position so that the notch area is not closer than 25 mm to the sides or bottom of the container, and no part of the specimen is in contact with the container. Place the device used to measure the temperature of the bath in the center of a group of the specimens. Agitate the bath and hold at the desired temperature within ±1 °C (±2 °F). Thermally condition the specimens for at least 5 min before testing, unless a shorter thermal conditioning time can be shown to be valid by measurements with thermocouples. Leave the device (tongs, for example) used to handle the specimens in the bath for at least 5 min before testing, and return the device to the bath between tests.

9.2.4.2 When using a gas medium, position the specimens so that the gas circulates around them and hold the gas at the desired temperature within ±1 °C (±2 °F) for at least 30 min. Leave the device used to remove the specimen from the medium in the medium except when handling the specimens.

NOTE 6—Temperatures up to +260 °C may be obtained with certain oils, but "flash-point" temperatures should be carefully observed.

NOTE 7—For testing at temperatures down to −196 °C (77 °K), standard testing procedures have been found to be adequate for most metals.

NOTE 8—A study has shown that a specimen heated to 100 °C in water can cool 10 °C in the 5 s allowed for transfer to the specimen supports.[4] Other studies, using cooling media that are above their boiling points at room temperature have also shown large changes in specimen temperature

[4] Nanstad, R. K., Swain, R. L. and Berggren, R. G., "Influence of Thermal Conditioning Media on Charpy Specimen Test Temperature," *Charpy Impact Test: Factors and Variables, ASTM STP 1072*, ASTM, 1990, pp. 195-210.

during the transfer of specimens to the machine anvils. In addition, some materials change temperature dramatically during impact testing at cryogenic temperatures due to adiabatic heating.[5]

9.3 *Charpy Test Procedure:*

9.3.1 The Charpy test procedure may be summarized as follows: the test specimen is thermally conditioned and positioned on the specimen supports against the anvils; the pendulum is released without vibration, and the specimen is impacted by the striker. Information is obtained from the machine and from the broken specimen.

9.3.1.1 The 8 mm striker shall be used, unless the 2 mm striker is specified.

NOTE 9—For some materials, the striker radius can significantly affect the results.

9.3.2 To position a test specimen in the machine, self-centering tongs similar to those shown in Fig. 5 should be used

[5] Tobler R. L. Et al.," Charpy Impact Tests Near Absolute Zero," *Journal of Testing and Evaluation*, Vol 19, 1 1992.

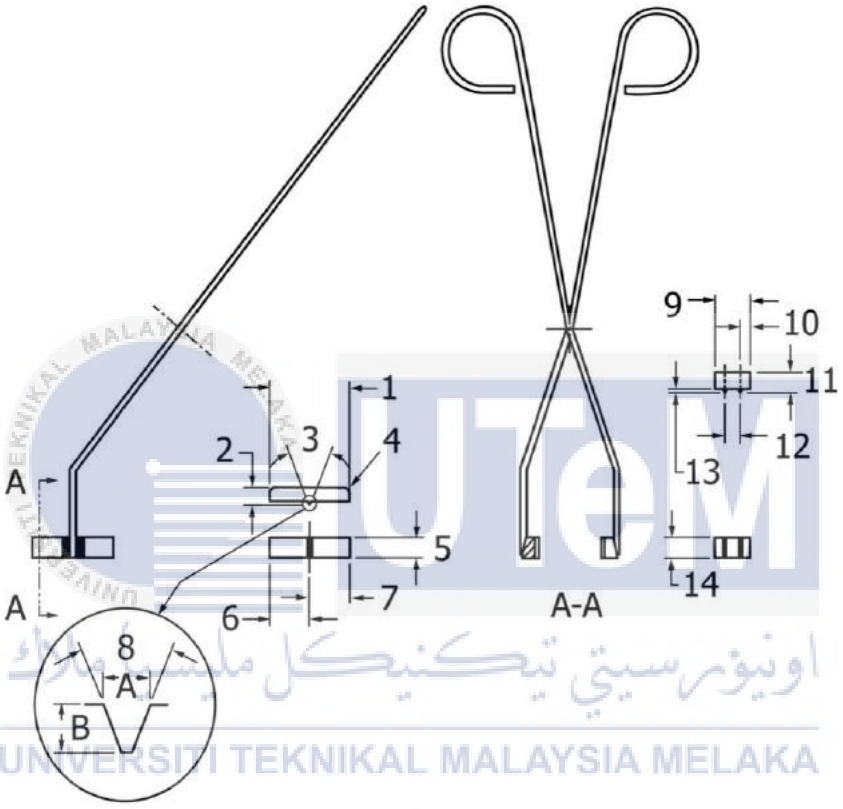

ID Number	Designation	Dimension, mm	ID Number	Designation	Dimension, mm
1	Support (notch side) length	39.93 + 0 −0.051	8B	10 mm specimen width	1.52 to 1.65
				5 mm specimen width	0.69 to 0.81
				3 mm specimen width	0.36 to 0.48
2	Support (notch side) height	7.94 ± 1	9	Solder pad length	17.46 ± 1
3	Insert angle	44.5 ± 0.5°	10	Solder pad extension	4.76 ± 1
4	Radius on support	2 ± 1	11	Solder pad height	9.5 ± 1
5	Support width	9.5 ± 1	12	rod	7.94 ± 1
6	Notch center	19.96	13		1.588 ± 1
7	Notch center	19.96	14	Solder pad width	9.5 ± 1
8A	10 mm specimen width	1.60 to 1.70			
	5 mm specimen width	0.74 to 0.80			
	3 mm specimen width	0.45 to 0.51			

FIG. 5 Centering Tongs for V-Notch Charpy Specimens

(see A1.10.1). The tongs illustrated in Fig. 5 are for centering V-notch specimens. If non V-notch specimens are used, modification of the tong design may be necessary. If an end-centering device is used, caution shall be taken to ensure that low-energy high-strength specimens will not rebound off this device into the pendulum and cause erroneously high recorded absorbed energy values. Many such devices are permanent fixtures of machines, and if the clearance between the end of a specimen in the test position and the centering device is not approximately 13 mm, the broken specimens may rebound into the pendulum.

9.3.3 To conduct the test, prepare the machine by raising the pendulum to the latched position, prepare the indicating device (set the analog scale pointer at the range capacity, or initialize the digital display, or both), position the specimen on the anvils, and release the pendulum. If a liquid bath or gas medium is being used for thermal conditioning, perform the following sequence in less than 5 s (for 10 × 10 × 55 mm specimens, see 9.2.4). Remove the test specimen from its cooling (or heating) medium with centering tongs that have been temperature conditioned with the test specimen, place the specimen in the test position, and release the pendulum smoothly. If a test specimen has been removed from the temperature conditioning bath and it is questionable that the test can be conducted within the 5 s time frame, return the specimen to the bath for the time required in 9.2 before testing.

9.3.3.1 If a fractured impact specimen does not separate into two pieces, report it as unbroken (see 10.2.2 for separation instructions). Unbroken specimens with absorbed energies of less than 80 % of the range capacity may be averaged with values from broken specimens. If the individual indicated absorbed energy values are not listed, report the percent of unbroken specimens with the average. If the absorbed energy exceeds 80 % of the range capacity and the specimen passes completely between the anvils, report the value as approximate (see 11.1) and do not average it with other values. If an unbroken specimen does not pass between the machine anvils, (for example, it stops the pendulum), the result shall be reported as exceeding the range capacity. A specimen shall never be struck more than once.

9.3.3.2 If a specimen jams in the machine, disregard the results and check the machine thoroughly for damage or misalignment, which would affect its direct verification, indirect verification, or both.

9.3.3.3 To prevent recording an erroneous indicated value, caused by jarring the analog scale pointer when locking the pendulum in its upright (ready) position, read the value for each test from the analog scale prior to locking the pendulum for the next test.

9.4 *Izod Test Procedure:*

9.4.1 The Izod test procedure may be summarized as follows: the test specimen is positioned in the specimen-holding fixture and the pendulum is released without vibration. Information is obtained from the machine and from the broken specimen. The details are described as follows:

9.4.2 Testing at temperatures other than room temperature is difficult because the specimen-holding fixture for Izod specimens is often part of the base of the machine and cannot be readily cooled (or heated). Consequently, Izod testing should be performed at room temperature.

9.4.3 Clamp the specimen firmly in the support vise so that the centerline of the notch is in the plane of the top of the vise within 0.125 mm. Prepare the indicating device (set the analog scale pointer at the range capacity or initialize the digital display, or both) and release the pendulum smoothly. Sections 9.3.3.1 – 9.3.3.3, also apply when testing Izod specimens.

10. Information Obtainable from Impact Tests

10.1 *The absorbed energy* shall be taken as the difference between the energy in the striking member at the instant of impact with the specimen and the energy remaining after breaking the specimen. This absorbed energy value is determined by the indicating device which has been corrected for total frictional losses.

10.2 *Lateral expansion measurement* methods shall take into account the fact that the fracture path seldom bisects the point of maximum expansion on both sides of a specimen. One half of a broken specimen may include the maximum expansion for both sides, one side only, or neither. Therefore, the expansion on each side of each specimen half shall be measured relative to the plane defined by the undeformed portion on the side of the specimen, as shown in Fig. 6. For example, if A_1 is greater than A_2, and A_3 is less than A_4, then the lateral expansion is the sum of $A_1 + A_4$.

10.2.1 Before making any lateral expansion measurements, it is essential that the two specimen halves are visually examined for burrs that may have formed during impact testing; if the burrs will influence the lateral expansion measurements, they shall be removed (by rubbing on emery cloth or any other suitable method), making sure that the protrusions to be measured are not rubbed during the removal of the burr. Then, examine each fracture surface to ascertain that the protrusions have not been damaged by contacting an anvil, a machine mounting surface, etc. Lateral expansion shall not be measured on a specimen with this type of damage.

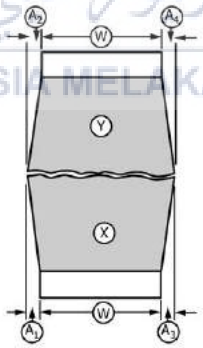

FIG. 6 Halves of Broken Charpy V-Notch Impact Specimen Illustrating the Measurement of Lateral Expansion, Dimensions A_1, A_2, A_3, A_4 and Original Thickness, Dimension W

10.2.2 Lateral expansion measurements shall be reported as follows. An unbroken specimen can be reported as broken if the specimen can be separated by pushing the hinged halves together once and then pulling them apart without further fatiguing the specimen, and the lateral expansion measured for the unbroken specimen (prior to bending) is equal to or greater than that measured for the separated halves. In the case where a specimen cannot be separated into two halves, the lateral expansion can be measured as long as the shear lips can be accessed without interference from the hinged ligament that has been deformed during testing. The specimen should be reported as unbroken.

10.2.3 Lateral expansion may be measured easily by using a gauge like the one shown in Fig. 7 (assembly and details shown in Fig. 8). Using this type of gauge the measurement is made with the following procedure: orient the specimen halves so that the compression sides are facing each other, take one half of the fractured specimen and press it against the anvil and indicator plunger and record the reading, make a similar measurement on the other half (same side) of the fractured specimen and disregard the lower of the two values, do the same for the other side of the fractured specimen, report the sum of the maximum expansions for the 2 sides as the lateral expansion for the specimen.

10.3 *The shear fracture appearance* may be determined using a variety of methods. The approach and the acceptable methods are defined in Annex A4. For each method, the user shall distinguish between regions formed by stable crack growth mechanisms, and regions formed by unstable crack growth mechanisms. For purposes of this Test Method, the "shear area" consists of those portions of the fracture surface that form by stable crack growth (Fracture Initiation Region, Shear Lips, and Final Fracture Region), as shown in Fig. 9.

The shear fracture appearance is typically calculated as the difference between the total fractured area (Fracture Initiation Region, Shear Lips, Unstable Fracture Region, and Final Fracture Region) and the area of unstable fracture region, divided by the total fractured area, times 100. The measurement methods described in Annex A4 provide estimates for the area of the unstable fracture region (directly or indirectly), but do not consider details of the fracture mode for the unstable region. The unstable fracture region could be 100 % cleavage, a mixture of cleavage and ductile-dimple fracture morphologies, a mixture of intergranular and ductile-dimple fracture morphologies, or a mixture of other fracture morphologies.

NOTE 10—Carbon steels often exhibit a classic cleavage region that identifies the unstable fracture region with a well-defined area of shiny fracture that is easy to recognize and measure. Other steels, such as quenched and tempered SAE 4340, alloys have a region of unstable fracture that consists of an intimate mixture of cleavage facets and ductile dimples (only apparent at high magnifications). Some embrittled steels can exhibit partially intergranular fracture, as well. In these cases the area of unstable fracture may not be as easy to identify.

11. Report

11.1 *Absorbed energy values above 80 %* of the range capacity are inaccurate and shall be reported as approximate. Ideally an impact test would be conducted at a constant impact velocity. In a pendulum-type test, the velocity decreases as the fracture progresses. For specimens that have absorbed energies approaching 80 % of the range capacity, the velocity of the pendulum decreases (to about 45 % of the initial velocity) during fracture to the point that accurate absorbed energies are no longer obtained.

11.2 *For commercial acceptance testing*, report the following information (for each specimen tested):

11.2.1 Specimen type,

11.2.2 Specimen size (if sub-size specimen),

11.2.3 Test temperature,

11.2.4 For Charpy testing specify the striker radius as 8 mm or 2 mm,

11.2.5 Absorbed energy, and

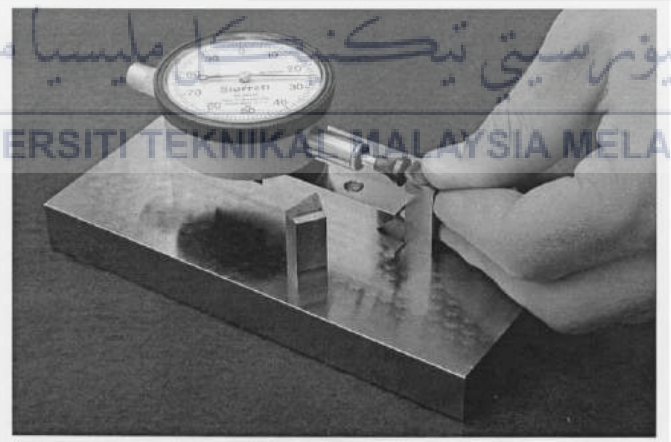

FIG. 7 Lateral Expansion Gauge for Charpy Impact Specimens

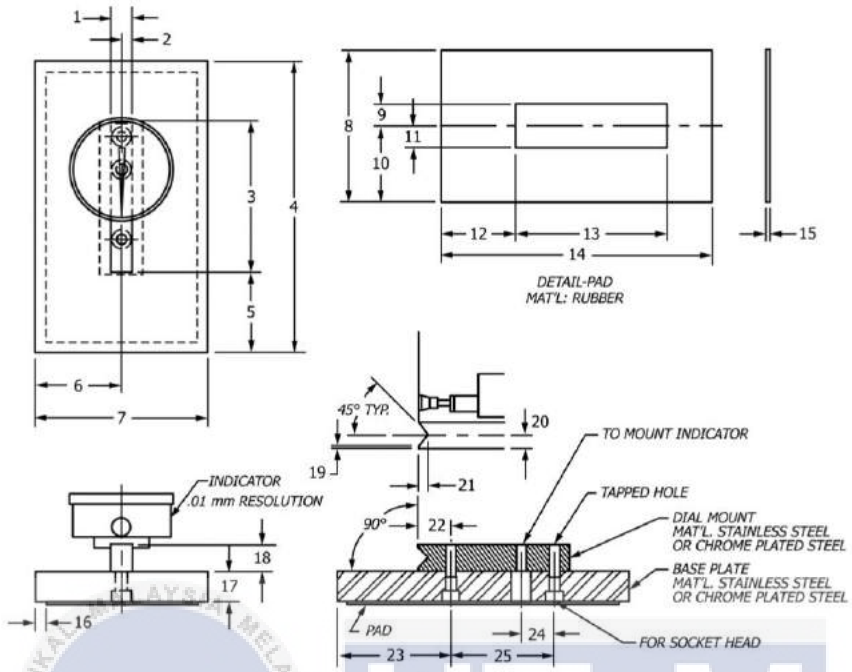

ID Number	Dimension, mm	ID Number	Dimension, mm
1	12.7	15	1.6
2	6.4	16	6.4
3	88.9	17	17.5
4	171.5	18	15.9
5	47.6	19	1.7
6	50.8	20	8.3
7	101.6	21	6.1
8	88.9	22	19.1
9	12.7	23	66.7
10	44.5	24	19.1
11	12.7	25	60.3
12	43.2		
13	88.9		
14	158.8		

FIG. 8 Assembly and Details for Lateral Expansion Gauge

11.2.6 Any other contractual requirements.

11.3 *For other than commercial acceptance testing* the following information is often reported in addition to the information in 11.2:

11.3.1 Lateral expansion,

11.3.2 Unbroken specimens,

11.3.3 Shear fracture appearance (See Note A4.1),

11.3.4 Specimen orientation, and

11.3.5 Specimen location.

NOTE 11—Even when the test temperature is specified as room temperature, report the actual temperature.

12. Precision and Bias

12.1 *An Interlaboratory study* used CVN verification specimens of low-energy and of high-energy to find sources of variation in the CVN absorbed energy. Data from 29 laboratories were included with each laboratory testing one set of five verification specimens of each energy level. Except being limited to only two energy levels (by availability of verification specimens), Practice E691 was followed for the design and analysis of the data; the details are given in ASTM Research Report No. RR:E28-1014.[6]

12.2 *Precision—The Precision* information given below is for the average CVN absorbed energy of five test determinations at each laboratory for each material.

[6] Supporting data have been filed at ASTM International Headquarters and may be obtained by requesting Research Report RR: RR:E28-1014.

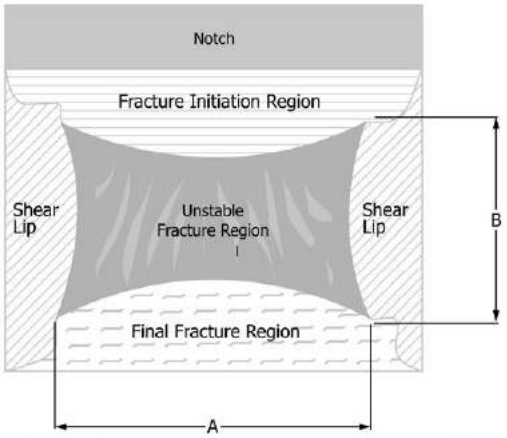

NOTE 1—Measure average dimensions A and B to the nearest 0.5 mm. Determine the shear fracture appearance using Table A4.1 or Table A4.2.

FIG. 9 Schematic of the Fracture Surface of a Charpy V-Notch Impact Test Specimen Showing the Various Region of Fracture

Material	Low-Energy J	High-Energy J
Absorbed Energy	15.9	96.2
95 % Repeatability Limits	2.4	8.3
95 % Reproducibility Limits	2.7	9.2

The terms repeatability and reproducibility limits are used as defined in Practice E177. The respective standard deviations among test results may be obtained by dividing the above limits by 2.8.

12.3 *Bias—Bias cannot be defined* for CVN absorbed energy. The physical simplicity of the pendulum design is complicated by complex energy loss mechanisms within the machine and the specimen. Therefore, there is no absolute standard to which the absorbed energy can be compared.

13. Keywords

13.1 Charpy test; shear fracture appearance; impact test; Izod test; notched specimens; pendulum machine

ANNEXES

(Mandatory Information)

A1. GENERAL REQUIREMENTS FOR IMPACT MACHINES

A1.1 *The machine frame* shall be equipped with a bubble level or a machined surface suitable for establishing levelness of the axis of pendulum bearings or, alternatively, the levelness of the axis of rotation of the pendulum may be measured directly. The machine shall be level to within 3:1000 and securely bolted to a concrete floor not less than 150 mm thick or, when this is not practical, the machine shall be bolted to a foundation having a mass not less than 40 times that of the pendulum. The bolts shall be tightened as specified by the machine manufacturer.

A1.2 *An anatog scate and digital display*, graduated in degrees or energy, on which readings can be estimated in increments of 0.25 % of the range capacity or less shall be furnished for the machine.

A1.2.1 The analog scales and digital displays may be compensated for total frictional losses. The error in the indicating device at any point shall not exceed 0.2 % of the range capacity or 0.4 % of the reading, whichever is larger. (See A2.3.8.)

A1.3 *The total frictional losses* of the machine during the swing in the striking direction shall not exceed 0.75 % of the range capacity, and pendulum energy loss from friction in the analog scale pointer mechanism shall not exceed 0.25 % of range capacity. See A2.3.8 for total frictional losses calculations.

A1.4 *The position of the pendulum*, when hanging freely, shall be such that the striker is within 2.5 mm from the test specimen. When the indicating device has been positioned to read zero energy in a free swing, it shall read within 0.2 % of the range capacity when the striker of the pendulum is held against the test specimen. The plane of swing of the pendulum shall be perpendicular to the transverse axis of the Charpy specimen anvils or Izod vise within 3:1000.

A1.5 *Transverse play of the pendulum* at the striker shall not exceed 0.75 mm under a transverse force of 4 % of the effective weight of the pendulum applied at the center of strike. Radial play of the pendulum bearings shall not exceed 0.075 mm.

A1.6 *The impact velocity* (tangential velocity) of the pendulum at the center of strike shall not be less than 3 nor more than 6 m/s.

A1.7 *The height of the center of strike* in the latched position, above its free hanging position, shall be within 0.4 % of the range capacity divided by the supporting force, measured as described in A2.3.5.1. If total frictional losses are compensated for by increasing the height of drop, the height of drop may be increased by not more than 1 %.

A1.8 *The mechanism for releasing the pendulum* from its initial position shall operate freely and permit release of the pendulum without initial impulse, retardation, or side vibration. If the same lever used to release the pendulum is also used to engage the brake, means shall be provided for preventing the brake from being accidentally engaged.

A1.9 *Specimen clearance* is needed to ensure satisfactory results when testing materials of different strengths and compositions. The test specimen shall exit the machine with a minimum of interference. Pendulums used on Charpy machines are of three basic designs, as shown in Fig. A1.1.

A1.9.1 When using a C-type pendulum or a compound pendulum, the broken specimen will not rebound into the pendulum and slow it down if the clearance at the end of the specimen is at least 13 mm or if the specimen is deflected out of the machine by some arrangement such as that shown in Fig. A1.1.

A1.9.2 When using a U-type pendulum, means shall be provided to prevent the broken specimen from rebounding against the pendulum (see Fig. A1.1). In most U-type pendulum machines, steel shrouds should be designed and installed to the following requirements: (*a*) thickness of approximately 1.5 mm, (*b*) minimum hardness of 45 HRC, (*c*) radius of less than 1.5 mm at the underside corners, and (*d*) positioned so that the clearance between them and the pendulum overhang (both top and sides) does not exceed 1.5 mm. In machines where the opening within the pendulum permits clearance between the ends of a specimen (resting on the specimen supports) and the shrouds, and this clearance is at least 13 mm, the requirements (*a*) and (*d*) need not apply.

A1.10 *Charpy Apparatus*:

A1.10.1 Means shall be provided (see Fig. A1.2) to locate and support the test specimen against two anvil blocks in such a position that the center of the notch is located within 0.25 mm of the midpoint between the anvils (see 9.3.2).

A1.10.2 The supports shall be of the forms and dimensions shown in Fig. A1.2. Other dimensions of the pendulum and supports should be such as to minimize interference between the pendulum and broken specimens.

A1.10.3 The center line of the striker shall advance in the plane that is within 0.40 mm of the midpoint between the supporting edges of the anvils. The striker shall be perpendicular to the longitudinal axis of the specimen within 5:1000. The striker shall be parallel within 1:1000 to the face of a perfectly square test specimen held against the anvils.

A1.10.4 The striker shall conform to dimensions and tolerances shown in Fig. A1.3. The standard 8 mm striker is shown in Fig. A1.3(a) and optional 2 mm striker is shown in Fig. A1.3(b).

A1.11 *Izod Apparatus*:

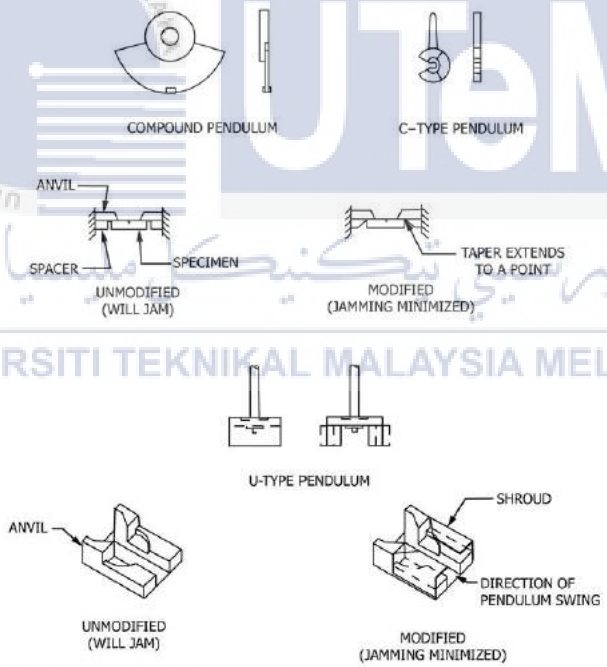

FIG. A1.1 Typical Pendulums and Anvils for Charpy Machines, Shown with Modifications to Minimize Jamming

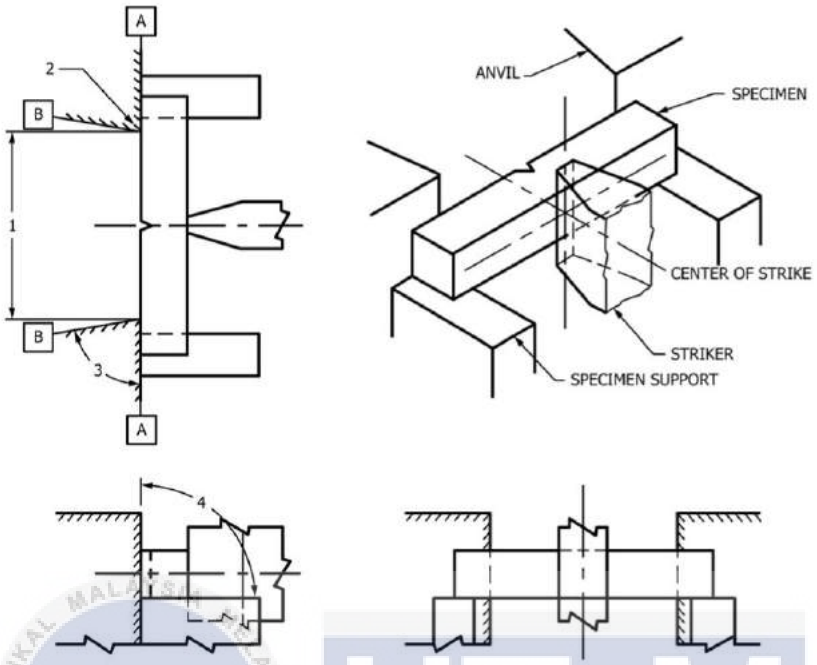

ID Num	Designation	Dimension	Tolerance
1	Span between anvils	40.00 mm	±0.05 mm
2	Anvil radius	1.00 mm	±0.05 mm
3	Anvil angle	80°	±2°
4	Anvil-Support angle	90°	±0.15°
A and B	Surface finish, Anvils	0.1 μm (R_a)	≤

FIG. A1.2 Charpy Anvils and Supports

A1.11.1 Means shall be provided (see Fig. A1.4) for clamping the specimen in such a position that the face of the specimen is parallel to the striker within 1:1000. The edges of the clamping surfaces shall be sharp angles of 90° ± 1° with radii less than 0.40 mm. The clamping surfaces shall be smooth with a 2 μm (R_a) finish or better, and shall clamp the specimen firmly at the notch with the clamping force applied in the direction of impact. For rectangular specimens, the clamping surfaces shall be flat and parallel within 0.025 mm. For cylindrical specimens, the clamping surfaces shall be contoured to match the specimen and each surface shall contact a minimum of π/2 rad (90°) of the specimen circumference.

A1.11.2 The dimensions of the striker and its position relative to the specimen clamps shall be as shown in Fig. A1.4.

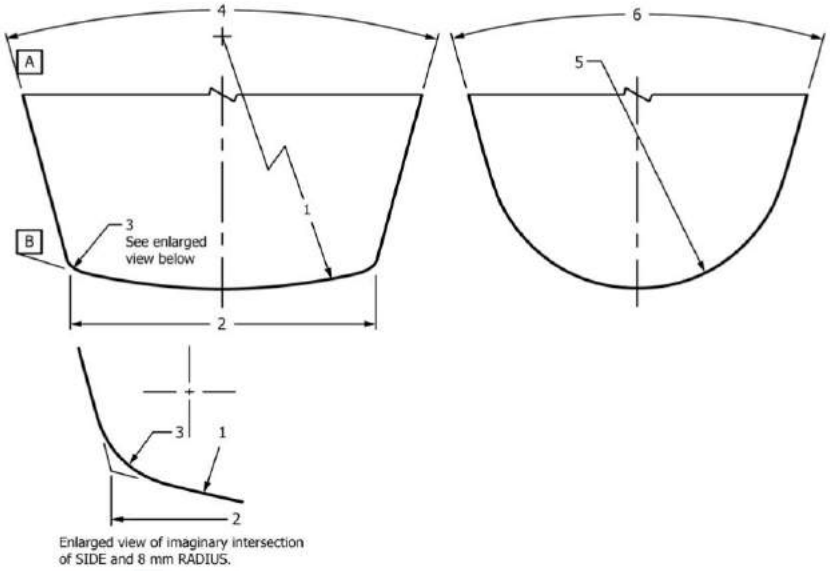

ID Num	Designation	Dimension	Tolerance
1	Striker radius, 8 mm Striker	8.00 mm	±0.05 mm
2	Striker width, 8 mm Striker	4.00 mm	±0.05 mm
3	Striker corner radii, 8 mm Striker	0.25 mm	+0.50/-0.05 mm
4	Striker angle, 8 mm Striker	30°	±2°
A and B	Striker Finish, 8 mm Striker	0.1 μm (R_a)	≤
5	Striker radius, 2 mm Striker	2.00 mm	+0.50/-0 mm
6	Striker angle, 2 mm Striker	30°	±1°

FIG. A1.3 Charpy Strikers

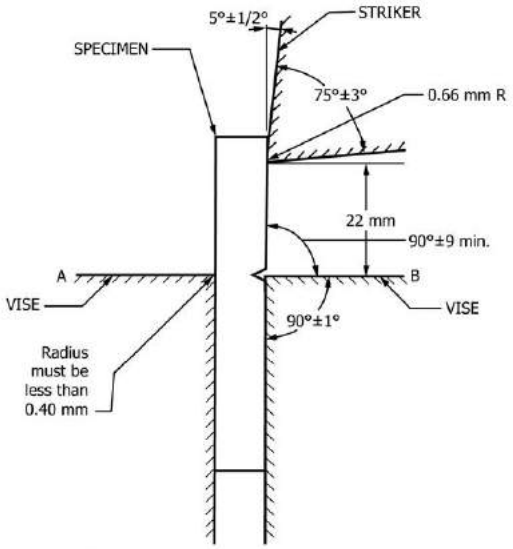

NOTE 1—All dimensional tolerances shall be ±0.05 mm unless otherwise specified.
NOTE 2—The clamping surfaces of A and B shall be flat and parallel within 0.025 mm.
NOTE 3— Surface finish on striker and vise shall be 2 µm (R_a).
NOTE 4—Striker width shall be greater than that of the specimen being tested.

FIG. A1.4 Izod (Cantilever-Beam) Impact Test

A2. VERIFICATION OF PENDULUM IMPACT MACHINES

A2.1 *The verification of impact machines has two parts:* direct verification, which consists of inspecting the machine to ensure that the requirements of this annex and Annex A1 are met, and indirect verification, which entails the testing of verification specimens.

A2.1.1 Izod machines require direct verification annually.

A2.1.2 Charpy machines require direct and indirect verification annually. Data is valid only when produced within 365 days following the date of the most recent successful indirect verification test. Charpy machines shall also be verified immediately after replacing parts that may affect the measured absorbed energy, after making repairs or adjustments, after they have been moved, or whenever there is reason to doubt the accuracy of the results, without regard to the time interval. These restrictions include cases where parts, which may affect the measured absorbed energy, are removed from the machine and then reinstalled without modification (with the exception of when the striker or anvils are removed to permit use of a different striker or set of anvils, or both and then are reinstalled, see A2.1.3). It is not intended that parts not subjected to wear (such as pendulum and indicating device linearity) require direct verification each year unless a problem is evident. Only the items cited in A2.2 require direct verification annually. Other parts of the machine require direct verification at least once, when the machine is new, or when parts are replaced.

A2.1.3 Charpy machines do not require immediate indirect verification after removal and replacement of the striker or anvils, or both, that were on the machine when it was verified provided the following safeguards are implemented: *(1)* an organizational procedure for the change is developed and followed, *(2)* high-strength low-energy quality control specimens (see A2.4.1.1 for guidance in absorbed energy range for these low-energy level specimens) are tested prior to removal and immediately after installation of the previously verified striker or anvils, or both within the 365 day indirect verification period, *(3)* the results of the before and after tests of the quality control specimens are within 1.4 J of each other, *(4)* the results of the comparisons are kept in a log book, and *(5)* before reattachment, the striker and anvils are visually inspected for wear and dimensionally verified to assure that they meet the

required tolerances of Fig. A1.2 and Fig. A1.3. The use of verification specimens with certified absorbed energy values is not required and internal quality control specimens are permitted.

A2.2 *Direct Verification of Parts Requiring Annual Inspection:*

A2.2.1 Inspect the specimen supports, anvils, and striker and replace any of these parts that show signs of wear. A straight edge or radius gage can be used to discern differences between the used and unused portions of these parts to help identify a worn condition (see Note A2.1).

NOTE A2.1—To measure the anvil or striker radii, the user may make a replica (casting) of the region of interest and measure cross sections of the replica. This can be done with the anvils and striker in place on the machine or removed from the machine. Make a dam with cardboard and tape surrounding the region of interest, then pour a low-shrinkage casting compound into the dam (silicon rubber casting compounds work well). Allow the casting to cure, remove the dam, and slice cross sections through the region of interest with a razor. Use these cross sections to make radii measurements on optical comparators or other instruments.

A2.2.2 Ensure the bolts that attach the anvils and striker to the machine are tightened to the manufacturer's specifications.

A2.2.3 Verify that the shrouds, if applicable, are properly installed (see A1.9.2).

A2.2.4 The pendulum release mechanism, which releases the pendulum from its initial position, shall comply with A1.8.

A2.2.5 Check the level of the machine in both directions (see A1.1).

A2.2.6 Check that the foundation bolts are tightened to the manufacturer's specifications. Expansion bolts or fasteners with driven-in inserts shall not be used for foundations.

NOTE A2.2—Expansion bolts or fasteners with driven-in inserts will work loose or will tighten up against the bottom of the machine indicating a false high torque value when the bolts are tightened.

A2.2.7 Check the indicating device zero and the percent friction and windage loss of the machine as described in 9.1.

A2.3 *Direct Verification of Parts to be Verified at Least Once:*

A2.3.1 Charpy anvils and supports or Izod vises shall conform to the dimensions shown in Fig. A1.2 or Fig. A1.4.

NOTE A2.3—The impact machine will be inaccurate to the extent that some energy is used in deformation or movement of its component parts or of the machine as a whole; this energy will be registered as used in fracturing the specimen and can result in erroneously high measurements of absorbed energy.

A2.3.2 The striker shall conform to the dimensions shown in Fig. A1.3 or Fig. A1.4. The mounting surfaces shall be clean and free of defects that would prevent a good fit. Check that the striker complies with A1.10.3 (for Charpy tests) or A1.11.1 (for Izod tests).

A2.3.3 The pendulum alignment shall comply with A1.4 and A1.5. If the side play in the pendulum or the radial play in the bearings exceed the specified limits, adjust or replace the bearings, or a combination thereof.

A2.3.4 *Determine the Center of Strike*—For Charpy machines the center of strike of the pendulum is determined using a half-thick specimen (10 × 5 × 55 mm) in the test position. With the striker in contact with the specimen, a line marked along the top edge of the specimen on the striker will indicate the center of strike. For Izod machines, the center of strike may be considered to be the contact line when the pendulum is brought into contact with a specimen in the normal testing position.

A2.3.5 *Determine the Potential Energy*—The following procedure shall be used when the center of strike of the pendulum is coincident with the radial line from the centerline of the pendulum bearings (herein called the axis of rotation) to the center of gravity (see Appendix X2). If the center of strike is more than 1.0 mm from this line, suitable corrections in elevation of the center of strike shall be made in A2.3.8.1 and A2.3.9, so that elevations set or measured correspond to what they would be if the center of strike were on this line. The potential energy of the system is equal to the height from which the pendulum falls, as determined in A2.3.5.2, times the supporting force, as determined in A2.3.5.1.

A2.3.5.1 To measure the supporting force, support the pendulum horizontally to within 15:1000 with two supports, one at the bearings (or center of rotation) and the other at the center of strike on the striker (see Fig. A2.1). Then arrange the support at the striker to react upon some suitable weighing device such as a platform scale or balance, and determine the weight to within 0.4 %. Take care to minimize friction at either point of support. Make contact with the striker through a round rod crossing the center of strike. The supporting force is the scale reading minus the weights of the supporting rod and any shims that may be used to maintain the pendulum in a horizontal position.

A2.3.5.2 Determine the height of pendulum drop for compliance with the requirement of A1.7. On Charpy machines determine the height from the top edge of a half-thick (or center of a 10 × 10 × 55 mm) specimen to the elevated position of the center of strike within 0.1 %. On Izod machines determine the height from a distance 22.66 mm above the vise to the release position of the center of strike within 0.1 %. The height may be determined by direct measurement of the elevation of the center of strike or by calculation from the change in angle of the pendulum using the following formulas (see Fig. A2.1):

$$h = S\,(1 - \cos\beta) \tag{A2.1}$$

$$h_1 = S\,(1 - \cos\alpha) \tag{A2.2}$$

where:

h = initial elevation of the striker, m,
S = length of the pendulum distance to the center of strike, m,
β = angle of fall,
h_1 = height of rise, m, and
α = angle of rise.

A2.3.6 Determine the impact velocity, v, of the machine, neglecting friction, by means of the following equation:

$$v = \sqrt{2gh} \tag{A2.3}$$

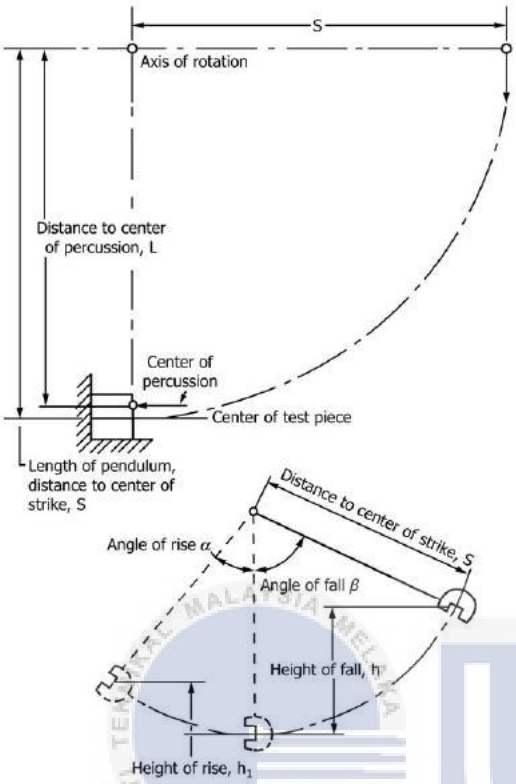

FIG. A2.1 Dimensions for Calculations

where:

v = velocity, m/s,
g = acceleration of gravity, 9.81 m/s^2, and
h = initial elevation of the striker, m.

A2.3.7 The center of percussion shall be at a point within 1 % of the distance from the axis of rotation to the center of strike in the specimen, to ensure that minimum force is transmitted to the point of rotation. Determine the location of the center of percussion as follows:

A2.3.7.1 Using a stop watch or some other suitable time-measuring device, capable of measuring time to within 0.2 s, swing the pendulum through a total angle not greater than 15° and record the time for 100 complete cycles (to and fro). The period of the pendulum then, is the time for 100 cycles divided by 100.

A2.3.7.2 Determine the center of percussion by means of the following equation:

$$L = \frac{gp^2}{4\pi^2} \quad \text{(A2.4)}$$

where:

L = distance from the axis to the center of percussion, m,
g = local gravitational acceleration (accuracy of one part in one thousand), m/s^2,
π = 3.1416, and
p = period of a complete swing (to and fro), s.

A2.3.8 *Determination of the Total Frictional Losses*—The friction and windage losses of the pendulum and friction in the indicating device, if not corrected, will be included in the energy loss attributed to breaking the specimen and can result in erroneously high measurements of absorbed energy. For machines recording in degrees, total frictional losses are usually not compensated for by the machine manufacturer, whereas in machines recording directly in energy, they are usually compensated for by increasing the starting height of the pendulum. Determine total frictional losses as follows.

A2.3.8.1 Without a specimen in the machine, and prepare the indicating device (set the analog scale pointer at range capacity or initialize the digital display, or both) release the pendulum from its starting position and record the energy value indicated. This value shall indicate zero absorbed energy if total frictional losses have been corrected by the manufacturer. Now raise the pendulum slowly until the indicating device is at the value obtained in the free swing. Secure the pendulum at this height and within 0.1 % determine the vertical distance from the center of strike to the top of a half-thick specimen positioned on the specimen supports (see A2.3.5). Determine the supporting force as in A2.3.5.1 and multiply by this vertical distance. The difference between this value and the initial potential energy is the total frictional losses. For analog scale, without resetting the analog scale pointer, repeatedly release the pendulum from its initial position until the pointer shows no further movement. The energy loss determined by the final position of the analog scale pointer is friction and windage losses of the pendulum alone. The friction in the analog scale pointer mechanism alone is then the difference between the total frictional losses and the friction and windage losses of the pendulum alone.

A2.3.9 The indicating device accuracy shall be checked to ensure that it is recording accurately over the entire range capacity (see A1.2.1). Check it at approximately 0, 10, 20, 30, 50, and 70 % of each range capacity. With the striker marked to indicate the center of strike, lift the pendulum and set it in a position where the indicating device reads, for example, 13 J. Secure the pendulum at this height and within 0.1 % determine the vertical distance from the center of strike to the top of a half-thick specimen positioned on the specimen supports (see A2.3.5). Determine the residual energy by multiplying the height of the center of strike by the supporting force, as described in A2.3.5.1. Increase this value by the total frictional losses for a free swing (see A2.3.8.1) multiplied by the ratio of the angle of swing of the pendulum from the latch to the energy value being evaluated to the angle of swing of the pendulum from the latch to the zero energy reading. Subtract the sum of the residual energy and proportional total frictional losses from the potential energy at the latched position (see A2.3.5). The indicating device shall agree with the energy calculated within the limits of A1.2.1. Make similar calculations at other points of the indicating device. Analog scales that indicate in degrees shall be checked using the above procedure. Degree readings

from the analog scale shall be converted to absorbed energy using the conversion formula or table normally used in testing. The analog scale pointer mechanism shall not overshoot or drop back with the pendulum. Make test swings from various heights to check visually the operation of the analog scale pointer over several portions of the analog scale.

NOTE A2.4—In this way the analog scale degree reading formula or table can also be checked for total frictional losses corrections.

A2.4 *Indirect Verification*:

A2.4.1 Indirect verification requires the testing of verification specimens with certified absorbed energy values to verify the accuracy of Charpy impact machines.

A2.4.1.1 Verification specimens with certified absorbed energy values are produced at low (typically 13 to 20 J), high (typically 88 to 136 J), and super-high (typically 176 to 244 J) energy levels. To meet the indirect verification requirements, the average absorbed energy value determined for a set of verification specimens at each energy level tested shall correspond to the certified absorbed energy values of the verification specimens within 1.4 J (1.0 ft lbf) or 5.0 %, whichever is greater.

A2.4.1.2 The certified absorbed energy values for the verification specimens shall be established on the three reference machines owned, maintained, and operated by NIST in Boulder, CO.

A2.4.2 The verified range of a Charpy range capacity is defined with reference to the lowest and highest energy level verification specimens tested. These values are determined from tests on sets of verification specimens at two or more energy levels, except in the case where a Charpy range capacity is too low for two energy levels to be tested. In this case, one energy level can be used for indirect verification.

A2.4.3 Determine the usable range of the range capacity prior to testing verification specimens. The usable range of an impact machine is dependent upon the resolution of the indicating device at the low end and the range capacity at the high end.

A2.4.3.1 The resolution of the indicating device establishes the lower limit of the usable range. The lower limit is equal to 25 times the resolution of the indicating device at 15 J.

NOTE A2.5—On analog scales, the resolution is the smallest change in energy that can be discerned on the analog scale. This is usually ¼ to ⅕ of the difference between two adjacent marks on the scale at the 15 J energy level.

NOTE A2.6—Digital displays usually incorporate devices, such as digital encoders, with a fixed discrete angular resolution. The resolution of these types of indicating devices is the smallest change in absorbed energy that can be consistently measured at 15 J. The resolution of these types of indicating devices is usually not a change in the last digit shown on the digital display because resolution is a function of the angular position of the pendulum and changes throughout the swing. One method for determining resolution of indicating devices that incorporate a verification mode, in which live absorbed energy is available, is to move the pendulum slowly in the area of 15 J. The smallest observable change in the indicating device is the resolution.

A2.4.3.2 The upper limit of the usable range is equal to 80 % of the range capacity.

A2.4.4 Only verification specimens that are within the usable range of the range capacity shall be tested. To verify the range capacity over its full usable range, test the lowest and highest energy levels of verification specimens commercially available that are within the range capacity's usable range. If the ratio between the highest and lowest verification specimens' certified absorbed energy values tested is greater than four, testing of a third set of intermediate energy level verification specimens is required (if the specimens are commercially available).

NOTE A2.7—Use the typical upper bound of the energy range given for the low, high, and super-high energy verification specimens (20, 136, and 244 J respectively) to determine the highest energy level verification specimens that can be tested. Alternately, use the typical lower bound of the energy range given for the verification specimens to determine the minimum energy level for testing.

A2.4.4.1 If the low energy verification specimens were not tested (only high and super-high verification specimens were tested), the lower limit of the verified range shall be one half the certified absorbed energy value of the lowest energy verification specimens set tested.

NOTE A2.8—For example, if the certified absorbed energy value of the high-energy verification specimens tested was 100 J, the lower limit would be 50 J.

A2.4.4.2 If the highest energy verification specimens commercially available for a given Charpy range capacity were not tested, the upper limit of the verified range shall be 1.5 times the certified absorbed energy value of the highest energy verification specimens tested.

NOTE A2.9—For example, if the machine being tested has a range capacity of 325 J and only low and high-energy verification specimens were tested, the upper limit of the verified range would be 150 J (100 J × 1.5 = 150 J), assuming that the high-energy verification specimens tested had a certified absorbed energy value of 100 J. To verify this range capacity over its full usable range, low-, high-, and super-high energy verification specimens would have to be tested, because super-high energy verification specimens can be tested on a 325 J range capacity (80 % of 325 J is 260 J, and the certified absorbed energy value of super-high energy verification specimens never exceeds 260 J). See Table A2.1.

TABLE A2.1 Verified Ranges for Various Range Capacities and Verification Specimens Tested[A]

Range Capacity J	Resolution J	Usable Range J	Verification Specimens Tested			Verified Range J
			Low	High	Super-high	
80	0.10	2.5 to 64	X	. . .	. . .	2.5 to 64
160	0.20	5.0 to 128	X	X	. . .	5.0 to 128
325	0.25	6.25 to 260	X	X	X	6.25 to 260
400	0.30	7.5 to 320	. . .	X	X	50 to 320
400	0.15	3.75 to 320	X	X	. . .	3.75 to 150
400	0.15	3.75 to 320	X	X	X	3.75 to 320

[A] In these examples, the high-energy verification specimens are assumed to have a certified absorbed energy value of 100 J.

A3. ADDITIONAL IMPACT TEST SPECIMEN CONFIGURATIONS

A3.1 *Sub-Size Specimen*—When the amount of material available does not permit making the standard impact test specimens shown in Fig. 1 and Fig. 2, smaller specimens may be used, but the results obtained on different sizes of specimens cannot be compared directly (X1.3). When Charpy specimens other than the standard are necessary or specified, they should be selected from Fig. A3.1. When reporting sub-size specimen dimensions, list the width, thickness, and length (for example, the upper left specimen in Fig. A3.1 would be 10 × 2.5 × 55 mm).

A3.2 *Supplementary Specimens*—For economy in preparation of test specimens, special specimens of round or rectangular cross section are sometimes used for cantilever beam test. These are shown as Specimens X, Y, and Z in Fig. A3.2 and Fig. A3.3. Specimen Z is sometimes called the Philpot specimen, after the name of the original designer. For hard materials, the machining of the flat surface struck by the pendulum is sometimes omitted. Types Y and Z require a different vise from that shown in Fig. A1.4, each half of the vise having a semi-cylindrical recess that closely fits the clamped portion of the specimen. As previously stated, the results cannot be reliably compared with those obtained using specimens of other sizes or shapes.

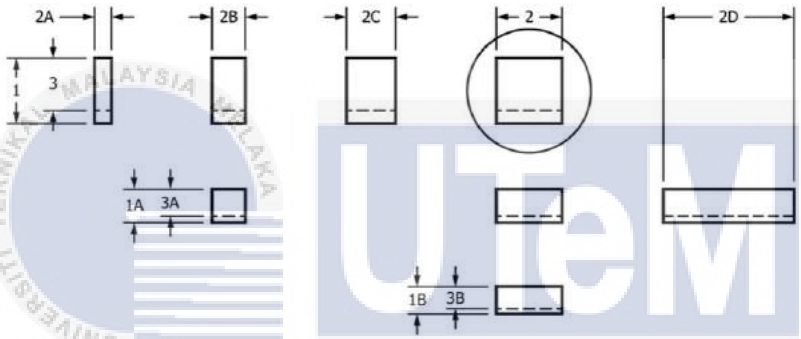

ID Number	Description	Dimension	Tolerance
1	Width, Standard	10.0 mm	±0.075 mm
1A	Width, Half	5.0 mm	±0.050 mm
1B	Width, Third	3.0 mm	±0.030 mm
2	Thickness, Standard	10.0 mm	±0.075 mm
2A	Thickness, Quarter	2.5 mm	±0.025 mm
2B	Thickness, Half	5.0 mm	±0.050 mm
2C	Thickness, Three-Quarters	7.5 mm	±0.075 mm
2D	Thickness, Double	20.0 mm	±0.075 mm
3	Ligament Length, Standard	8.0 mm	±0.025 mm
3A	Ligament Length, Half	4.0 mm	±0.025 mm
3B	Ligament Length, Third	2.4 mm	±0.025 mm

NOTE 1—The circled specimen is the standard V-notch specimen (see Fig. 1).

NOTE 2—On sub-size specimens the length, notch angle, notch radius, surface finish are constant with V-notch specimens (see Fig. 1); width, thickness, and ligament length vary as indicated above.

FIG. A3.1 Sub-Size Charpy (Simple-Beam) V-Notch Impact Test Specimens

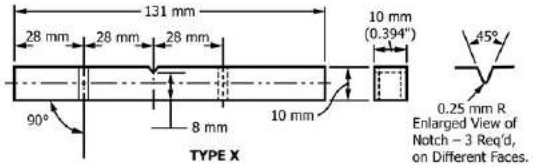

NOTE 1—Permissible variations for type X specimens shall be as follows:

Perpendicularity of notch axis	± 2°
Adjacent (90°sides) shall be at	± 10 min
Ligament length	±0.025 mm

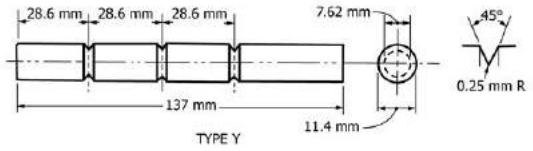

NOTE 2—Permissible variations for both specimens shall be as follows:

Cross-section dimensions	±0.025 mm
Lengthwise dimensions	+0, –2.5 mm
Angle of notch	±1°
Radius of notch	±0.025 mm
Notch diameter of Type Y specimen	±0.025 mm

FIG. A3.2 Izod (Cantilever-Beam) Impact Test Specimens, Types X and Y

The flat shall be parallel to the longitudinal centerline of the specimen and shall be parallel to the bottom of the notch within 2:1000.

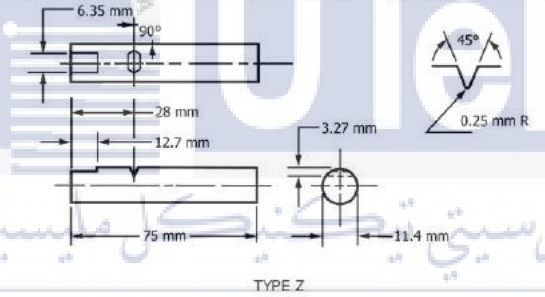

NOTE 1—Permissible variations shall be as follows:

Perpendicularity between notch length and longitudinal centerline	± 2°
Cross-section dimensions	±0.025 mm
Length of specimen	+0, –2.5 mm
Angle of notch	±1°
Radius of notch	±0.025 mm
Notch depth	±0.025 mm

FIG. A3.3 Izod (Cantilever-Beam) Impact Test Specimen (Philpot), Type Z

A4. DETERMINATION OF THE SHEAR FRACTURE APPEARANCE

A4.1 These shear fracture appearance methods are based on the concept that 100 % shear (stable) fracture occurs above the transition-temperature range and brittle unstable fracture occurs below the range, as shown by the instrumented Charpy data in Fig. A4.1 (see also Test Method E2298). This shear measurement process was developed for carbon steels that undergo a distinct ductile to brittle transition that results in a clearly defined region of cleavage fracture (unstable) on the surface of the specimen. Fracture surface interpretation is complicated in materials that exhibit mixed-mode fracture during unstable crack extension.

In the transition-temperature range, fracture is initiated at the root of the notch by fibrous tearing. A short distance from the notch, unstable crack extension occurs (F_{bf}) as the fracture mechanism changes to cleavage, mixed mode, or another low energy fracture mode, which often results in distinct radial markings in the central portion of the specimen (indicative of fast, unstable fracture). After several microseconds the unstable crack extension arrests (F_a). Final fracture occurs at the remaining ligament and at the sides of the specimen in a stable manner. As shear-lips are formed at the sides of the specimen, the plastic hinge at the remaining ligament ruptures. In the ideal case, a "picture frame" of fibrous "shear" (stable) fracture surrounds a relatively flat area of unstable fracture.

The five methods used below may be used to determine the shear fracture appearance. The user should qualitatively characterize the fracture mode of the unstable fracture zone, and provide a description of how the shear measurements were made. The methods are grouped in order of increasing precision. In the case where a specimen does not separate into two halves during the impact test and the fracture occurs without any evidence of unstable crack extension, the shear fracture appearance can be considered to be 100 % and the specimen should be reported as unbroken.

NOTE A4.1—Round robin data (five U.S. companies, 1990) estimates of the shear fracture appearance for five quenched and tempered 8219 steels and four microalloyed 1040 steels indicated the following: (1) results using method A4.1.1 systematically underestimated the percent shear (compared with method A4.1.4), (2) the error using method A4.1.2 was random and, (3) the typical variation in independent measurements using method A4.1.4 was on the order of 5 to 10 % for microalloyed 1040 steels.

A4.1.1 Measure the length and width of the unstable fracture region of the fracture surface, as shown in Fig. 9, and determine the shear fracture appearance from Table A4.1 and Table A4.2 depending on the units of measurement.

A4.1.2 Compare the appearance of the fracture of the specimen with a shear fracture appearance chart such as that shown in Fig. A4.2.

A4.1.3 Magnify the fracture surface and compare it to a precalibrated overlay chart or measure the shear fracture appearance by means of a planimeter.

A4.1.4 Photograph the fracture surface at a suitable magnification and measure the shear fracture appearance by means of a planimeter.

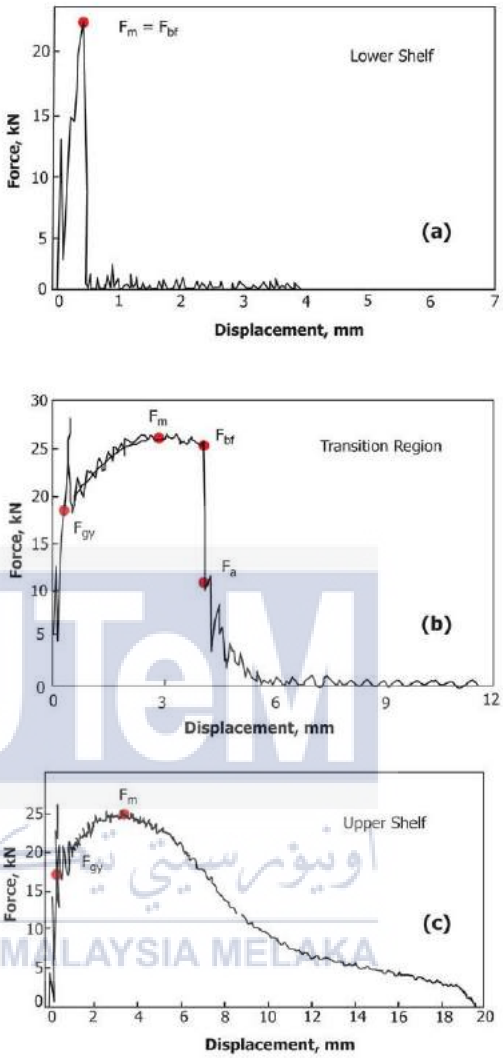

FIG. A4.1 Instrumented Charpy impact data showing behavior of steels in the (a) lower shelf, (b) transition, and (c) upper shelf regions. The symbols are defined as: *(1)* F_{gy}, general yield force, *(2)* F_m, maximum force, *(3)* F_{bf}, force at initiation of unstable crack propagation, and *(4)* F_a, force at end of unstable crack propagation (arrest force).

A4.1.5 Capture a digital image of the fracture surface and measure the shear fracture appearance using image analysis software.

TABLE A4.1 Shear Fracture Appearance for Measurements Made in Millimetres

NOTE 1—100 % shear fracture appearance is to be reported when either *A* or *B* is zero.

Dimension *B*, mm	Dimension *A*, mm																	
	1.0	1.5	2.0	2.5	3.0	3.5	4.0	4.5	5.0	5.5	6.0	6.5	7.0	7.5	8.0	8.5	9.0	9.5	10
1.0	99	98	98	97	96	96	95	94	94	93	92	92	91	91	90	89	89	88	88
1.5	98	97	96	95	94	93	92	92	91	90	89	88	87	86	85	84	83	82	81
2.0	98	96	95	94	92	91	90	89	88	86	85	84	82	81	80	79	77	76	75
2.5	97	95	94	92	91	89	88	86	84	83	81	80	78	77	75	73	72	70	69
3.0	96	94	92	91	89	87	85	83	81	79	77	76	74	72	70	68	66	64	62
3.5	96	93	91	89	87	85	82	80	78	76	74	72	69	67	65	63	61	58	56
4.0	95	92	90	88	85	82	80	77	75	72	70	67	65	62	60	57	55	52	50
4.5	94	92	89	86	83	80	77	75	72	69	66	63	61	58	55	52	49	46	44
5.0	94	91	88	85	81	78	75	72	69	66	62	59	56	53	50	47	44	41	37
5.5	93	90	86	83	79	76	72	69	66	62	59	55	52	48	45	42	38	35	31
6.0	92	89	85	81	77	74	70	66	62	59	55	51	47	44	40	36	33	29	25
6.5	92	88	84	80	76	72	67	63	59	55	51	47	43	39	35	31	27	23	19
7.0	91	87	82	78	74	69	65	61	56	52	47	43	39	34	30	26	21	17	12
7.5	91	86	81	77	72	67	62	58	53	48	44	39	34	30	25	20	16	11	6
8.0	90	85	80	75	70	65	60	55	50	45	40	35	30	25	20	15	10	5	0

TABLE A4.2 Shear Fracture Appearance for Measurements Made in Inches

NOTE 1—100 % shear fracture appearance is to be reported when either *A* or *B* is zero.

Dimension *B*, in.	Dimension *A*, in.																
	0.05	0.10	0.12	0.14	0.16	0.18	0.20	0.22	0.24	0.26	0.28	0.30	0.32	0.34	0.36	0.38	0.40
0.05	98	96	95	94	94	93	92	91	90	90	89	88	87	86	85	85	84
0.10	96	92	90	89	87	85	84	82	81	79	77	76	74	73	71	69	68
0.12	95	90	88	86	85	83	81	79	77	75	73	71	69	67	65	63	61
0.14	94	89	86	84	82	80	77	75	73	71	68	66	64	62	59	57	55
0.16	94	87	85	82	79	77	74	72	69	67	64	61	59	56	53	51	48
0.18	93	85	83	80	77	74	72	68	65	62	59	56	54	51	48	45	42
0.20	92	84	81	77	74	72	68	65	61	58	55	52	48	45	42	39	36
0.22	91	82	79	75	72	68	65	61	57	54	50	47	43	40	36	33	29
0.24	90	81	77	73	69	65	61	57	54	50	46	42	38	34	30	27	23
0.26	90	79	75	71	67	62	58	54	50	46	41	37	33	29	25	20	16
0.28	89	77	73	68	64	59	55	50	46	41	37	32	28	23	18	14	10
0.30	88	76	71	66	61	56	52	47	42	37	32	27	23	18	13	9	3
0.31	88	75	70	65	60	55	50	45	40	35	30	25	20	18	10	5	0

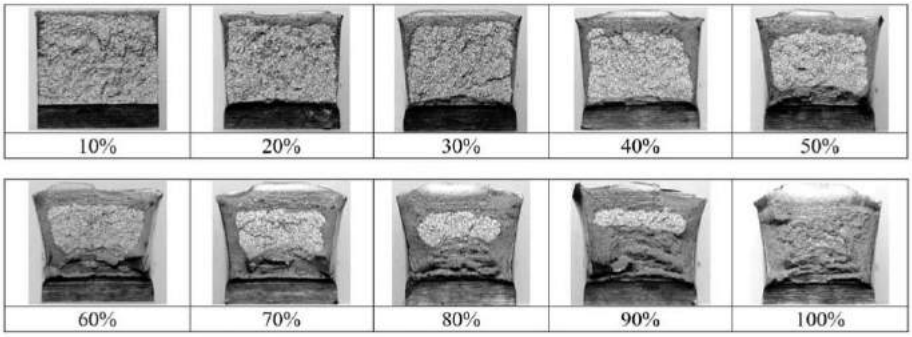

(a) Shear Fracture Appearance Charts

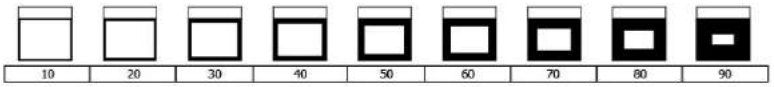

(*b*) Guide for Estimating Shear Fracture Appearance

FIG. A4.2 Shear Fracture Appearance

APPENDIXES

(Nonmandatory Information)

X1. NOTES ON SIGNIFICANCE OF NOTCHED-BAR IMPACT TESTING

X1.1 *Notch Behavior*:

X1.1.1 The Charpy V-notch (CVN) impact test has been used extensively in mechanical testing of steel products, in research, and in procurement specifications for over three decades. Where correlations with fracture mechanics parameters are available, it is possible to specify CVN toughness values that would ensure elastic-plastic behavior for fracture of fatigue cracked specimens subjected to minimum operating temperatures and maximum in-service rates of loading.

X1.1.2 The notch behavior of face-centered cubic metals and alloys, a large group of nonferrous materials and austenitic steels can be judged from their common tensile properties. If they are brittle in tension, they will be brittle when notched, while if they are ductile in tension they will be ductile when notched, except for unusually sharp or deep notches (much more severe than the standard V-notch Charpy or Izod specimens). Even low temperatures do not alter this characteristic of these materials. In contrast, the behavior of ferritic steels under notch conditions cannot be predicted from their properties as revealed by the tension test. For the study of these materials the Charpy and Izod type tests are accordingly very useful. Some metals that display normal ductility in the tension test may nevertheless break in brittle fashion when tested or when used in notched condition. Notched conditions include constraints to deformation in directions perpendicular to the major stress, or multi axial stresses, and stress concentrations. It is in this field that the Charpy and Izod tests prove useful for determining the susceptibility of a steel to notch-brittle behavior though they cannot be directly used to appraise the serviceability of a structure.

X1.2 *Notch Effect*:

X1.2.1 The notch results in a combination of multi-axial stresses associated with restraints to deformation in directions perpendicular to the major stress, and a stress concentration at the base of the notch. A severely notched condition is generally not desirable, and it becomes of real concern in those cases in which it initiates a sudden and complete failure of brittle type. Some metals can be deformed in a ductile manner even down to very low temperatures, while others may crack. This difference in behavior can be best understood by considering the cohesive strength of a material (or the property that holds it together) and its relation to the yield point. In cases of brittle fracture, the cohesive strength is exceeded before significant plastic deformation occurs and the fracture appears crystalline. In cases of ductile or shear type of failure, considerable deformation precedes the final fracture and the broken surface appears fibrous instead of crystalline. In intermediate cases, the fracture comes after a moderate amount of deformation and is part crystalline and part fibrous in appearance.

X1.2.2 When a notched bar is loaded, there is a normal stress across the base of the notch which tends to initiate

fracture. The property that keeps it from cleaving, or holds it together, is the cohesive strength. The bar fractures when the normal stress exceeds the cohesive strength. When this occurs without the bar deforming it is the condition for brittle fracture.

X1.2.3 In testing, though not in service because of size effects, it happens more commonly that plastic deformation precedes fracture. In addition to the normal stress, the applied force also sets up shear stresses which are about 45° to the normal stress. The elastic behavior terminates as soon as the shear stress exceeds the shear strength of the material and deformation or plastic yielding sets in. This is the condition for ductile failure.

X1.2.4 This behavior, whether brittle or ductile, depends on whether the normal stress exceeds the cohesive strength before the shear stress exceeds the shear strength. Several important facts of notch behavior follow from this. If the notch is made sharper or more drastic, the normal stress at the root of the notch will be increased in relation to the shear stress and the bar will be more prone to brittle fracture (see Table X1.1). Also, as the speed of deformation increases, the shear strength increases and the likelihood of brittle fracture increases. On the other hand, by raising the temperature, leaving the notch and the speed of deformation the same, the shear strength is lowered and ductile behavior is promoted, leading to shear failure.

X1.2.5 Variations in notch dimensions will affect the results of the tests. Tests on E4340 steel specimens[7] have shown the effect of dimensional variations on Charpy results (see Table X1.1).

X1.3 *Size Effect*:

X1.3.1 Increasing either the thickness or the width of the specimen tends to increase the volume of metal subject to distortion, and by this factor tends to increase the absorbed energy. However, any increase in size, particularly in thickness, also tends to increase the degree of constraint and by tending to induce brittle fracture, may decrease the absorbed energy. Where a standard V-notch specimen is on the verge of brittle fracture, this is particularly true, and a double-thick specimen may actually require less absorbed energy to rupture than one of standard thickness.

X1.3.2 In studies of such effects where the size of the material precludes the use of the standard specimen, for example when the material is a 6.35-mm plate, sub-size specimens are used. Such specimens (Fig. A3.1) are based on the V-notch specimen of Fig. 1.

X1.3.3 A general correlation between the absorbed energy values obtained with specimens of different size or shape is not feasible, but limited correlations may be established for specification purposes on the basis of special studies of particular materials and particular specimens. On the other hand, in a study of the relative effect of process variations, evaluation by use of some arbitrarily selected specimen with some chosen notch will in most instances place the methods in their proper order.

X1.4 *Temperature Effect*:

X1.4.1 The testing conditions also affect the notch behavior. So pronounced is the effect of temperature on the behavior of steel when notched that comparisons are frequently made by examining specimen fractures and by plotting absorbed energy values and shear fracture appearance versus temperature from tests of notched bars at a series of temperatures. When the test temperature has been carried low enough to start cleavage fracture, there may be an extremely sharp drop in absorbed energy or there may be a relatively gradual falling off toward the lower temperatures. This drop in energy value starts when a specimen begins to exhibit some crystalline appearance in the fracture. The transition temperature at which this embrittling effect takes place varies considerably with the size of the part or test specimen and with the notch geometry.

X1.5 *Testing Machine*:

X1.5.1 The testing machine itself must be sufficiently rigid or tests on high-strength low-energy materials will result in excessive elastic energy losses either upward through the pendulum shaft or downward through the base of the machine. If the anvil supports, the striker, or the machine foundation bolts are not securely fastened, tests on ductile materials in the range of 108 J may actually indicate values in excess of 122 to 136 J.

X1.5.2 A problem peculiar to Charpy-type tests occurs when high-strength, low-energy specimens are tested at low temperatures. These specimens may not leave the machine in the direction of the pendulum swing but rather in a sidewise direction. To ensure that the broken halves of the specimens do

[7] Fahey, N.H., "Effects of Variables on Charpy Impact Testing," *Material Research & Standards*, Vol 1 No.11, November 1961, p. 872.

TABLE X1.1 Effect of Varying Notch Dimensions on Standard V-Notch Specimens

	High-Energy Specimens, J	Medium-Energy Specimens, J	Low-Energy Specimens, J
Specimen with standard dimensions	103.0 ± 5.2	60.3 ± 3.0	16.9 ± 1.4
Depth of notch, 2.13 mm[A]	97.9	56.0	15.5
Depth of notch, 2.04 mm[A]	101.8	57.2	16.8
Depth of notch, 1.97 mm[A]	104.1	61.4	17.2
Depth of notch, 1.88 mm[A]	107.9	62.4	17.4
Radius at base of notch 0.13 mm[B]	98.0	56.5	14.6
Radius at base of notch 0.38 mm[B]	108.5	64.3	21.4

[A] Standard 2.0 ± 0.025 mm (0.079 ± 0.001 in.).
[B] Standard 0.25 ± 0.025 mm (0.010 ± 0.001 in.).

not rebound off some component of the machine and contact the pendulum before it completes its swing, modifications may be necessary in older model machines. These modifications differ with machine design. Nevertheless the basic problem is the same in that provisions must be made to prevent rebounding of the fractured specimens into any part of the swinging pendulum. Where design permits, the broken specimens may be deflected out of the sides of the machine and yet in other designs it may be necessary to contain the broken specimens within a certain area until the pendulum passes through the anvils. Some low-energy high-strength steel specimens leave impact machines at speeds in excess of 15.2 m/s although they were struck by a pendulum traveling at speeds approximately 5.2 m/s. If the force exerted on the pendulum by the broken specimens is sufficient, the pendulum will slow down and erroneously high absorbed energy values will result. This problem accounts for many of the inconsistencies in Charpy results reported by various investigators within the 14 to 34 J range. Fig. A1.1 illustrates a modification found to be satisfactory in minimizing jamming.

X1.6 *Velocity of Straining:*

X1.6.1 Velocity of straining is likewise a variable that affects the notch behavior of steel. The impact test shows somewhat higher absorbed energy values than the static tests above the transition temperature and yet, in some instances, the reverse is true below the transition temperature.

X1.7 *Correlation with Service:*

X1.7.1 While Charpy or Izod tests may not directly predict the ductile or brittle behavior of steel as commonly used in large masses or as components of large structures, these tests can be used as acceptance tests or tests of identity for different lots of the same steel or in choosing between different steels, when correlation with reliable service behavior has been established. It may be necessary to perform the tests at properly chosen temperatures other than room temperature. In this, the service temperature or the transition temperature of full-scale specimens does not give the desired transition temperatures for Charpy or Izod tests since the size and notch geometry may be so different. Chemical analysis, tension, and hardness tests may not indicate the influence of some of the important processing factors that affect susceptibility to brittle fracture nor do they comprehend the effect of low temperatures in inducing brittle behavior.

X2. SUGGESTED METHODS FOR MEASURING THE POSITION OF THE CENTER OF STRIKE

X2.1 *Position of the Center of Strike Relative to the Center of Gravity:*

X2.1.1 Since the center of strike can only be marked on an assembled machine, only the methods applicable to an assembled machine are described as follows:

X2.1.1.1 The fundamental fact on which all the methods are based is that when the friction forces are negligible, the center of gravity is vertically below the axis of rotation of a pendulum supported by the bearings only (herein referred to as a free hanging pendulum). Section A1.3 limits the total frictional losses in impact machines to a negligible value. The required measurements may be made using specialized instruments such as transits, clinometers, or cathometers. However, simple instruments have been used as described in the following to make measurements of sufficient accuracy.

X2.1.1.2 Suspend a plumb bob from the frame. The plumb line should appear visually to be in the plane of swing of the striking edge.

X2.1.1.3 Place a massive object on the base close to the latch side of the pendulum. Adjust the position of this object so that when back lighted, a minimal gap is visible between it and the pendulum. (See Fig. X2.1.)

X2.1.1.4 With a scale or depth gage pressed lightly against the striking edge at the center of strike, measure the horizontal distance between the plumb line and striking edge. (Dimension *B* in Fig. X2.1.)

X2.1.1.5 Similarly, measure the distance in a horizontal plane through the axis of rotation from the plumb line to the clamp block or enlarged end of the pendulum stem. (Dimension *A* in Fig. X2.1.)

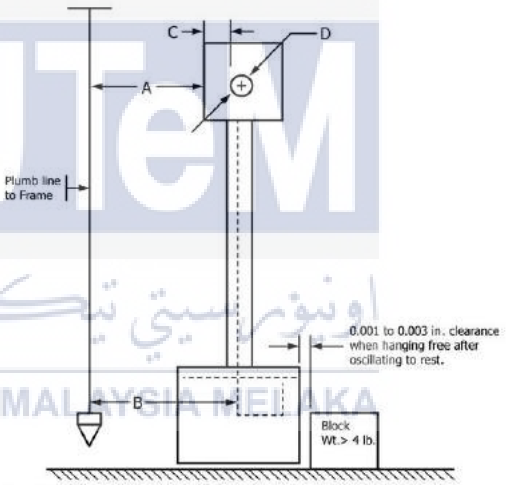

FIG. X2.1 Measurement of Deviation of Center of Strike from Vertical Plane through Axis of Rotation when Pendulum is Hanging Free

X2.1.1.6 Use a depth gage to measure the radial distance from the surface contacted in measuring *A* to a machined surface of the shaft which connects the pendulum to the bearings in the machine frame. (Dimension *C* in Fig. X2.1.)

X2.1.1.7 Use an outside caliper or micrometer to measure the diameter of the shaft at the same location contacted in measuring *C*. (Dimension *D* in Fig. X2.1.)

X2.1.1.8 Substitute the measured dimensions in the equation

$$X = A + C + D/2 - B \quad \text{(X2.1)}$$

where:

X = deviation of the center of strike from a line from the center of rotation through the center of gravity.

X3. INSTRUCTIONS FOR TESTING SUB-SIZE CHARPY SPECIMENS

X3.1 When testing sub-size specimens (see Fig. A3.1), the specimen support height should be changed to ensure that the center of strike is maintained (see A2.3.4 and A2.3.7 for instructions). To comply with this change, new specimen supports can be manufactured or shims may be added to the specimen supports in a secure manner so that they do not interfere with the test.

X3.2 In order to maintain the center of strike requirements, the following procedure should be used when testing a sub-size specimen. The height of the specimen supports should be changed to ensure that the centerline of the sub-size specimen will coincide with the centerline of the standard specimen. Higher specimen supports should be used when testing a smaller thickness specimen and lower specimen supports should be used when testing a larger thickness specimen.

X3.3 Determine the nominal thickness of the sub-size specimen. When testing smaller thickness specimens, subtract this value from the standard thickness specimens (10 mm). Divide this value by two. This amount shall be added to the standard specimen support height. For larger thickness specimens, the result of the subtraction is a negative number. Therefore, the thickness of the supports shall be reduced by the amount calculated.

SUMMARY OF CHANGES

Committee E28 has identified the location of selected changes to this standard since the last issue (E23 – 16b) that may impact the use of this standard. (Approved June 1, 2018.)

(1) Section 3, 3.1, 3.1.1, 3.1.2, 3.1.3, 3.1.4, 3.1.4.1, 3.1.5, 3.1.5.1, 3.1.6, and 8.2.4 were added and subsequent sections renumbered.
(2) 4.1, 8.1.4, 9.1.1.2, 9.3.2, 9.3.3.1, 10.1, 11.1, 11.3, A2.1.2, A2.1.3, Note A2.3, A2.3.8.1, A2.3.9, Note A2.6, X1.3.1, X1.3.3, X1.4.1, X1.5.2, and X1.6.1 were revised with absorbed energy.
(3) 7.2.1, 7.2.2, 9.3.3.2 and A2.1.2 were revised with direct verification.
(4) 7.2.2, 9.3.3.2, A2.1.2, A2.1.3, and A2.4.1.1 were revised with indirect verification.
(5) 9.1.1.3, 9.3.3, 9.3.3.1, 9.4.3, 11.1, A1.2, A1.2.1, A1.3, A1.4, A2.3.8.1, A2.3.9, A2.4.2, A2.4.3, A2.4.3.2, A2.4.4, A2.4.4.2, Note A2.9, and Table A2.1 were revised with range capacity.
(6) 1.1, 10.3, 11.3.3, Section 13, Fig. 9, Annex A4, A4.1, Note A4.1, A4.1.1, A4.1.2, A4.1.3, A4.1.4, A4.1.5, Table A4.1, Table A4.2, Fig. A4.2 and X1.4.1 were revised with shear fracture appearance.
(7) 9.3.3.3, A1.2, A1.2.1, A2.3.8.1, A2.3.9, Note A2.4 and Note A2.5 were revised with analog scale.
(8) 9.1.1.3, Note 5, 9.3.3, 9.3.3.3, 9.4.3, A1.3, A2.3.8.1 and A2.3.9 were revised with analog scale pointer.
(9) 4.1, 9.1.1.2, 9.1.1.3, 9.3.3, 9.4.3, 10.1, A1.2.1, A1.4, A2.1.2, A2.2.7, A2.3.8, A2.3.8.1, A2.3.9, A2.4.3, A2.4.3.1 and Note A2.6 were revised with indicating device.
(10) 9.4.3, A2.3.8.1 and Note A2.6 were revised with digital display.
(11) Note 5, A2.3.8, and A2.3.8.1 were revised with friction and windage losses.
(12) 9.1.1.3, Note 5, and A2.2.7 were revised with percent friction and windage loss.
(13) 9.1.1.2, 10.1, A1.2.1, A1.3, A1.7, A2.3.8, A2.3.8.1, A2.3.9, Note A2.4 and X2.1.1.1 were revised with total frictional losses.
(14) A2.1.3, A2.4.1, A2.4.1.1, A2.4.1.2, A2.4.4, A2.4.4.1, A2.4.4.2, Note A2.8, Note A2.9 and Table A2.1 were revised with certified absorbed energy value.
(15) A2.1.3, A2.4.2, A2.4.4 and Note A2.7 were revised with energy level.
(16) 12.1, A2.4.1, A2.4.2, A2.4.4, A2.4.4.1, A2.4.4.2, Note A2.8, and Note A2.9 were revised with verification specimens.
(17) 9.3.2, 10.2, 10.2.1, 10.3, Fig. A1.4 (Note 4), A2.3.2, and A2.3.5 were revised from "must" to "shall".
(18) 7.2.1, 7.2.2, A2.1.1 and A2.1.2 were revised to use required.

(19) 9.1.1, 9.2.1, 9.3.2, 9.4.2, A3.1 and A4.1 were revised from "recommended" to "should".
(20) 9.1.1.2 and A2.3.8.1 were revised from "should" to "shall".
(21) 9.1.1.2, 10.1, A1.9.2, A2.2.6 and A2.3.9 were revised to include requirements from Notes following the section (other Notes were renumbered where necessary).
(22) Note 2 was added with information from 8.2.2 and subsequent notes renumbered.
(23) Note 3 was revised to eliminate "shall".
(24) Note 6 was revised from "must to "should".
(25) Note A2.1 was revised from "recommended" to "may".
(26) 10.2.3 changed "gage" to "gauge" and "dial gage" to "indicator".
(27) Fig. 7 title changed "gage" to "gauge".
(28) Fig. 8 deleted ID numbers 20 and 22 and subsequent ID numbers renumbered. Changed "gage" to "gauge" in title.
(29) Note A2.7 and A2.4.4.1 were revised with typically or typical.
(30) A2.4.4.2 and Note A2.9 were revised with limit.
(31) 9.1.1.2 was revised with free swing.

APPENDIX B

GANTT CHART (BDP 1)

ACTIVITIES	STATUS	WEEK (BDP 1)															
		1	2	3	4	5	6	7	8	9	10	11	12	13	14	15	16
TOPIC CONFIRMATION AND MEETING WITH SUPERVISOR	PLAN																
	ACTUAL																
FINDING JOURNAL RESEARCH	PLAN																
	ACTUAL																
CHAPTER 1: INTRODUCTION	PLAN																
	ACTUAL																
CHAPTER 2: LITERATURE REVIEW	PLAN																
	ACTUAL																
CHAPTER 3: METHODOLOGY	PLAN																
	ACTUAL																
DRAFT REPORT	PLAN																
	ACTUAL																
REVISE THE DRAFT REPORT	PLAN																
	ACTUAL																
FINAL REPORT	PLAN																
	ACTUAL																
PREPARATION AND PRESENTATION BDP 1	PLAN																
	ACTUAL																

APPENDIX C

GANTT CHART (BDP 2)

ACTIVITIES	STATUS	WEEK (BDP 1)															
		1	2	3	4	5	6	7	8	9	10	11	12	13	14	15	16
MEETING AND DICUSSION	PLAN																
	ACTUAL																
CONDUCTING THE EXPERIMENT	PLAN																
	ACTUAL																
COLLECT AND ANALYSIS THE DATA	PLAN																
	ACTUAL																
CHAPTER 4: RESULT AND DISCUSSION	PLAN																
	ACTUAL																
CHAPTER 5: CONCLUSION AND RECOMMENDATION	PLAN																
	ACTUAL																
SUBMISSION THE FIRST DRAFT BDP 2	PLAN																
	ACTUAL																
REVISE THE DRAFT REPORT	PLAN																
	ACTUAL																
FINALIZE THE CORRECTION OF FULL REPORT	PLAN																
	ACTUAL																
PREPARATION AND PRESENTATION BDP 2	PLAN																
	ACTUAL																

APPENDIX D, TURNITIN REPORT

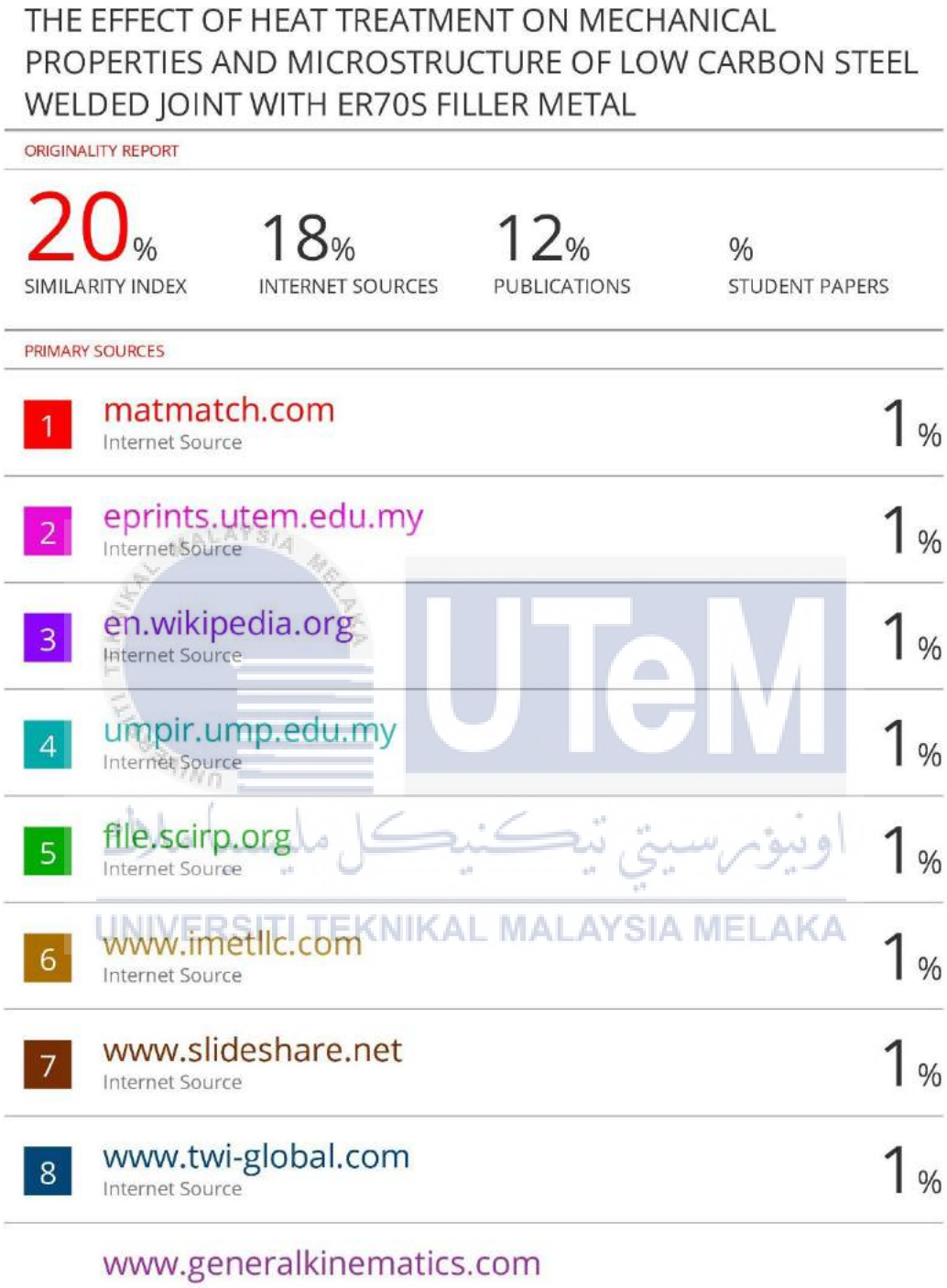

THE EFFECT OF HEAT TREATMENT ON MECHANICAL PROPERTIES AND MICROSTRUCTURE OF LOW CARBON STEEL WELDED JOINT WITH ER70S FILLER METAL

ORIGINALITY REPORT

20%	18%	12%	%
SIMILARITY INDEX	INTERNET SOURCES	PUBLICATIONS	STUDENT PAPERS

PRIMARY SOURCES

1	matmatch.com Internet Source	1%
2	eprints.utem.edu.my Internet Source	1%
3	en.wikipedia.org Internet Source	1%
4	umpir.ump.edu.my Internet Source	1%
5	file.scirp.org Internet Source	1%
6	www.imetllc.com Internet Source	1%
7	www.slideshare.net Internet Source	1%
8	www.twi-global.com Internet Source	1%
	www.generalkinematics.com	

UNIVERSITI TEKNIKAL MALAYSIA MELAKA

BORANG PENGESAHAN STATUS LAPORAN PROJEK SARJANA

TAJUK: **THE EFFECT OF HEAT TREATMENT ON MECHANICAL PROPERTIES AND MICROSTRUCTURE OF LOW CARBON STEEL WELDED JOINT WITH ER70S FILLER METAL**

SESI PENGAJIAN: **2021/22 Semester 1**

Saya **NUR ALIYA ALINA BT AB RADZAK**

mengaku membenarkan tesis ini disimpan di Perpustakaan Universiti Teknikal Malaysia Melaka (UTeM) dengan syarat-syarat kegunaan seperti berikut:

1. Tesis adalah hak milik Universiti Teknikal Malaysia Melaka dan penulis.
2. Perpustakaan Universiti Teknikal Malaysia Melaka dibenarkan membuat salinan untuk tujuan pengajian sahaja dengan izin penulis.
3. Perpustakaan dibenarkan membuat salinan tesis ini sebagai bahan pertukaran antara institusi pengajian tinggi.
4. **Sila tandakan (✓)

☐	SULIT	(Mengandungi maklumat yang berdarjah keselamatan atau kepentingan Malaysia sebagaimana yang termaktub dalam AKTA RAHSIA RASMI 1972)
☐	TERHAD	(Mengandungi maklumat TERHAD yang telah ditentukan oleh organisasi/badan di mana penyelidikan dijalankan)
☑	TIDAK TERHAD	

Disahkan oleh:

Alamat Tetap:

Lot 2531, Taman Durian Burung,

Jalan Cengal Lapan,

20050 Kuala Terengganu, Terengganu

Tarikh: 16 Januari 2022

Cop Rasmi: NUR AIMAN HANIS BINTI HASIM
Pensyarah
Jabatan Teknologi Kejuruteraan Pembuatan
Fakulti Teknologi Kejuruteraan Mekanikal dan Pembuatan
Universiti Teknikal Malaysia Melaka

Tarikh: 18 January 2022

** Jika tesis ini SULIT atau TERHAD, sila lampirkan surat daripada pihak berkuasa/organisasi berkenaan dengan menyatakan sekali sebab dan tempoh laporan PSM ini perlu dikelaskan sebagai SULIT atau TERHAD.

UNIVERSITI TEKNIKAL MALAYSIA MELAKA

Universiti Teknikal Malaysia Melaka
Hang Tuah Jaya,
76100 Durian Tunggal,
Melaka, Malaysia.

+606 270 1000
+606 270 1022
www.utem.edu.my

FAKULTI TEKNOLOGI KEJURUTERAAN MEKANIKAL DAN PEMBUATAN

Tel : +606 270 1184 | Faks : +606 270 1064

Rujukan Kami (Our Ref):
Rujukan Tuan (Your Ref):
Tarikh (Date): 31 Januari 2021

Chief Information Officer
Perpustakaan Laman Hikmah
Universiti Teknikal Malaysia Melaka

Melalui

Dekan
Fakulti Teknologi Kejuruteraan Mekanikal dan Pembuatan
Universiti Teknikal Malaysia Melaka

Tuan

PENGKELASAN TESIS SEBAGAI TERHAD BAGI TESIS PROJEK SARJANA MUDA

Dengan segala hormatnya merujuk kepada perkara di atas.

2. Dengan ini, dimaklumkan permohonan pengkelasan tesis yang dilampirkan sebagai TERHAD untuk tempoh **LIMA** tahun dari tarikh surat ini. Butiran lanjut laporan PSM tersebut adalah seperti berikut:

Nama pelajar : NUR ALIYA ALINA BT AB RADZAK (B091810078)
Tajuk Tesis : THE EFFECT OF HEAT TREATMENT ON MECHANICAL PROPERTIES AND MICROSTRUCTURE OF LOW CARBON STEEL WELDED JOINT WITH ER70S FILLER METAL

3. Hal ini adalah kerana IANYA MERUPAKAN PROJEK YANG DITAJA OLEH SYARIKAT LUAR DAN HASIL KAJIANNYA ADALAH SULIT.

Sekian, terima kasih.

"BERKHIDMAT UNTUK NEGARA"
"KOMPETENSI TERAS KEGEMILANGAN"

Saya yang menjalankan amanah,

NUR AIMAN HANIS BINTI HASIM
Penyelia Utama/ Pensyarah Kanan
Fakulti Teknologi Kejuruteraan Mekanikal dan Pembuatan
Universiti Teknikal Malaysia Melaka

THE EFFECT OF HEAT TREATMENT ON MECHANICAL PROPERTIES AND MICROSTRUCTURE OF LOW CARBON STEEL WELDED JOINT WITH ER70S FILLER METAL

by Nur Aliya Alina Ab Radzak

THE EFFECT OF HEAT TREATMENT ON MECHANICAL PROPERTIES AND MICROSTRUCTURE OF LOW CARBON STEEL WELDED JOINT WITH ER70S FILLER METAL

NUR ALIYA ALINA BT AB RADZAK
B091810078

BACHELOR OF MANUFACTURING ENGINEERING TECHNOLOGY (PROCESS AND TECHNOLOGY) WITH HONOURS

2022

UNIVERSITI TEKNIKAL MALAYSIA MELAKA

Faculty of Mechanical and Manufacturing Engineering Technology

THE EFFECT OF HEAT TREATMENT ON MECHANICAL PROPERTIES AND MICROSTRUCTURE OF LOW CARBON STEEL WELDED JOINT WITH ER70S FILLER METAL

Nur Aliya Alina Binti Ab Radzak

Bachelor of Manufacturing Engineering Technology (Process and Technology) with Honours

2022

THE EFFECT OF HEAT TREATMENT ON MECHANICAL PROPERTIES AND MICROSTRUCTURE OF LOW CARBON STEEL WELDED JOINT WITH ER70S FILLER METAL

NUR ALIYA ALINA BINTI AB RADZAK

A thesis submitted
in fulfillment of the requirements for the degree of
Bachelor of Manufacturing Engineering Technology (Process and Technology) with Honours

Faculty of Mechanical and Manufacturing Engineering Technology

UNIVERSITI TEKNIKAL MALAYSIA MELAKA

2022

DECLARATION

I declare that this Choose an item. entitled "The Effect of Heat Treatment on Mechanical Properties and Microstructure of Low Carbon Steel Welded Joint with ER70s Filler Metal" is the result of my own research except as cited in the references. The Choose an item. has not been accepted for any degree and is not concurrently submitted in candidature of any other degree.

Signature : 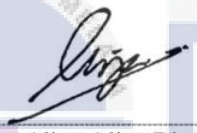

Name : Nur Aliya Alina Binti Ab Radzak

Date : 16 January 2022

APPROVAL

I hereby declare that I have checked this thesis and in my opinion, this thesis is adequate in terms of scope and quality for the award of the Bachelor of Manufacturing Engineering Technology (Process and Technology) with Honours.

Signature : .....

Supervisor Name : Puan Nur Aiman Hanis Binti Hasim

Date : .....

Signature : .....

Co Supervisor Name : Dr Mohd Fauzi Bin Mamat

Date : .....

DEDICATION

This report is dedicated to my beloved family in perticular, for their endless love, support and encouragement. To my main supervisor Puan Nur Aiman Hanis Binti Hasim and my co supervisor, Dr Mohd Fauzi Bin Mamat who has guided me along the way to finish this project. Thank you for all your support, and give me strength untill this project is finished.

ABSTRACT

Welding process such as GMAW appear to be growing the fastest, with recent years showing the greatest growth. However, the process during welding, rapid heating and cooling takes place which produce severe thermal cycle near weld line region of any metal that gets submerged in the heating zone. Gas Metal Arc Welding (GMAW), sometimes known as metal inert gas (MIG) welding, is a type of welding method in which an electric arc is produced between a consumable wire electrode and the workpiece metal(s), heating, melting, and joining them. The main objective of this study were to study the welded joint of low carbon steel joint with filler metal ER70s. Next, to carry out the non-destructive test by using radiography testing and liquid penetrant inspection. Last but not least,to study the effect of heat treatment on the mechanical and microstructure properties by performing hardness and impact test. Radiography and liquid penetrant test were conducted to investigate the surface defects on the sample. After that, the sample were cut into 9 samples with the dimension of 55mm x 10mm x 12mm using abrasive water jet. The samples were prepared through two types of heat treatment process which is annealing with the temperature of 900 and tempering 450˚C. Next, the material characterization were confirmed through optical microscope and Scanning Electron Microscope (SEM/EDX). The macro hardness test were done by using Rockwell machine to evaluate the microhardness behaviour of treated and untreated samples. Meanwhile, for the impact test, the Charpy test were used to determine the relative toughness or impact toughness of the sample. The impact test results showed similar value of three samples with value 49.885J for untreated sample, 49.860J for tempered sample and 49.884J for annealed were tough and strong enough to break at the welded connection, however at the HAZ area, the annealed sample with value 49.884J is stronger than the tempered which have 48.860J and untreated samples with 47.885J. At annealed sample, the result of the graph showed that the line pattern of each area were in average compared to graph of untreated and tempered sample. Even though the line pattern of annealed sample were in average, but the annealed sample have the lowest value of hardness at HAZ and weld joint compared to tempered and untreated sample. Next, by performing SEM, it shown the presence of Iron (Fe) in the welded joint with 94.95% at untreated sample meanwhile after performing a heat treatment test, it showed that the structure has changed by showing the presence of manganese in the welded join area with 97.56% at tempered sample and 92.72% at annealed sample.

ABSTRAK

Proses kimpalan seperti GMAW nampaknya berkembang dengan pantas, dengan beberapa tahun kebelakangan ini menunjukkan pertumbuhan yang paling besar. Walau bagaimanapun, proses semasa mengimpal, pemanasan pantas dan penyejukan berlaku yang menghasilkan kitaran haba yang teruk berhampiran kawasan garisan kimpalan mana-mana logam yang terendam dalam zon pemanasan. Kimpalan Arka Logam Gas (GMAW), kadang-kadang dikenali sebagai kimpalan gas lengai logam (MIG), ialah sejenis kaedah kimpalan di mana arka elektrik dihasilkan antara elektrod wayar boleh guna dan logam bahan kerja, pemanasan, lebur, dan menyertai mereka. Objektif utama kajian ini adalah untuk mengkaji sambungan kimpalan sambungan keluli karbon rendah dengan pengisi ER70s. Seterusnya, untuk menjalankan ujian tanpa musnah dengan menggunakan ujian radiografi dan pemeriksaan penembus cecair. Akhir sekali, untuk mengkaji kesan rawatan haba ke atas sifat mekanikal dan struktur mikro dengan melakukan ujian kekerasan dan hentaman. Radiografi dan ujian penembusan cecair telah dijalankan untuk menyiasat kecacatan permukaan pada sampel. Selepas itu, sampel dipotong kepada 9 sampel berdimensi 55mm x 10mm x 12mm menggunakan pancutan air yang kasar. Sampel disediakan melalui dua jenis proses rawatan haba iaitu *annealing* dengan suhu 900˚C dan *tempering* 450˚C. Seterusnya, pencirian bahan disahkan melalui mikroskop optik dan Mikroskop Elektron Pengimbasan (SEM/EDX). Ujian kekerasan makro dilakukan dengan menggunakan mesin *Rockwell* untuk menilai tingkah laku kekerasan mikro bagi sampel yang dirawat dan tidak dirawat. Manakala bagi ujian impak, ujian *Charpy* digunakan untuk menentukan keliatan relatif atau keliatan impak sampel. Keputusan ujian impak menunjukkan nilai yang hampir sama bagi tiga sampel dengan nilai 49.885J untuk sampel yang tidak dirawat, 49.860J untuk sampel *tempered* dan 49.884J untuk *annealed* adalah lasak dan cukup kuat untuk pecah pada sambungan yang dikimpal, namun pada kawasan HAZ, sampel *annealed* dengan nilai 49.884J adalah lebih kuat daripada sampel *tempered* yang mempunyai nilai 48.860J dan sampel yang tidak dirawat dengan nilai 47.885J. Pada sampel *annealed*, keputusan graf menunjukkan bahawa corak garisan setiap kawasan adalah secara purata berbanding dengan graf sampel yang tidak dirawat dan *tempered*. Walaupun corak garisan sampel *annelaed* adalah secara purata, tetapi sampel *annealed* mempunyai nilai kekerasan yang paling rendah pada HAZ dan sambungan kimpalan berbanding sampel *tempered* dan tidak dirawat. Seterusnya, dengan melakukan SEM menunjukkan kehadiran *Iron* (Fe) dalam sambungan kimpalan dengan 94.95% pada sampel yang tidak dirawat manakala selepas melakukan ujian rawatan haba, ia menunjukkan bahawa struktur telah berubah dengan menunjukkan kehadiran *manganese* dalam cantuman yang dikimpal. kawasan dengan 97.56% pada sampel *tempered* dan 92.72% pada sampel *annealed*.

ACKNOWLEDGEMENTS

In the Name of Allah, the Most Gracious, the Most Merciful

First and foremost, I would like to thank and praise Allah the Almighty, my Creator, my Sustainer, for everything I received since the beginning of my life. I would like to extend my appreciation to the Universiti Teknikal Malaysia Melaka (UTeM) for providing the research platform.

My utmost appreciation goes to my main supervisor, Puan Nur Aiman Hanis Binti Hasim and my co supervisor, Dr. Mohd Fauzi Bin Mamat for all their support, advice, and inspiration. Their constant patience for guiding and providing priceless insights will forever be remembered.

I would like to give a special thanks to my beloved mother, Hamah Binti Yong for her endless support, love, and prayers. I dedicated this thesis for you. I would also like to thank my friends especially to my housemates, 807-K for the great supports and friendship. I also would like to thank seven beautiful individuals, BTS for always being there along ups and down in my life. Finally, thank you to all the individual(s) who had provided me the assistance, support, and inspiration to embark on my study.

TABLE OF CONTENTS

		PAGE
DECLARATION		
APPROVAL		
DEDICATION		
ABSTRACT		**i**
ABSTRAK		**ii**
ACKNOWLEDGEMENTS		**iii**
TABLE OF CONTENTS		**iv**
LIST OF TABLES		**vi**
LIST OF FIGURES		**vii**
LIST OF SYMBOLS AND ABBREVIATIONS		**x**
APPENDICES		**xi**
CHAPTER 1	**INTRODUCTION**	**1**
1.1	Background of Study	1
1.2	Problem Statement	2
1.3	Objective of Study	3
1.4	Scope of Study	3
1.5	Significant of Study	4
CHAPTER 2	**LITERATURE REVIEW**	**5**
2.1	Introduction	5
2.2	Welding Process	5
	2.2.1 Welding Gas Metal Arc Welding (GMAW)	7
	2.2.2 Filler metal	9
2.3	Welding Metallurgy	10
	2.3.1 Area at fusion weld – Heat Affected Zone (HAZ)	11
2.4	Welding Parameter	12
2.5	Defects in Welding	12
2.6	Carbon Steel as Base Material	19
	2.6.1 Low Carbon Steel	21
	2.6.2 Medium Carbon Steel	22
	2.6.3 High Carbon Steel	22
	2.6.4 Application of Carbon Steel in Oil and Gas Industry	23
2.7	Heat Treatment Process	23
	2.7.1 Stages of Heat Treatment	26

2.7.2 Types of Heat Treatment 28
2.7.3 Heat Treatment on Welded Joint 35
2.8 Summary of Literature Review 36

CHAPTER 3 METHODOLOGY 38
3.1 Introduction 38
3.2 Preparation of Sample 40
3.2.1 Welding Procedures 40
3.3 Non-Destructive Test (NDT) 41
3.3.1 Liquid Penetrant Inspection 42
3.3.2 Radiographic Testing 44
3.4 Sample Preparation for Testing 45
3.4.1 Procedure of waterjet cutting 46
3.5 Heat Treatment Process 47
3.6 Mechanical Test 48
3.6.1 Hardness Test (Rockwell Hardness) 49
3.6.2 Impact Test 50
3.7 Microstructure Characterization 53
3.7.1 Optical Microscope 53
3.7.2 Scanning Electron Microscopy (SEM) Energy Dispersive X-Ray Spectroscopy (EDX) 55

CHAPTER 4 RESULTS AND DISCUSSION 56
4.1 Introduction 56
4.2 Composition of analysis 56
4.3 Complete welded joint 57
4.4 Non destructive test 58
4.4.1 Radiographic testing 58
4.4.2 Liquid penetrant testing 59
4.5 Heat Treatment Process 60
4.6 Mechanical Test 61
4.6.1 Impact Testing 61
4.6.2 Macro hardness Analysis 64
4.7 Microstructure Analysis 71
4.7.1 Optical microscope 71
4.7.2 Line Scanning 75
4.7.3 Elemental Mapping 78

CHAPTER 5 CONCLUSION AND RECOMMENDATIONS 80
5.1 Conclusion 82
5.2 Recommendations for future 85

REFERENCES 86

APPENDICES Error! Bookmark not defined.

LIST OF TABLES

TABLE	TITLE	PAGE
Table 2.1	Typical welding parameters of mild and low alloy for GMAW	8
Table 2.2	The comparison of the carbon content, microstructure, and properties	20
Table 2.3	The comparison result of heat treatment on welded joint of previous study	24
Table 2.4	Table comparison of heat treatment process	29
Table 4.1	Chemical composition of low carbon steel	57
Table 4.2	Result of Charpy test	62
Table 4.3	Result from the macro hardness test of untreated sample	65
Table 4.4	Result from the macro hardness test of tempered sample	67
Table 4.5	Result from the macro hardness test of annealed sample	69

LIST OF FIGURES

FIGURE	TITLE	PAGE
Figure 2.1	Types of welding process	6
Figure 2.2	Gas Metal Arc Welding (GMAW)	7
Figure 2.3	The letter-number designations of filler metal	9
Figure 2.4	Zones and boundaries in the heat affected zone	11
Figure 2.5	Classification of welding defects	13
Figure 2.6	Welding crack	15
Figure 2.7	Spatter	16
Figure 2.8	Uniformly distributed porosity	17
Figure 2.9	Diagram of incomplete fusion	19
Figure 2.10	The example of pipeline structure in oil and gas	23
Figure 2.11	a) Temperature b) Its reaction to the TTT diagram	27
Figure 2.12	Iron-carbon phase diagram	29
Figure 2.13	Grain metals in annealing stages	32
Figure 2.14	Hardening process	33
Figure 2.15	Tempering steel colour chart used	34
Figure 2.16	Difference on pearlitic structure due to annealing and normalizing	35
Figure 3.1	Process flow chart of study	39
Figure 3.2	Dimension of sample preparation	40
Figure 3.3	The procedure of liquid penterant inspection	43
Figure 3.4	The applicant used in liquid penentrant testing	44
Figure 3.5	Indication using liquid penetrant inspection	44

Figure 3.6	Radiography using x-ray	45
Figure 3.7	Flow Mach 2 1313B Abrasive Water Jet Machine	46
Figure 3.8	The procedures of waterjet cutting	46
Figure 3.9	Workpiece that were cut by waterjet machine	47
Figure 3.10	The procedure of the sample for tempering process	48
Figure 3.11	The procedure of the sample for annealing process	48
Figure 3.12	Mitutoyo HR-400 Rockwell Hardness Tester	49
Figure 3.13	The sample were put to get the value of hardness of each layers	50
Figure 3.14	Instron CEAST 9050 Pendulum Impact Tester	51
Figure 3.15	The Charpy test	52
Figure 3.16	Charpy (Simple-Beam) impact test specimens (ASTM, 2015)	52
Figure 3.17	Zeiss AxioLab A1 Upright Light Microscope with AxioCam Erc 5s	54
Figure 3.18	ZEISS EC EPIPLAN objectives lens	54
Figure 3.19	JEOL JSM 6010 PLUS/LV Scanning Electron Microscope	55
Figure 4.1	Complete welded low carbon steel plate	58
Figure 4.2	The film of workpiece under film viewer	59
Figure 4.3	Sample after developer were applied	60
Figure 4.4	Visual appearances after treated	61
Figure 4.5	The bar graph of impact test for welded joint (centre)	62
Figure 4.6	The bar graph of impact test for Heat Affected Zone (HAZ)	63
Figure 4.7	Indentation done on multiple layer on the same surface	64
Figure 4.8	Graph result of macro hardness of untreated sample	66
Figure 4.9	Graph result of macrohardness of tempered sample	68
Figure 4.10	Graph result of macrohardness of annealed sample	70

Figure 4.11 Microstructure of each area on untreated sample 72

Figure 4.12 Microstructure of each area of tempered sample 73

Figure 4.13 Microstructure of each area of annealed sample 74

Figure 4.14 Interface of untreated sample 76

Figure 4.15 Interface of tempered sample 77

Figure 4.16 Interface of annealed sample 78

Figure 4.17 Elemental mapping analysis for untreated sample 79

Figure 4.18 Elemental mapping analysis for tempered sample 80

Figure 4.19 Elemental mapping analysis for annealed sample 81

LIST OF SYMBOLS AND ABBREVIATIONS

GMAW	-	Gas Metal Arc Welding
MIG	-	Metal Inert Gas
GTAW		Gas Tungsten Arc Welding
HAZ	-	Heat Affected Zone
NDT	-	Non-Destructive Test
SEM	-	Scanning Electron Microscope
LPT	-	Liquid Penetrant Testing
EDX	-	Energy Dispersive X-Ray
FCC	-	Face Centered Cubic
BCC	-	Body Centered Cubic
CO_2	-	Carbon Dioxide
ASRC	-	Alloy Steels Research Committee
HSLA	-	High- Strength, Low-Alloy Steel
PWHT	-	Post-Weld Heat Treatment
EBSD	-	Electron Backscatter Diffraction

APPENDICES

APPENDIX	TITLE	PAGE
APPENDIX A	ASTM E23	90
APPENDIX B	Gantt Chart (BDP 1)	116
APPENDIX C	Gantt Chart (BDP 2)	117
APPENDIX D	Turnitin Report	118

CHAPTER 1

INTRODUCTION

1.1 Background of Study

The arc welding segment of the industry appears to be growing the fastest, with recent years showing the greatest growth. Welding is the most common joining method, and most common steels are weldable. These days, it become the most important activity in any manufacturing process, and the quality of welding has a direct effect on the performance of the endproduct. Welding can be defined as the process of joining materials into a single piece (Vural, 2014). As widely known, GMAW is a popular welding technique, particularly in industrial sectors. Gas Metal Arc Welding (GMAW), sometimes known as metal inert gas (MIG) welding, is a type of welding method in which an electric arc is produced between a consumable wire electrode and the workpiece metal(s), heating, melting, and joining them (Hajili, 2017). GMAW produces welds with enhanced mechanical characteristics and is often used because it results in welds that are more attractive as well as of higher quality. This technology is increasingly being applied in the construction industry, as well as pipe joining in the oil and gas industry.

Although the oil and gas industries has an incredible safety record over many decades, failures occasionally occur. Corrosion failures, fatigue failures, and ductile and brittle metal failures are the most common reasons of these failures. Due to the heat treatment process, infrastructure and equipments used in the oil and gas industry tend to last for many years because of the properties in the structures and it became stronger, and can survive severe pressures, temperatures, weights, and conditions (Pourazizi et al.,

2020). Heat treatment is the process of heating a metal to a specified temperature, keeping it there, and then cooling it down (Chandra Kandpal et al., 2020). Mechanical characteristics of the metal part will alter during the process. This is due to the fact that high temperatures affect the microstructure of the metal. To sum up, heat treatment is critical for obtaining the appropriate mechanical characteristics and microstructure for a variety of applications. The present study will investigate the mechanical properties and microstructure of low carbon steel joint with ER70s filler metal with different type of heat treatments.

1.2 Problem Statement

During the welding process, rapid heating and cooling occur, causing a severe thermal cycle along the weld line region of any metal submerged in the heating zone. Due to the thermal cycle, the material is not uniformly heated and cooled, resulting in a harder heat affected zone (HAZ), sustaining stress, and a preponderance of cold cracking in the weld metal and base metal. Hazardous stressors that persist regularly cause and impact a wide variety of heating and cooling temperatures. When steel is heated to a certain temperature, it welds well; moreover, the heat generated on it has an unique microstructure from that of the base metal, referred to as the heat affected zone (HAZ) (Pisarski & Pargeter, 1984). Why do weld usually fails in HAZ? It is because when the HAZ is exposed to enough heat for a long enough time, the layer develops microstructure and properties that are different from the parent metal. These property adjustments are normally undesirable, and they end up becoming the component's weakest point. Microstructural changes, for example, can result in residual stresses, decreased material strength, increased brittleness, and decreased corrosion and/or crack resistance (Nayak et al., 2015). As a result, there are several faults in the HAZ. A pre- and/or post-weld heat

treatment can help to reduce HAZ issues. Heat treatment, as is well known, modifies the mechanical and microstructural qualities of the material, making it suitable for the purpose for which it is intended. Nam et al., (1999) proposed that during annealing, the microstructure softens and sometimes recrystallizes and recovers. They also proposed that the morphology of carbides is bound to vary throughout time. Steel's machinability, ductility, hardness, tensile strength, and impact strength are all improved by heat treatment. In this project, two types of heat treatment process which is annealing and tempering will be used.

1.3 Objective of Study

i. To study the welded joint of low carbon steel joint with filler ER70s.

ii. To carry out the non-destructive test by using radiography testing and liquid penetrant inspection.

iii. To study the effect of heat treatment on the mechanical and microstructure properties by performing hardness and impact test.

1.4 Scope of Study

The scope of this study:

i. Gas metal arc welding (GMAW) are used as welding method on the low carbon steel joint.

ii. Performing non –destructive test (NDT) by using radiography testing and liquid penetrant inspection to detect internal and external defects in the welded joint.

iii. Using abrasive water jet to cut the welded metal to the dimension 55mm x 10mm x 12mm.

iv. Mechanical testing of microhardness is carried out on the sample to investigate the resistant of the sample to indentation or penetration.

v. Investigate the material characterization using optical microscope, scanning electron microscope (SEM) and energy dispersive x-ray analysis (EDX) to analyse microstructure and fracture mode on welded cross section.

vi. Visual observation and inspection of the experiments are used to evaluate and analyse them.

1.5 Significant of Study

The oil and gas industry plays a very important role in the global energy supply as well as the world economy. Many technologies are crucial to the existence and functioning of this multi-billion-dollar industry. The oil and gas industry utilizes various highly complex infrastructure such as rigs, pipelines, platforms, bridges, offshore and onshore structure and ships. The vast majority of these infrastructures are built using welding technologies. Welding is important in oil and gas operations, both for new project construction and for the maintenance of existing facilities. Regarding this project, heat treatment will help to increase the mechanical properties. The purpose of this research is to help the oil and gas industry so that they will improve the future production in term of using suitable heat treatment process and reduce the cost of processing, time and energy of the workers.

CHAPTER 2

LITERATURE REVIEW

2.1 Introduction

Welding is the most critical operation in any manufacturing process, and the quality of the welding directly affects the ultimate product's quality. According to Kumar et al., (2019), welding is a procedure that permanently binds two materials (typically metals) together through the use of a specific mixture formed by the proper combination of temperature, weight, and metallurgical conditions. Additionally, he claimed that a range of welding forms have been developed depending on the relationship between temperature and weight, ranging from high temperatures with no weight to large weights with a low temperature. Nowadays, numerous welding techniques are used. The most often used varieties in industrial sectors are Gas Metal Arc Welding (GMAW) or MIG, Gas Tungsten Arc Welding (GTAW) or TIG, Flux Core Arc Welding, and Stick Welding. Apart from that, welding can be done underwater; nevertheless, this demands highly skilled operators who are aware with the conditions and scenarios encountered while working in the water.Welding Process

Metal is melted to form a bridge between the components to be connected, and when the weld metal solidifies, the components become connected. Welding is frequently accomplished by the use of pressure, perhaps in combination with heat (Jenney & O'Brien, 1991). Welding processes are classified into two categories as shown in figure 2.1:

i) Fusion - The surfaces of two components to be connected are cleaned, pressed together, and heated, resulting in the formation of a pool of molten metal connecting the components.

ii) Solid state - The joining metals are not melted. Rather than that, they are heated by friction created by the components moving together under normal load. This process softens the metals and cleans the surface. After then, the sliding is halted, the normal load is raised, and the two surfaces are joined.

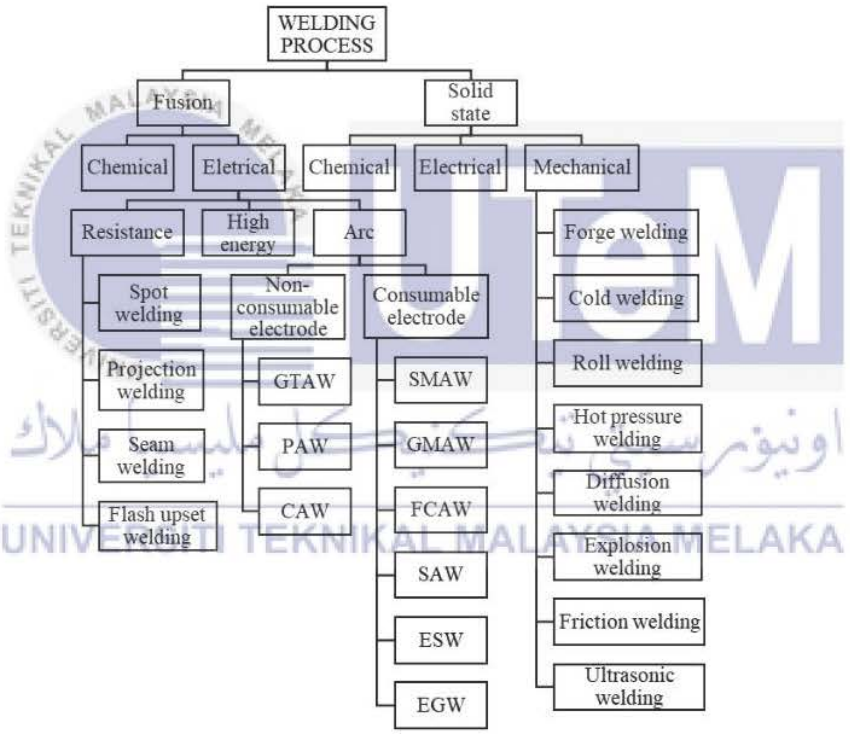

Figure 2.1: Types of welding process (https://www.weldingandndt.com/, 2017)

2.1.1 Welding Gas Metal Arc Welding (GMAW)

Gas Metal Arc Welding (GMAW), also known as metal inert gas (MIG) welding, is a process that involves the formation of an electric arc between a consumable wire electrode and the workpiece metal(s), heating and pressing them together to melt and join (Hajili, 2017). In addition to the wire electrode, a shielding gas is fed into the welding gun, effectively isolating the process from airborne pollutants. Techniques might be semi-automatic or totally automated. While GMAW is commonly driven by a constant voltage, direct current source, it can also be run on constant current or alternating current. External shielding gas protects molten metal from ambient oxides and nitrides during the welding process. There are four fundamental metal transfer processes in GMAW as in Figure 2.2 which were globular, short-circuiting, spray, and pulsed-spray, each having its own set of characteristics, advantages, and disadvantages.

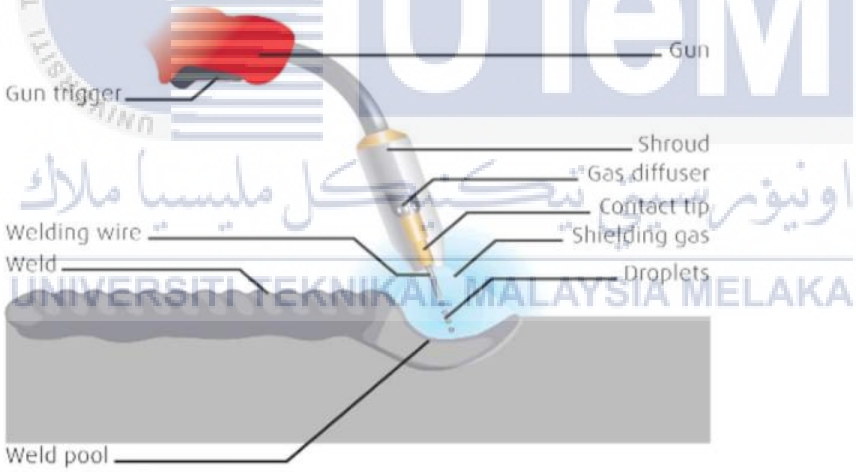

Figure 2.2: Gas Metal Arc Welding (GMAW) (https://www.sparkerweld.com/en, 2018)

Gas metal arc welding (GMAW) is a regularly utilised arc welding technology for joining large metal sections due to its unique properties. These advantages include an enhanced rate of wire electrode deposition, regulated high thermal energy dissipation, no

oxidation due to the use of shielding gas, and increased process efficiency (Wahab, 2014). Additionally, GMAW produces weldments with improved mechanical qualities and is frequently employed because it produces more visually appealing and high-quality welds than the shielded metal arc welding (SMAW) process (Abioye et al., 2019). This technique is increasingly being utilised in the construction industry, as well as the oil and gas business, to link pipes. In GMAW, argon is frequently utilised as the shielding gas. This is because the single-atom gas has a low thermal conductivity and ionisation potential, resulting in inefficient heat transmission to the arc's surface. As a result, argon offers deep but limited penetration into welds.

Table 2.1 showed the typical welding parameters of mild and low alloy for GMAW. These two methods of metal transfer usually used as parameter when welding the mild and low alloy steels.

Table 2.1: Typical welding parameters of mild and low alloy for GMAW (https://www.haynesintl.com/, 2017)

Process	Diameter Of Wire		Voltage	Amperage	Shielding Gas
	inch	mm	(V)	(A)	
Spray transfer	.035	0.9	28 – 32	165 – 200	98% Argon + 2% Oxygen or 75% Argon + 25% CO_2
	.045	1.14	30 – 34	180 – 220	
	1/16	1.6	30 – 34	230 – 260	
Short circuiting transfer	.035	0.9	22 – 25	100 – 140	100% CO_2
	.045	1.14	23 – 26	120 – 150	75% Argon + 25% CO_2

2.1.2 Filler metal

Filler metals liquefy and melt when heated, providing a brazed or soldered connection between two closely fitted components. Capillary attraction distribution occurs in correctly prepared joints when a filler metal has suitable melting and flow characteristics. Filler metals contribute to the formation of joints that meet service requirements for strength and corrosion resistance, among other characteristics. Seven factors must be considered when selecting a filler metal: the base material to be welded, the welding location, regulatory specifications and regulations, design requirements, shielding gas, post-weld heat treatment, and welding equipment. The welder can select an appropriate filler metal by referring to the letter-number designations for each type of filler metal as indicated in Figure 2.3.

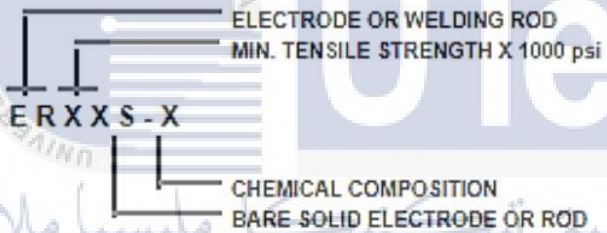

Figure 2.3: The letter-number designations of filler metal (Primo, 2014)

The silicon level in carbon steel electrodes is determined by the electrode classification, with ER70S-3 and ER70S-6 being the most popular. Because of its lower silicon levels, ER70S-2, ER70S-4, and ER70S-7 are sometimes used in pipe applications for open-root work. Lower silicon results in a firmer puddle and more control over the back bead design (Primo, 2014). Because the S-6 type has a larger degree of silicon and the puddle is more fluid, it can be used with less inductance in an open-root weld than an S-2 type electrode (Primo, 2014). It is critical to maintain a steady contact tip-to-work distance

in short-circuit transfer to ensure a smooth transfer. For carbon steel electrodes, the most common shielding gas and short-circuit transfer mode is 75% Ar and 25% CO_2.

2.2 Welding Metallurgy

Metallurgy is the science that investigates how metals behave. It explains how metals behave, their properties, and their internal structure are determined. Additionally, metallurgy refers to the treatments and techniques that enable us to customise a metal's qualities to a certain use. The metallurgy described in this case study is gas metal arc welding's ability to join two mechanically identical or different metals, specifically ferrous and non-ferrous metals. As Rahman et al., (2016) mentioned in their research, several studies in the field of metallurgical engineering are being conducted to investigate how heat treatment can be used to improve the physical and mechanical properties of low carbon steel. As is generally known, the atomic structure of a material has an effect on its properties; for instance, face-centered cubic FCC metals and alloys exhibit extraordinary ductility. Each crystal (grain) contains an ordered array of atoms, and when the grains come into contact, a mismatch in the ordered atoms causes a grain boundary. Imperfections in the crystal structure, such as point defects (such as solute atoms and vacancies) and dislocations, have a wide range of characteristics (Krauss, 2017).

The crystal structure of the metal determines the welding type that is required to meet the weldment criteria. Low carbon steels have body centred cubic (BCC) microstructures that can fluctuate during weld pool formation and joining, resulting in a heterogeneous microstructure on the welded surface. Due to the fact that welding employs heat to unite the metals, the required melting ranges, which span from solid to liquid, for the efficient application of the steel welding process are often referred to as phase diagrams. When a sufficient amount of heat is given to a surface, the ferrite BCC structure

converts to the face-centred cubic (FCC) structure known as austenite. While welding may be advantageous for the connecting method, the temperature variations induced by the welding process may damage the features in certain cases (Magudeeswaran et al., 2018).

2.2.1 Area at fusion weld – Heat Affected Zone (HAZ)

The heat affected zone (HAZ) of a metal or thermoplastic material is the area that is exposed to heat. While HAZ does not melt, heat-intensive processing can alter the material's characteristics and microstructure. Typically, mechanical qualities are altered during welding or high-heat cutting. HAZ refers to the region between the welded or cut surface and the base metal. These zones vary in size and severity depending on the material properties, the heat intensity and concentration, and the procedure used. When subjected to high temperatures for a sustained length of time, the HAZ undergoes structural and physical changes that identify it from the parent metal (Jeong et al., 2021). Typically, these property changes are undesirable and contribute to the material's weakness. For example, microstructural changes may result in residual stresses, decreased material strength, increased brittleness, and reduced resistance to corrosion or cracking. As a result of this, the HAZ has a high rate of failure. The zones and bounds of the heat-affected zone are illustrated in Figure 2.4 below.

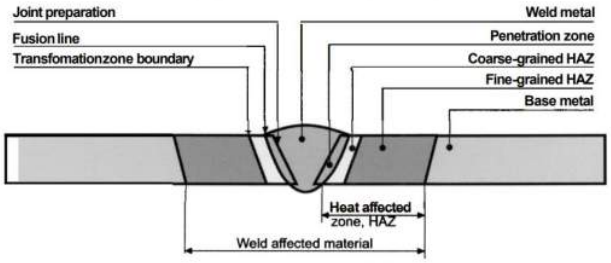

Figure 2.4: Zones and boundaries in the heat affected zone (https://whatispiping.com/, 2021)

2.3 Welding Parameter

The GMAW welding parameters have an impact on the quality, productivity, and cost of the welding joint. If all the welding parameters are in place, the perfect arc will be achieved. Major parameters contain:

i. welding current and voltage

ii. welding travel speed

iii. Flow rate of gas

According to Owolabi et al., (2016), the welding current is the most critical variable in the arc welding process since it affects the melting rate, deposition rate, penetration depth, and amount of base metal melted. His research proved that raising the welding current increases the hardness of the weld up to 115A and 116A for mild steel and low carbon steel, respectively, but declines with increasing the welding current. The ultimate tensile strength of mild steel decreases with increasing welding current but increases with 200A and 115A welding currents, respectively. The yield and impact strengths of the two samples decrease with increasing welding current.

2.4 Defects in Welding

As with any other industrial process, welding is prone to faults. The shape and size of the metal structure may alter slightly during the operation. It is likely that this condition is produced by the employment of an ineffective welding approach or technique. While it is difficult to achieve a defect-free welding joint, various procedures can help minimise defects to a considerable extent. Welding flaws are classified into two types: exterior defects and internal problems. External flaws are visible on the welded material's upper

surface, whereas internal imperfections are visible at a greater depth. Figure 2.5 below is the classification of some of welding defects in GMAW.

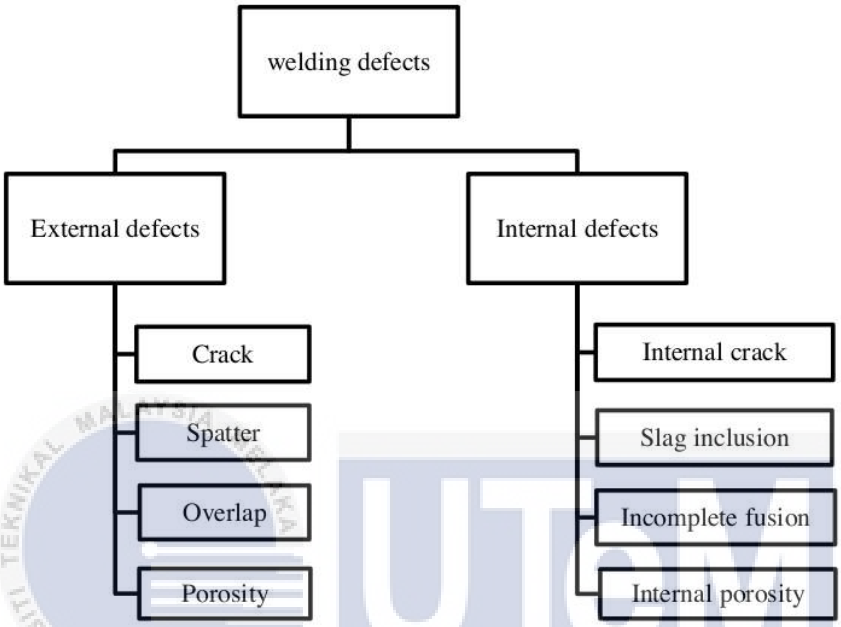

Figure 2.5: Classification of welding defects (https://whatispiping.com/, 2020)

2.4.1.1 Type of Defects

There are some of the most common welding flaws that can be found in welding field such as crack, spatter, porosity and incomplete fusion. These are the sort of flaws that commonly can be see found when a weld is complete either a single pass or a complete weld, depending on the defect itself. Most of it are easy to be detected.

1) Crack

Cracks are frequently planar discontinuities with a large distance between their length and diameter. Cracks can form at either elevated or low temperatures and in three locations: the weld, the base metal's heat affected zone, or at the weld-to-base metal fusion

line. Furthermore, cracking indicates a breakdown in metallurgical control. Cracks can be classified into several types based on the temperature at which they occur:

i. Hot cracks: Hot weld cracking occurs at high temperatures, typically exceeding 1000 degrees Fahrenheit (538 degrees Celsius), and the fault appears practically immediately (though not always visibly) after the weld hardens. Hot cracking nearly always occurs parallel to or immediately next to the longitudinal direction of the weld bead.

ii. Cold cracks: Occurs primarily when the weldment's temperature has returned to atmospheric levels. It can happen instantly or a week later, and it can happen with or without loading. Additionally, it may arise as a result of loading stress or as a result of stress concentrations generated by the notch effect of surface discontinuities.

iii. Crater cracks: These take place at the end of the welding process, shortly before the operator makes a pass over the weld joint. They are often seen after the finish of a weld. When the weld pool cools and solidifies, it must retain enough volume to compensate for any shrinkage in the weld metal. If this is not done, a crater fracture will form.

As a result, cracks, particularly surface cracks, are regarded as the most harmful of all flaws, and practically all specifications restrict the admission of any crack observable by conventional methods of analysis. Cracks can reveal themselves in a variety of forms and locations. Factors that contribute to crack formation include the following:

i. Temperature gradients that result in thermal stresses in the weld zone as a result of the weld bead's solidification and contraction relative to the surrounding structure.

ii. Differences in the weld zone's composition.

iii. Grains' borders become fragile.

iv. Lack of contraction of the welded metal during cooling.

Figure 2.6 below shows the example of cracks that usually happen in weldment.

Figure 2.6: Welding crack (https://allgas.us/, 2019)

Select base and filler materials with care to avoid cracks. Additionally, it may be quite advantageous to store the filler material appropriately. Cracks created by spreading the bead too thinly can be rectified by applying sufficient filler and ensuring that the parts fit together properly. Apart from the base and filler materials, adjusting the travel speed and voltage settings frequently results in sufficient filler material to withstand internal pressures caused by metal shrinkage. Contaminants can also have an effect on the strength of the weld, therefore thoroughly clean the workpiece. In some instances, preheating may be required.

2) Spatter

Spatter is a term that refers to droplets of molten material that occur at or near the welding arc. It is frequently regarded as a nuisance and should be taken into account while developing an application. Spatter happens when the weld pool is disrupted to the point where molten metal spits or sprays out of the weld, as illustrated in figure 2.7. Spatter is a frequent occurrence during GMAW welding. The primary reason for this is that wire transmission into the weld causes a disruption in the molten weld pool. This is frequently

the result of an amperage-voltage mismatch. This occurs when the welding voltage is either too high or too low for the particular wire and gas combination. The arc is too cool in this scenario to keep the wire and pool molten, resulting in a stubbing action on the wire. This can occur when the current is either too high or too low. Additionally, as a result of the gas created, scattering may occur. While using CO_2 in GMAW increases arc energy and is extremely cost effective, but it results in increased weld spatter. Argon is commonly used to prevent CO_2 splatter.

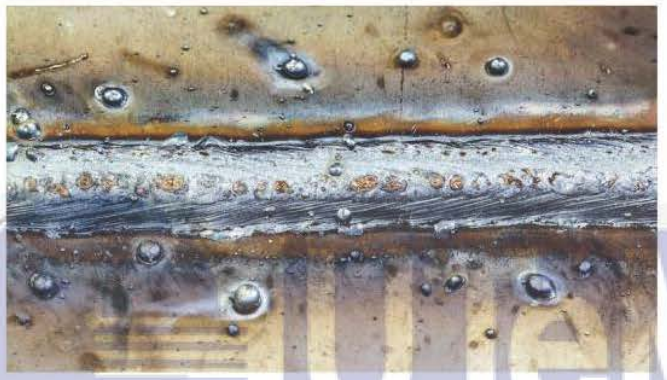

Figure 2.7: Spatter (https://weldguru.com/, 2021)

There are some ways to reduce the spatter. Firstly, the arc voltage should be adjusted. If the voltage setting is not adjusted properly, it can result in a large number of spatters. Low voltage settings produce spatter because the wire is repeatedly shorted in the weld pool, resulting in small explosions at the wire tip. This is typical for short-arc MIG welding, but if the arc voltage is set properly, the expelled spatter will be extremely little and will not adhere to your workpiece or surrounding fixtures. On the other hand, due to the massive arc force, an excessive voltage might result in severe splatter. Another option is to eliminate the protrusion. The stick-out length, or the length of wire that extends beyond the contact tip that forms the weld, has an effect on the arc's amperage. If the stick-out is excessively long, it can reduce amperage, resulting in spatter escaping the weld due

to the weld not reaching deep enough. If it is too short, the amperage is increased, which results in material falling out of the weld owing to the arc's force.

Apart from that, welding equipment should be improved. Due to the high expense of spatter, certain modern welding power sources place a premium on spatter reduction. They also provide other benefits that enhance overall weld quality and readily justify the cost.

3) Porosity

Cavities or pores formed by trapped gases in molten metal during the solidification process are referred to as porosity. In other words, porosity can be thought of as a trapped gas bubble within the welded metal. Porosity can take on a variety of shapes and sizes, including dispersed pores, wormhole pores, surface-breaking pores, and crater pipes.

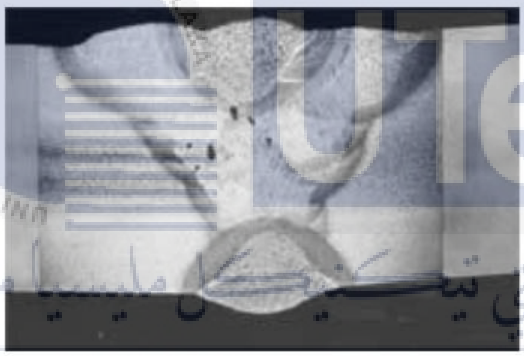

Figure 2.8: Uniformly distributed porosity (https://www.twi-global.com/)

The porosity is created when nitrogen, oxygen, and hydrogen are absorbed in the molten weld pool and subsequently released and trapped in the solidified weld metal. Inadequate gas shielding is the most common source of nitrogen and oxygen absorption in the weld pool. Distributed porosity may be created with as little as 1% air entrainment in the shielding gas, but more than 1.5% results in gross surface breaking pores. Apart from that, porosity is typically caused by gas line leaks, high gas flow rates, draughts, and an

excessive amount of weld pool turbulence. Hydrogen can be generated when moisture from wet electrodes, fluxes, or the workpiece surface condenses.

There are a few methods for overcoming it. To begin, pretreatment of material surfaces before to welding can be just as critical to creating a clean weld as welding itself. Without proper cleaning, the aftereffects of manufacturing might result in surface contamination and porosity. Next, take note on the flow of gas from the gas shield. The more powerful the gas flow, the more air is disrupted. This can result in impurities combining with the weld puddle, resulting in an impure weld. Although flow rates might vary, it is critical to choose the appropriate flow rate for each application. Last but not least, always do checking on the equipment. Hoses might leak and wire might become exposed or damaged over time. Before striking an arc, double-check all connections to ensure an exact flow from the gas shield. Check the weld gun tip for cleanliness; sometimes the tip becomes clogged, resulting in contaminants in the weld.

4) Incomplete fusion

Incomplete fusion occurs when there is insufficient fusion between the weld metal and the fusion faces or nearby weld beads, as seen in Figure 2.9. This absence of fusion can occur in any location inside the weld joint, but is most visible in fillet and groove welds. Incomplete fusion can occur as a result of the base material's or previously deposited weld metal's melting temperature not being increased sufficiently during the welding process. It is frequently encountered on one leg of a fillet weld and is produced by an insufficient welding angle, which results in an uneven distribution of heat between the two sides of the joint. Additionally, it could be caused by a failure to clean the surface of the base material with which the deposited weld metal must fuse.

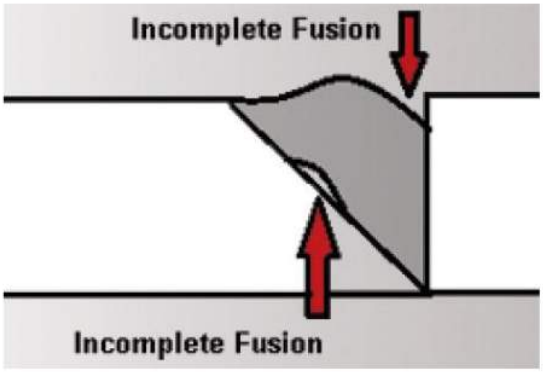

Figure 2.9: Diagram of incomplete fusion (https://weldingengineers.co.nz/)

Numerous precautions must be taken to ensure the full fusion of two or more pieces of metal. After completing a weld, always clear away any slag. Leaving slag in place can result in structural discontinuities, such as insufficient fusion. Incomplete fusion, like a large number of other welding problems, is typically the result of insufficient technique. Inadequate travel speed and welding angle will make thoroughly fusing separate pieces of metal problematic. Additionally, it is vital to select the appropriate welding procedure for the application. Attempting to fuse together thick metal pieces with GMAW welding is an example of selecting the inappropriate welding procedure. The strength of the MIG welding method is its ability to join a wide variety of thinner metals.

2.5 Carbon Steel as Base Material

Steel is an alloy metal that is generally made of iron and carbon, as well as trace metals. Due to its high tensile strength and low manufacturing cost, it is a preferred metal among manufacturers. However, steel comes in a variety of varieties, each with its unique set of properties. Carbon steel, for instance, is frequently preferred over other types of steel. Carbon steels are defined by the Alloy Steels Research Committee (ASRC) as "steels that include less than 0.5% manganese and 0.5% silicon, with all other steels classed as

alloy steels" (Metals. & International., 1997). The fundamental alloying elements used in steel are manganese, lead, nickel, chromium, molybdenum, vanadium, niobium, silicon, and cobalt (Metals. & International., 1997),(Frihat, 2015). Carbon steels are categorised into three groups based on their carbon content: low carbon steel, medium carbon steel, and high carbon steel. The carbon content, microstructure, and characteristics of these materials are compared in Table 2.2 below.

Table 2.2: The comparison of the carbon content, microstructure, and properties (https://matmatch.com/)

Type of Carbon	Carbon Content (Wt.%)	Microstructure	Properties	Examples
Low carbon steel	< 0.25	Ferrite, pearlite	• Low hardness and cost. • High ductility, toughness, machinability and weldability.	AISI 304, ASTM A815, AISI 316L
Medium carbon steel	0.25 – 0.60	Martensite	• Low hardenability, medium strength, ductility and toughness.	AISI 409, ASTM A29, SCM 435
High carbon steel	0.60 – 1.25	Pearlite	• High hardness, strength, low ductility.	AISI 440C, EN 10088-3

2.5.1 Low Carbon Steel

Low-carbon steel is the most often used kind of carbon steel. Typically, these steels have a carbon content of less than 0.25 percent. Due of these materials' inability to be hardened through heat treatment (to form martensite), they are frequently hardened using cold work. Frequently, carbon steels are delicate and brittle. They do, however, possess a high degree of ductility, which makes them ideal for machining and welding, as well as being reasonably priced. While high-strength, low-alloy steels (HSLA) are occasionally referred to as low-carbon steels, they also include other elements such as copper, nickel, vanadium, and molybdenum. These can make up up to 10% of the steel's composition. As the name implies, high-strength, low-alloy steels have been heat treated to improve their strength. Additionally, they retain their ductility, allowing them to be moulded and machined easily. Corrosion resistance is increased in HSLA steels over ordinary low-carbon steels.

It is primarily composed of ferrite, a solid solution phase of carbon dissolved in alpha-iron that crystallises as a body-centered cubic (BCC) crystal (Evans, 2012). Ferrite is steel's softest phase, and it substantially contributes to low carbon steel's superior machinability as compared to other carbon and alloyed steels. As the carbon content of steel increases, the amount of pearlite produced in the microstructure of the metal increases proportionally. The microstructure of pearlite is made of alternating layers of ferrite and iron carbide (cementite). Low carbon steels are frequently employed in the fabrication of pipes, structural forms (I-beams, channel, and angle iron), building and bridge components, food cans, and vehicle body components.

2.5.2 Medium Carbon Steel

Carbon concentrations vary between 0.25 and 0.60 percent, whereas manganese concentrations range between 0.60 and 1.65 percent. The autenitising, quenching, and tempering processes improve the mechanical characteristics of this steel, resulting in a martensitic microstructure. Although heat treatment is only possible on extremely thin sections, extra alloying elements such as chromium, molybdenum, and nickel can be added to improve the steel's heat treatment capacity and therefore hardening capability. While hardened medium-carbon steels provide more strength than low-carbon steels, they sacrifice ductility and toughness in the process. These steels are mostly used to produce shafts, axles, gears, crankshafts, couplings, and forgings. Rails, railway wheels, and rail axles are composed of steels containing between 0.40 and 0.60 percent carbon (Singh, 2020).

2.5.3 High Carbon Steel

The carbon level is between 0.60 and 1.25 percent by weight, whereas the manganese concentration is between 0.30 and 0.90 percent by weight. It is the strongest and most durable carbon steel available, but it is also the least ductile. High-carbon steels are extremely resistant to wear due to their virtually universal hardening and tempering. Tool and die steels are chromium-vanadium-molybdenum-tungsten-alloyed high-carbon steels. Combining these metals results in a highly hard, wear-resistant steel due to the creation of carbide compounds such as tungsten carbide (WC) (Qiao et al., 2021). High-carbon steels are applied in cutting tools, springs, great-strength wire, and dies due to their high wear resistance and toughness.

2.5.4 Application of Carbon Steel in Oil and Gas Industry

Carbon steel, as we all know, is a strong metal with a great resistance to wear. It is the most often used steel type in the oil and gas industries. It is used to construct pipelines, structural components, platforms, and other objects. Carbon steel is critical in the oil and gas sectors because it is an iron alloy that contains up to 2% carbon, which enhances the material's strength and offers corrosion resistance (Wahab, 2014). Furthermore, the steel contains trace quantities of other metals such as nickel and chromium. Additionally, carbon steel has enough structural and thermal strength, is economical, and its surfaces may be protected against corrosion using well-known corrosion inhibitors. The figure 2.10 below illustrates a typical oil and gas pipeline structure.

Figure 2.10: The example of pipeline structures in oil and gas (https://www.codesteel.com/2017)

2.6 Heat Treatment Process

Heat treatment is widely utilised in the steelmaking and welding and joining sectors today, with post-weld heat treatment focusing on the weld bead and joining metal. Heat treatment is a procedure that includes controlling the rate of heating and cooling and involves the application of a range of steel treatments for a variety of metalworking purposes (Rahman et al., 2016). The physical and mechanical characteristics of the metal

will change during annealing, tempering, annealing, and quenching, and other variables will also impact the heat-treated metal. The hardness, toughness, and strength of the metal, as well as its brittleness, may be increased by heat treatment, resulting in more dependable and superior characteristics (Chandra Kandpal et al., 2020). Apart from that, it is a method of enhancing the shapeability, machining, and manufacturability of the metal (Hnizdil & Chabicovsky, 2018). Heat treatment is employed in this study to determine the efficacy of changes made to the characteristics of low carbon steel in order to make it more stable and steady.

Table 2.3: The comparison result of heat treatment on welded joint of previous study

Author	Title	Material	Process	Finding
čerová et al., (2019)	Microstructure analysis and mechanical properties of low alloyed steel with retained austenite obtained by heat treatment	Low carbon low alloyed steel.	Annealing	With decreasing retained austenite volume fraction, the retained austenite carbon content dropped. In all treatments, the volume fraction of retained austenite ranged between 11% and 18%. Slower cooling produced coarser microstructures, longer retained austenite laths, lower retained austenite carbon concentrations, and more prominent retained austenite lath bainite morphology.
Reyes et al., (2017)	Effect of heat treatment on the mechanical and microstructural properties of a low carbon steel	Low carbon steel	Annealing Tempering Hardening Normalizing	The investigation of the effect of heat treatment on the steel sample reveals that there is always a trade-off between two properties. Tempering reduces the steel's toughness and tensile strength while increasing its hardness slightly. The microstructure of the untreated control phases exposes ferrite and pearlite, while the hardened

				micrograph displays mainly coarse martensite. The microstructure of the tempered sample indicates a martensite phase with recrystallization of ferrite.
Chandra Kandpal et al., (2020)	Effect of heat treatment on properties and microstructure of steels	Alloy steel (EN 31, EN 24 and EN 8)	Annealing Normalizing Hardening	From the data obtained, it can be claimed that mechanical qualities depend greatly on the different heat treatment processes and cooling rate. It will deliver satisfactory results for high ductility and minimum toughness. This treatment is indicated as final following manufacture. Hardened sample showed the maximum tensile strength and hardness compared to other heat-treated samples, with the lowest ductility and impact strength.
Prabakaran & Kannan, (2021)	Effects of post-weld heat treatment on dissimilar laser welded joints of austenitic stainless steel to low carbon steel	Austenitic stainless steel (AISI316) and low carbon steel (AISI1018)	Annealing	The effects of PWHT on a variety of metal complexes were thoroughly investigated. Tensile strength and elongation of the joint were significantly increased with PWHT at 960°C. Following PWHT at 960°C, the chromium carbide was successfully dissolved and did not precipitate again in the weld zone's grain and grain boundari
Valdes-Tabernero et al., (2020)	The sensitivity of the microstructure and properties to the peak temperature in an ultrafast heat treated low carbon-steel	Hot-rolled 6 mm thick low carbon steel sheets	Annealing	The rise in peak temperature favours the production of austenite. These activities ult in a decrease in the volume fraction of ferrite as the volume fraction of inter-critical austenite increases. Due to the increased dislocation density of non-recrystallized ferrite, it is tougher than recrystallized ferrite.

2.6.1 Stages of Heat Treatment

To achieve the desired outcome, the metal or alloy is heated to a specific temperature, sometimes as high as 1300°C, held there for a specified amount of time, and then cooled. When a metal is heated, its physical structure, sometimes referred to as microstructure, changes, resulting in changes in the metal's physical properties. The period of time required to heat the metal is referred to as the 'soak time.' The duration of the soak time has an influence on the properties of a metal, as metal that has been soaked for an extended period of time will exhibit distinct microstructure changes in comparison to metal that has been soaked for a brief period of time (Mesquita et al., 2017). After the soak time, the cooling procedure has an influence on the metal's outcome. Metals can be swiftly cooled, a process known as quenching, or gradually cooled in the furnace to ensure the correct end is obtained. The soak temperature, soak time, cooling temperature, and cooling duration all contribute to the desirable characteristics of a metal or alloy. When a metal is heat treated numerous times throughout the production process, the characteristics of the metal are altered, and some metals may be treated several times.

Based on figure 2.11, heat treatment is comprised of three steps: progressively heating the metal to provide uniform temperature distribution, soaking the metal at a certain temperature for a specified period of time, and cooling the metal to room temperature to achieve the desired characteristics. The heating stage, the soaking stage, and the cooling stage are the three steps of heat treatment.

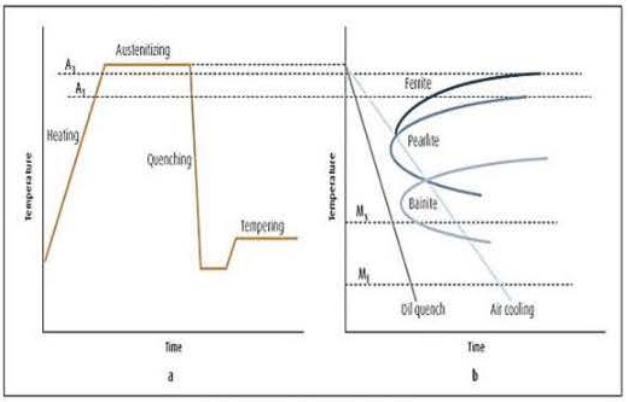

Figure 2.11: a) Temperature b) Its relation to the TTT diagram

(https://www.slideshare.net/,2015)

1) The heating stage

The first step in a heat-treating procedure is heating. When alloys are heated to a given temperature, it is done to change their structure. At room temperature, the alloy is said to be either a solid solution, a mechanical mixture, or a combination of both. In a solid solution, two or more metals are bonded together to generate a solution which does not show the elements when observed under the microscope. The elements and compounds are easily noticeable and compressed by a base metal matrix in a mechanical mixture.

2) The soaking stage

Soaking is the stage when the entire structure of the heated metal undergoes a thorough transformation. The objective of the soaking stage is to maintain a constant temperature for the metal until the necessary internal structure develops. The time required to soak the metal is dependent by its mass. In other terms, soaking happens when a section of a metal becomes evenly red as a result of prolonged exposure to heat.

3) The cooling stage

The third and last stage of the heat treatment procedure is cooling. Additionally, depending on the cooling method used, it alters the chemical properties of the soaked metal. The metal can be directly contacted with a cooling medium, which can be a gas, a liquid, or a solid, or a mixture of these. The speed at which the metal cools is determined by the metal itself and the desired end result.

There is no way to bypass any of the three phases of heat treatment. The heating stage assists in the change of the metal's structure from room temperature to the soaking stage, which occurs when the metal develops a consistent red colour. Cooling is the stage at which the metal completely transforms into its new characteristics as a result of the cooling process.

2.6.2 Types of Heat Treatment

Heat treatment is important for achieving the optimal characteristics of a metal and can be used to soften or condition it, as in normalising and annealing, or to harden it, as in hardening, quenching, and tempering. These treatments result in the formation of three distinct microstructures: pearlite, bainite, and martensite. There are four primary types of heat treatment processes that are often employed in the steelmaking industry: annealing, tempering, hardening, and normalizing. The exact heat treatment required in manufacturing will be determined by the metal chemistry, the part's size, and the desired characteristics. Heat treatment is frequently used in forging and post weld heat treatment, or preheat (Singh, 2020). The iron-carbon phase diagram (figure 2.12) is often used to understand the various phases of steel and cast iron. As we know, steel and cast iron are both made of iron and carbon. In table 2.3, there are table comparison of each of the heat treatment process.

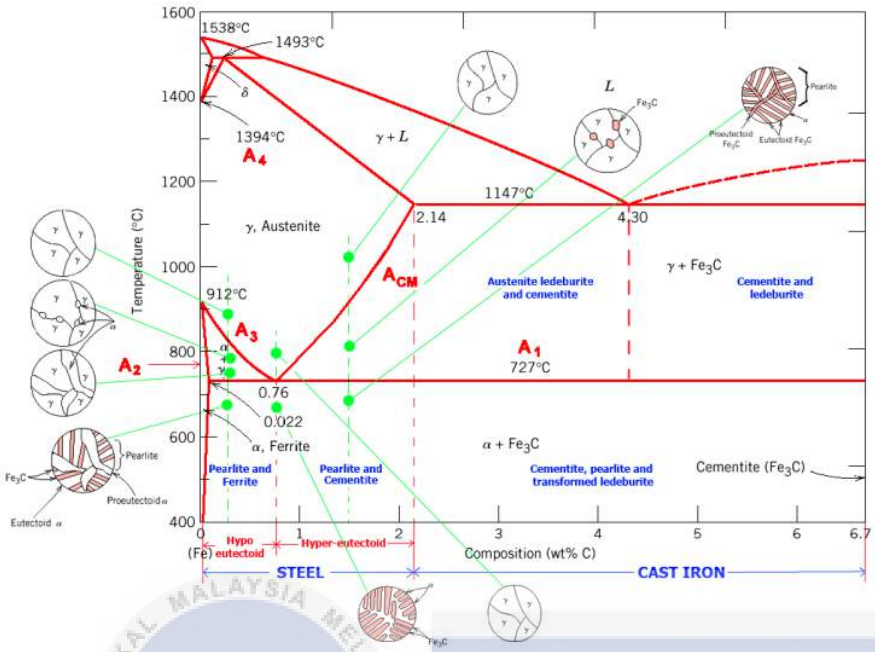

Figure 2.12: Iron-carbon Phase Diagram (https://www.tf.uni-kiel.de/en, 2021)

Table 2.4: Table comparison of heat treatment process

Type of Heat Treatment	Definition	Process	Temperature	Purpose	Application
Annealing	Is a process to soften metal in order to get desired chemical and physical properties.	Involves heating a metal to or near critical temperature and then slowly cooling it to room temperature.	260˚C- 950˚C	To soften the materials.	Used for metals and metal alloys.
Hardening	Is a process used to increase the hardness of a metal.	The metal is heated until it reaches the austenitic crystal phase, then pidly cooled.	Between 800˚C- 900˚C	To increase the hardness of a metal.	Used for metal alloys with a high carbon and alloy content.
Tempering	Is the process of removing excess hardness,	By heating it to produce austenite and then quenching it to produce	As high as 950 °C for up to 20 hours	To make metals less brittle.	Used mainly for steel.

	and thus brittleness, caused by hardening.	martensite.			
Normalizing	Is a process used to relieve internal tensions produced by processes such as welding, casting, or quenching.	Involves heating the steel to about 40˚Celsius beyond its upper critical temperature limit, holding it at this temperature for a period of time, and then cooling it in air.	Between 750°C-980°C	To improves toughness, ductility while still maintaining high strength level.	Used mainly for material that require impact strength or have to withstand huge external stresses.

The following subject will go into full detail about the types of heat treatment that are usually advantageous in welding.

i. Annealing

Annealing is a chemical and physical process that softens metals to get the desired chemical and physical properties. During annealing, the metal is heated to its upper critical temperature and then slowly cooled to room temperature. It improves the ability of the metal to be cold worked and formed. Additionally, it improves the machinability, ductility, and toughness of the metal. Annealing is a process that is commonly used in ferrous alloys. It involves heating the metal over the upper critical temperature and then cooling slowly to create pearlite or ferrite. Annealing is used to soften pure metals and a range of alloys that cannot be heat treated (Reyes et al., 2017). The metal is sufficiently heated to produce recrystallization, which corrects defects caused by plastic deformation. (Phoumiphon et al., 2016). In general, the pace at which these metals cool has little influence on them. The bulk of heat treatable nonferrous alloys are also

annealed to reduce the hardness of cold working. These can be gradually chilled to cause full crystallisation and the formation of a fine microstructure.

Ferrous alloys are frequently referred to be 'completely annealed' or 'process annealed'. Full annealing requires extremely slow cooling rates to create coarse pearlite. In process annealing, the cooling rate may be increased up to and including normalizing. The fundamental objective of process annealing is to produce a microstructure that is consistent. Nonferrous alloys are often annealed in a number of ways, including 'recrystallization annealing,' 'partial annealing,' 'complete annealing,' and 'final annealing'. The figure 2.13 below shows the grain of metals in annealing stages. In figure 2.13, a small increase in the annealing temperature initiates the second step, which entails dislocation rearrangement and elimination. At rearrangement temperature, opposing dislocations caused by diffusion are reduced, resulting in a reduction in the material's total internal stresses. Following the annihilation of opposite sign dislocations, the remaining dislocations begin to expand in order to mitigate the effects of internal stresses. This process of rearranging remaining dislocations is referred to as polygonization, in which edge dislocations unite to form tilt boundaries and screw dislocations combine to form twist boundaries. As the steel annealing temperature is increased higher, the activation energy increases and the high-angle grain boundary begins to migrate. Only dislocations and point defects are moving entities that reduce internal stresses in the material below the recrystallization temperature. Following the recrystallization process, freshly created grains begin to expand. The growth of large grains occurs at the expense of crystallised fine grains. The greater the steel annealing temperature, the more aggressive the growing process will be. This force is linked to grain boundaries. Higher grain border area in conjunction with increased grain size results in a decrease in total energy per unit area.

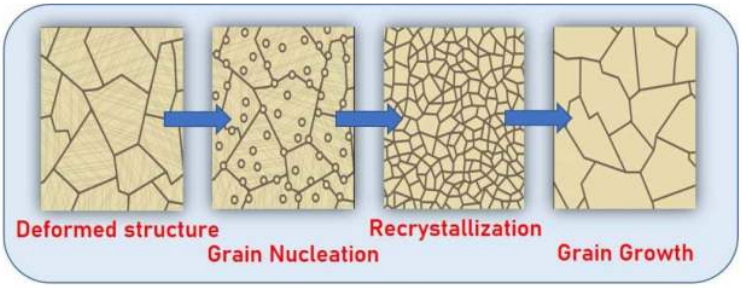

Figure 2.13: Grain of metals in annealing stages (https://materials-today.com/, 2020)

ii. Hardening

The most often used heat treatment procedure is hardening, which is used to improve a metal's hardness. To harden a metal (usually steel or cast iron) by quenching, it must be heated above its upper critical temperature and then rapidly cooled. Cooling can be accomplished using forced air or other gases, depending on the alloy and other factors (such as the exchange between maximum hardness and fracture and distortion) (such as nitrogen). Liquids such as oil, water, a polymer diluted in water, or brine may be used because of their increased heat resistance (Rahman et al., 2016). When austenite is rapidly cooled (depending on the alloy composition), a part of it changes into martensite, a hard, brittle crystalline structure. The chemical composition and quenching process of a metal determine its quenched hardness. The figure 2.14, it shows the steel rapidly cooled by using water after heated.

Figure 2.14: Hardening process (https://www.wasatchsteel.com/, 2018)

iii. Tempering

Tempering is a process that improves the toughness of hardened steel by heating it to produce austenite and then quenching it to produce martensite. Untempered martensite is a strong, tough, brittle material. The more brittle it is, the stronger and tougher it is. The strength and hardness of martensite are due to elastic strain within the martensite, which is caused by an excess of carbon atoms in the gaps between the iron atoms in the martensite. The martensite strength and hardness increase as the quantity of carbon in a steel increases (up to roughly 0.8w% carbon).

During the tempering process, the carbon atoms in martensite migrate out of the spaces between the iron atoms, forming iron carbide particles (Singh, 2020). The strain is released as the carbon atoms separate from the iron atoms in martensite. As a result, steel toughness is improved at the price of strength. The amount of tempering required is dependent on the steel's intended usage. Because toughness is not always needed, tempering at a low temperature for a brief period of time is sometimes suitable. When extremely strong and tough steel is required, a high carbon steel tempered at a high

temperature may be used. Figure 2.15 below shows the tempering steel colour chart that used in heat treatment process.

Figure 2.15: Tempering steel colour chart used (https://materials-today.com/, 2020)

iv. Normalizing

Normalizing is a type of heat treatment that is used to relieve internal stresses caused by welding, casting, or quenching. Normalizing produces not just pearlite but also martensite and, in certain circumstances, bainite, resulting in a harder, stronger steel with less ductility than complete annealing of the same composition. The normalization process involves heating the steel to about 40˚Celsius over its upper critical temperature limit, keeping it there for an extended length of time, and then cooling it in air. Normalized steels are more difficult to work with and stronger than annealed steel (Rahman et al., 2016). Indeed, steel is stronger than any other material in

its normalized state. This is why parts requiring impact resistance or the ability to tolerate extremely high external pressures are often normalized. The figure 2.16 below illustrates the variation in the spacing of the cementite plates in pearlite between annealing and normalising. Ferrite is a very soft structure, whereas cementite is extremely hard. By bringing the cementite plates closer together in normalised medium pearlite, they tend to stiffen the ferrite, preventing it from yielding as easily, hence enhancing hardness.

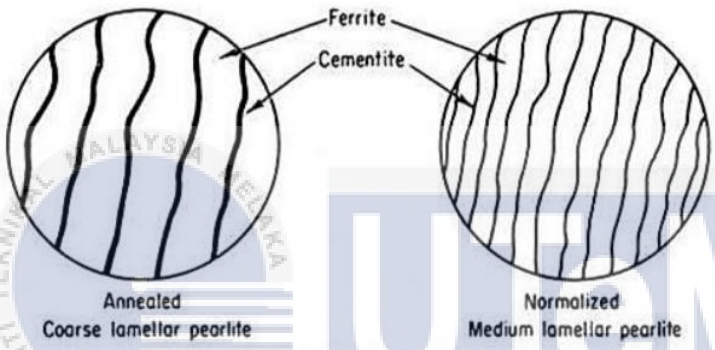

Figure 2.16: Difference on pearlitic structure due to annealing and normalizing (https://www.ques10.com/, 2018)

2.6.3 Heat Treatment on Welded Joint

Welding is a critical component in operating and maintaining assets in the oil and gas (upstream, midstream, and downstream) industries, as well as the chemical processing industries. While welding has a wide range of applications, it can unintentionally damage equipment by transferring residual stresses into the material, resulting in decreased material properties. Post Weld Heat Treatment (PWHT) is a process that is routinely used to guarantee that the material strength of a component is maintained following welding. PWHT can be used to reduce residual stresses, control hardness, and assist in material

strength enhancement (Moore & Booth, 2015). Heat treatment may be conducted following welding for one or more of the following reasons:

i. To achieve dimensional stability in order to preserve tolerances during machining operations or during service shake-down.

ii. To design and fabricate novel metallurgical structures in order to achieve the necessary mechanical properties.

iii. To reduce the possibility of in-service problems such as stress corrosion or brittle fracture by reducing the residual stress in the welded component.

If PWHT is conducted incorrectly or not at all, residual stresses can combine with load stresses to exceed the design limitations of a material. This can result in weld failures, enhanced cracking potential, and increased sensitivity to brittle fracture. In general, the higher the carbon content of a material, the more probable it will require PWHT following welding procedures. Similarly, the higher the alloy content and the greater the cross-sectional thickness of the material, the more likely it will require PWHT.

2.7 Summary of Literature Review

Gas Metal Arc Welding (GMAW), sometimes referred to as metal inert gas (MIG) welding, is a type of welding in which an electric arc is formed between a wire electrode and the workpiece metal. GMAW produces welds that are more attractive and of higher quality than those produced by shielded metal arc welding (SMAW). In the arc welding process, the welding current is the most important variable. Carbon steels are defined by the Alloy Steels Research Committee (ASRC) as "steels containing less than 0.5 percent manganese and 0.5 percent silicon, with all other steels classed as alloy steels." Carbon steel is classified into three types based on its carbon content which is low carbon, medium carbon, and high carbon steel. Carbon steel is critical in the oil and gas industries because

it is an iron alloy that contains up to 2% carbon, which indirectly enhances the material's strength. Heat treatment is frequently employed in steel manufacturing, as well as welding and joining, with post-weld heat treatment concentrating on the weld bead and joining metal. The duration of the soak time has an effect on the characteristics of a metal, since metal that has been soaked for a long period of time will exhibit differential microstructure changes compared to metal that has been soaked for a short amount of time. Heat treatment is essential for attaining the best characteristics and may be used to soften or condition a metal, as with normalizing and annealing, or to harden a metal, as with hardening, quenching, and tempering.

CHAPTER 3

METHODOLOGY

3.1 Introduction

This chapter were described in details the process of finding the effects of heat treatment on mechanical properties and microstructure of low carbon steel joint with 70s filler metal. Based on previous study, the students or professors had also researched, tested and performed the effect of heat treatment on low carbon steel. This information were provided more perspectives into how this work is to be carried out and the studies and processes for potential use of particular fields and areas that are included in this subject.

The flowchart of overall process in this study were depicted in Figure 3.1. This study began by initiating specimen preparation and were proceed with the welding process which were GMAW with butt joint design. And then, were followed by carried out non-destructive test to check any flaws of the specimen. After that, the sample were cut into small pieces with the dimensions of 55mm x 10mm x 12mm. These samples were carried out in two heat treatment process which are annealing and tempering. When the samples are done with heat treatment process, the samples were tested to observe the mechanical by hardness test and impact test. To identified the material characterization, analytical scanning such as optical microscope, Energy Dispersive X-Ray Spectroscopy (EDX) and Electron Backscatter Diffraction (EBSD) were used to study the microstructure element of the welded low carbon steel. Lastly, all the data were analyzed to conclude the study.

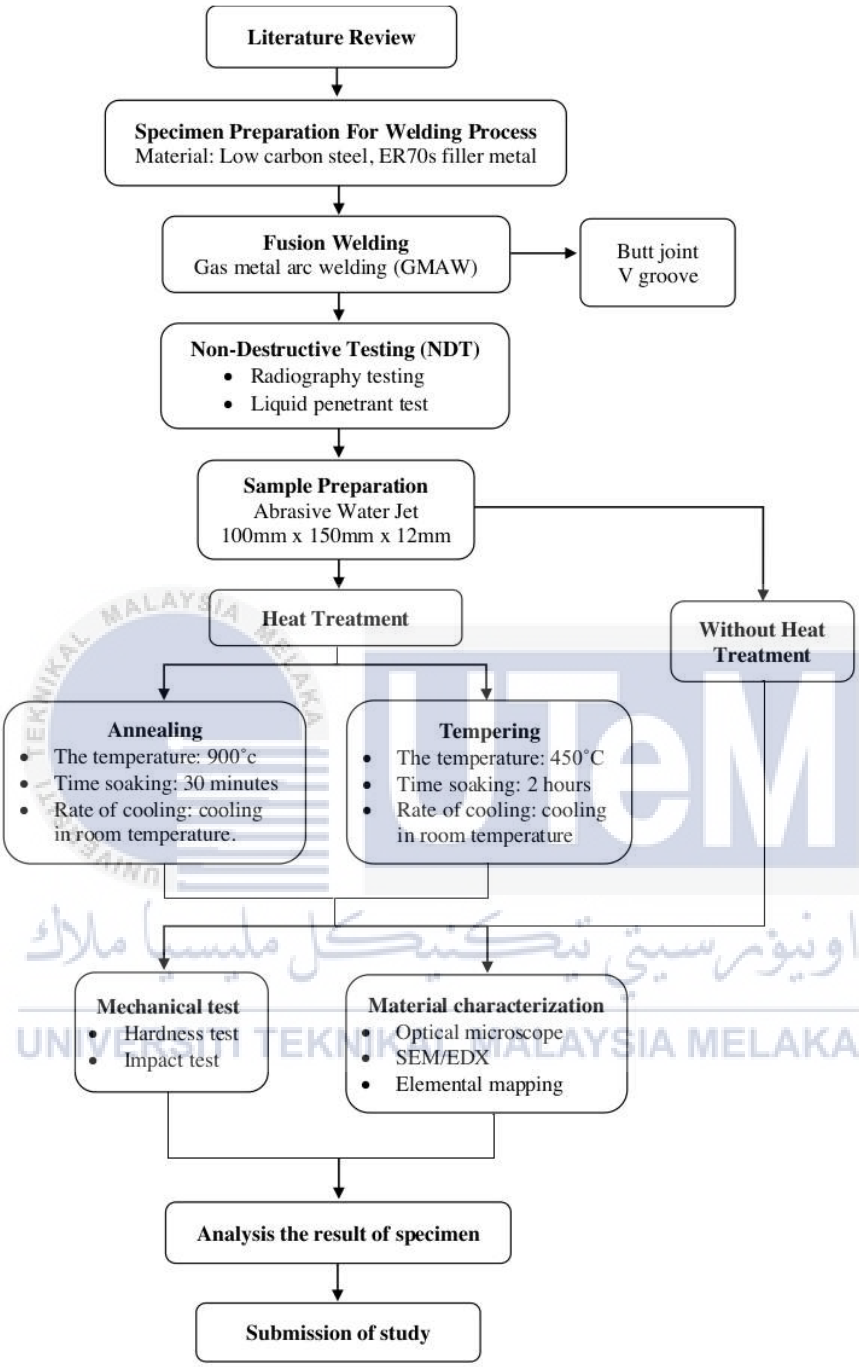

Figure 3.1: Process flow chart of study

3.2 Preparation of Sample

Prior to cut the sample to the desired size, the metal was inspected for flaws and defects and then were cleansed to remove foreign objects such as small holes or indentation that could result in the development of pitting corrosion and to ensured that the raw materials are free of microstructure changes.

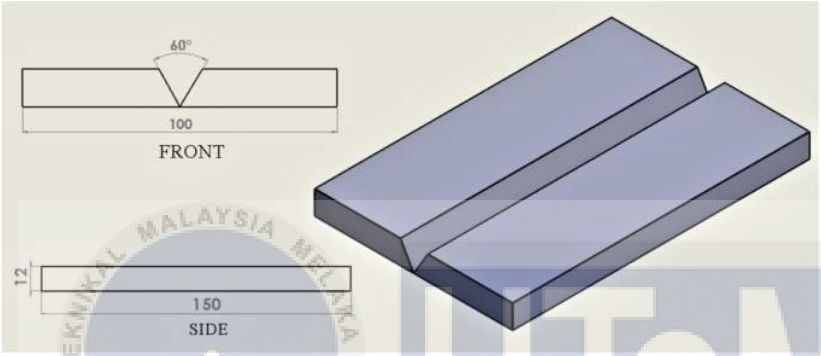

Figure 3.2: Dimension of sample preparation

The dimensions of the samples were cut to a smaller length and width by using an appropriate cutting tool for the desired dimension. The type of joint used in this study is the butt joint, which were the most commonly used and widely recognized as the simplest design welding to manufacture weldment.

3.2.1 Welding Procedures

The joint type that were used in this study is a butt joint, which were a well-known form of joint that was applied in accordance with the American Welding Society (AWS) standard. The idea of the butt joint is similar to that seen in the welding industry. The welding technique that must be applied in order to maintain the quality of welding activity were shielded metal arc welding, and the welding type used in this study were shielded

metal arc welding (GMAW). GMAW was chosen because of its support of a wide variety of industries and its simplicity of use, needing no additional safeguards. Precautions must be taken, however, to guarantee safety and good welding. The process for performing GMAW welding were as follows:

i. The butt joint design can take on a variety of forms however, the V groove was chosen for this study.
ii. The electrode used in the welding butt joint were ER70s filler metal.
iii. Current setup and amp were set as appropriated.
iv. The travel speed of the welding to ensure the good penetration on the welded joint.

This parameter must be monitored closely in ordered to avoid and eliminate internal flaws and cracks produced by inadequate welding techniques. When the current were abnormally weak, the suitable speed should also be reduced. The groove must be entirely filled to eliminated corrosion risk and ensured the welded joint's integrity.

3.3 Non-Destructive Test (NDT)

Non-destructive testing (NDT) were a method of analyzing the properties of a material, component, structure, or system for unique variations or welding defects and discontinuities without causing damage to the original part. This type of inspection were performed to check the sample's quality prior to the sample set's heat treatment test. To ensure the quality of the sample, the welded joint, and the continuity of the sample used in this study, liquid penetrant tests and radiography were used.

3.3.1 Liquid Penetrant Inspection

The sample were inspected using liquid penetrant testing, which would look for undetected defects on the weld sample. Firstly, the sample were first be cleaned using a cleaner to eliminate any foreign substance from its surface. Following that, the liquid penetrant were softly sprayed onto the clean surface of the test plate. The sample were allowed to dry for around 7-10 minutes, depending on the base metal's temperature. Then, the surface were wiped cleanly using the cleanser to eliminate any remaining penetrant. Then, wait another 2-5 minutes till it dried completely. The developer were applied by spraying a little layer on the surface and wait approximately 10 minutes for the indication to appear as shown the process in figure 3.3. The figure 3.4 showed the applicant used in liquid penentrant testing meanwhile figure 3.5 showed the indication using liquid penetrant inspection.

1. 	2. 
First of all, brush the surface of the plate using a wire brush to remove any rust.	Then, spray the cleaner on the lint-free cloth and rubbed it on top of the surface plate to remove any foreign substance. Allow for a while for it to evaporate.

3. 	4. 
Next, spray the liquid penetrant on top of the surface and allow to dry for around 7-10 minutes.	And then, wipe the surface off to remove all the penetrant. Allow it dry around 2-5 minutes.
5. 	6. 
Lastly, spray light coating of the developer on the surface. Wait around 4-6 minutes for the indication to appear.	After done evaluating the weld, clean the surface by using a cleaner.

Figure 3.3: The procedure of liquid penetrant inspection

Figure 3.4: The applicant used in liquid penentrant testing; (a) Fluxo S190 Solvent Remover, (b) Fluxo P125 Red Dye Penetrant, (c) Fluxo R175 Developer

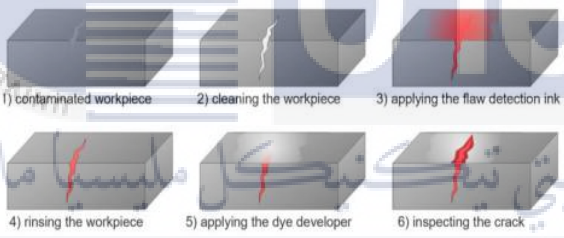

Figure 3.5:Indication using liquid penetrant inspection (https://www.tec-science.com/)

3.3.2 Radiographic Testing

Radiographic Testing (RT), as seen in Figure 3.6, is a non-destructive testing (NDT) technique that used x-rays or gamma rays to analyzed the internal structure of produced components in order to discover defects or flaws. The sample were sandwiched between the radiation source and a piece of sensitive film or detector during radiography testing. Once the x-ray or gamma-ray radiation were initiated, the test part's material density and

thickness would absorbed some of the radiation. A thicker, denser specimen were enabled less radiation to flow through it. The film (or electronic device) captured the quantity of radiation (referred to as radiograph) that passed through the test specimen and reached the film. Defects can simply be identified by examining the radiograph data. If the material were sound and free of defects, whole rays were flowed through it equally. However, for materials with imperfections, rays traveling through the faults were absorbed to a minor level due to the density changed. Due to the fact that defects in the parent metal diminished its density, they transmitted radiation far more efficiently than the sound metal. As a result, the radiograph film were looked darker in the defect-exposes area.

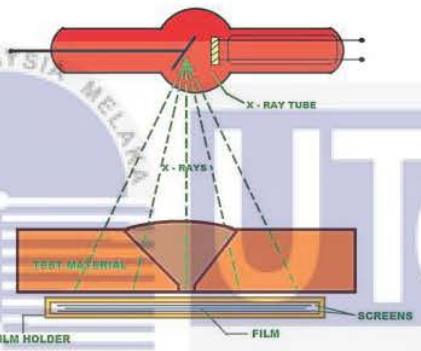

Figure 3.6: Radiography using x-ray (https://www.weldingandndt.com/, 2017)

3.4 Sample Preparation for Testing

To enhance the data collection, the sample were cut to the measurements required for sample analysis and experimentation. Before started the weld, the raw material were selected and were processed to remove any impurities. After butted the plates together, the welded plate were cut to the correct length and width using an watejet machine as shown in figure 3.7 below. Before undergone waterjet process, the drawing of the sample were done using Solidworks and the sample size is 55mm x 10mm x 12mm.

Figure 3.7: Flow Mach 2 1313B Abrasive Water Jet Machine

3.4.1 Procedures of waterjet cutting

The waterjet machine was used to cut into small samples by cutting a tiny line into a piece of material using a high-pressure spray of water as shown in figure 3.8. A granular abrasive is added to the waterjet to enhance the cutting power required to cut to the specified dimension. Figure 3.9 is the finished workpiece after were cut by using abrasive water jet.

The workpiece were placed on the slats and were clamped on the worktable by using speader.	The water nozzle were cut right to the place that want to be cut.

Figure 3.8: The procedures of waterjet cutting

Figure 3.9: Workpiece that were cut by waterjet machine

3.5 Heat Treatment Process

Among the other tests, heat treatment were the most important for this research. This due to the fact that whether or not heat treatment affected the performance of the sample had a significant impact on the overall research. In this project, two types of heat treatment process which was tempering and annealing were used as parameter. The figure 3.10 below showed the procedure of the sample for tempering process meanwhile figure 3.11 shown the procedure of the sample for annealing process.

The samples were put in the furnace with the temperature 450˚C	The samples were soak for about 2 hours.	Lastly, the samples were cooled to the room temperature

Figure 3.10: The procedure of the sample for tempering process

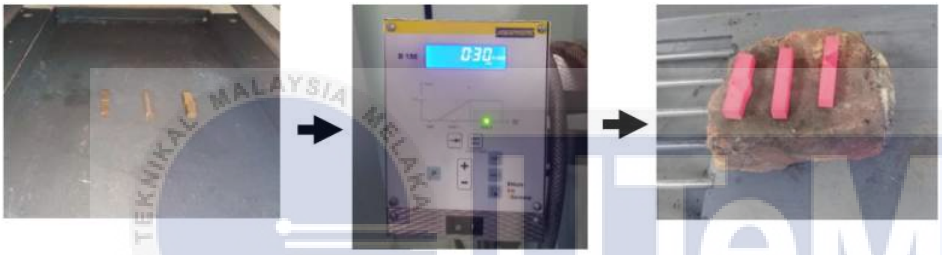

The samples were put in the furnace with the temperature 900˚C	The samples were soak for about 30 minutes.	Lastly, the samples were cooled to the room temperature.

Figure 3.11: The procedure of the sample for annealing process

To sum up, three temperature were used during the testing process which are 900°C for annealing, 450°C for tempering, and 30°C for the untreated sample and lastly were cooled in room temperature.

3.6 Mechanical Test

Mechanical properties are those of materials that need a response to an applied load. The mechanical characteristics of metals influenced the material's range of utility and, consequently, the expected service life. The most often examined characteristics are strength, ductility, hardness, impact resistance, and fracture strength. Mechanical

characteristics of the material are not constant and regularly fluctuated in response to temperature, loading rate, and other variables. Macro hardness test and impact resistance of materials were evaluated using Rockwell hardness and their behaviour at high deformation rates were investigated using Charpy testing.

3.6.1 Macro Hardness Test (Rockwell Hardness)

A macro hardness tester as depicted in figure 3.12 were the most often used technique to evaluated the macrohardness behaviour of treated and untreated materials. The samples were indented with a ball indenter. The indentation were produced on the surface of three primary regions: base metal, weld material, and heat-affected zone (HAZ). Additionally, numerous layers of indentation testing were done to verified and confirmed the sample data.

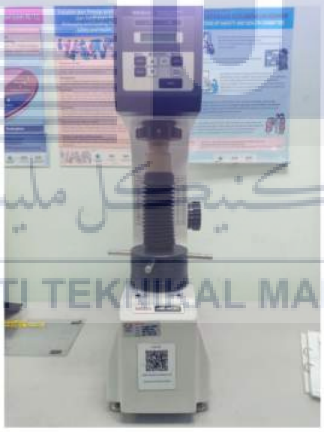

Figure 3.12: Mitutoyo HR-400 Rockwell Hardness Tester

Figure 3.13: The sample were put to get the value of hardness of each layers

3.6.2 Impact Test

Impact testing were used to evaluate the relative toughness or impact toughness of materials. Impact tests are beneficial because they can determined the amount of energy absorbed by a material during fracture. This absorbed energy is an indicator for a material's toughness and would used to investigate the temperature-dependent brittle-ductile transition. The purpose were to determined if a material is brittle or ductile. For this experiment, the impact test were conducted using the Charpy technique and ASTM E23 standards. The aim is to analyze whether the materials are brittle or ductile. Also, the Charpy test and ASTM E23 standards were used as when do impact test.

3.6.2.1 The Charpy Test

The Charpy impact tester as shown in figure 3.15 also known as the Charpy V-notch test, is a strain rate test that included impacting a standard notched sample with a controlled weight pendulum swinging from a predetermined height. The specimens shown in figure 3.14 were those most widely used and most generally satisfactory. For this study, a specimen of type A as in figure 3.16 which are the typical Charpy V-notch specimen with dimension 55mm long, 10mm square, and has a 2mm deep notch machines on one

face with a tip radius of 0.25mm were used. The sample were supported at both ends by an anvil and struck by the pendulum on the opposite face to the notch. The amount of energy absorbed in breaking the sample were measured, and this would give an approximation of the test material's notch toughness. During the test, the pendulum swings over, with the height of the swing represented the amount of energy absorbed in breaking the sample.

Figure 3.14: Instron CEAST 9050 Pendulum Impact Tester

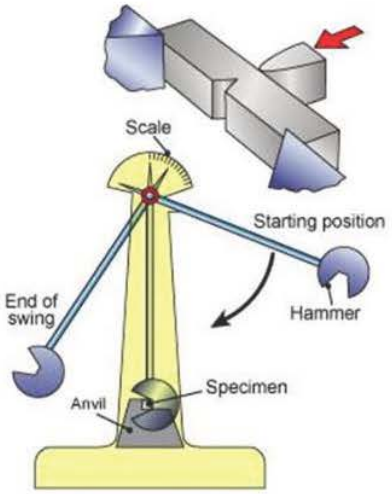

Figure 3.15:The Charpy test (https://builderssolutiongroup.blogspot.com/)

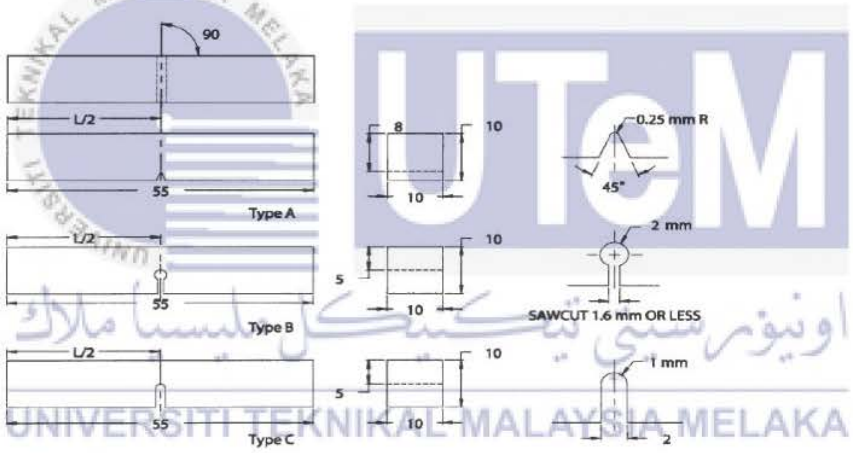

Notch length to edge	90 ±2°
Adjacent sides shall be at	90° ± 10 min
Cross-section dimensions	± 0.075 mm
Length of specimen (L)	+0, −2.5 mm
Centering of notch (L/2)	± 1 mm
Angel of notch	±1°
Radius of notch	±0.025 mm
Ligament Length:	±0.025 mm
Type A specimen	±0.025 mm
Type B and C specimen	±0.075 mm
Finish requirements	2 µm on notched surface and opposite face; 4 µm on other two surfaces

Figure 3.16: Charpy (Simple-Beam) impact test specimens (ASTM E23, 2015)

3.7 Microstructure Characterization

The microstructure is a material that were a very tiny scale structure, defined as the structure of a material's prepared surface as revealed by an optical microscope over 25 magnification. The microstructure of a material (such as metals, polymers, ceramics, or composites) could have a significant impact on physical properties including strength, toughness, ductility, hardness, corrosion resistance, high or low temperature behaviour, or wear resistance. The microstructural analysis were crucial. Generally, the microstructure is were examined using an optical microscope in conjunction with suitable metallurgical preparation and Scanning Electron Microscopy (SEM) Energy Dispersive X-Ray Spectroscopy (EDX). The sample is polished with sandpaper of various sizes, including 1000μ, 2000μ, and diamond polishing pieces, to achieve a mirror-like surface. The sample will then be etched for 10 seconds in Nital solution to allow the microstructure machine to see the sample structure.

3.7.1 Optical Microscope

An optical microscope as in figure 3.17 combined one or more lenses to magnified the image of a sample placed inside the lens's focal plane. The components of an optical microscope were sometimes rather complicated, and it is critical that the microscope is set up properly in order to obtain an accurate image. The fundamental principles related to the operation of an optical microscope are rather simple. An optical microscope's objective lens as in figure 3.18 were comparable to that of an extremely strong magnifying glass. As it is a small focal length lens, it should be held near to the sample that were study. This caused the light from the sample to concentrate around 160 mm within the microscope's tube, resulting in an enlarged and inverted picture of the subject. The objective lens created the genuine picture, which the ocular lens enlarged further so that it may be viewed by an

individual. The compound lens eyepiece used on the majority of optical microscopes has one lens in the front and another at the back of the eyepiece tube. This results in the formation of a couplet, which enabled the virtual image to focus between the lenses, allowing the eye to concentrate on it. The stage were lowered after utilized an optical microscope to facilitate the removal of the microscope slide.

Figure 3.17: Zeiss AxioLab A1 Upright Light Microscope with AxioCam Erc 5s

Figure 3.18 : ZEISS EC EPIPLAN objectives lens (http://zeiss-campus.magnet.fsu.edu/)

3.7.2 Scanning Electron Microscopy (SEM) Energy Dispersive X-Ray Spectroscopy (EDX)

Scanning electron microscopy (SEM) is a technique used to examine cells in a sample at a high magnification. Sample preparation is fairly simple, and when it comes to diverse samples, it does not require processing for ultra-thin sheets to perform the SEM procedure. This is due to the fact that SEM may be used to analyse and calculate evaluations on a millimetre or nanometer scale. SEM can receive a large sample size at one time at low magnification, while at greater magnification, high-resolution images of specific regions can be acquired. Each SEM has energy-dispersive X-ray (EDX, commonly known as EDS) spectroscopy functions. When subjected to an electron beam, an atom generates characteristic X-rays that are unique to its atomic number; this allows the elemental composition of a material to be analysed, whether at a single spot or over a vast region, using techniques such as line scanning and elemental mapping. Semi-quantitative analysis can also be used to determine the chemical composition of a material. When combined with standard SEM analysis, EDX can provide a more comprehensive view of a sample's local composition.

Figure 3.19: JEOL JSM 6010 PLUS/LV Scanning Electron Microscope

CHAPTER 4

RESULTS AND DISCUSSION

4.1 Introduction

The outcomes of this study are used to forecast the likely outcome or result of the upcoming test that was being researched. However, when the analyzed actual results are obtained, the findings may be debated. The preliminary outcomes from the sample tests are also discussed, although they are not the final data that will define the research's course. This subject is used to identify and investigate the original data expectations.

4.2 Composition of analysis

Chemical composition involves qualitative approach testing of numerous sample components, combined with structured analytical approaches, which may require the synthesis and production of delicate chemical composites and chemical reactions. In addition to quantitative analysis to analyze the correlation coefficients of substances in various chemical reagents, the molecular structure of the discovered substance was detected and validated throughout many platforms (Boumerzoug et al., 2010). Table 4.1 showed the chemical composition of the ER70s filler metal material and the low carbon steel material.

Table 4.1: Chemical composition (%wt) of low carbon steel and filler used

Alloy Elements	Low carbon steel	Filler metal ER70s
C	0.137	0.104
Mn	0.560	0.521
P	0.0320	0.0229
S	0.0337	0.0108
Si	0.140	0.238
Cr_2	0.127	0.0702
Ni_2	0.157	0.486
Cu_2	0.276	0.277
Fe	98.4	98.1

Carbon content on low carbon steel showing at table 4.1 proved that the carbon content is below than <0.30%.

4.3 Complete welded joint

Low carbon steel plate was welded together as in figure 4.1 using current and voltage that were appropriate for the speed and thickness of the steel plate. The slag on the weld bead was then carefully scraped away to avoid any damage to the weld bead itself or to the surface of the plate. Following the completion of the weld, the steel plate is allowed to cool to room temperature slowly by being exposed to the air rather than being immersed in water.

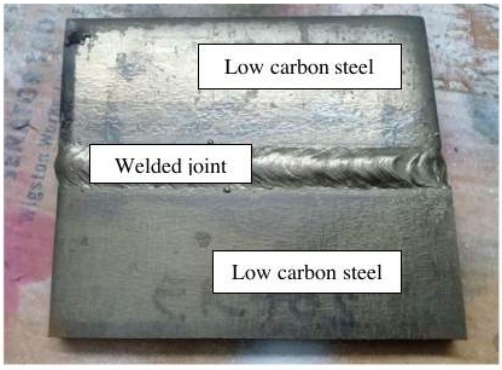

Figure 4.1: Complete welded low carbon steel plate

4.4 Non destructive test

Non-Destructive Testing refers to a group of inspection methods that allow inspectors to evaluate and collect data about a material, system, or component without permanently affecting it. Radiographic and liquid penetrant tests are used in this study to ensure the quality of the sample, the welded joint, and the continuity of the sample.

4.4.1 Radiographic testing

Radiographic Testing (RT) is a non-destructive testing (NDT) approach that examines the interior structure of produced components to discover flaws or defects using either x-rays or gamma rays. The test-part is positioned between the radiation source and the film in radiography testing (or detector). It is based on the idea that radiation is absorbed and scattered as it travels through an item. If the thickness or density of an object varies (for example, due to faults), more or less radiation goes through and affects the film exposure (Deepak et al., 2020). Flaws appear on the film as dark patches. The figure 4.2 below showed the film of workpiece. Based on figure 4.2 below, theres no signs of cracks at the workpiece.

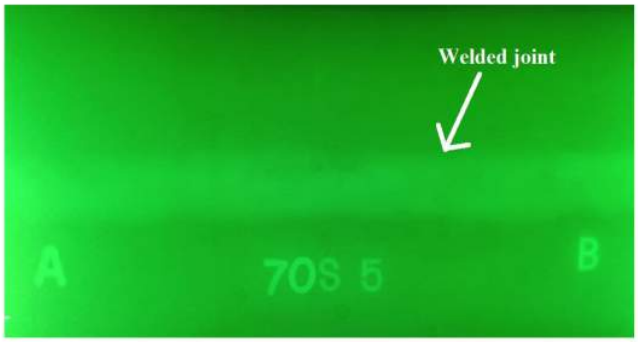

Figure 4.2: The film of workpiece under film viewer

4.4.2 Liquid penetrant testing

The liquid penetrant is pulled into the surface-breaking crack by capillary action, and surplus surface penetrant is then removed; a developer (usually a dry powder) is then applied to the surface, drawing out the penetrant in the fracture and producing a surface indication (Deepak et al., 2020). It is possible to detect cracks as small as 150 nanometres. The created indicators are significantly wider than the real fault and hence more obvious.

Liquid penetrant testing can be used on any non-porous clean material, metallic or non-metallic, although it is not appropriate for unclean or extremely rough surfaces (Deepak et al., 2020). Surface cleaning is an important step in the penetrant testing process. The process can be fully automated, semi-automatic, or manual. Penetrant inspection and continuous-operation production lines, in which specimens are cleaned, dipped, rinsed, dried, and so on, are prevalent. As can see in figure 4.3, after a few minutes were sprayed by developer there are no signs of cracks or any defects on the surface of workpiece and welding area.

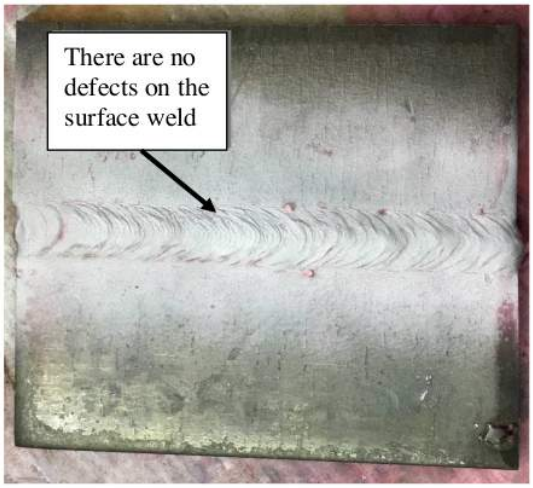

Figure 4.3: Sample after developer were applied

4.5 Heat Treatment Process

There were three parameters that were determined for each sample group to be evaluated and studied. The first treatment parameter is annealing, which has a high temperature but is below the melting point of low carbon steel. The sample was heated to 900˚C inside the furnace before being allowed to cool down with the furnace's lowering ambient temperature. The second treatment parameter is tempering, which has a temperature of 450˚C and was left in the furnace for 2 hours before the sample was taken out to cool to the surrounding temperature. Finally, the third sample group was made up of untreated samples. The look of each sample varied as shown in figure 4.4 below. The looks of each sample group can be identified by naked eyes, with the annealed sample having a crispy dark grey coating outside its surface, the tempered sample having a brownish colour, and the untreated sample retaining its original appearance.

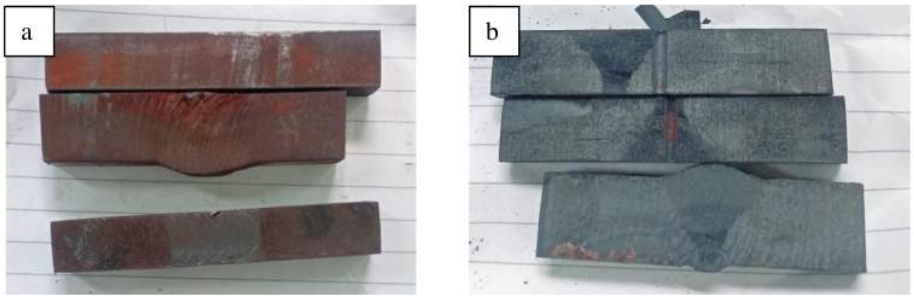

Figure 4.4: Visual appearances after treated; (a) Annealed, (b) Tempered

4.6 Mechanical Test

Mechanical properties are the characteristics of materials that must respond to a load applied to them. The mechanical properties of metals had an impact on the material's range of application and, as a result, on the estimated service life of the material. Strength, ductility, hardness, impact resistance, and fracture strength are the qualities that are most frequently investigated (Adedayo et al., 2010). The mechanical characteristics of the material are not constant and fluctuate on a regular basis in reaction to changes in temperature, loading rate, and other variables (Owolabi et al., 2016). Macro hardness testing was used to evaluate material hardness and impact resistance, while Charpy testing was used to explore their behaviour at high deformation rates.

4.6.1 Impact Testing

43

An impact test is performed to observe the mechanics that a material will exhibit when subjected to a shock loading that causes the specimen to immediately deform, fracture, or break completely. In addition, the Charpy test and ASTM E23 standard were applied for performing impact tests. Table 4.2 below showed the result of impact test meanwhile for figure 4.5 and 4.6 depicted the bar graph of impact test.

Table 4.2: Result of Charpy test

Type of sample	Part	Impact value(kJ/m^2)	Energy consumed (J)
Untreated	Centre	1293.56	49.885
	HAZ	1293.53	47.884
Tempering	Centre	1292.92	49.860
	HAZ	1292.92	48.860
Annealing	centre	1293.53	49.884
	HAZ	1293.53	49.884

The figure 4.5, the bar graph showed that the toughness of the heat-treated samples and untreated sample were not have significant result of values. This is because the welded joint area is strong, the structure remains the same so thats why the result does not show a significant difference.

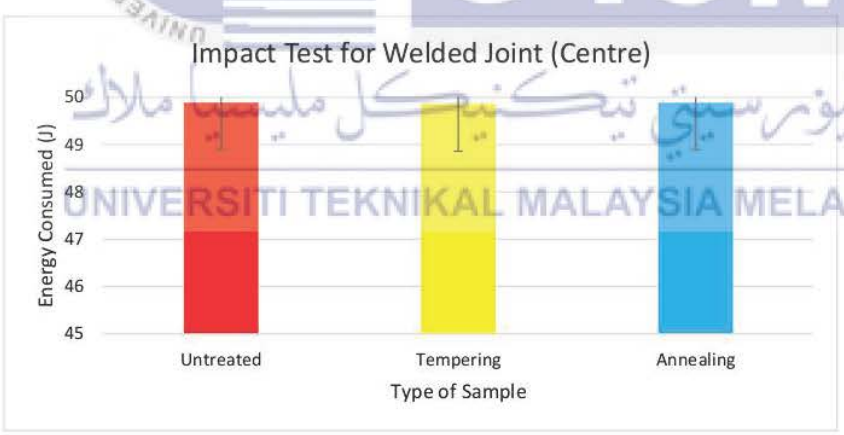

Figure 4.5: The bar graph of impact test for welded joint (centre)

However in figure 4.6, it showed there were significant value at the HAZ area for each sample. As can see, annealed sample still does not show a change in value compared to annealed value at welded joint. This is because each surface of the annealed sample is approximately have the same structure. The toughness of tempered sample were decrease at HAZ area because the structure of surface area were more subtle (Adedayo et al., 2010).

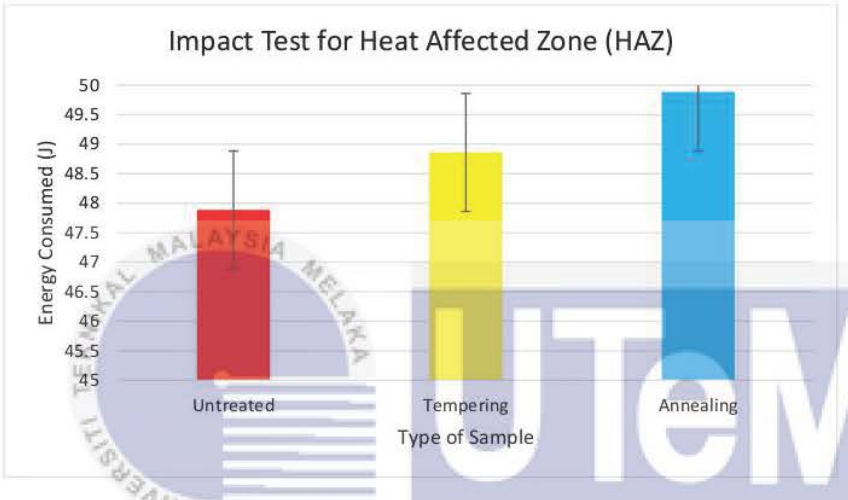

Figure 4.6: The bar graph of impact test for Heat Affected Zone (HAZ)

4.6.2 Macro hardness Analysis

Macro hardness is a phrase that is commonly used in the testing of hardness by applied load impacting materials. For this testing, Rockwell method were chosen and used ball indenter because of type of material were low carbon steel. Macro hardness variability were measured at three separate layers, with micro hardness tests done at the top, centre, and bottom of the sample as shown in figure 4.7.

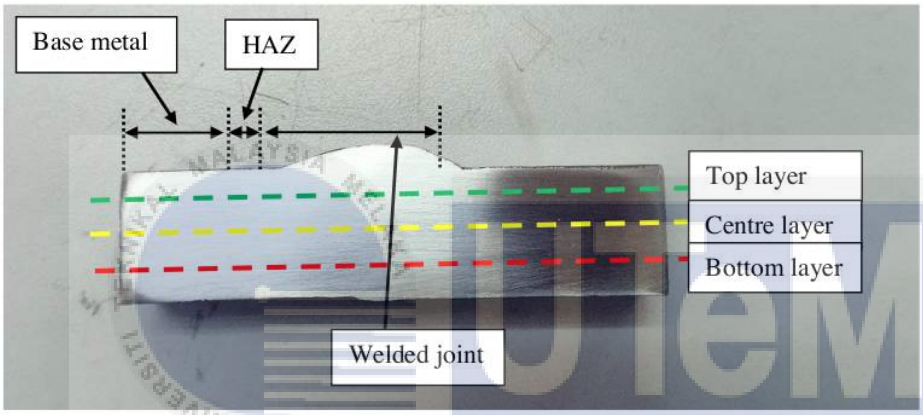

Figure 4.7: Indentation done on multiple layer on the same surface

The measurement was conducted in a distributed way, and the transverse area of cross sectional area that was given the most attention is the area of Heat Affected Zone (HAZ) and weld joint , in which the fusion reaction and microstructure variations growing actively occur (Boumerzoug et al., 2010), as shown in table 4.3.

Table 4.3: Result from the macro hardness test of untreated sample

No	Area	Top (HRB)	Centre (HRB)	Bottom (HRB)
1	Base metal	74.3	74.2	73.8
2		73.9	76.8	75.8
3		74.2	77.5	76.0
4		76.3	75.9	75.4
5		75.8	75.6	75.2
6	HAZ	79.7	78.7	76.9
7		81.3	77.6	79.2
8		81.5	79.2	79.2
9	Welded joint	83.9	82.9	80.5
10		84.4	84.6	85.6
11		85.9	84.3	82.5
12		85.7	82.6	83.5
13	HAZ	78.6	80.0	78.1
14		75.2	81.3	79.5
15		77.1	78.2	79.5
16	Base metal	77.1	75.3	75.0
17		74.8	76.7	76.0
18		74.6	75.0	76.3
19		75.6	74.9	74.0
20		75.8	75.5	74.5

Figure 4.8 showed a line graph for an untreated sample. The line patten is not in average. As can see at the weld joint area it were higher than the HAZ and base metal. This is because the structure at weld joint were subtle compared to other areas.

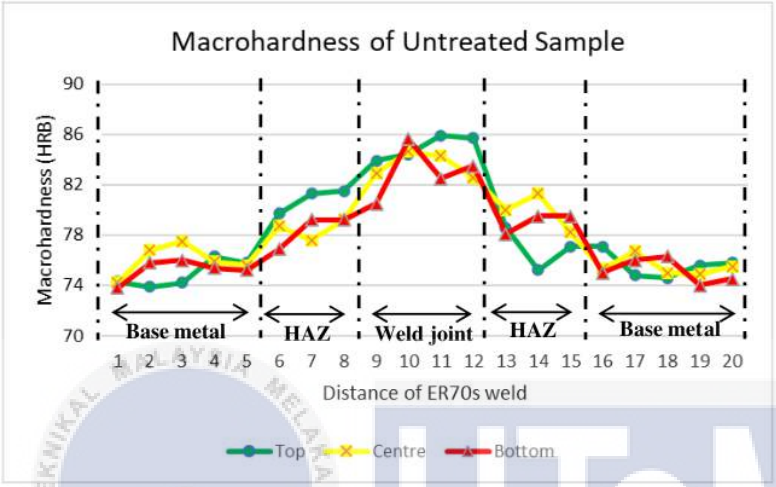

Figure 4.8: Graph result of macro hardness of untreated sample

Table 4.4: Result from the macro hardness test of tempered sample

No	Area	Top (HRB)	Centre (HRB)	Bottom (HRB)
1	Base metal	75.0	75.3	74.5
2		75.0	74.6	75.3
3		75.7	74.9	75.7
4		74.8	75.1	75.4
5		75.6	76.3	76.3
6	HAZ	80.0	79.9	79.5
7		81.3	81.8	80.9
8		81.5	80.3	81.3
9	Welded joint	84.8	82.2	82.2
10		85.6	82.1	84.2
11		84.2	82.5	84.2
12		82.4	81.8	83.6
13	HAZ	81.2	80.8	80.2
14		80.7	79.8	79.1
15		80.2	79.9	78.6
16	Base metal	74.9	75.8	75.9
17		74.9	75.5	75.1
18		74.8	75.2	75.3
19		75.7	74.7	75.4
20		75.1	74.9	74.9

According to the graph in figure 4.9 below as for tempered sample, it also showed that the line pattern were not in average. At the HAZ area, we can see that the line pattern were higher compared to the line pattern for untreated sample. This because tempered sample have more subtle structure surface compared from untreated sample. Other than that, at area weld joint, we can see that it has similar line pattern to the untreated sample. The smoother the surface structure, the higher the hardness value.

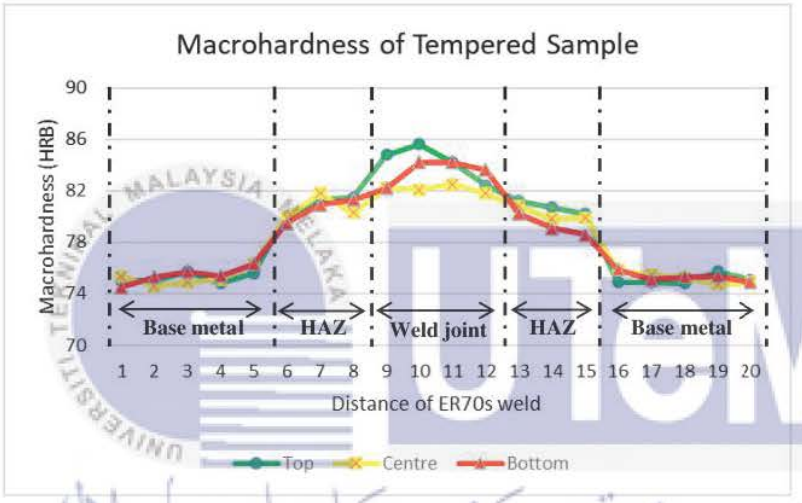

Figure 4.9: Graph result of macrohardness of tempered sample

Table 4.5: Result from the macro hardness test of annealed sample

No	Area	Top (HRB)	Centre (HRB)	Bottom (HRB)
1	Base metal	75.8	75.7	74.0
2		76.0	76.0	75.2
3		76.6	75.7	75.5
4		75.6	75.9	75.8
5		76.1	77.2	75.3
6	HAZ	77.7	79.5	76.8
7		79.3	79.8	77.2
8		76.3	78.0	78.4
9	Welded joint	77.1	79.6	80.6
10		76.4	79.9	78.8
11		77.0	78.7	80.9
12		76.9	78.7	80.1
13	HAZ	76.7	75.9	75.1
14		78.7	77.7	75.4
15		78.2	77.5	75.3
16	Base metal	76.2	75.8	73.2
17		76.2	75.9	72.4
18		76.0	76.3	74.5
19		76.4	76.6	74.2
20		76.1	75.7	73.4

Figure 4.10 showed the result of annealed sample for macro hardness. The line pattern of each area were in average compared to untreated sample of graph. The value at each area quite similar because annealing process were helped to stabilize the microstructure of the sample. Even though the line pattern in average but the annealed sample have the lowest value of hardness at HAZ and weld joint compared to tempered and untreated sample.

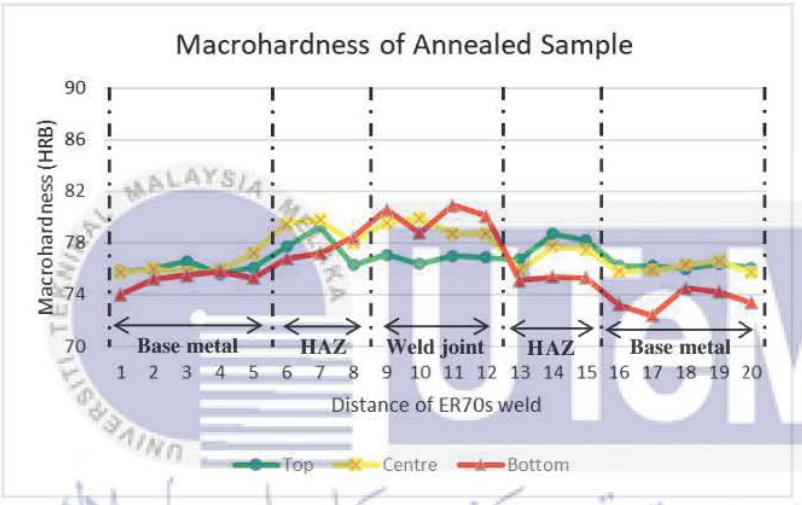

Figure 4.10: Graph result of macrohardness of annealed sample

4.7 Microstructure Analysis

The microstructure resting method was an alternative strategy to identifying and recognizing the characteristics of all three group samples. This testing is used to identify grit size by employing microscope-assisted equipment, as stated in the methodology.

4.7.1 Optical microscope

134
This test is used to determine the grain size utilising microscope-assisted equipment, as discussed in the methodology.

Figure 4.11 depicted the appearance of untreated sample's grain growth. According to the figure below, the results of the microstructural examination revealed that the initial grain size had a significant impact on the phases formed in the intercritical HAZ (b). Also, there is the presence of pearlite and martensite as can be seen in (c) and (e). The fusion line of HAZ and welded metal low carbon steel can be seen in (d).

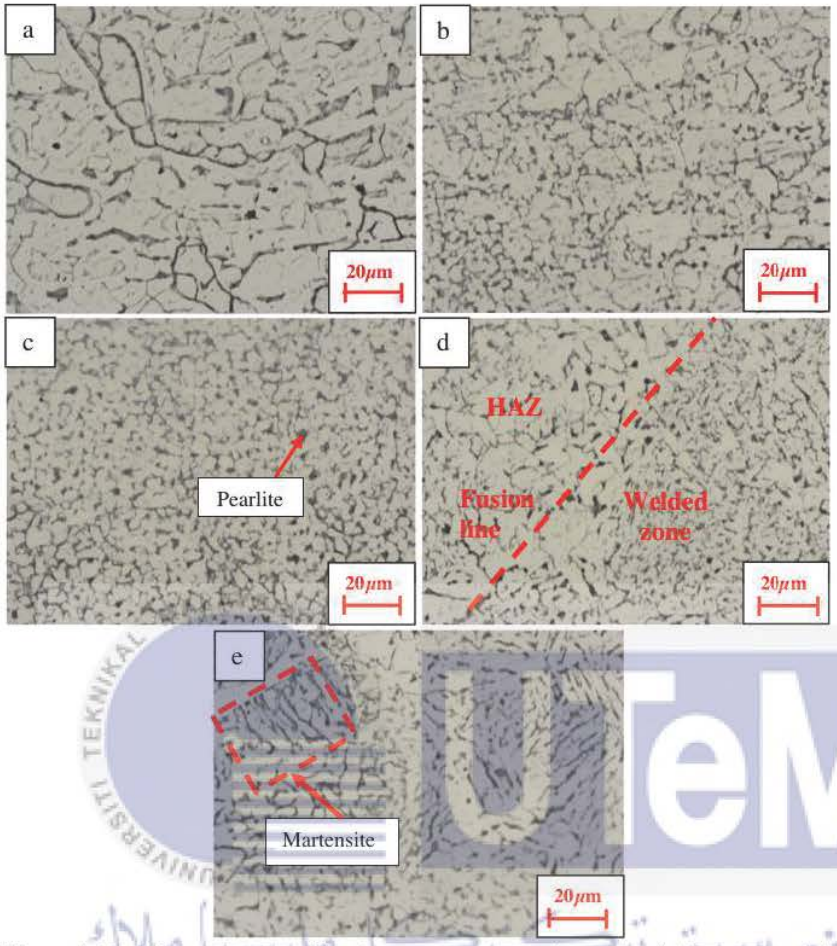

Figure 4.11: Microstructure of each area on untreated sample; (a) base material, (b) Intercritical zone (IGHAZ), (c) Fine grained zone (FGHAZ), (d) Fusion boundary between HAZ and welded zone, (e) Welded zone

After done tempered at 450˚C, the microstructure as in figure 4.12 below, the pearlite were seen at the (b). White areas indicated ferrite formation, while black patches indicated pearlite or cementite formation. At the welded zone (e), its being gradually transformed into fine needle-like (fragmented) tempered martensite.

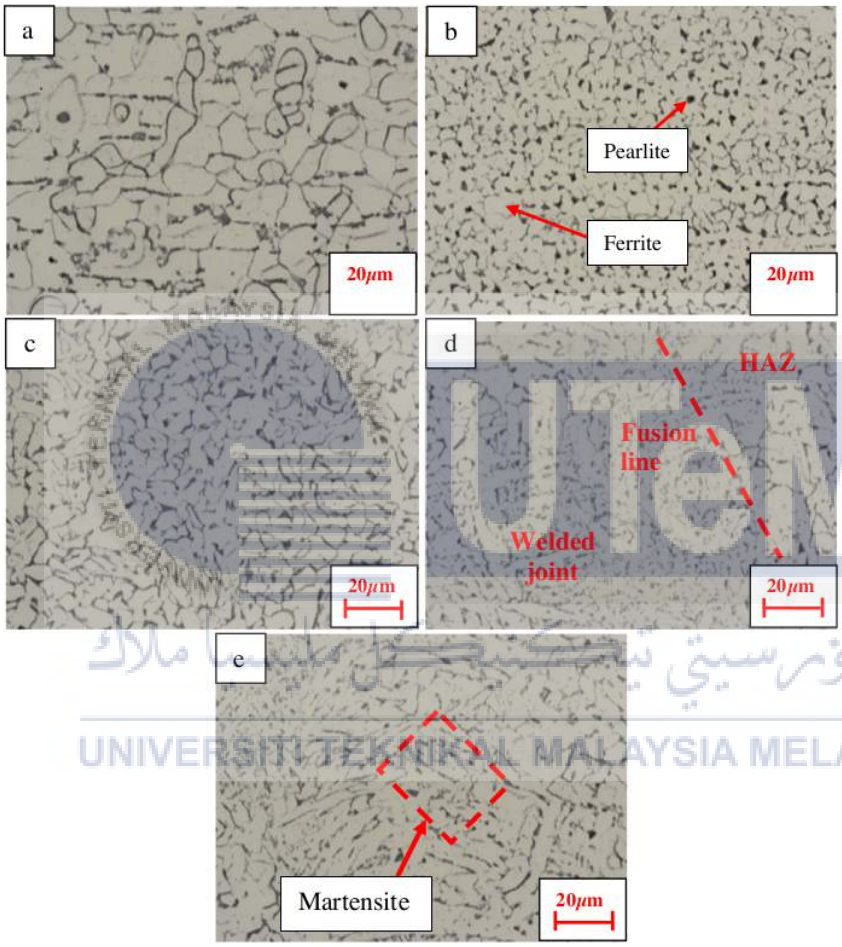

Figure 4.12: Microstructure of each area of tempered sample; (a) base material, (b) Fine grained zone (FGHAZ), (c) Coarse grained zone (CGHAZ), (d) Fusion boundary between HAZ and welded zone, (e) Welded zone

Figure 4.13 depicted the microstructure of each area of annealed sample. Slow cooling in annealing, which is room temperature cooling, led in the change of austenite to soft pearlite, which was then combined with ferrite or cementite (Chandra Kandpal et al., 2020). At the base metal (a), the grain size of the microstructure were more small compared to grain size of untreated sample. The more pearlite gives the steel higher strength, but lower ductility (Owolabi et al., 2016). Also, there were no significant microstructure changes between each area. This is because there were no structure fine needle-like at the welded area.

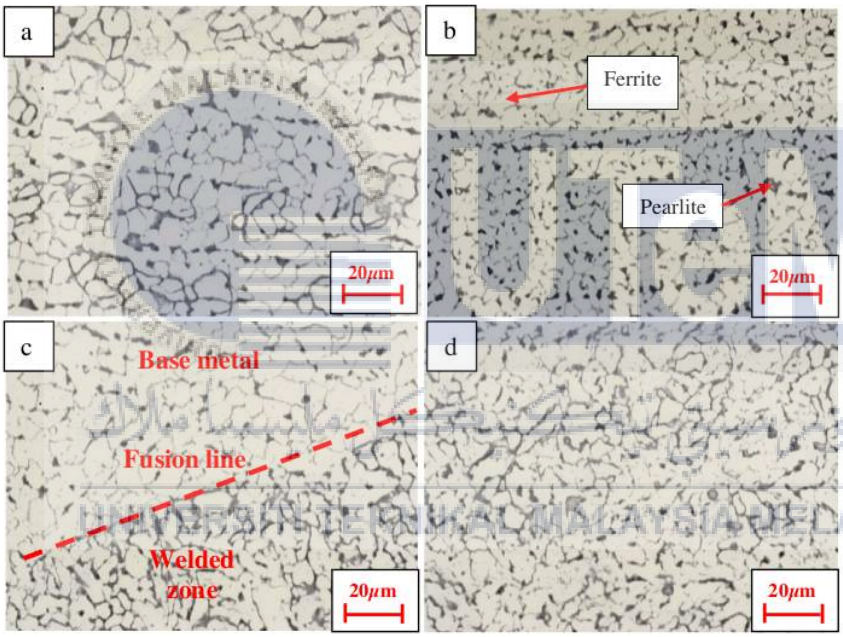

Figure 4.13: Microstructure of each area of annealed sample; (a) base material, (b) Fine grained zone (FGHAZ), (c) Fusion Boundary between base metal and welded zone, (d) Welded zone

4.7.2 Line Scanning

One of the features of an EDX machine is the ability to evaluate the elements and compounds detected in the sample utilizing a low vacuum mode (Saito et al., 2021). It has displayed the results of the analysis of the sample provided.

A line scanning test was performed on the surface of the low carbon steel sample, as shown in figure 4.14. The colour that represents the element content in the sample between the base and welded areas. Based on figure 4.14, it showed elements that have in untreated sample which is Carbon (C), Silicon (Si), Iron (Fe), and Manganese (Mn). Red colour graph represent for Carbon (C) element, green colour showed Silicon (Si) meanwhile blue light showed Iron (Fe) element detected on sample and purple colour for Manganese (Mn) element. It showed that Iron element have highest weight percentage with 94.95% compared to other elements, followed by Carbon with 4.06% and Silicon 0.99%.

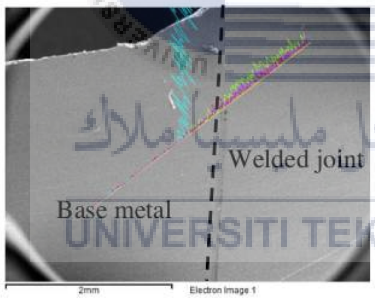

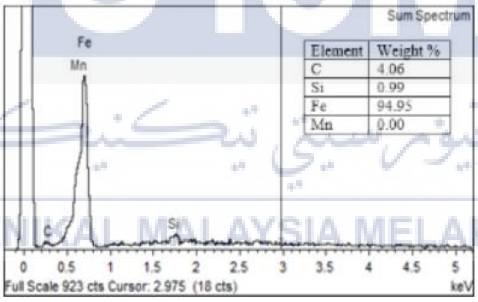

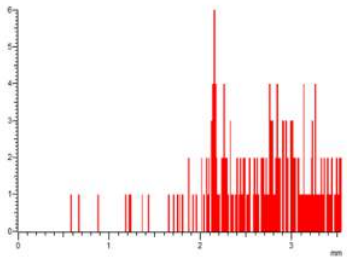

Carbon, C

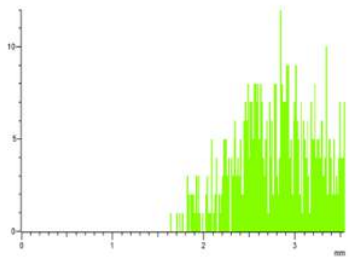

Silicon, Si

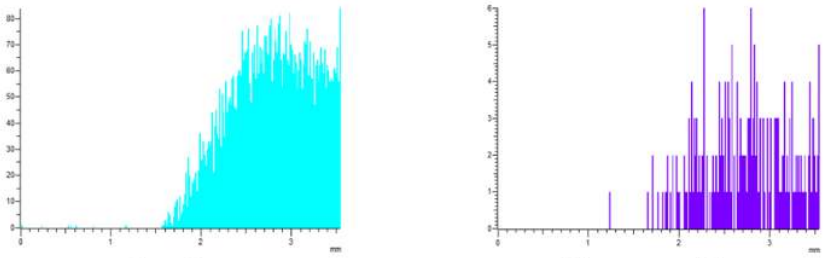

Iron, Fe Manganese, Mn

Figure 4.14: Interface of untreated sample

The surface of base metal and welded joint area sample was performed a line scanning test was conducted on, referring to Figure 4.15, the colour representing the content of the element between the base metal and welded joint. Based on figure 4.15, it showed the element content found between base metal and welded joint area. Different colours have shown the sample contains various type of elements. The red graph was showed an element containing Carbon (C) meanwhile the green graph has shown that the sample contains the element Silicon (Si). In addition, the blue light coloured graph containing Iron (Fe) element and the purple graph showed Manganese (Mn). Manganese elements were shown that the manganese element have a high chemical contain in the welded metal area compared to the base metal in tempered sample.

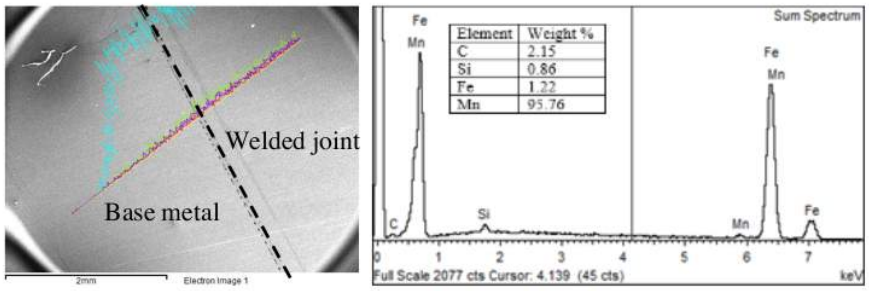

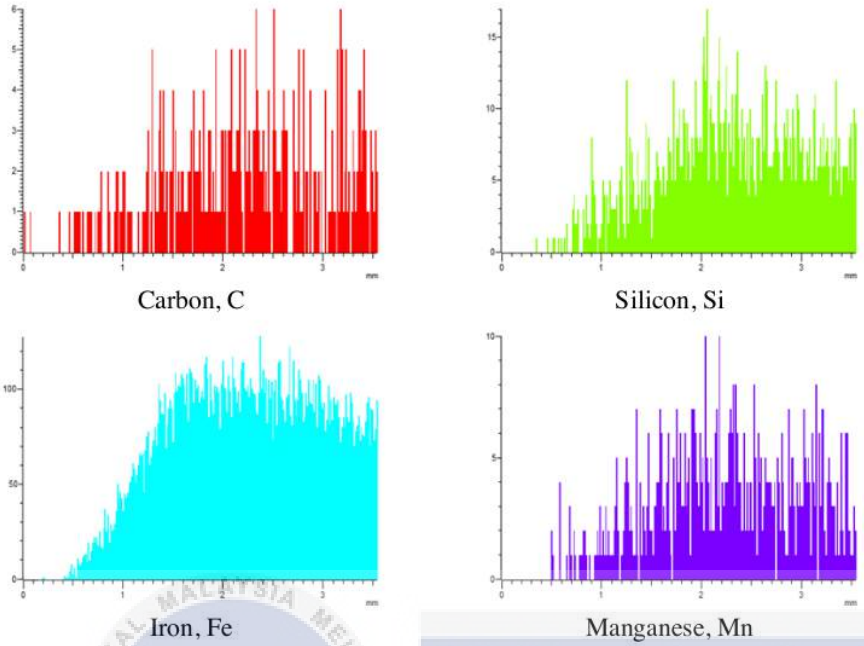

Figure 4.15: Interface of tempered sample

Based on figure 4.16, it showed the element content found between base metal and welded joint area. Different colours have shown the sample contains various type of elements. The red graph was showed an element containing Carbon (C) meanwhile the green graph has shown that the sample contains the element Silicon (Si). In addition, the blue light coloured graph containing Iron (Fe) element and the purple graph showed Manganese (Mn). Manganese elements were shown that the manganese element have a high chemical contain in the base metal compared to the welded metal area in annealed sample.

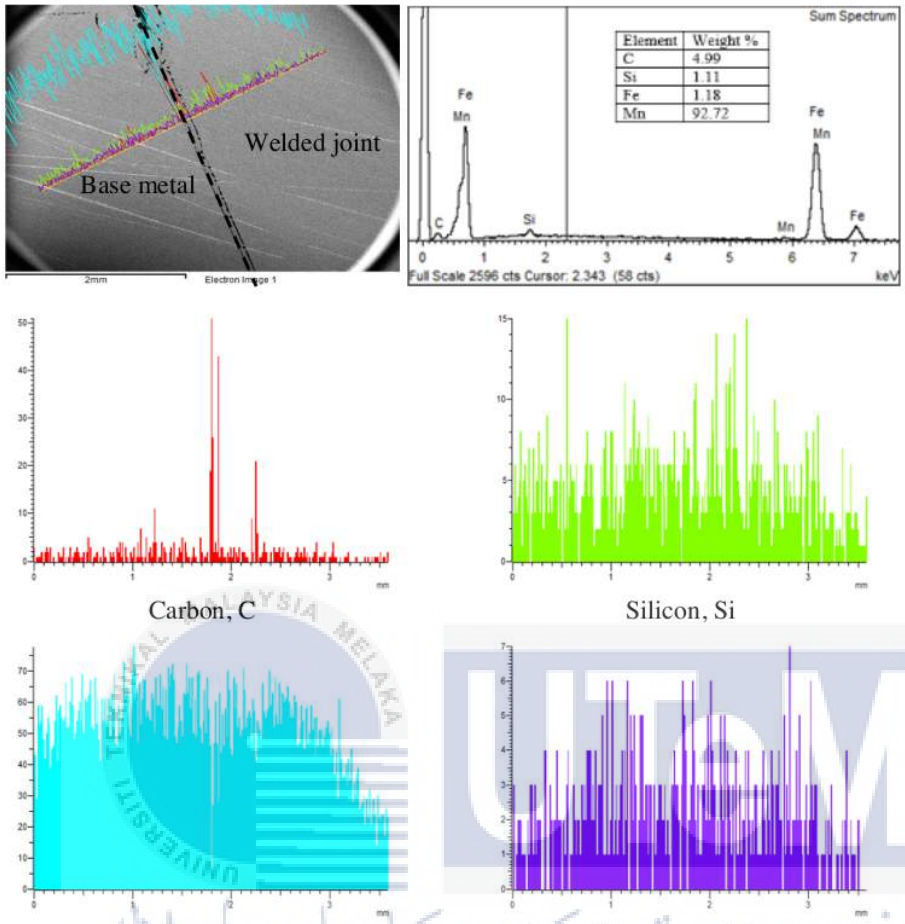

Figure 4.16: Interface of annealed sample

4.7.3 Elemental Mapping

One of the procedures used for element analysis or chemical characterization of samples is EDX analysis. This is to prove the presence of other chemical elements after the sample were done do heat treatment (Senthur Prabu et al., 2021).

Based on figure 4.17, the content of the element can be seen in the graph where the highest content on the graph is the Iron (Fe) element which in blue colour have 94.95% at

welded area. Carbon (C) elements that were in red colour have 4.06% in surface between base metal and welded zone for untreated sample.

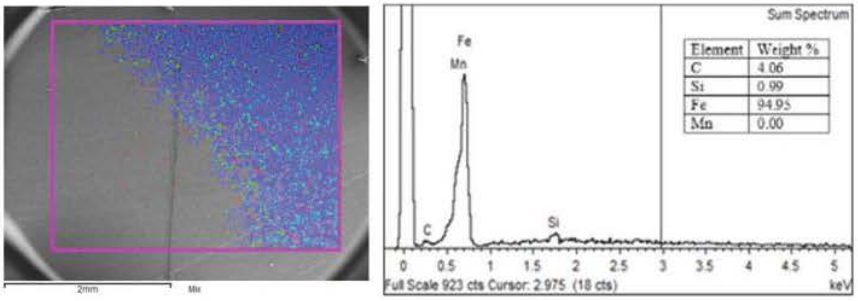

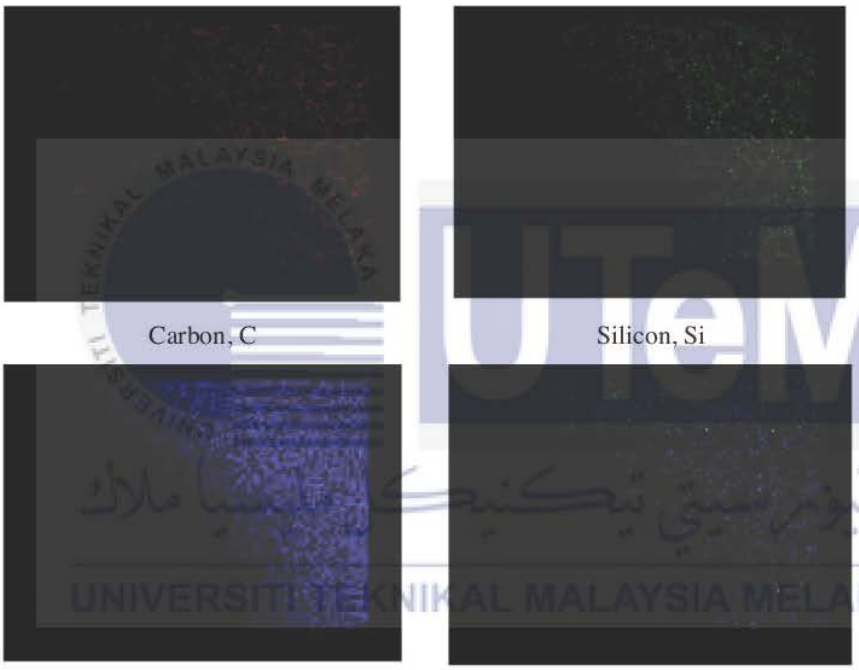

Carbon, C Silicon, Si

Iron, Fe Manganese, Mn

Figure 4.17: Elemental mapping analysis for untreated sample

For the figure 4.18, supposedly there are manganese (Mn) in blue color covering the surface because it has the highest content of element which is 95.76% compared to other elements. Besides, Carbon (C) elements which is in red colour have 2.15% in welded zone meanwhile Iron (Fe) elements were 1.22% and Silicon (Si) elements were 0.86% for tempered sample.

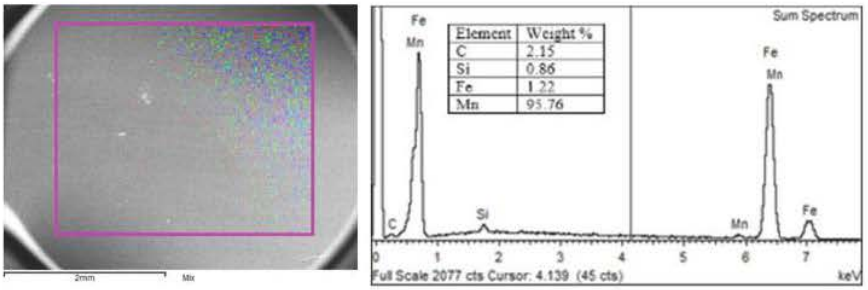

Carbon, C

Silicon, Si

Iron, Fe

Manganese, Mn

Figure 4.18: Elemental mapping analysis for tempered sample

Based on figure 4.19, the blue colour elements containing Manganese (Mn) which have the highest content percentage which are 92.71% when compared to other elements. The red graph depicted element containing Carbon (C) where it have 4.99% content element in the sample, whereas the Iron (Fe) have 1.18% slight higher than Silicon (Si) which is 1.11%.

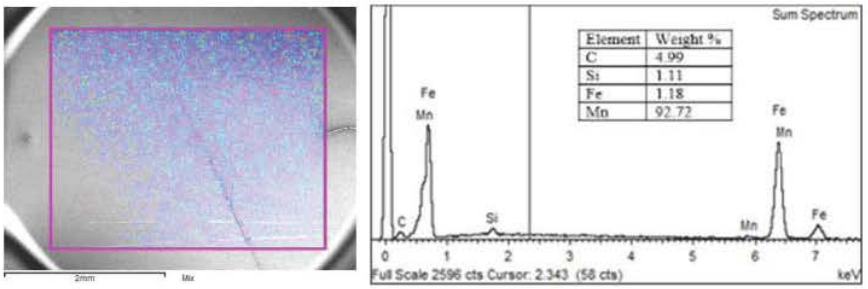

Carbon, C

Silicon, Si

Iron, Fe

Manganese, Mn

Figure 4.19: Elemental mapping analysis for annealed sample

CHAPTER 5

CONCLUSION AND RECOMMENDATIONS

5.1 Conclusion

i. During this process, were able to study the welded joint of low carbon steel joint with filler ER70s and the effect of heat treatment on the mechanical and microstructure properties by performing hardness and impact test. In addition, were able to carry out the non-destructive test by using radiography testing and liquid penetrant inspection. This study was conducted to find out how heat treatment can effect on the mechanical and microstructure at HAZ and welded joint area. This study is also used in the oil and gas industry.

ii. NDT is a non-destructive test that is always used on non-porous materials to detect surface defects using two separate procedures. These tests are particularly effective because the specimens are tested in methods that do not affect the reliability or functionality of the material being analyzed. After completing a dye penetrant test and radiography testing to examine if there was a surface defect against the welded joint, the specimen showed that no surface defect was found.

iii. After being cut with an abrasive water jet, the specimen must go through the tempering and annealing processes. This study includes three parameters: untreated, tempered, and annealed samples. The sample for tempering had to soak for 2 hours in the furnace at 450˚celsius, while the sample for annealing had to soak for 30 minutes in the furnace at 900˚celsius, and both had to be cooled in

room temperature. The outcome of the heat treatment method is that the looks of each sample group can be recognized by naked eyes, with the annealed sample having a crispy dark grey coating outside its surface, the tempered sample having a brownish colour, and the untreated sample preserving its original appearance.

iv. After the heat treatment is completed, a mechanical test must be performed. The impact and hardness tests were conducted for mechanical testing. The impact test results showed similar value of three samples with value 49.885J for untreated sample, 49.860J for tempered sample and 49.884J for annealed were tough and strong enough to break at the welded connection, however at the HAZ area, the annealed sample with value 49.884J is stronger than the tempered which have 48.860J and untreated samples with 47.885J.

v. For hardness test, Rockwell method were chosen and used ball indenter because of type of material were low carbon steel. Macro hardness variability were measured at three separate layers, with micro hardness tests done at the top, centre, and bottom of the sample. At annealed sample, the result of the graph showed that the line pattern of each area were in average compared to graph of untreated and tempered sample. Even though the line pattern of annealed sample were in average, but the annealed sample have the lowest value of hardness at HAZ and weld joint compared to tempered and untreated sample. Hardness test also revealed that heat treatment can strengthen the structure, resulting in a more ductile and stronger sample.

vi. material characterization, two methods were used, including an optical microscope and a Scanning Electron Microscopy (SEM) machine. First, the

sample must be polished with sandpaper and a diamond polisher sheet until it resembles a mirror. The sample must next be etched for 10 seconds with Nital. Nital is used to see the structure more clearly under an optical microscope with different lens diameters. The microstructure test results showed at the tempered sample have subtle structure especially at welded joint area and there's have fine grained structure at HAZ area meanwhile for annealed sample, the microstructure were similar at each area. There also no structure fine needle-like at the welded area were detected.

5.2 Recommendations for future

During the period, some difficulties and limitations in this study were encountered. During the polishing process to prepare the sample for microstructure and etching, the polished surface must not be touched or swept with a dry cloth since contact with a foreign surface may reduce the integrity of the polished surface and a scratch may occur. In addition to the process before the microstructure analyses, the duration spend immersing the sample in the Nital solution liquid during the etching should not exceed 10 seconds to avoid over etching on the surface sample. If over etching occurs, the polishing procedure must be repeated from the beginning.

Excessive heat from equipment and tools must not be introduced to the samples throughout the heat treatment study's sample preparation and data collecting phase prior to the heat treatment performed on the samples. This is done to avoid changes in microstructure and grain growth caused by the affected heat apart from heat treatment. Other test such as Electron Backscatter Diffraction (EBSD) to examine the microstructure, also can be done. In addition to all the recommendations, we can undertake additional heat treatment studies in the future to prevent failure in the region of HAZ, particularly at pipeline structures that were used in the oil and gas industry.

REFERENCES

Abioye, T. E., Ariwoola, O. E., Ogedengbe, T. I., Farayibi, P. K., & Gbadeyan, O. O. (2019). Effects of welding speed on the microstructure and corrosion behavior of dissimilar gas metal arc weld joints of AISI 304 stainless steel and low carbon steel. Materials Today: Proceedings, 17, 871–877. https://doi.org/10.1016/j.matpr.2019.06.383

Adedayo, A. V, Ibitoye, S. A., & Oyetoyan, O. A. (2010). Annealing Heat Treatment Effects on Steel Welds. 9(6), 547–557.

ASTM. (2015). E23-07a - Standard Test Methods for Notched Bar Impact Testing of Metallic Materials. ASTM International, 14(C), 28. https://doi.org/10.1520/E0023-07AE01.2

Boumerzoug, Z., Derfouf, C., & Baudin, T. (2010). Effect of Welding on Microstructure and Mechanical Properties of an Industrial Low Carbon Steel. Engineering, 02(07), 502–506. https://doi.org/10.4236/eng.2010.27066

Chandra Kandpal, B., Gupta, D. K., Kumar, A., Kumar Jaisal, A., Kumar Ranjan, A., Srivastava, A., & Chaudhary, P. (2020). Effect of heat treatment on properties and microstructure of steels. Materials Today: Proceedings, 44, 199–205. https://doi.org/10.1016/j.matpr.2020.08.556

Deepak, J. R., Bupesh Raja, V. K., Srikanth, D., Surendran, H., & Nickolas, M. M. (2020). Non-destructive testing (NDT) techniques for low carbon steel welded joints: A review and experimental study. Materials Today: Proceedings, 44, 3732–3737. https://doi.org/10.1016/j.matpr.2020.11.578

Evans, R. (2012). 2 - Selection and testing of metalworking fluids. In V. P. Astakhov & S. Joksch (Eds.), Metalworking Fluids (MWFs) for Cutting and Grinding (pp. 23–78). Woodhead Publishing. https://doi.org/https://doi.org/10.1533/9780857095305.23

Frihat, M. H. (2015). Effect of Heat Treatment Parameters on the Mechanical and Microstructure Properties of Low-Alloy Steel. Journal of Surface Engineered Materials and Advanced Technology, 05(04), 214–227. https://doi.org/10.4236/jsemat.2015.54023

Hajili, S. (2017). School Of Industrial And Information Welding processes for joining dissimilar metals and plastics.https://www.researchgate.net/ publication/323254307_Advanced_Manufacturing_Welding_processes_for_joining_dissimilar_metals_and_plastics/references

Hnizdil, M., & Chabicovsky, M. (2018). Experimental study of in-line heat treatment of 1.0577 structural steel. Procedia Manufacturing, 15, 1596–1603. https://doi.org/https://doi.org/10.1016/j.promfg.2018.07.305

Jenney, C. L., & O'Brien, A. (1991). Welding Handbook_Volume 1_Welding Science And Technology. American Welding Society, 1, 982.

Jeong, S., Lee, Y., Park, G., Kim, B., Moon, J., Park, S.-J., & Lee, C. (2021). Phase transformation and the mechanical characteristics of heat-affected zones in austenitic Fe–Mn–Al–Cr–C lightweight steel during post-weld heat treatment. Materials Characterization, 177, 111150. https://doi.org/https://doi.org/10.1016/j.matchar.2021.111150

Krauss, G. (2017). 4 - Physical metallurgy of steels: An overview.In R. Rana & S. B. Singh (Eds.), Automotive Steels (pp. 95–111). Woodhead Publishing. https://doi.org/https://doi.org/10.1016/B978-0-08-100638-2.00004-3

Kučerová, L., Jandová, A., & Rubešová, K. (2019). Microstructure analysis and mechanical properties of low alloyed steel with retained austenite obtained by heat treatment. Manufacturing Technology, 19(2), 243–247. https://doi.org/10.21062/ujep/277.2019/a/1213-2489/mt/19/2/243

Kumar, H., Kumar, N., & Engineering, R. N. C. (2019). A Survey on Gas Metal Arc Welding (GMAW) -Review. 7(01), 595–600.

Magudeeswaran, G., Balasubramanian, V., & Madhusudan Reddy, G. (2018). Metallurgical characteristics of armour steel welded joints used for combat vehicle construction. Defence Technology, 14(5), 590–606. https://doi.org/10.1016/j.dt.2018.07.021

Mesquita, R. A., Barbosa, C. A., & Machado, A. R. (2017). 2.9 Heat Treatment of Tool Steels. In M. S. J. Hashmi (Ed.), Comprehensive Materials Finishing (pp. 214–245). Elsevier. https://doi.org/https://doi.org/10.1016/B978-0-12-803581-8.09191-8

Metals., A. S. for, & International., A. S. M. (1997). Metals handbook. Volume 1, Volume 1,. ASM International.

Moore, P., & Booth, G. (2015). 13 - Improving the fracture performance and fatigue life of welded joints. In P. Moore & G. Booth (Eds.), The Welding Engineer's Guide to Fracture and Fatigue (pp. 185–195). Woodhead Publishing. https://doi.org/https://doi.org/10.1533/9781782423911.2.185

Nayak, S. S., Biro, E., & Zhou, Y. (2015). 5 - Laser welding of advanced high-strength steels (AHSS). In M. Shome & M. Tumuluru (Eds.), Welding and Joining of Advanced High Strength Steels (AHSS) (pp. 71–92). Woodhead Publishing. https://doi.org/https://doi.org/10.1016/B978-0-85709-436-0.00005-9

Owolabi, O. B., Aduloju, S. C., Metu, C. S., Chukwunyelu, C. E., & Okwuego, E. C. (2016). Evaluation of the Effects of Welding Current on Mechanical Properties of Welded Joints Between Mild Steel and Low Carbon Steel. American Journal of Materials Science and Application, 4(1), 1–4.

Phoumiphon, N., Othman, R., & Ismail, A. B. (2016). Improment in Mechanical Properties Plain Low Carbon Steel Via Cold Rolling and Intercritical Annealing. Procedia Chemistry, 19, 822–827. https://doi.org/https://doi.org/10.1016/j.proche.2016.03.108

Pisarski, H. G., & Pargeter, R. J. (1984). Fracture Toughness Of Weld Heat Affected Zones (Hazs) In Steels Used In Constructing Offshore Platforms. In Welding in Energy-Related Projects (pp. 415–428). Pergamon. https://doi.org/https://doi.org/10.1016/B978-0-08-025412-8.50044-9

Pourazizi, R., Mohtadi-Bonab, M. A., & Szpunar, J. A. (2020). Investigation of different failure modes in oil and natural gas pipeline steels. Engineering Failure Analysis, 109, 104400. https://doi.org/10.1016/j.engfailanal.2020.104400

Prabakaran, M. P., & Kannan, G. R. (2021). Effects of post-weld heat treatment on dissimilar laser welded joints of austenitic stainless steel to low carbon steel. International Journal of Pressure Vessels and Piping, 191(January), 104322. https://doi.org/10.1016/j.ijpvp.2021.104322

Primo, J. (2014). Gas Metal Arc Welding – GMAW Best Practices. ME Mechanical, 514.

Qiao, L., Zhu, J., & Wang, Y. (2021). Coupling physics in machine learning to predict interlamellar spacing and mechanical properties of high carbon pearlitic steel. Materials Letters, 293, 129645. https://doi.org/https://doi.org/10.1016/j.matlet.2021.129645

Rahman, S. M. M., Karim, K. E., & Simanto, M. H. S. (2016). Effect of Heat Treatment on Low Carbon Steel: An Experimental Investigation. Applied Mechanics and Materials, 860, 7–12. https://doi.org/10.4028/www.scientific.net/amm.860.7

Reyes, A., Bedolla, E., Perez, R., & Contreras, A. (2017). Effect of heat treatment on the mechanical and microstructural characterization of Mg-AZ91E/TiC composites. Composite Interfaces, 24(6), 593–609. https://doi.org/10.1080/09276440.2017.1248201

Saito, G., Zhang, T., Sakaguchi, N., Ohno, M., Matsuura, K., Takeuchi, M., Sano, T., Minoguchi, K., & Yamaoka, T. (2021). In-situ observation of abnormal grain growth in a low-alloyed carbon steel using SEM-EBSD. Materialia, 15, 100985. https://doi.org/10.1016/j.mtla.2020.100985

Senthur Prabu, S., Devendranath Ramkumar, K., & Arivazhagan, N. (2021). Microstructural evolution and elemental variation across the fusion interface of AISI 904L and Inconel 625 dissimilar weldments. Materials Today: Proceedings, 46(xxxx), 8260–8265. https://doi.org/10.1016/j.matpr.2021.03.246

Singh, R. (2020). 6 - Classification of steels. In R. Singh (Ed.), Applied Welding Engineering (Third Edition) (Third Edit, pp. 53–60). Butterworth-Heinemann. https://doi.org/https://doi.org/10.1016/B978-0-12-821348-3.00014-8

Valdes-Tabernero, M. A., Kumar, A., Petrov, R. H., Monclus, M. A., Molina-Aldareguia, J. M., & Sabirov, I. (2020). The sensitivity of the microstructure and properties to the peak temperature in an ultrafast heat treated low carbon-steel. Materials Science and Engineering A, 776(January), 138999. https://doi.org/10.1016/j.msea.2020.138999

Vural, M. (2014). 6.02 - Welding Processes and Technologies. In S. Hashmi, G. F. Batalha, C. J. Van Tyne, & B. Yilbas (Eds.), Comprehensive Materials Processing (pp. 3–48). Elsevier. https://doi.org/https://doi.org/10.1016/B978-0-08-096532-1.00603-8

Wahab, M. A. (2014). 6.03 - Manual Metal Arc Welding and Gas Metal Arc Welding. In S. Hashmi, G. F. Batalha, C. J. Van Tyne, & B. Yilbas (Eds.), Comprehensive Materials Processing (pp. 49–76). Elsevier. https://doi.org/https://doi.org/10.1016/B978-0-08-096532-1.00610-5

Exclude quotes	Off	Exclude matches	Off
Exclude bibliography	Off		